UNIVERSITAT POLITÈCNICA DE VALÈNCIA

DEPARTAMENTO DE MAQUINAS Y MOTORES TÉRMICOS

Influence of the mixture preparation on the combustion in Direct Injection engines

DOCTORATE THESIS

presented by

Patrick Gastaldi

directed by

Professor Francisco Payri Gonzalez

Valencia, January 2015

DOCTORATE THESIS

Influence of the mixture preparation on the combustion in Direct Injection engines

Presented by:

Patrick Gastaldi

Directed by:

Professor Francisco Payri

DEFENSE COMMITTEE

President: Professor Jose Desantes

Secretary: Professor Magin Lapuerta

Member: Dr Shuji Kimura

EXTERNAL EVALUATORS

Professor Octavio Armas

Dr Amin Velji

Dr Shuji Kimura

Valencia, January 2015

ABSTRACT

During the last two centuries, the development of the internal combustion engine has followed the evolution of the customer expectations. From the race for pure performances, high power, and fun to drive, perfectly well illustrated by the fabulous Mercedes 300 SL, the focus moved towards fuel efficient engines under the pressure of the still increasing oil prices. The well-known Diesel powertrain, up to this period limited to industrial vehicles, suddenly became the object of many researches, even for automotive manufacturers, specialists for sport cars. Technologic developments, mainly concerning turbocharging and injection, allowed the opening of the passenger cars market to CI engines due to acceptable noise, power and still unreachable efficiency. On the gasoline side, direct injection moved from racing to economic cars by the introduction of the stratified combustion. More recently, the pressure rose for dramatically reducing the air pollution, both in urban areas, by limiting NOx and soot, but also, at the scale of the earth, for managing CO_2 rejections and thereby enlarging the efforts on efficiency.

The two first combustion systems described in this document are concerning spray guided and air guided design alternatives to obtain a fuel stratification, and thereby operate the gasoline engine without throttling the air intake, aiming at a better fuel efficiency.

The first concept, called MID3S, was based on a 3 valve combustion chamber with a large squish area and a high compression ratio over 12; inspired from the May Fireball system, it was developed with a house made high pressure injector operating up to 80 bars with an outwardly opening needle. An ultra-lean flame-able mixture was formed at WOT in the vicinity of the spark plug for different operating points as low as idle, while the maximum performances were quite close to the targeted 37 kW/l. The efficiency was significantly improved compared to a similar MPI engine while CO and HC were quite acceptable. On the contrary, NOx and soot would have to be improved. The robustness of the squish aerodynamic motion was unfortunately balanced by the sensitivity of spray angle and penetration versus the back pressure and thereby late injection timings, creating plug wetting and fouling. The hollow cone structure of the fuel plume was clearly responsible of this behavior, especially because of the effect of the air entrainment inside the spray. An increase of the injection pressure from 30 to 80 bar, and probably upper, would probably reduce this effect. Concerning methodologies, a dedicated cylinder head was designed with two endoscope locations in order to visualize the interaction between spray, air, walls and combustion –or more precisely soot- with a high speed camera operating within visible wavelengths. The spray structure, formed by a succession of ligaments at the surface of the plume, was clearly emphasized in atmospheric conditions.

The second design, called K5M, was based on an adjustable high tumble motion generated in the intake port. A swirl injector provided by Siemens and located between the two intake valves of the pent roof chamber, was operated until 80 bar. Mixture preparation was relying on the interaction between the air motion and the spray, the tumble velocity deviating fuel droplets towards the spark plug situated at the center of the chamber. 3D CFD simulation, PIV and LIF visualization techniques

on an optical single cylinder engine were used in parallel in order to understand the spatial evolution of the equivalence ratio during the cycle and the ability to operate the engine at WOT, even at part load. At low BMEP and speed, the natural reduction of the tumble intensity might have been followed by a significant reduction of the injection pressure in order to secure an accurate balance between the two momentum energies; unfortunately, both high cycle to cycle aerodynamic fluctuations and a poor spray atomization at 30 bar didn't allow to achieve an acceptable ignition stability at low loads due to a too lean mixture in the plug vicinity. Protruded electrodes could have been a solution to the problem but their reliable use in serial life was not secured. On the contrary, mid load performances were globally adequate.

The third concept is concerning Diesel combustion aiming at very low NOx and soot emissions by using an innovative injection system. The basic idea relies on the use of a quite homogeneous combustion at low load –called Mild HCCI- and on a diffusion controlled one at higher loads.
Based on two injections close one of the other in the vicinity of TDC, the Mild HCCI allows to moderate the combustion noise inherent to the premixed burning phase as the fuel injected during the second injection cools down the first combustion; the advantages of very low NOx and soot emissions until around 8 bar BMEP are meanwhile maintained. Above this value, the noise level becomes unacceptable for automotive applications and the come back to a conventional diffusive combustion becomes mandatory. Based on early academic investigations pointing out the positive effect of small nozzle holes associated to high injection pressures in terms of soot via a significant difference between the lift-off length and the liquid penetration length, an innovative injection system was adapted to a conventional combustion chamber.
The first conclusion was concerning a significant improvement of the NOx/soot trade-off at mid and high loads with quite usual EGR rates. This advantage was due to a much better fuel atomization linked to both small holes and high pressures.
The second conclusion was related to the possibility to achieve a "0 soot/ 0 NOx" combustion at high loads while very much increasing EGR and air mass flows. In this case, a Lifted Flame Diffusion Controlled combustion was generated, confirming on a scale 1 engine the results obtained in academic conditions. Nevertheless, the use of 3D simulation allowed to demonstrate that mixture preparation was only one part of the result; the location of the different stages of the combustion in a Kamimoto diagram, much away from the NOx and soot peninsula, highlighted the impact of the LTC (Low Temperature Combustion) thermodynamics. Unfortunately, despite these good results, industrially available EGR and air systems are not able to provide the necessary mass flows.
Concerning tools, the development steps were followed by intensive spray visualizations for both the liquid and the vapor phases, in conditions closer and closer to the actual engine. These measurements allowed to precisely evaluate the impact of the diameter size, the rail pressure and the oxygen content on the difference between lift-off and liquid lengths.

Finally, the importance of coupling investigation tools like visualization and 3D simulation in conditions as close as possible to the actual engine in terms of temperature, pressure and timing –eg the ability to record a complete mixture and combustion cycle- has been emphasized for both future SI and Diesel engines. In particular, the forecasted increase of the rail pressures will lead to re-optimize the different available spray models and eventually to re-adapt them in terms of physical

phenomena because of the great variations of the spray velocity and of the Weber number. The presence of cavitation in the nozzle holes will also have to be taken into account as it has a key role versus coking.

In conclusion, it is quite clear that the development of stratified gasoline and low emissions Diesel engines will more and more rely on the mixture preparation and on its association with low gas temperatures.

RESUMEN

Durante las últimas dos décadas, el desarrollo del motor de combustión interna ha seguido la evolución de las expectativas del cliente. Desde la carrera por la pura obtención de prestaciones, alta potencia y el fun-to-drive, perfectamente ilustrada por el fabuloso Mercedes 300 SL, el planteamiento se cambió hacia motores eficientes bajo la presión de los aún crecientes precios de petróleo. La bien conocida planta motriz Diesel, hasta este periodo limitada a vehículos industriales, de repente fue el objeto de muchas investigaciones, incluso para fabricantes de automoción, especialistas en coches deportivos. Los desarrollos tecnológicos, principalmente concernientes a sobrealimentación e inyección, permitieron la apertura del mercado de los vehículos automóviles a los motores de encendido por compresión debido a los niveles aceptables de ruido, potencia y su aún imbatible eficiencia. Por la parte de la gasolina, la inyección directa pasó de los coches de carrera a los utilitarios con la introducción de la combustión estratificada. Más recientemente se incrementó la presión para reducir la contaminación del aire tanto en zonas urbanas, limitando NOx y hollín, como a escala planetaria, para gestionar emisiones de CO2 y por tanto aumentar los esfuerzos en la parte de eficiencia.

Los dos primeros sistemas de combustión descritos en este documento tratan las alternativas de guiado por chorro y guiado por aire para obtener una estratificación de combustible, y por tanto operar el motor de gasolina sin estrangulamiento de la admisión, con miras a conseguir mejor eficiencia.

El primer concepto, denominado MID3S, se basó en una cámara de combustión de 3 válvulas con una gran área de squish y una relación de compresión de más de 12; inspirado en el sistema May Fireball, se desarrolló con un inyector casero de alta presión operado hasta 80 bar con una aguja que se abría hacia afuera. Se formaba una mezcla inflamable ultra pobre con la mariposa totalmente abierta en las proximidades de la bujía para condiciones de operación tan bajas como relentí, mientras que las prestaciones máximas estaban cerca del objetivo de 37 kW/l. El rendimiento se mejoró significativamente respecto a un motor de inyección multipunto, mientras que el CO y HC eran bastante aceptables. Por el contrario, los NOx y hollín tenían que mejorar. Desafortunadamente, la robustez del movimiento aerodinámico de squish estaba compensado por la sensibilidad del ángulo de chorro y la penetración a la contrapresión, y por tanto las inyecciones en tiempos tardíos creaban mojado y fallos de la bujía. La estructura de cono hueco del chorro de combustible era la responsable de este comportamiento, especialmente debido al efecto de englobamiento del aire dentro del chorro. El aumento de la presión de inyección de 30 a 80 bar, y probablemente por encima, habría reducido este efecto. Por lo que respecta a las metodologías, se diseñó una culata a propósito con dos accesos endoscópicos para visualizar la interacción entre el chorro, el aire, las paredes y la combustión (o más precisamente el hollín) con una cámara de alta velocidad operando en longitudes de onda visibles. La estructura del chorro, formada por una sucesión de ligamentos en la superficie del mismo, mostraba claramente las condiciones de operación atmosféricas.

El segundo diseño, denominado K5M, se basaba en un movimiento ajustable de alto tumble generado en el colector de admisión. Se utilizaba un inyector de Siemens

localizado entre las dos válvulas de admisión de la cámara de combustión tipo pent-roof, con una presión de hasta 80 bar. La preparación de la mezcla se confiaba a la interacción entre el movimiento del aire y el chorro, donde la velocidad del tumble desviaba las gotas hacia la bujía situada en el centro de la cámara. Se usaron simulaciones 3D CFD y técnicas de visualización PIV y LIF en un motor óptico en paralelo, para comprender la evolución espacial del dosado durante el ciclo, y la posibilidad de operar el motor con la mariposa totalmente abierta, incluso a carga parcial. A baja carga y velocidad, la reducción natural de la intensidad del tumble podría haber sido seguida por una reducción significativa de la presión de inyección, con el objeto de asegurar un balance exacto entre las dos energías de momento; desafortunadamente, tanto las altas fluctuaciones ciclo a ciclo, como la pobre atomización a 30 bar no permitieron alcanzar una estabilidad de encendido aceptable a baja carga debido a una mezcla demasiado pobre en las proximidades de la bujía. El uso de electrodos que sobresalieran podría haber sido una solución al problema, pero no se aseguraba un uso confiable en la vida de serie. Por el contrario, las prestaciones a media carga eran globalmente adecuadas.

El tercer concepto es refiere a la combustión Diesel que pretende conseguir muy bajas emisiones de NOx y hollín usando un sistema de inyección innovador. La idea básica se apoya en el uso de una combustión bastante homogénea a baja carga – denominada Mild HCCI – y en una de difusión a alta carga.

Basada en dos inyecciones cercanas entre ellas en las proximidades del PMS, la Mild HCCI permite moderar el ruido de combustión inherente a la fase de combustión premezclada, puesto que el combustible inyectado durante la segunda fase enfría la primera combustión; se mantienen las ventajas de las bajas emisiones de NOx y soot hasta 8 bar de PME. Por encima de este valor, el nivel de ruido llega a ser inaceptable para aplicaciones de automoción y se hace obligatorio volver a una combustión convencional difusiva. Basado sobre investigaciones académicas que señalan el efecto positivo de los orificios de tobera reducidos asociados a altas presiones de inyección en términos de hollín via una diferencia significativa entre la distancia de lift-off y la longitud de penetración líquida, se adaptó un sistema de inyección innovador a una cámara de combustión convencional.
La primera conclusión es una mejora significativa del balance NOx/soot a media y alta carga con tasas de EGR bastante usuales. Esta ventaja fue debida a una atomización mucho mejor unida tanto a los pequeños orificios como a las altas presiones.
La segunda conclusión se relaciona con la posibilidad de alcanzar una combustión “0 hollín/0 NOx” a alta carga, aumentando mucho el EGR y la masa de aire. En este caso se generó una combustión controlada por difusión con llama despegada, confirmando a escala de motor real los resultados obtenidos en investigaciones académicas. Sin embargo, el uso de simulaciones 3D permitieron demostrar que la preparación de la mezcla era solamente una parte del resultado; la localización de las diferentes etapas de la combustión en un diagrama de Kamimoto, muy lejos de la península de NOx y soot, señala el impacto de la termodinámica de la LTC (Combustión a Baja Temperatura). Desafortunadamente, a pesar de estos resultados los sistemas disponibles de EGR y aire no pueden proporcionar los gastos necesarios de masa.
Por lo que respecta a las herramientas, los pasos de desarrollo fueron seguidos por visualizaciones intensivas de chorro para las fases líquida y vapor, en condiciones cada vez más cercanas al motor real. Estas medidas permitieron evaluar precisamente

el impacto del diámetro, la presión de inyección y el contenido en oxígeno sobre la diferencia entre las longitudes líquida y de lift-off.

Finalmente, se ha enfatizado en la importancia de acoplar herramientas de investigación como visualización y simulaciones 3D en condiciones tan cerca como sea posible a las del motor real en términos de temperatura, presión y timing (p.ej. la posibilidad de registrar un ciclo completo de mezcla y combustión) para los futuros motores tanto de Encendido Provocado como por Compresión. En particular, el aumento predicho de presión de inyección llevará a reoptimizar los diferentes modelos disponibles de chorro y finalmente a readaptarlos en términos de los fenómenos físicos, debido a las grandes variaciones de la velocidad de chorro y del número de Weber. La presencia de cavitación en los orificios de la tobera también tendrá que ser tenida en cuenta, puesto que tiene un papel fundamental en lo que respecta al coking.

En conclusión, es evidente que el desarrollo de motores de gasolina de carga estratificada y Diesel de bajas emisiones se apoyará cada vez más en la preparación de la mezcla y en su asociación con las temperaturas de gas bajas.

RESUM

Durant les últimes dos dècades, el desenvolupment del motor de combustió interna ha seguit l'evolució de les expectatives del client. Des de la carrera per la pura obtenció de prestacions, alta potència i el fun-to-drive, perfectament il·lustrada pel fabulós Mercedes 300 SL, el plantejament es va canviar cap a motors eficients davall la pressió dels encara creixents preus de petroli. La bé coneguda planta motriu Dièsel, fins a este període limitada a vehicles industrials, de sobte va ser l'objecte de moltes investigacions, inclús per a fabricants d'automoció, especialistes en cotxes esportius. Els desenvolupments tecnològics, principalment concernents a sobrealimentació i injecció, van permetre l'obertura del mercat dels vehicles automòbils als motors d'encesa per compressió degut als nivells acceptables de soroll, potència i a la seua encara imbatible eficiència. Per la part de la gasolina, la injecció directa va passar dels cotxes de carrera als utilitaris amb la introducció de la combustió estratificada. Més recentment es va incrementar la pressió per a reduir la contaminació de l'aire tant en zones urbanes, limitant NOx i sutja, com a escala planetària, per a gestionar emissions de CO2 i per tant d'augmentar els esforços en la part d'eficiència.

Els dos primers sistemes de combustió descrits en este document tracten les alternatives de guiat per doll i guiat per aire per a obtenir una estratificació de combustible, i per tant operar el motor de gasolina sense estrangulació de l'admissió, amb vista a aconseguir millor eficiència

El primer concepte, denominat MID3S, es va basar en una cambra de combustió de 3 vàlvules amb una gran àrea de squish i una relació de compressió de més de 12; inspirat en el sistema May Fireball, es va desenrotllar amb un injector casolà d'alta pressió operat fins a 80 bar amb una agulla que s'obria cap a fora. Es formava una mescla inflamable ultra pobre amb la papallona totalment oberta en les proximitats de la bugia per a condicions d'operació tan baixes com ralentí, mentre que les prestacions màximes estaven prop de l'objectiu de 37 kW/l. El rendiment es va millorar significativament respecte a un motor d'injecció multipunt, mentre que el CO i HC eren prou acceptables. Al contrari, els NOx i sutja havien de millorar. Desafortunadament, la robustesa del moviment aerodinàmic de squish estava compensat per la sensibilitat de l'angle de doll i la penetració a la contrapressió, i per tant les injeccions en temps tardans creaven mullat i fallades de la bugia. L'estructura de con buit del doll de combustible era la responsable d'este comportament, especialment a causa de l'efecte d'englobament de l'aire dins del doll. L'augment de la pressió d'injecció de 30 a 80 bar, i probablement per damunt, hauria reduït este efecte. Pel que fa a les metodologies, es va dissenyar una culata a propòsit amb dos accessos endoscòpics per a visualitzar la interacció entre el doll, l'aire, les parets i la combustió (o més precisament la sutja) amb una càmera d'alta velocitat operant en longituds d'onda visibles. L'estructura del doll, formada per una successió de lligaments en la superfície del mateix, mostrava clarament les condicions d'operació atmosfèriques.

El segon disseny, denominat K5M, es basava en un moviment ajustable d'alt tumble generat en el col·lector d'admissió. S'utilitzava un injector de Siemens localitzat entre les dos vàlvules d'admissió de la cambra de combustió tipus pent-roof, amb una pressió de fins a 80 bar. La preparació de la mescla es confiava a la interacció entre el

moviment de l'aire i el doll, on la velocitat del tumble desviava les gotes cap a la bugia situada en el centre de la cambra. Es van usar simulacions 3D CFD i tècniques de visualització PIV i LIF en un motor òptic en paral·lel, per a comprendre l'evolució espacial del dosatge durant el cicle, i la possibilitat d'operar el motor amb la papallona totalment oberta, inclús a càrrega parcial. A baixa càrrega i velocitat, la reducció natural de la intensitat del tumble podria haver sigut seguida per una reducció significativa de la pressió d'injecció, amb l'objecte d'assegurar un balanç exacte entre les dos energies de moment; desafortunadament, tant les altes fluctuacions cicle a cicle, com la pobra atomització a 30 bar no van permetre aconseguir una estabilitat d'encesa acceptable a baixa càrrega degut a una mescla massa pobra en les proximitats de la bugia. L'ús d'elèctrodes que sobreïsqueren podria haver sigut una solució al problema, però no s'assegurava un ús confiable en la vida de sèrie. Al contrari, les prestacions a mitja càrrega eren globalment adequades.

El tercer concepte és refereix a la combustió Dièsel que pretén aconseguir molt baixes emissions de NOx i sutja usant un sistema d'injecció innovador. La idea bàsica es recolza en l'ús d'una combustió prou homogènia a baixa càrrega - denominada Mild HCCI - i en una de difusió a alta càrrega.

Basada en dos injeccions properes entre elles en les proximitats del PMS, la Mild HCCI permet moderar el soroll de combustió inherent a la fase de combustió premesclada, ja que el combustible injectat durant la segona fase refreda la primera combustió; es mantenen els avantatges de les baixes emissions de NOx i soot fins a 8 bar de PME. Per damunt d'este valor, el nivell de soroll arriba a ser inacceptable per a aplicacions d'automoció i es fa obligatori tornar a una combustió convencional difusiva. Basat sobre investigacions acadèmiques que assenyalen l'efecte positiu dels orificis de tovera reduïts associats a altes pressions d'injecció en termes de sutja via una diferència significativa entre la distància de lift-off i la longitud de penetració líquida, es va adaptar un sistema d'injecció innovador a una cambra de combustió convencional.
La primera conclusió és una millora significativa del balanç NOx/soot a mitja i alta càrrega amb taxes d'EGR prou usuals. Este avantatge va ser degut a una atomització molt millor unida tant als xicotets orificis com a les altes pressions.
La segona conclusió es relaciona amb la possibilitat d'aconseguir una combustió "0 hollín/0 NOx" a alta càrrega, augmentant molt l'EGR i la massa d'aire. En este cas es va generar una combustió controlada per difusió amb flama enlairada, confirmant a escala de motor real els resultats obtinguts en investigacions acadèmiques. No obstant això, l'ús de simulacions 3D va permetre demostrar que la preparació de la mescla era només una part del resultat; la localització de les diferents etapes de la combustió en un diagrama de Kamimoto, molt lluny de la península de NOx i soot, assenyala l'impacte de la termodinàmica de la LTC (Combustió a Baixa Temperatura). Desafortunadament, a pesar d'estos resultats els sistemes disponibles d'EGR i aire no poden proporcionar els cabdals necessaris de massa.
Pel que fa a les ferramentes, els passos de desenvolupament van ser seguits per visualitzacions intensives de doll per a les fases líquida i vapor, en condicions cada vegada més pròximes al motor real. Estes mesures van permetre avaluar precisament l'impacte del diàmetre, la pressió d'injecció i el contingut en oxigen sobre la diferència entre les longituds líquida i de lift-off.

Finalment, s'ha emfatitzat en la importància d'acoblar ferramentes d'investigació com ara la visualització i simulacions 3D en condicions tan prop com siga possible a les del motor real en termes de temperatura, pressió i timing (p.ej. la possibilitat de registrar un cicle complet de mescla i combustió) per als futurs motors tant d'Encesa Provocada com per Compressió. En particular, l'augment predit de pressió d'injecció portarà a reoptimitzar els diferents models disponibles de doll i finalment a readaptar-los en termes dels fenòmens físics, a causa de les grans variacions de la velocitat de doll i del número de Weber. La presència de cavitació en els orificis de la tovera també haurà de ser tinguda en compte, ja que té un paper fonamental pel que fa el coking.

En conclusió, és evident que el desenvolupament de motors de gasolina de càrrega estratificada i Dièsel de baixes emissions es recolzarà cada vegada més en la preparació de la mescla i en la seua associació amb les temperatures de gas baixes.

RESUME

Au cours des deux siècles précédents le développement des moteurs à combustion interne a été impulsé par la demande et les souhaits des clients. D'une course aux performances, à la puissance pure et au plaisir de conduite, illustrée par la merveilleuse Mercedes 300 SL, le focus s'est déplacé vers une amélioration du rendement énergétique sous la pression des prix du pétrole. Le bien connu moteur Diesel, jusque-là réservé aux véhicules industriels, devint rapidement l'objet de maintes recherches, même chez les constructeurs automobiles spécialistes de voitures de sport. Les développements technologiques, principalement dans les domaines de la suralimentation et de l'injection, permirent d'ouvrir le marché de la voiture particulière aux moteurs à allumage par compression de par les progrès réalisés en matière de bruit, de puissance et toujours de meilleur rendement. Du côté des moteurs à essence, l'injection directe migra des voitures de course aux véhicules économiques via l'introduction de la charge stratifiée. Les dernière décennies furent marquées par la nécessité de très fortement réduire la pollution de l'air, à la fois en milieu urbain en limitant NOx et particules, mais aussi à l'échelle de la planète en mieux gérant les rejets de CO_2.

Les deux premiers systèmes décrits dans ce document concernent des alternatives basées sur soit un guidage par le jet, soit un guidage par l'air afin de stratifier le carburant et ainsi utiliser le moteur à essence sans vannage de l'admission, avec comme premier objectif le rendement énergétique.
Le premier concept, appelé MID3S, était basé sur une chambre de combustion à 3 soupapes avec une large zone de chasse et un taux de compression élevé, supérieur à 12 ; inspiré du système May Fireball, il fut développé avec un injecteur haute pression à aiguille sortante réalisé en interne et fonctionnant jusqu'à 80 bars. Un mélange inflammable était formé au voisinage de la bougie pour différents points de fonctionnement obtenus à pleine ouverture papillon, et ce jusqu'au ralenti, avec des richesses très faibles ; les performances maximales étaient proches de l'objectif de 37 kW/l. Le rendement était largement amélioré par comparaison avec un moteur à injection indirecte similaire alors que HC et CO étaient cantonnés à des valeurs raisonnables. Par contre, les NOx et les suies restaient à réduire. La robustesse du mouvement aérodynamique était malheureusement perturbée par la sensibilité de l'angle et de la pénétration de jet vis-à-vis de la contre pression, et par là même de l'avance à l'injection, générant un mouillage et un encrassement des électrodes de la bougie. La structure du jet en cône creux était clairement responsable de ce comportement, en particulier de par l'effet d'entraînement d'air à l'intérieur du jet. Une augmentation de pression d'injection de 30 à 80 bars, et probablement au-delà, réduirait cet effet néfaste. Concernant les méthodologies, une culasse dédiée fut dessinée en intégrant le passage de deux endoscopes permettant de visualiser l'interaction entre le jet, l'air et la combustion –ou plus précisément les suies- avec une caméra rapide opérant dans le visible. La structure du jet formé par une succession de filaments fut clairement mise en évidence en conditions atmosphériques.
Le second concept, appelé K5M, était basé sur un mouvement de tumble d'intensité variable généré à l'admission. Un injecteur à swirl fourni par Siemens et situé entre les deux soupapes d'admission de la chambre en toit était utilisé jusqu'à 80 bars. La

préparation du mélange reposait sur l'interaction entre le mouvement d'air et le jet, le mouvement de tumble entraînant les gouttelettes de carburant vers la bougie située au centre de la chambre. La simulation 3D, les visualisations par PIV et LIF réalisées sur un moteur monocylindre optique furent utilisées en parallèle afin de comprendre l'évolution spatiale du champ de richesse durant le cycle et la capacité d'utiliser le moteur sans papillon même à charge partielle. A faible PME et faible régime, la réduction naturelle de l'intensité de tumble aurait dû être accompagnée d'une réduction significative de la pression d'injection afin d'assurer un bon équilibre entre les deux quantités de mouvement ; malheureusement, à la fois les fluctuations cycle à cycle de l'aérodynamique et une atomisation défaillante en deçà des 30 bars ne permirent pas d'obtenir une stabilité suffisante aux faibles charges de par la richesse trop pauvre au niveau de la bougie. Des électrodes projetées auraient pu constituer une solution au problème mais leur utilisation en grande série n'était pas suffisamment sûre. A contrario, les performances à mi charge étaient globalement satisfaisantes.

Le troisième système est de type Diesel à très faibles niveaux de NOx et de suies via une injection innovante. L'idée de base consiste en l'utilisation d'une combustion quasi homogène à faible charge –appelée Mild HCCI- et d'une combustion de diffusion contrôlée aux charges plus élevées.
Basée sur deux injections rapprochées au voisinage du PMH, le Mild HCCI permet de contenir le bruit de combustion inhérent au prémélange, la seconde injection refroidissant la première combustion, tout en conservant les avantages de faibles niveaux de NOx et de suies jusqu'à environ 8 bars de PME. Au-delà de cette valeur, le bruit devient inacceptable pour une application automobile et le retour à une combustion de diffusion devient obligatoire. Basée sur des travaux académiques démontrant l'effet positif de buses à petits diamètres de trous associées à de fortes pression rail en terme de suies via une différence significative entre longueurs de lift-off et de pénétration liquide, un système d'injection innovant fut adapté à une chambre conventionnelle.
La première conclusion concernait une amélioration significative du compromis NOx/suies aux charges moyennes et élevées avec les taux d'EGR usuels. Cet avantage était dû à une bien meilleure atomisation du carburant via à la fois les faibles diamètres de trous et les pressions élevées.
La seconde conclusion était relative à la possibilité d'obtenir une combustion sans suies et sans NOx aux charges élevées en augmentant significativement les débits d'EGR et d'air. Dans ce cas une combustion LFDC (Lifted Flame Diffusion Controlled combustion) était obtenue, confirmant sur moteur réel les résultats obtenues dans des conditions de laboratoire. Néanmoins, l'utilisation du calcul 3D permit de montrer que la préparation du mélange était à la source de seulement une partie du résultat ; le suivi de la combustion au cours du cycle, positionnée dans le diagramme de Kamimoto bien au-delà des péninsules de formation des NOx et des suies, mit en évidence le rôle de la thermodynamique et de la combustion faible température LTC. Malheureusement, malgré ces bons résultats, les systèmes d'EGR et de suralimentation actuellement disponibles en série ne permettent pas d'atteindre les débits identifiés comme nécessaires.
Concernant les outils, les étapes du développement furent accompagnées par de nombreuses visualisations des jets, à la fois pour les phases liquide et vapeur, dans des conditions de plus en plus proches du fonctionnement réel sur moteur. Ces mesures permirent d'évaluer précisément l'impact du diamètre de trou, de la pression rail et de

la concentration en oxygène sur la différence entre longueur de lift-off et pénétration liquide.

En conclusion, l'importance du couplage entre les outils de simulation 3D et la visualisation dans des conditions aussi proches que possible du moteur réel en termes de température, pression et temps –ie la capacité à enregistrer un cycle complet de préparation du mélange et de combustion- a été mise en évidence pour à la fois les futurs moteurs à allumage commandé et Diesel. En particulier, l'augmentation prévisible des pressions d'injection conduira à ré-optimiser les différents modèles de jets disponibles et éventuellement les réadapter au niveau des phénomènes physiques à cause des fortes variations de vitesse de jet et de nombre de Weber. La présence de cavitation dans les trous de buse devra également être prise en compte en raison de son fort impact sur l'encrassement.

Il est ainsi clair que le développement de moteurs essence à charge stratifiée et de Diesel à faibles émissions sera de plus en plus dépendant de la préparation du mélange et de son interaction avec la température des gaz.

Acknowledgements

For an engineer working in the industry, deciding to achieve a PhD thesis during the second part of the life can look like a quite strange story. It is perhaps one of these decisions you sometimes take even if they are not entirely motivated by the reason, but by something else!
After almost 30 years spent in Research and Advanced Development teams, I really felt the need to gather and share the technical experiences –scientific would certainly be a too heavy word- I had the opportunity to acquire along the projects which have the largest place in my heart. I thereby wished to achieve this work within the frame of an institution whose reputation in my field of expertise, Mixture Preparation and Combustion, could not be discussed.

Among the people who helped me during these years, I would like to thank Professor Francisco Payri and many of his collaborators at CMT; after having accepted to supervise the such particular student I was, Professor Payri provided me scientific recommendation and encouragements of first importance in order to synthetize all the available results into an actual PhD report.

It is obvious that this task would not have been achieved without the agreement and the support of Renault management, and especially from Mr Pierrick Cornet, VP for Powertrain Development, Mr Christophe Monnereau and Mr Denis Reverseau. I am grateful for their comprehensive understanding of my motivation and for the time I had available to achieve this work.

This short page would also be dedicated to engineers and technicians I have been proud to manage or more simply to work with during these investigations; all of them would have had the right to be co-authors of this document because, without their innovative ideas, their valuable scientific contribution or their ability to set up and drive new kind of tests or simulations which seemed to be impossible, most of the presented results would not have been obtained. An exhaustive list would probably have been much too long, with the fear to forget one of them; nevertheless, the related bibliography highlights the participation of some of my closest collaborators.

If much of the work has been achieved within Renault Research Division and Renault Powertrain Division, I would also like to associate all our partners, CMT, CERTAM, IFPEN, KIT, but also Delphi…., public and private institutions, NISSAN, for the quality of the exchanges I had with them and for the benefits I could learn from their experience. I really believe that this “multi-cultural” world-wide relationship between the industry and the laboratories was and remains a key for the success of advanced developments.

As a conclusion, and for younger PhD students who are going to read this report, I would like to remember how rare are the individual success in techniques and sciences, but that human relations are at the basis of much of the advances.

Nomenclature

Definition

Equivalence Ratio = (mass of Fuel / mass of Air) / (mass of Fuel / mass of Air)st

Symbols

a (suffix)	ambiant	
d	diameter	[µm]
L	liquid length	[mm]
H	lift-off length	[mm]
P	pressure	[Pa]
Q	mass flow	[kg/s]
st (suffix)	stoechiometric	
T	temperature	[K]
U	velocity	[m/s]
V	volume	[m^3]
ρ	density	[kg/m^3]
W	work	[J]
γ	polytropic exponent	[-]
η	efficiency	[-]
ξ	mixture fraction	[-]

Abbreviations

ASOI	After Start Of Injection
AVL	AVL List GmbH
BDC	Bottom Dead Center
BMEP	Brake Mean Effective Pressure
BTDC	Before Top Dead Center
CA	Crank Angle
CERTAM	Centre d'Etude et de Recherche Technologique en Aérothermique et Moteurs
CI	Compression Ignition
CMT	CMT-Motores Térmicos
CORIA	COmplexe de Recherche Interprofessionnel en Aérothermochimie

CR	Common Rail
CSF	Catalytic Soot Filter
DICO	DIffusive COmbustion (consortium)
ECN	Engine Combustion Network
EGR	Exhaust Gas Recirculation
ELSA	Eulerian Lagrangian Spray Atomization
FARLIF	Fuel Air Ratio Laser Induced Fluorescence
FPIV	Fluorescent Particles Image Velocimetry
FTP	Federal Testing Procedure
GDI	Gasoline Direct Injection
HCCI	Homogeneous Combustion Compression Ignition
hp	high pressure cycle
HRR	Heat Release Rate
IFP	Institut Français du Pétrole
IFPEN	IFP Energies Nouvelles
IMEP	Indicated Mean Effective Pressure
IMFT	Institut de Mécanique des Fluides de Toulouse
ISFC	Indicated Specific Fuel Consumption
KIT	Karlsruhe Institut für Technologie
LEM	Laser Extinction Method
LFDC	Lifted Flame Diffusion Controlled combustion
LIEF	Laser Induced Exciplex Fluorescence
LIF	Laser Induced Fluorescence
LII	Laser Induced Incandescence
LTC	Low Temperature Combustion
MIT	Massachusetts Institute of Technology
MPI	Multi Points Injection
NADIA	New Advanced Direct Injection Analysis (Consortium)
NEDC	New European Driving Cycle
NVH	Noise Vibration Harshness
PAH	Poly-Aromatic Hydrocarbons
PCCI	Premixed Combustion Compression Ignition
PIV	Particles Image Velocimetry
PLII	Planar Laser Induced Incadescence
RANS	Reynolds-averaged Navier Stokes
RCM	Rapid Compression Machine
RON	Research Octane Number
SCR	Selected Catalytic Reduction
SI	Spark Ignition
SMD	Sauter Mean Diameter

SNL	Sandia National Laboratory
SOI	Start Of Injection
TCV	Tumble Control Valve
TDC	Top Dead Center
VCO	Valve Covered Orifice
WLTP	World Light duty Testing Procedure
WOT	Wide Open Throttle
WWII	World War II

Contents

Chapter 1

Introduction

1.1. Energy and environment challenges for automotive engines.

1.1.1 Evolution of the transportation demand.

Since the very early stage of the earth, humans need to move from one location to the other, firstly to survive, by finding food or to preserve themselves from natural disasters or from wars, and then to transport goods for trading or later on for business. During the last centuries, muscular power, provided by their own legs or by animals, natural sources, like wind, have been step by step replaced by vapor and combustion of fossil energies.

This fundamental need has been both emphasized by the development of international trade and commercial exchanges, but also by the increasing interest for tourism and leisure, first in the western industrialized regions, but more and more in the newly developed countries like China, India and, tomorrow, Africa. Techniques and technologies have been developed to fulfill these human demands –we would now say these customer expectations. Besides the need of reduced transportation times, or increased reliability, the ideas of performances, driving pleasure, comfort, individual freedom wherever the client is, and of course affordability, became more and more important.

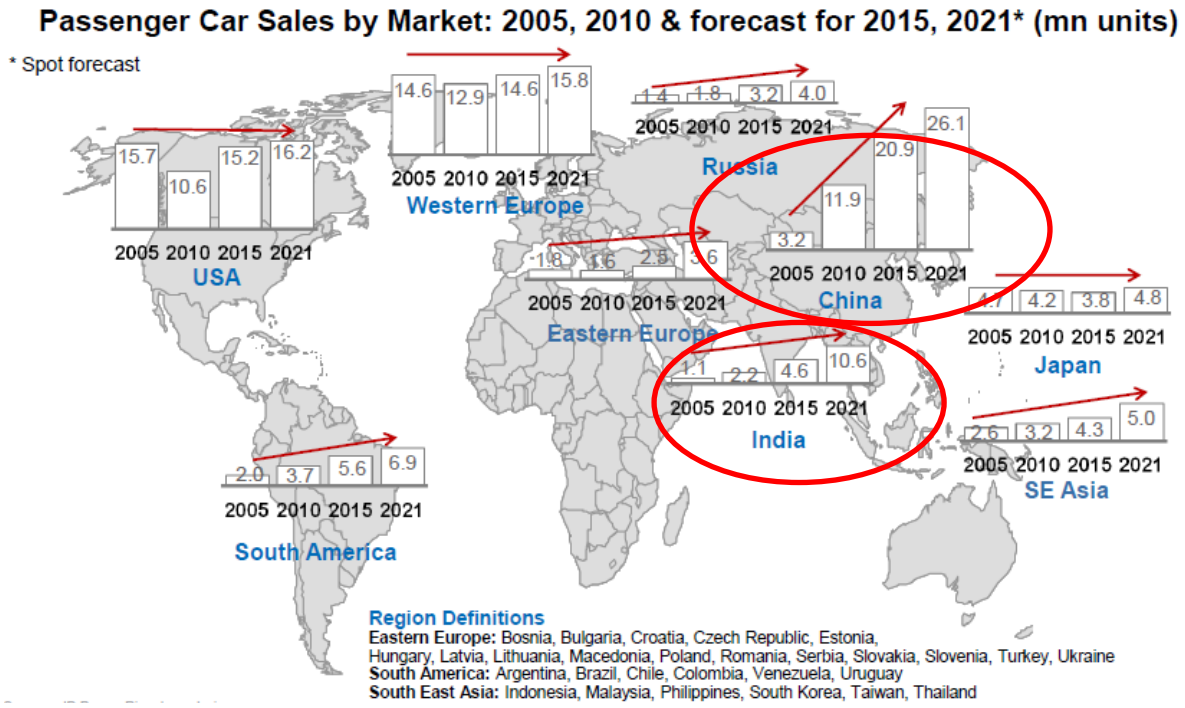

Figure 1-1: evolution of the main passenger car sales until 2021 [1-1]

This trend leads to an increase of the number of automobiles over the world; for instance, between 2010 and 2015, passenger cars sales will double in China and India and they will still increase by at least 30% between 2015 and 2021according to JD.Power forecasts (Figure1-1).
By its relatively low production cost, by the availability of fuels in most of the regions over the world, by a quite wide autonomy capacity, the internal combustion engine has been and will remain a key actor of road and sea transportation.

1.1.2. Energy context.

This forthcoming development will obviously generate an increase of the energy consumption, particularly in currently developing countries, as presented by Figure 1-2, with a rough rate of 30% between 2008 and 2035; due to high production prices and despite local efforts or incentives to promote their use in Europe, in North America or in Japan, alternative solutions, like biofuels, will remain quite marginal within the 25 upcoming years. Conventional fuels will thereby provide the dominant (90%) energy source even in the case of a high increase of the barrel price as illustrated in Figure 1-3.

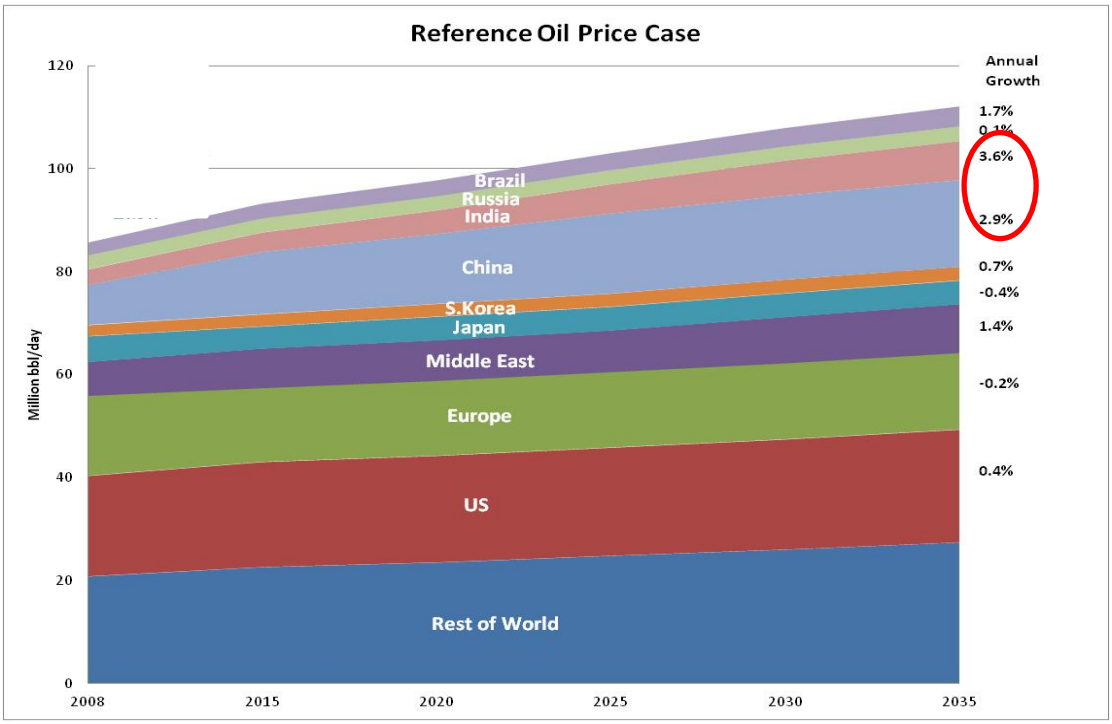

Figure 1-2: geographic distribution of the liquid fuels used for transportation [1-2]

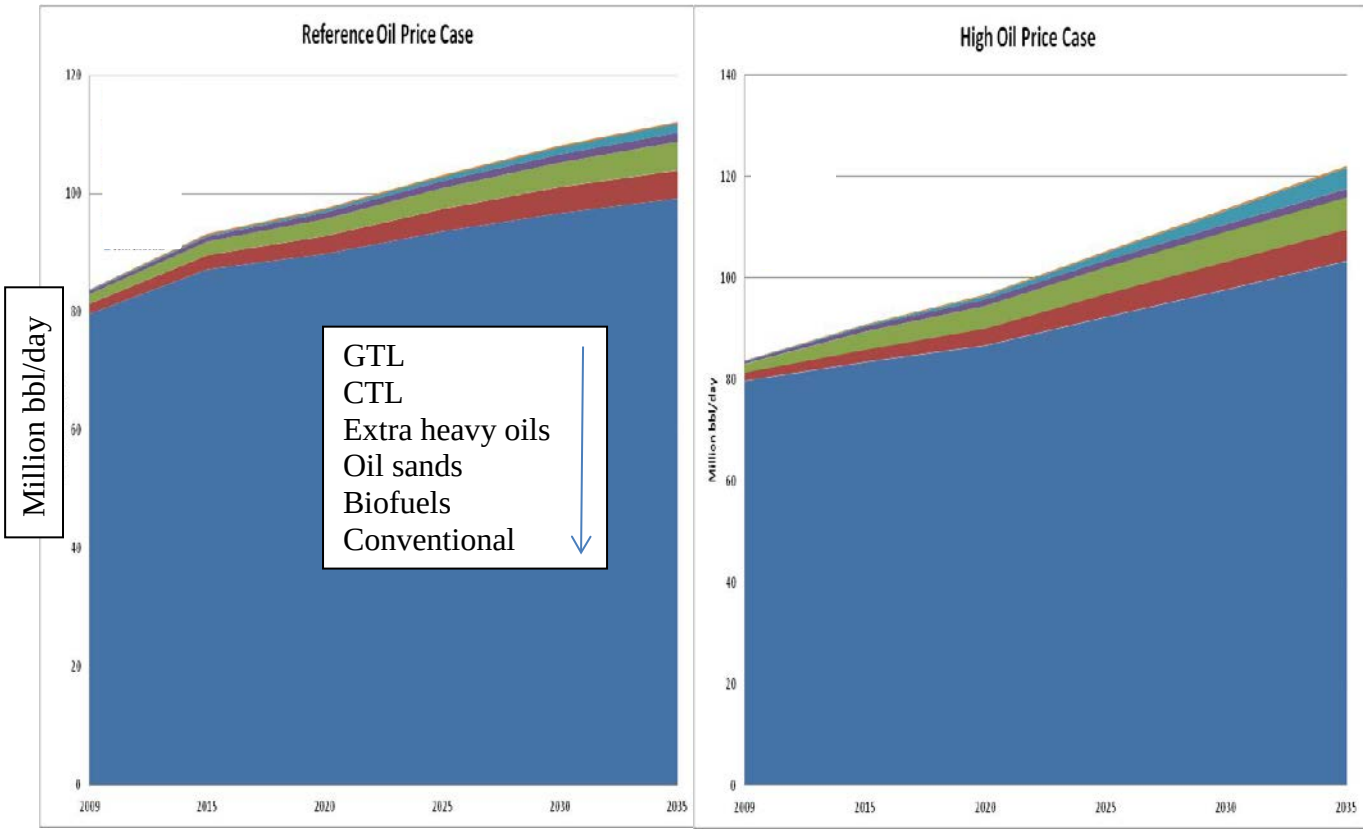

Figure 1-3: global total fuels projection [1-2]

Nevertheless, if the energy crunch, often evocated in the past, hopefully seems to be more and more improbable in the following years as proven resources with heavy bitumen or shell oils are far larger than the current production, “the stone age didn’t end because of lack of stones”; the international political context, and thereby the security of supply or the price of crude oil, are threatens which have to be considered for the future.
But the most important aspect linked to the increase of the energy demand is probably not related to economic considerations but to the environmental situation.

1.1.3. Environment context.

1.1.3.1. The Green House effect.

Since the beginning of the industrial revolution, the emissions of greenhouse gases, and particularly CO_2, in the atmosphere, have dramatically increased by around 30% as illustrated by Figure 1-4.

Without any significant measure, this trend would not stop in the future. It is the reason why all the domains of the industry have to drastically reduce their basic emissions; concerning transportation, a target of 24% would have to be achieved in 2050 –see Figure 1-5- to reach the BLUEMap target of 14 Gt of CO_2 per year.

Since 1995, the automotive manufacturers already have begun to improve the efficiency of the vehicles as demonstrated by Figure 1-6, even if the customer requirements for performances, safety and comfort –respectively illustrated by the power level and the vehicle weight- increased. The effort must nevertheless be strengthened in the future to compensate the dramatic increase of the number of vehicles.

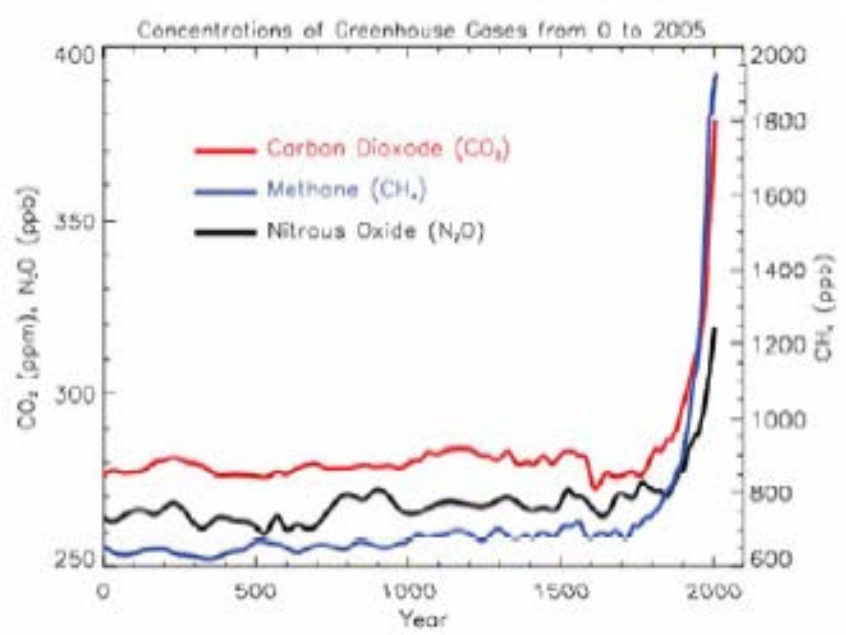

Figure 1-4: evolution of the greenhouse gases until 2005 [1-3]

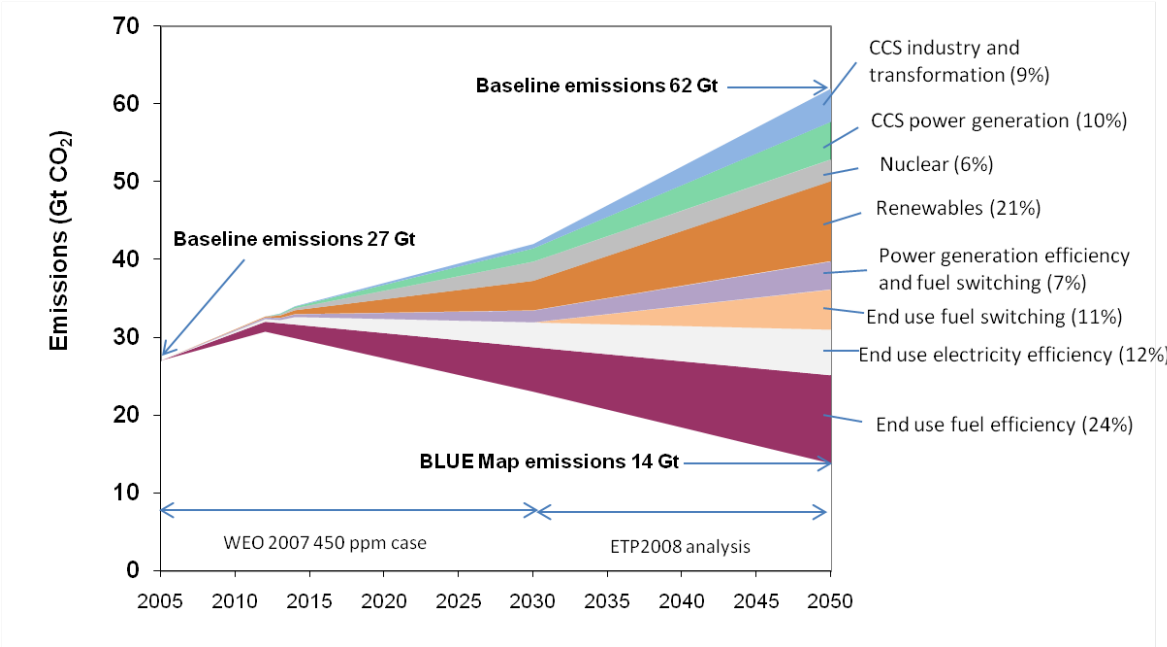

Figure 1-5: 2050 target for a reduction of the worldwide CO_2 emissions [1-2]

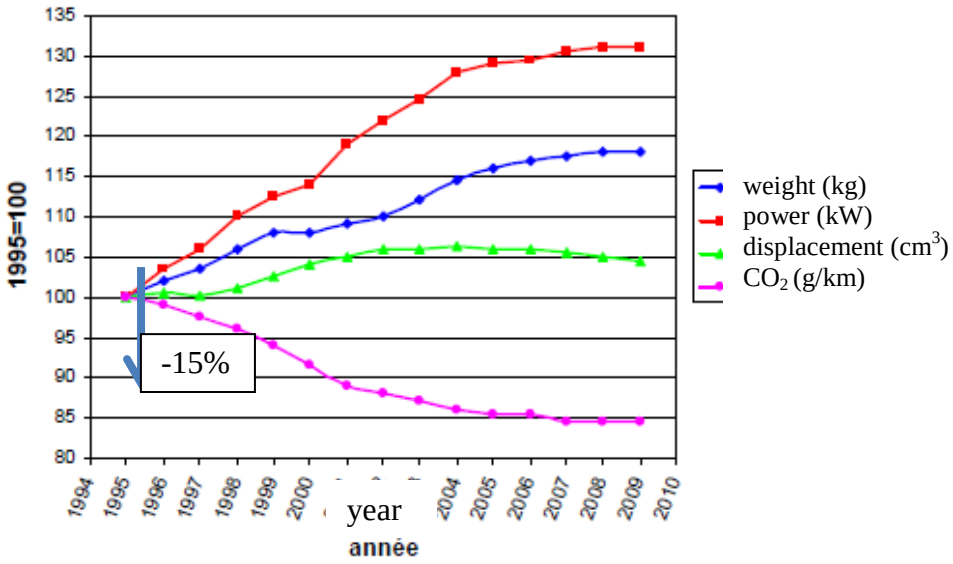

Figure 1-6: evolution of some passenger cars characteristics in Europe [1-4]

1.1.3.2. Local pollution.

Several spectacular events linked to the atmospheric pollution in large cities have illustrated the recent history, like the “big smog” in London in 1952 or the current pollution in Linfen (China).

Figure 1-7: London, 1952 and Linfen, 2012

The automotive traffic obviously has a significant part of responsibility concerning emissions of pollutants like nitrogen oxides (NOx) and particles but other actors, mainly urban heating and air conditioning or agriculture, also have their part of responsibilities as illustrated by Figure 8.

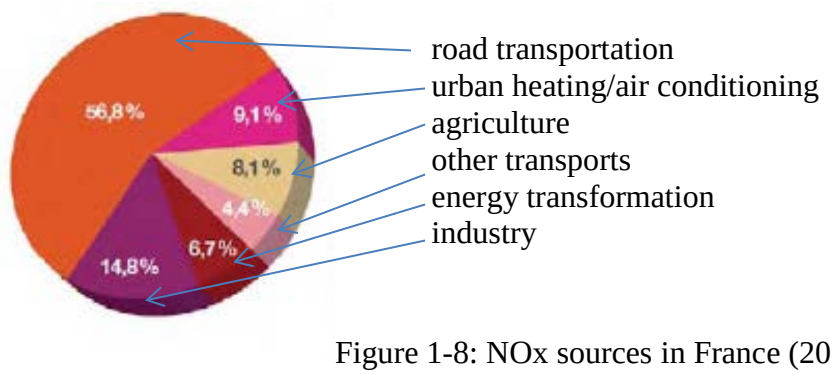

Figure 1-8: NOx sources in France (2011) [1-4]

The local pollution has undoubtedly an impact on the health situation of people living or working in urban areas; even if it is always difficult to make a clear difference between deaths caused by pollution or by more "natural" reasons, the necessary reduction of NOx and particles can't be discussed anymore and the automotive industry has significantly contributed to an improvement of the situation; for instance, NOx emissions due to the road transportation have decreased by 5% in France between 1990 and 2011and particles by 5.5% during the same period, despite the traffic increase.

1.2. R&D context.

In the industry, and particularly in the automotive domain, the development of a new concept is not limited to a simple use of already existing methodologies and tools. Changes in project requirements, such as a new regulation on pollutant emissions or a different power/efficiency trade-off, or the availability of new components, improved injectors, digital ignition systems, must often lead to investigate new possibilities in engine design and tuning. For instance, the introduction of the injection for gasoline powertrains opened the way to a charge stratification which was completely impossible with carburetors.

These new fields of investigation necessitate in parallel tools for understanding and thereby governing the physical phenomena linked to the new concepts; thereby, the economic necessity to speed up development times offered unexplored possibilities to numerical simulation.

Figure 1-7 is summarizing a V representation of what could be the cycle of development of such a project.

During the research phase, the actual potential of the idea has to be clearly evaluated in terms of cost to benefit for the final customer; this important job sometimes necessitates new tools to capture the inherent physical phenomena and to provide methodological guidelines for the forthcoming pre-development.
Ideally, these tools currently exist in the company or in academic laboratories –see Figure 1-8- because their necessity has been anticipated earlier, but in some cases they have to be developed, or adapted, during the project.
Because of a short timing, the optimization phase and the development of the final product could only be supported by easy to use tools whose methodologies have been well established.

These two necessities explain why a close cooperation between Research, this word covers both internal activities but also partnerships with universities and laboratories, and Industry is mandatory.

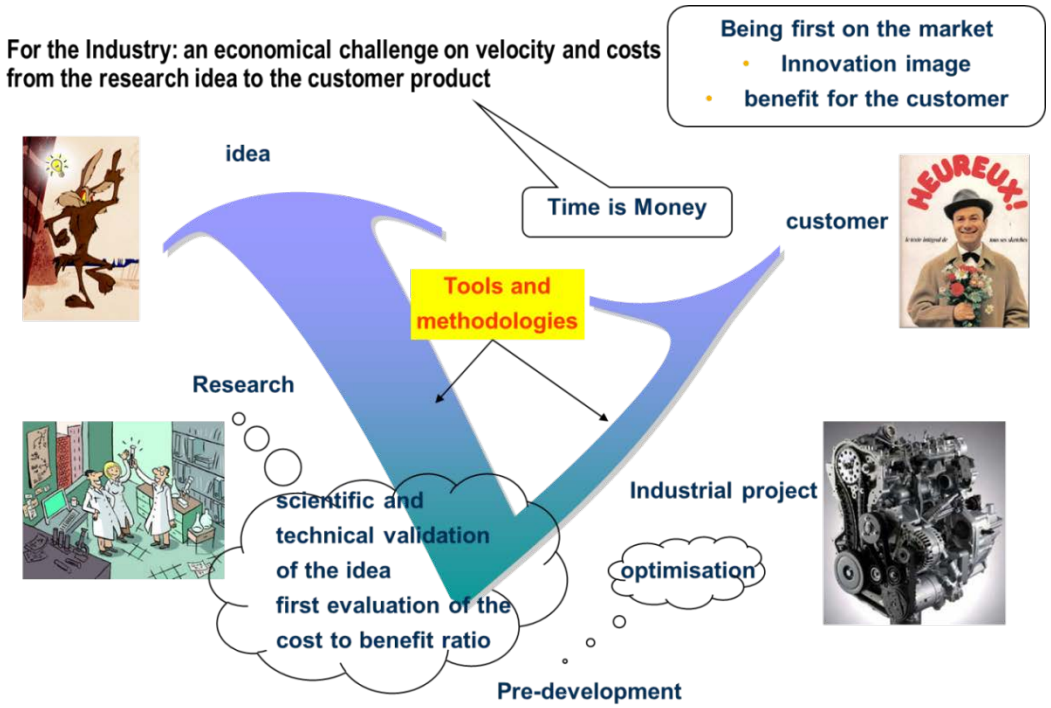

Figure 1-7: schematic overview of a project development scheme

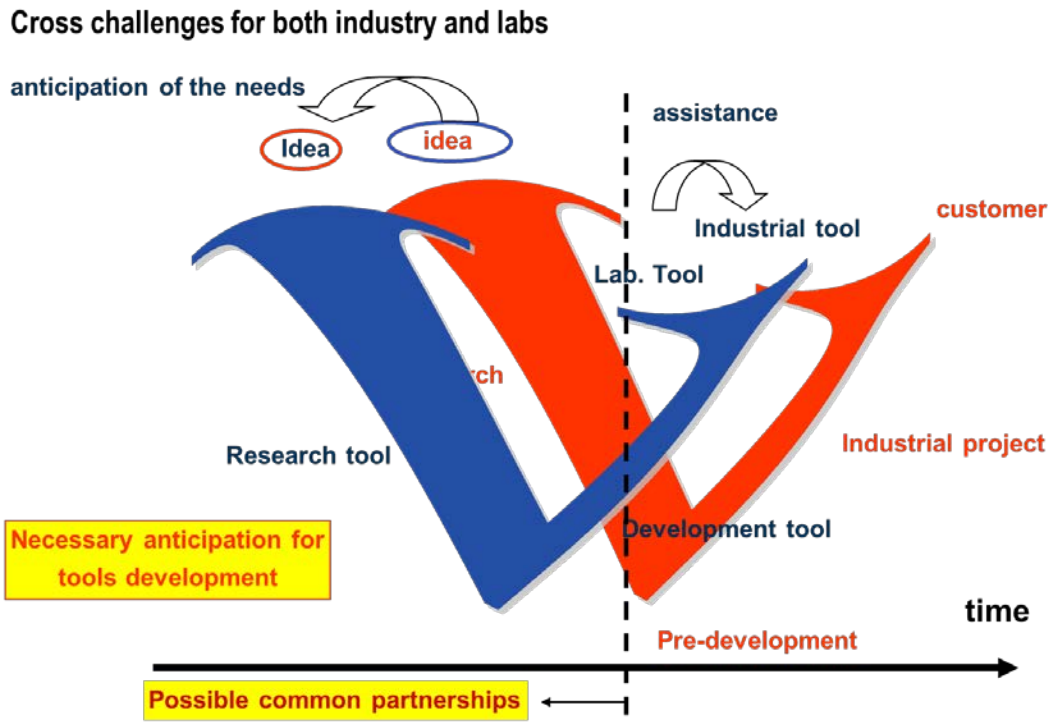

Figure 1-8: ideal timing for tools and project development

1.3. Motivation.

The combustion engine is the heart of a car or a truck; it is responsible of the pleasure and the satisfaction the customer will have but also of the environmental foot print the vehicle will generate in usage. This trade-off between performances, consumption and pollutant emissions nowadays constitutes a great challenge, not only in the industry but also in the Research centers.

Understanding and improving the way fuel is burning has always been a key driver for engineers; number of combustion chambers, more or less sophisticated, more or less efficient, have been developed and patented for both Spark Ignition (SI) and Diesel engines over the years; meanwhile, the most famous universities over the world have created dedicated departments to develop theoretical knowledge and experimental tools between the two World Wars.
But, quite recently, the rapid and dramatic improvements achieved by injector manufacturers led to understand that Mixture Formation was at the base of the combustion process. Governing the way fuel is distributed in the chamber and mixed with the air, so governing the equivalence ratio distribution, is already a success key to improve the trade-off between high performances, high efficiency and low pollutant emissions. It became then obvious that the term “combustion system” might now include the chamber, as usual, but also the injector and the aerodynamic pattern, ie the swirl, the tumble or the squish levels.

This work has therefore been dedicated to the development of three different combustion systems, or let’s say, three different mixture preparation systems, concerning SI and Diesel engines; for each one, a first, noticeable, part is concerning the spray description; a second one is emphasizing the way fuel and air are mixed and the last one is showing how the inherent combustion is responding to a particular trade-off between customer expectations and legal requirements.

Even if its physics is a quite complex topic –see Figure 1-9-, a good understanding of the fuel spray behavior and its interaction with the internal aerodynamics was necessary to secure the target achievement. The development of the liquid phase after the nozzle outlet and its atomization, the formation of the vapor and the surrounding gas engulfment, and finally the combustion by auto ignition or with an external spark had to be considered and understood.

As explained in the previous paragraph, the development of new tools has meanwhile been necessary to understand, but also to provide guidelines, for designing and optimizing the three concepts. It is the reason why a significant part of the work presented in the present document is dedicated to optical and numerical methodologies which have been used all along the projects, in parallel with the conventional single cylinder tests.

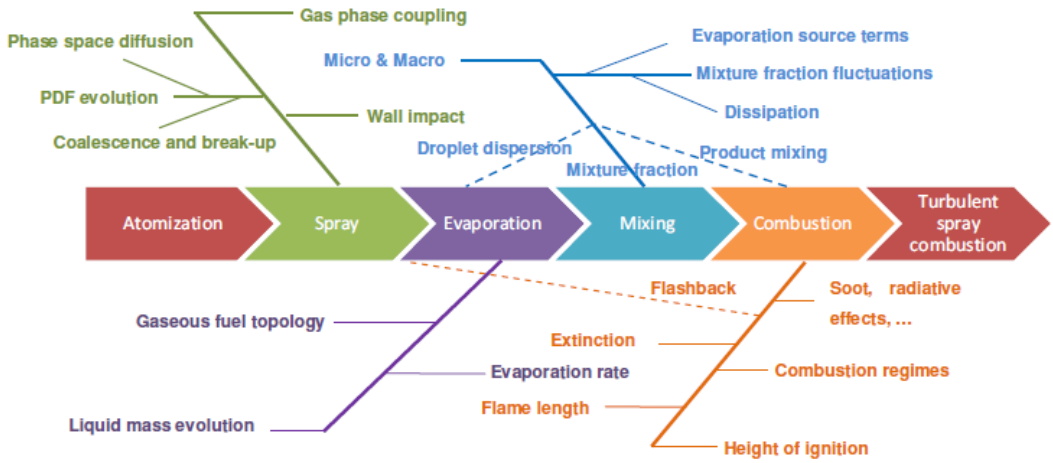

Figure 1-9: complex phenomenon in the combustion chamber [1-5]

1.4. General methodology.

As far as it is possible, the investigation of a new concept, and particularly a new combustion system, might always follow the same methodology.

At first, a theoretical analysis of the problem has to be achieved with the help of the currently available tools; the different physical behaviors, the relative influence of the involved parameters, have to be identified with simple models when they are existing; the recent advances in simulation allow to improve the corresponding output data.
A second phase consists in observing past and already existing realizations whose targets were similar to the object of the work.
The last one is to design and optimize the system with the help of all the possible tools, while eventually developing new ones if they really help to understand the different phenomena.

The development of the combustion systems described thereafter respected this methodology as far as it was possible within the frame of tools and time availability.

1.5. Outline of the thesis.

The document is split in 8 chapters, as follows:

The **"Introduction"** presented in **Chapter 1** describes the macroscopic challenges the combustion engine has to solve and its responsibility in terms of the world energy management and of the global protection of the environment.

Chapter 2, **"General context and historical background",** is more focused on the evolution of the customer demand and of the different regulations in terms of reduction of the pollutant emissions. A technical description of the main evolutions in terms of direct injection is provided for both SI and Diesel powertrains.

Chapter 3, **"The spray structure and its impact on combustion",** investigates the physics of the spray for high pressure gasoline and Diesel injections; essentially based on visualizations issued from the bibliography, it describes the main mechanisms leading to the fuel dispersion in the chamber and points out the essential parameters governing the physical phenomena.

In **Chapter 4**, **"Tools and methodologies",** the different experimental and numerical tools used during the work are described and the followed methodologies explained, especially in the fields of direct visualization or fluorescence. Several innovations in the use of a cylinder head originally designed with endoscope locations and optimized to characterize the spray behavior in actual thermodynamic conditions, in the vicinity of the spark plug, are presented. The 3D simulation has been used as far as possible, taking into account the limitations of the sub-models describing the spray.

Chapters 5 to **7** are concerning three different concepts, the two first being dedicated to SI engines – **"The MID3S spray guided stratified engine"** and **"The K5M air guided stratified engine",** as the third one to Diesel, **"The Lifted Flame Diffusion Controlled (LFDC) combustion"**. A state of the art review provides the basic guidelines concerning the global design of the combustion systems, as defined § 1.2. Two stratification modes, based on the use of completely different injectors and aerodynamic motions, have been optimized in order to improve the fuel efficiency. For Diesel, the necessity of working on the diffusion controlled phase of the combustion was clarified and the use of innovative injectors constituted the basis of a new concept for low emissions.

Chapter 8 proposes several **Conclusions** for the achieved work as well as some indications concerning future developments. Following the red line of the thesis, these ideas are not only concerning the "product" but also the development tools and methodologies which could be useful in the near future.

Bibliography.

[1-1] JD Power forecast 2012 release

[1-2] EIA International Energy Outlook 2011

[1-3] GIEC, Climate Change 2007, The Physical Science Basis
Cambridge University Press 2007

[1-4] E.Baron: Elements d'automobiles - Pollution
Techniques de l'ingénieur - 2013

[1-5] Khuong Ahn Dung: The Eulerian-Lagrangian Spray Atomization (ELSA) model of the Jet Atomization in CFD
PhD report – Valencia 2012

Chapter 2

General context and historical background

2.1. Introduction.

On an engine, a torque demand from the driver is directly or indirectly –via the quantity of flammable mixture- transduced in term of energy by an amount of fuel to be introduced in the cylinders; this first task, called "fuel metering", has to be fulfilled by the fuel system, whatever the chosen technology is.

The second task, whose importance appeared later on during the history, is concerning the mixture preparation –eg the way fuel and air are mixed before combustion. As long as fuel economy or pollutant emissions were not considered as a first order of importance, this requirement was marginally taken into account and only some work was achieved during the last tuning periods of the engine development, mainly to check the cold start ability.

The evolution of the fuel system is thereby very well correlated with the automotive history, and, on a more technical aspect, with the significant evolution of the air systems, from normally aspirated engines to highly efficient turbocharged ones. This trend can be summarized by three different periods: the first one, called "the race for power" in this document, went on until the last 80's; the second one, called "the race for fuel economy", roughly finished at the end of the 20th century, and finally "the race for low pollutant emissions" is still concerning all the manufacturers.

The association of these two elements explains why the carburetor survived more than one century for gasoline engines and the Diesel pre-chamber a bit more than 50 years, even if much better solutions already existed for a long time.

2.2. The race for power.

2.2.1. Context.

Between the end of the first World War and the crisis of 1929, the economy significantly grew, entraining the development of wealthy social classes in the USA, in Great Britain and in France. Passenger cars were mainly used by rich people traveling from one part of the continents to the other and wishing comfort, reliability, driving pleasure but also high performances and speed. The link between racing and tourism models was noticeably strong and technical solutions were first applied in competition and then on tourism cars by almost all the manufacturers.

After the dark worldwide depression, this tendency remained unchanged on the luxury market where prestige automobiles were synonym of technical knowledge and sometimes political leadership, like Mercedes, Horch or Auto-

Union, which fought on the tracks but also on the new highways. Only some very marginal models just began to prepare a more popular diffusion, like pre War projects as the Citroën 2CV or the VW Beetle.

During these years, obtaining a higher power output was the main target for engine designers and the easiest way to burn more gasoline was naturally to increase the displacement and/or to introduce more air, generally by the mean of a mechanically driven compressor.

2.2.2. The pre-war period.

For fuel metering on Spark Ignition powertrains, the carburetor was a satisfactory solution as it offered both a fine atomization of the gasoline, thanks to the venturi effect, and an "automatic" –but not perfect- regulation of the equivalence ratio versus the air flow; difficulties to cope with a wide air flow range or with long intake manifolds were eventually solved by adapting one carburetor per cylinder or per group of cylinders.

Nevertheless, the first gasoline direct injection engine due to the Swedish engineer Jonas Hesselman appeared in 1925 on buses and trucks (Figure 2-1); this innovative design followed a different and "local" target; with a "dual fuel" approach, it was dedicated to burn cheap heavy fuels, like kerosene or Diesel oils, in a low compression ratio engine with moderate combustion peak pressures and therefore quite a simple mechanical architecture; gasoline was mainly used to start and warm up the engine. This solution was used by VOLVO until 1947 and produced in the USA by Waukesha until 1951.

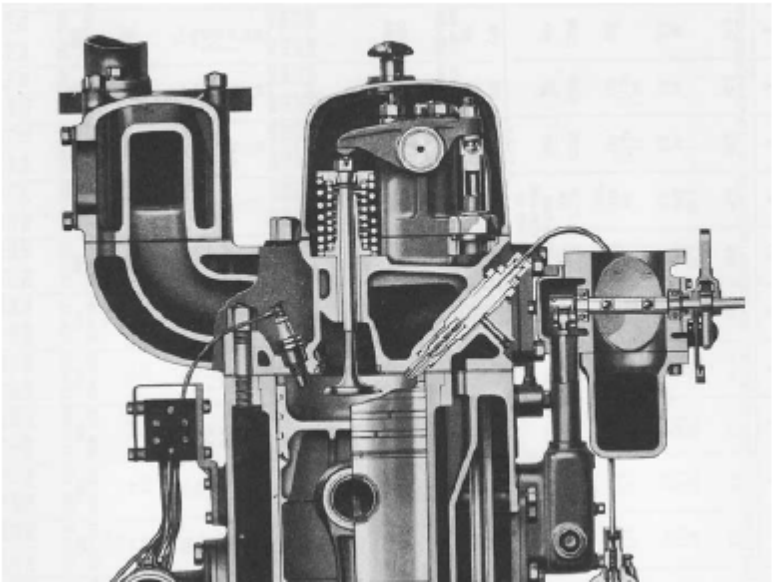

Figure 2-1: the Waukesha Hesselmann engine

The situation of the Diesel engine was quite different. Born in 1893, it was first dedicated to submarines and boats and, later on, to trucks, first with a pre-chamber combustion system located either in the cylinder head, either in the

piston; this technology was chosen because currently available single hole injectors were unable to correctly mix fuel and air in the wide volume of an open chamber, generating a poor efficiency and a very low torque.

The adaptation to passenger cars even represented a more difficult challenge due to the limited dimensions of the combustion chamber. The high weight of the engine and thereby its poor power density greatly limited performances; as the Citroën Rosalie, first presented in 1933, was not produced due to the financial difficulties of the French constructor, only 2000 Mercedes 260 D (Figure 2-2) came out of the factories between 1936 and 1940 despite a significant advantage of around 40% in fuel consumption compared to the equivalent gasoline model; the German cars were equipped with a L4 2.5 liter pre-chamber (Figure 2-3) engine developing 45 HP –eg a more than modest power density of roughly 13 kW/l.

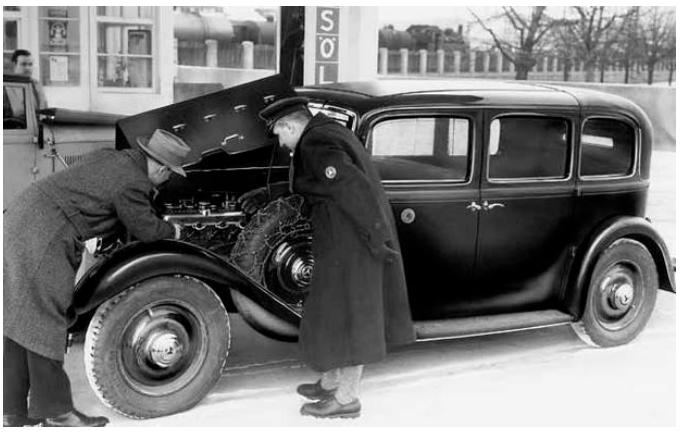

Figure 2-2: Mercedes 260 D

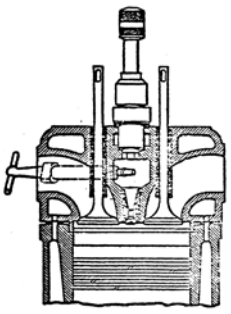

Figure 2-3: Mercedes pre-chamber

Mixture preparation in the Diesel open chamber was related to the use of the air quantity introduced in the cylinder; as the “fuel had to find air”, the evolution of the spray in the cylinder began to be investigated during this period. The target was to generate a maximum fuel penetration while avoiding wall wetting, which led to smoke –even if that problem was not too important- but also to a decrease of the efficiency and to a dilution in the lubricating oil, which had a severe impact on the engine reliability. Bird [2-1] and Gelalles [2-

2], respectively in 1930 and 1931, were probably among the first to publish papers related to nozzles and sprays for large engines, focusing their work on the efficiency of the holes and on the impact on the spray penetration.

2.2.3. The close pre-war and the war periods: the aeronautic experience.

But the most interesting advances, and especially the introduction of direct injection, where achieved for aircraft applications just before, with the development of long range civil flights over continents and oceans, and unfortunately as usual, during the War for combat air planes.

Due to both very high fire hazards during frequent crashes at take-off and landing and the necessity to increase the aircraft autonomy, civil companies like Air France or Condor asked for the development of "heavy oil" compression ignition engines. The most advanced power units were developed by the French engineer Clerget with the first two stage turbo charger Diesel presented in 1938 [2-3]; due do a direct injection in an open combustion chamber, the 14Fcs engine (14 cylinders, 34 liter displacement, 600 CV at take-off, charging system from Rateau – see Figure 2-4) achieved a specific power of 13 kW/l and a quite fine specific fuel consumption of 265 g/kWh. The two injectors per cylinder, necessary to distribute the oil in the chamber, were internally developed by Clerget.

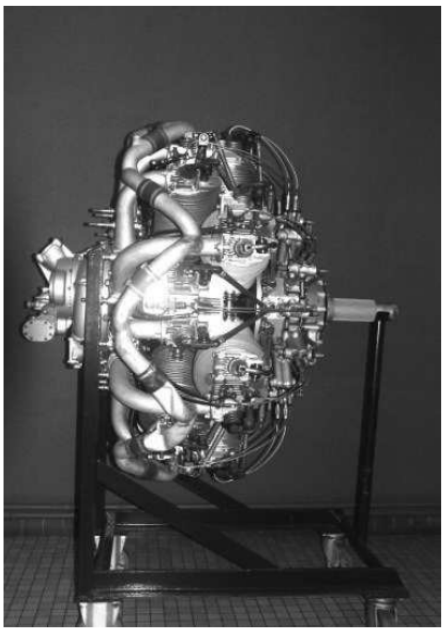

Figure 2-4: the Clerget F14 engine

On the SI side, the competition to develop lighter and more powerful engines dedicated to fighters was hard and in 1937 both Daimler Benz, with the DB 601A (Figure 2-5), and Jumo, with the 210 and 211, both V12 supercharged engines, first equipped the Luftwaffe with a direct injection gasoline system developed with Bosch and associated to an open combustion chamber. The four valves per cylinder, twin spark, Daimler engine in its first version offered

a power density of 25.5 kW/l at take-off in 1937. Later on, in 1944, the maximum performances reached 35 kW/l with over-boost and water injection, and a compression ratio increasing from 6.9 up to 8.5; these relatively low values were due to a great variability of the Octane Number presented by the synthetic fuels produced in Germany during this period. The 1940 version offered specific fuel consumptions between 340 g/kWh at take-off and 300 g/kWh at the best point corresponding to 75% of the maximum load [2-4] – only +13% compared to the Clerget engine as far as these data are really comparable.

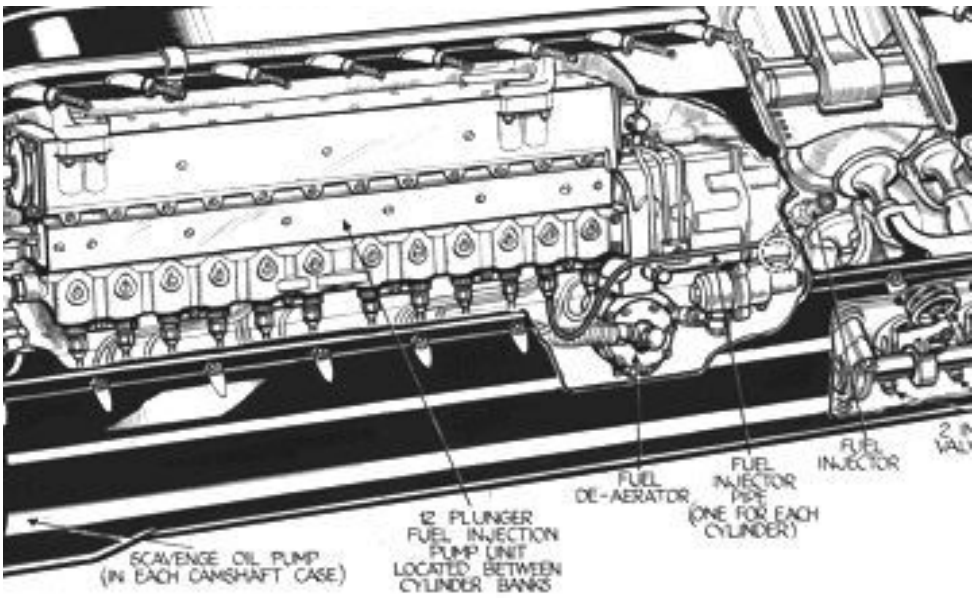

Figure 2-5: detail of the Daimler DB 601A engine

Gasoline was provided by a 12 plunger in line pump, mechanically distributed to the cylinders at a rail pressure of maximum 90 bars, and injected in the cylinders after the exhaust valve closure; a large valve overlap was therefore possible, offering a good air breathing in the cylinders without wasting fuel directly at the exhaust and therefore significantly improving the fuel consumption and the plane autonomy – see in Figure 2-6 a comparison with the original carbureted Daimler and the Rolls Royce Merlin engines.

A very interesting point concerned the evolution of the injector; as a conventional single hole pintle needle design was used at the beginning of the War, Bosch shifted to multi hole nozzles in 1944 and greatly improved the knock resistance of the engine, probably due to a much better mixture homogeneity in the open chamber.

The direct injection was later on adopted by Shvetsov in the USSR in 1943 on Lavochkin fighters and by Wright in the USA in 1944.

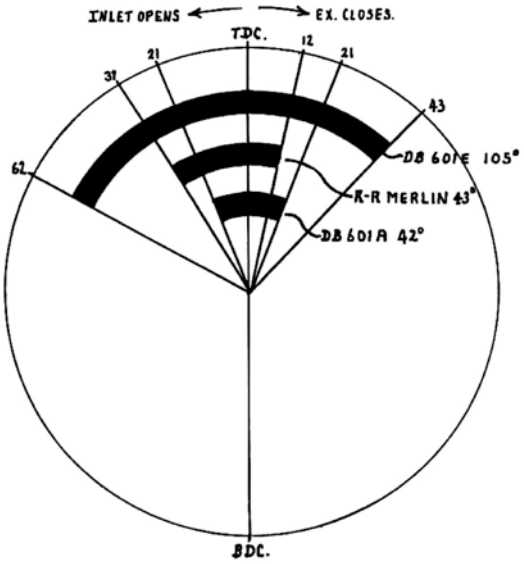

Figure 2-6: compared valve timing of different aircraft engines

2.2.4. The post-war period.

After the War, the need for relatively cheap and easy to manufacture cars led the German two stroke engine specialists Gutbrod and Goliath to develop the first small direct injection gasoline powertrains, respectively for the Superior and the GP700 which both appeared in 1951; at Gutbrod, the program was driven by Hans Scherenberg, a former engineer of the team who designed the DB 601 A for Daimler. To achieve a 30% decrease of the fuel consumption compared to the carburetor versions, he used the same capability provided by direct injection as on the fighter engine -eg an injection phasing during the compression stroke when the exhaust ports were closed.

In 1952, Scherenberg moved back to Daimler to lead the development of the 6 cylinders in line engine designed to power the fantastic Mercedes 300 SL "Gull Wing"; the direct injection was adapted in place of the initial carburetors, allowing a dramatic 30% power increase, one time again using the same principles as on the aircraft engines. Only 7 years after the end of the War, the race for power was back! But due to reliability problems, this technical solution was replaced by a low pressure port injection. Other sport and luxury cars very slowly shifted to this new technology because of the difficulties encountered with carburetors, first to monitor the air/fuel ratio in all conditions with larger and larger ranges of air mass flow between idle and full load as power increased, and second to improve the transients.

For the other largely commercialized cars, the main target was to keep manufacturing costs as low as possible but also to offer larger and more comfortable family limousines at an acceptable price. Technical solutions were quite conventional and the carburetor remained the main solution for fuel metering, with a large quantity of versions from single to quadruple barrels realizations.

Penalized by the same drawbacks as before the War, the Diesel engine was still marginally used and almost only the European specialists Mercedes and Peugeot dedicated a large part of their production for taxis or light duty vehicles. The pre-chamber technology was still in use even if Peugeot used the Comet design from Ricardo, but mixture formation and combustion were very close one from the other.
For trucks and industrial engines, a significant work was conducted, for instance by Pischinger [2-5] or Wakuri [2-6], to understand the parameters which govern the spray penetration.

2.3. The race for fuel economy.

2.3.1. Context.

In the autumn 1973, the price of the crude oil suddenly increased from 3 up to 10 $ per barrel, and then, hopefully relatively quickly, decreased. The alert was hard for the automotive manufacturers but there was no reason to drastically change the technical strategy used since the end of the War; only some high performance cars like the Citroën SM or some gas guzzlers like the rotary engine applications were badly affected. In the USA, the large displacement V8 powertrains were still successful.

The second oil crisis happened six years later and was noticeably longer. Its effects on the world economy also were much more severe and the fuel consumption really became a challenge for a long time. The necessity to significantly improve the engine efficiency appeared for all the automotive manufacturers, in Europe but also in the USA and in Japan.

2.3.2. The development of the Diesel for automotive applications.

The first trend was to take benefits of the good efficiency provided by the Diesel cycle while avoiding its major drawbacks. Despite its cost, the turbo charging technology was therefore introduced to significantly increase a power density which did not change very much since 1936, but the pre-chamber system remained quite unchanged! (Figure 2-7). Compressor and turbine size were optimized to fit with small engines and air coolers were quickly associated to improve the charging efficiency. Finally, after 2010, double stage turbochargers began to be used for high performance cars.

A second significant step for fuel consumption was made during the 90's with the development of the direct injection adapted from truck engines. Thanks to the availability of small multi holes nozzles, this technological solution allowed to dramatically reduce the heat losses in the cylinder, heat losses which were quite high with pre-chamber systems, and thereby to access to efficiencies closer to industrial powertrains. Mixture preparation became much more challenging, with a main difficulty at full load with an optimized use of the air present in the cylinder and a limited smoke level. At high load, the noise level significantly increased compared to the previous engines; despite

several improvements on the purely hydraulically driven systems –like the possibility to generate a pilot injection-, engineers had to wait until the late 90's to solve the problem thanks to the arrival of Common Rail systems with a rail pressure of 1200 bars and multi injection capabilities, paving the way to an infinite number of trade-off between NVH, emissions and performances.

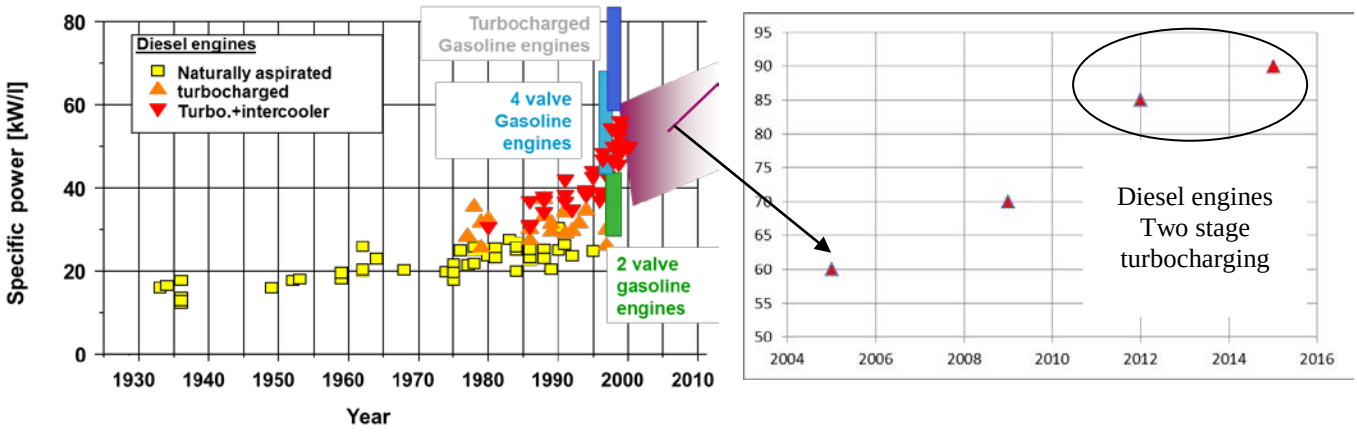

Figure 2-7: evolution of the Diesel specific power

The parallel development of injection and turbo-charging technologies explained the dramatic success of the Diesel for private customer applications as illustrated in Figure 2-8, with a market share of 50% in Europe, fairly constant from 2004 up to now. A noticeable new balance between small passenger cars, for which the CI engine became too expensive, and larger vehicles, taking benefit from the increased power and torque, appeared around 2010.

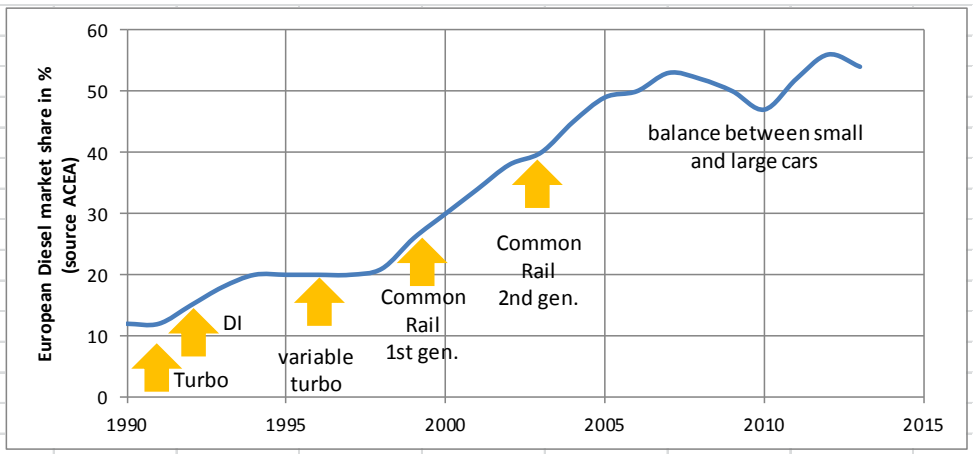

Figure 2-8: evolution of the Diesel market share in phase with technology improvements

Mainly based on the work achieved for gaseous jets, investigations concerning the development of the fuel spray increased; in particular, Reitz and Braco [2-7 & 2-8] in the USA developed new techniques to visualize the mixture in the chamber. In France, Haupais [2-9] tried to access to the evolution of the fuel concentration along the spray axis and in the radial direction, as Cummins

[2-10] tried to propose a model for the interaction of spray and air –see Figure 2-9. In 1985, Hiroyasu [2-11] summarized the different available models and correlations concerning spray angle, liquid penetration but also Sauter Mean Diameter, auto-ignition and flame propagation in the diffusion controlled mode.

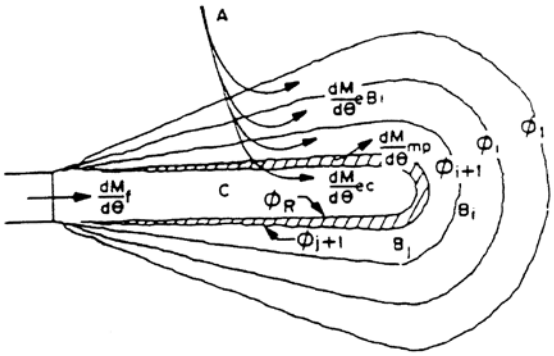

Figure 2-9: schematic representation of combustion zones and entrainment rates, Cummins model

2.3.3. The gasoline lean burn and stratified engines.

The second trend consisted in improving the efficiency of gasoline engines with two parallel solutions: the conventional homogeneous charge lean burn combustion and the stratified charge. For both of them, the idea was to increase the compression ratio and to reduce pumping and heat losses with a diluted mixture as on the Diesel. One time again, mixture preparation was not the main parameter to work on because of the difficulties encountered with such combustions.

Lean burn was intensively developed by almost all manufacturers and laboratories with high turbulence chambers to speed up the flame front despite the reduced equivalence ratio; some examples were given by the FIAT CHT (Controlled High Turbulence) with an additional air jet in the chamber generating swirl [2-12] –see Figure 2-10-, the Nebula chamber from Ricardo [2-13] or the May Fireball system [2-14] with high squish areas.

A lot of difficulties, including misfiring, high HC and CO emissions at low loads, bad transient behavior or reduced power densities due to the low efficiency of the intake port, slowed down their introduction on the market. Finally, the reduction of the NOx limit in the different state regulations forbid any possibility of improvement and this interesting solution disappeared despite significant advantages in fuel consumption, letting the place for a lambda 1 mixture and 3 way catalysts technology. The necessary accurate regulation of the equivalence ratio around the value of 1.0 strongly increased the complexity of the carburetors and led to their complete replacement by multi point injection systems (MPI). But fuel metering was still the key word for this evolution.

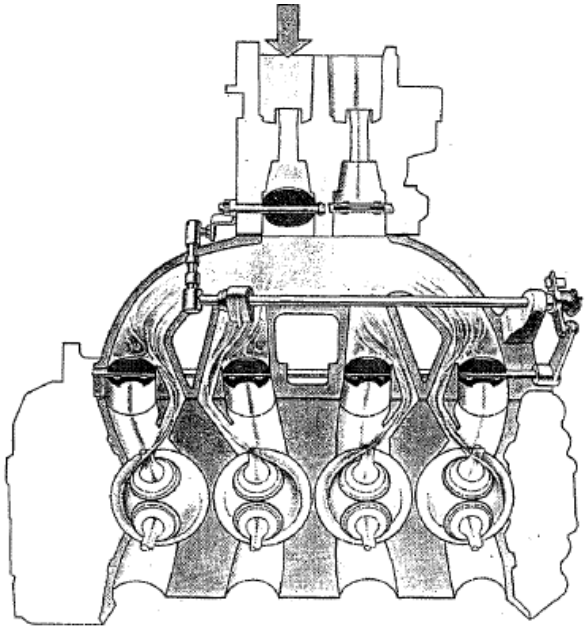

Figure 2-10: combustion system of the FIAT CHT 2.0 liter

In parallel, several tentative for Direct Injection were also investigated, for instance at Ford with the PROCO or at TEXACO with the TCCS (Texaco Controlled Combustion System) [2-15]; their basic design was greatly inspired from the Diesel technology –see Figure 2-11- and, for fuel consumption purposes, a charge stratification around the spark plug was awaited to secure a wide open throttle operation at part load without misfiring. Diesel hydraulically governed injection systems and single hole nozzles were adapted to the low gasoline lubricity.

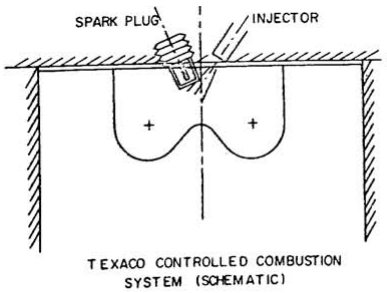

Figure 2-11: the Ford PROCO combustion system

Most of them had been previously developed for multi fuel applications, mainly for the US Army, but high costs and poor full load performances were not adapted to large diffusion civil vehicles. Some of the most interesting realizations will be detailed thereafter in Chapter 5.

Even if quite a few publications have been dedicated to mixture preparation in gasoline direct injection, for the first time, this item became mandatory for the development of a combustion chamber; global visualizations of the spray and of the combustion flame were observed with relatively simple techniques, focusing the work on the region near the spark plug.

2.4. The race for low emissions.

2.4.1. Regulations.

During the late eighties, the necessity to strongly reduce the local pollution, especially in large urban areas, led to a dramatic decrease of the limited emissions as hydrocarbons, carbon monoxide, nitrogen oxydes and particles.
For gasoline engines, the three way catalyst associated with a lambda 1 regulation of the equivalence ratio allowed to quite easily fulfill the legislation with MPI systems.

The situation was much more difficult on Diesel applications as illustrated in Figure 2-12 with the evolution of the European limits for Diesel passenger cars; some very similar schedules also exist for the USA and for Japan.

In 1990, the particles level had to be reduced by 70% and the HC+NOx by 40%. In 2010, the soot level represented less than 10% of the value accepted before 1990. This tremendous evolution was allowed by the development of the injection systems, whose rail pressure regularly increased from 1200 up to 2000 bars nowadays and probably around 2500 bars in the near future, in parallel with the reduction of the nozzle holes diameter. On the other side, smaller turbochargers associated to more efficient air coolers permitted to increase the mass air flow in the whole speed range of the engine.

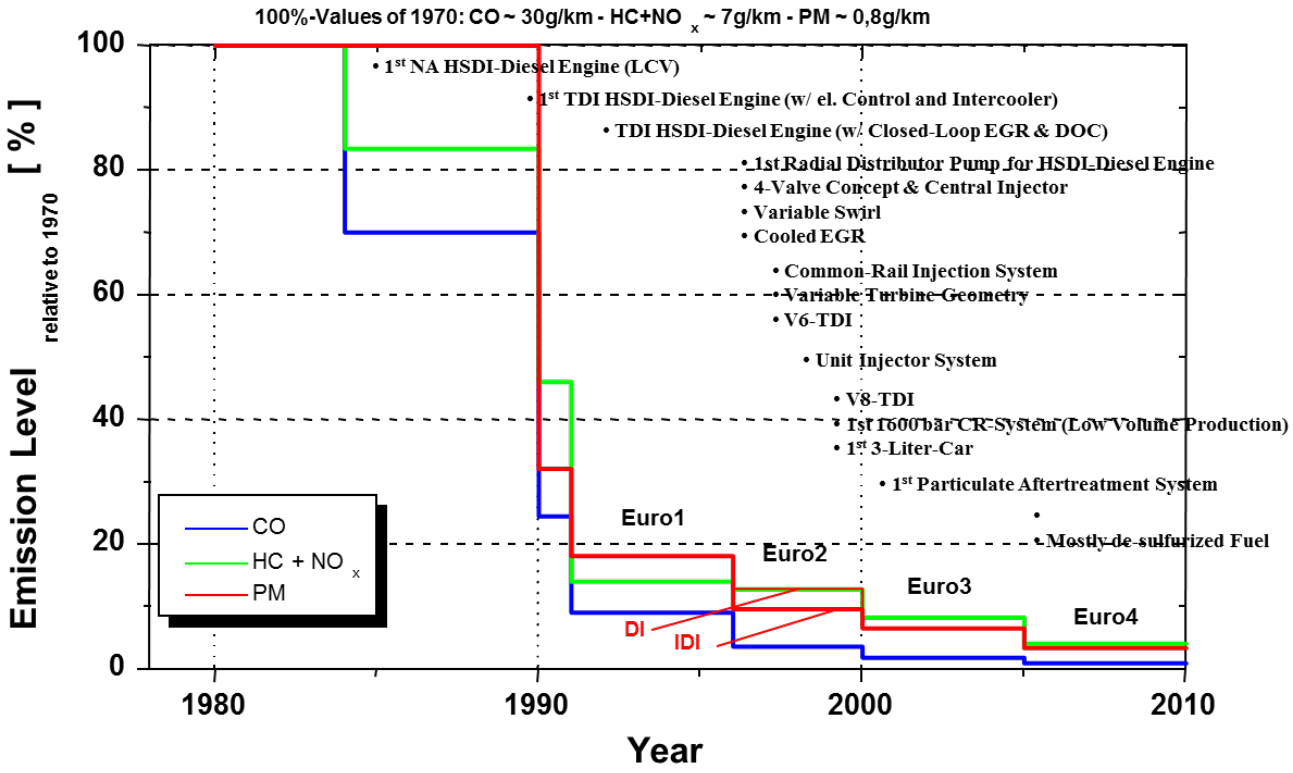

Figure 2-12: evolution of the European regulation for Diesel passenger cars and technical advances until 2010

After 2010, the shift from Euro4 to Euro5 mainly concerned soot and the particle filter became mandatory, but the evolution to Euro6 will be focused on NOx emissions as can be observed in Figure 2-13.

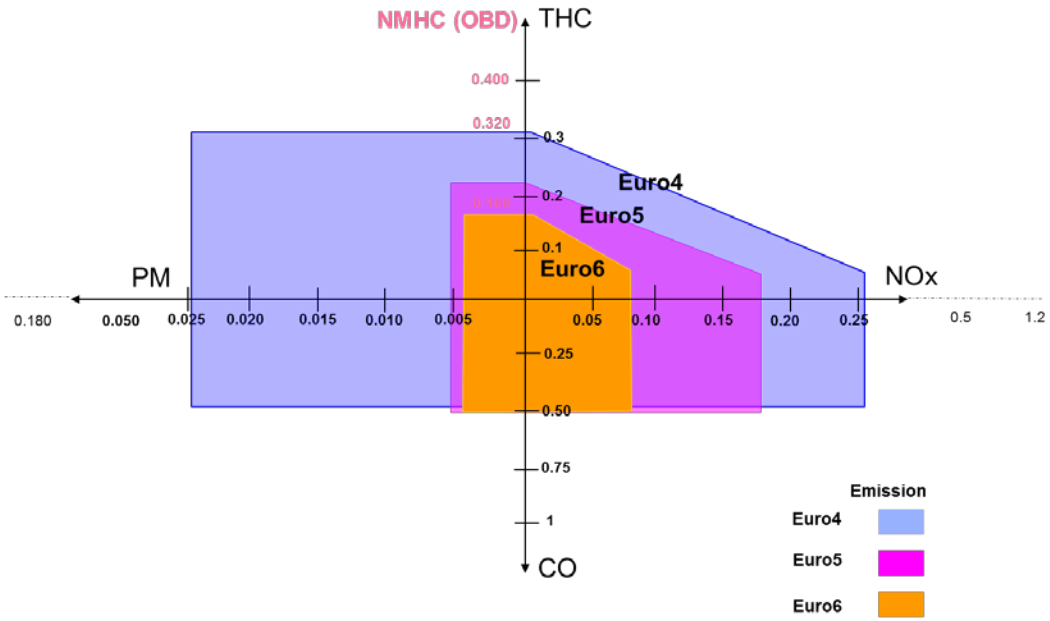

Figure 2-13: current (Euro5) and future (Euro6) European regulation for Diesel passenger cars

At the same time, the regulators wish to measure the emissions on cycles which would be closer to the actual use of the customers. Even if the final decisions have not been taken yet, some hypothesis –see Figure 2-14, WLTP- are currently used for the car developments. In particular, the engines will be submitted to higher loads at higher speeds compared to the currently used cycles (NEDC for Europe). This situation will enhance the difficulties to find a compromise between NOx and soot emissions.

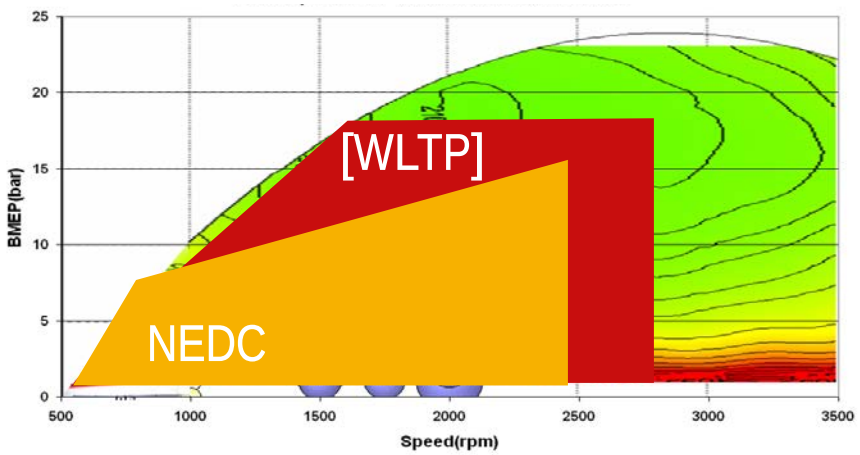

Figure 2-14: comparison of current NEDC and supposed new WLTP cycles on the BMEP/N range of a current Diesel passenger car

2.4.2. The challenge of the Diesel engine.

Figure 2-15 compares the evolution of the total cost of the same gasoline and Diesel engines between Euro3 and Euro5; for the Diesel version, this cost increased by 25% due to the after-treatment system; for the gasoline version it was only marginally affected. In the future, for Euro6 and after, the potential introduction of NOx traps or SCR (Selected Catalytic Reduction) would one time again extend the differences between the two combustion systems, threatening the customer acceptance for the Diesel and thereby the reduction of the CO2 footprint for vehicles.
One investigated solution is therefore to significantly reduce the NOx engine out emissions in order to avoid, or at least to minimize, the size and the cost of the after-treatment system.

Monitoring the engine out emissions clearly necessitates to govern the local air/fuel ratio and temperature –eg the mixture preparation and the fuel repartition in the chamber as illustrated by the well-known diagram of Kamimoto. This activity has therefore dramatically grown in the academic world but also in the industry, with the help of sophisticated 3D simulation codes or optical techniques.

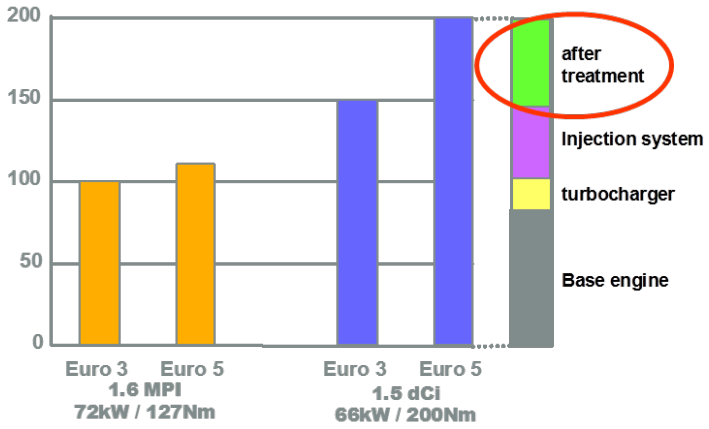

Figure 2-15: comparison of gasoline and Diesel engine costs (base 100 for Euro3 versions)

2.4.3. The CO_2 reduction.

A much more global aspect of the pollution is linked to the global warming of the earth, probably generating big storms or other severe weather disasters. This climatic evolution seems to be linked to the destruction of the ozone layer in the atmosphere, destruction caused by several gases like methane or carbon dioxide.
Even if the road transportation is far away from being the sole contributor to the emissions of CO_2, its importance can't be hidden and all the countries have set up new rules to stop their increase. Figure 2-16 presents the current situation in Europe but also a forecast in newly developed countries.

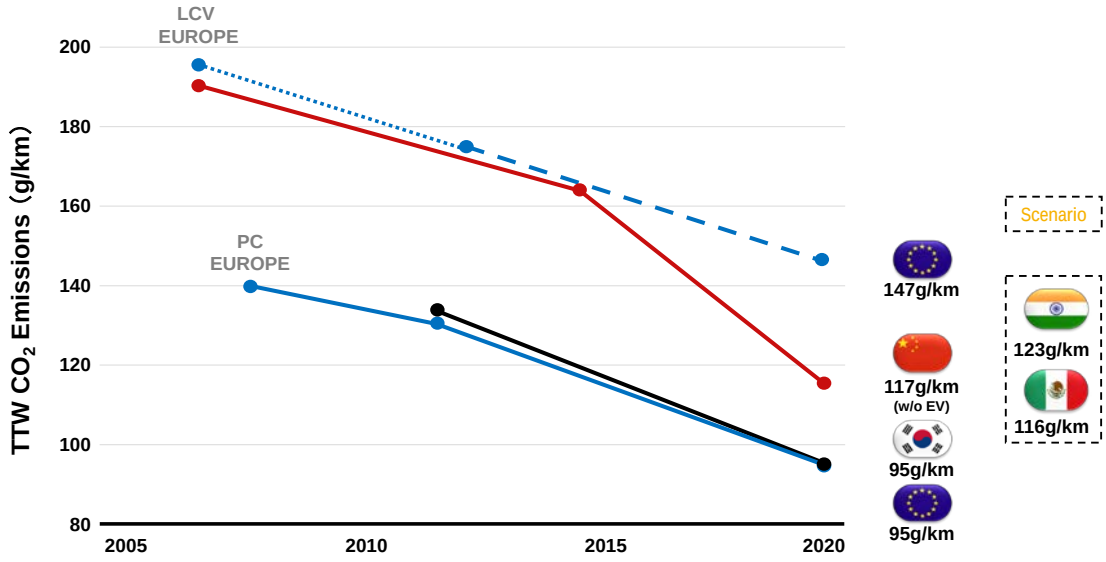

Figure 2-16: evolution target of the CO_2 emissions until 2020

To fulfill this ambitious commitment –more than a 40% decrease in CO_2 rejections between 2007 and 2020- , car manufacturers rely on different new technologies like electric and hybrid vehicles but the conventional powertrain has still a great future because of is cost, its reliability and its range.
For both spark ignited and Diesel engines, down-sizing and down-speeding are two solutions to reduce fuel consumption, and thereby CO_2 emissions.

The reduction of the total displacement directly impacts the pumping losses, especially in urban traffic for throttled engines, and possibly the friction level as a trade-off with a high effective pressure. If decreasing the number of cylinders from 8 to 6 or from 6 to 4 is not a problem, the use of 3 cylinders is more difficult due to vibrations. On the other hand, the reduction of the cylinder displacement leads to small combustion chambers with a high surface to volume ratio and thereby high heat losses, and a more difficult mixture preparation and combustion due to the wall effects.

The basic idea for down-speeding is to reduce the friction losses at constant power by lowering the engine speed. Associated to a high low end torque and longer gear ratios, some significant gains in fuel economy can as well be obtained.

2.5. Conclusion.

The importance and the interest concerning mixture preparation globally followed the increase of severity concerning the regulation of the pollutant emissions. As long as the aim of the combustion system optimization was concerning full load performances and fuel efficiency, the thermodynamics and therefore the combustion chamber design and the global aerodynamics definition, played the key role. The fuel system was chosen in order to provide the best possible fuel metering, securing a smooth engine operation from idle to maximum power, including transients, with the

capability to operate in all ambient temperatures. During this period, mixture preparation was only very macroscopically considered with the global position of the fuel in the chamber and therefore took a very little place in books relatively to engine technology or even in the universities; for Diesel engines, quantifying the liquid spray penetration was the main target for a long time.

When the center of gravity of the difficulties moved from power and efficiency to pollutant emissions, and from premixed (in SI engines or, roughly, in Diesel pre-chambers) to stratified combustion in both SI and Diesel, it became necessary to change the observation scale –eg to understand what really happened in the combustion chamber in terms of fuel and temperature repartition. This step clearly marked the introduction of mixture preparation as a key topic for engineers.

The following chapters will describe the work achieved on gasoline direct injection engines and roughly corresponding to the first period defined above, and, finally, to a Diesel application with a deep investigation of the mixture preparation corresponding to the second period.

Bibliography.

[2-1] A.L.Bird: Characteristics of nozzles and sprays for oil engines
Second World Power Conference- Berlin 1930

[2-2] A.G.Gelalles: Effect of orifice length diameter ratio on fuel sprays for compression ignition engines
NACA report 402 – 1931

[2-3] G.Hartmann: Clerget (1875 – 1943), un motoriste de génie
Editions de l'Officine, 2004

[2-4] Daimler Benz DB601A
Luftwaffe Handbuch – October 1940

[2-5] A&F Pischinger: Gemischbildung und Verbrennung in Dieselmotor
Springer Verlag Wien - 1957

[2-6] Wakuri: Studies of the penetration of fuel spray in a Diesel engine
JSME n°9 – 1960

[2-7] Reitz, Bracco: On the dependence of the spray angle and other spray parameters on nozzle design and operating conditions
SAE 790494

[2-8] Reitz, Bracco: Ultra high speed filming of atomizing jets
Physic fluids - 1979

[2-9] A.Haupais: Contribution à l'étude de la combustion dans un moteur Diesel
PhD report – Lyon 1981

[2-10] S.M.Shahed, W.Chiu, W.T.Lyn : A mathematical model of Diesel combustion
I.Mech – Cranfield – 1975

[2-11] H.Hiroyasu : Diesel Engine Combustion and its Modeling
Comodia - 1985

[2-12] F.Cavallino: Fuel Efficiency Evolution and Air Quality Improvement in Italy
SAE 962484

[2-13] C.D.de Boer, D.W.Grigg: Gasoline Engine Combustion – The Nebula Combustion Chamber
SAE 885148

[2-14] M.G.May : The high compression lean burn spark ignited 4-stroke engine
I Mech E 1979

[2-15] B.C.Jain, J.M.Rife, J.C.Keck: A Performance Model for the Texaco Controlled Combustion, Stratified Charge Engine
SAE 760116

Chapter 3

The spray structure and its impact on combustion

3.1. Introduction.

The importance of the spray/air interaction and its impact on combustion results via the local equivalence ratio, in terms of velocity and pollutant formation, has become a crucial topic as direct injection was adopted for Diesel and for gasoline engines. The results were not governed by the global "homogeneous" richness for conventional carbureted or port injected gasoline engines and by the ratio between air and oil with the pre-chamber Diesel but were the conclusion of complex physical phenomena involving the injector nozzle and the detailed aerodynamics in the chamber.

The aim of this chapter, essentially issued from the bibliography, is to briefly overview the main mechanisms involved in the mixture preparation and to point out the boundary parameters influencing the destruction of the liquid jet. The presented results are mainly based on visualizations obtained in the last decades due to a dramatic progress in optical techniques, results which have led to improve or to significantly modify the numerical models. A more detailed investigation has been achieved when necessary in the following chapters, focused on the actual boundary conditions occurring for the different combustion concepts.

3.2. Macroscopic interaction between the spray and the Diesel combustion.

For Diesel engines, and particularly during the diffusion controlled phase of the combustion, the spray structure and the spray behavior play a key role in the combustion development and thereby in efficiency and pollutant emissions. The physical phenomena find their origin in the nozzle hole of the injector and thereafter in different steps combining the plume development and the thermodynamic conditions in the chamber as illustrated by Figure 3-1.

The photograph on the left hand side of the Figures is relative to a 10 hole prototype nozzle operating at 2000 bars [3-1]; the dark part of the photograph is liquid, the white part is vapor and flame. The different steps during the spray development are illustrated in Figures 3-1a to d as follows:

- Figure 3-1a is showing an example of the velocity field within the hole and at its outlet, provided by a 3D simulation with Star CD for a prototype single hole nozzle. The cavitation generated by the curvature radius at the hole inlet is responsible of the vapor propagation and of the dissymmetry of the outlet flow [3-1].
- Figure 3-1b presents a representation of the air entrainment with a prototype single hole nozzle [3-2]. The intensity of the phenomenon is governing the air/fuel ratio in the spray and so combustion velocity and temperature.
- Figure 3-1c is highlighting the lift-off length –eg the distance from the nozzle where combustion is occurring at first [3-1].

- Figure 3-1d is an example of soot visualization at the spray tip [3-1].

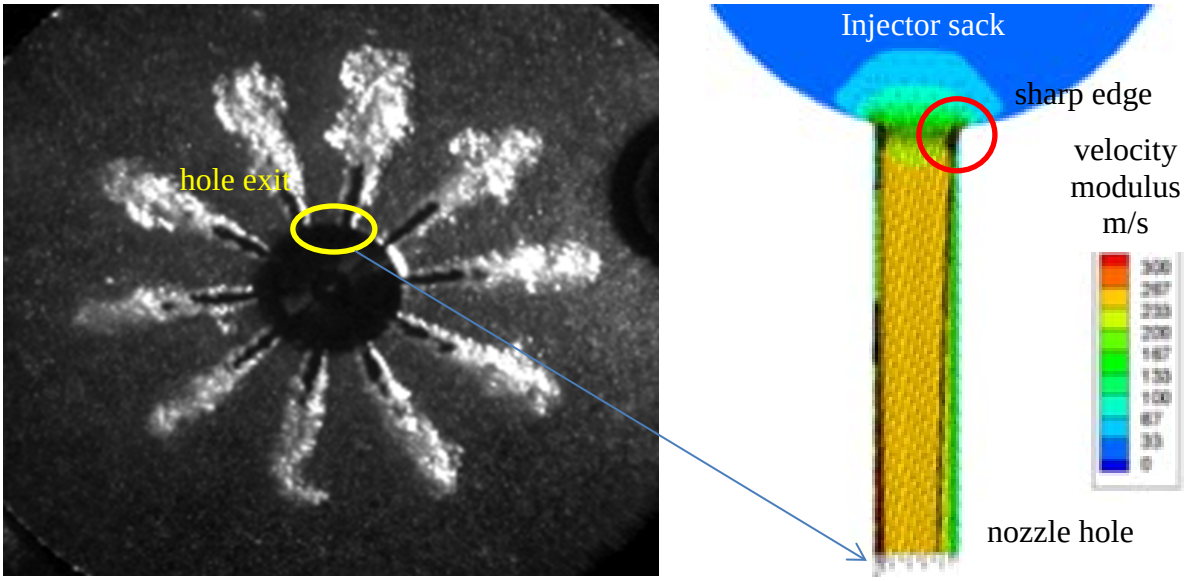

Figure 3-1a: velocity field characteristic at the hole outlet (3D simulation with Star CD), showing the inhomogeneous velocity profile at the hole exit

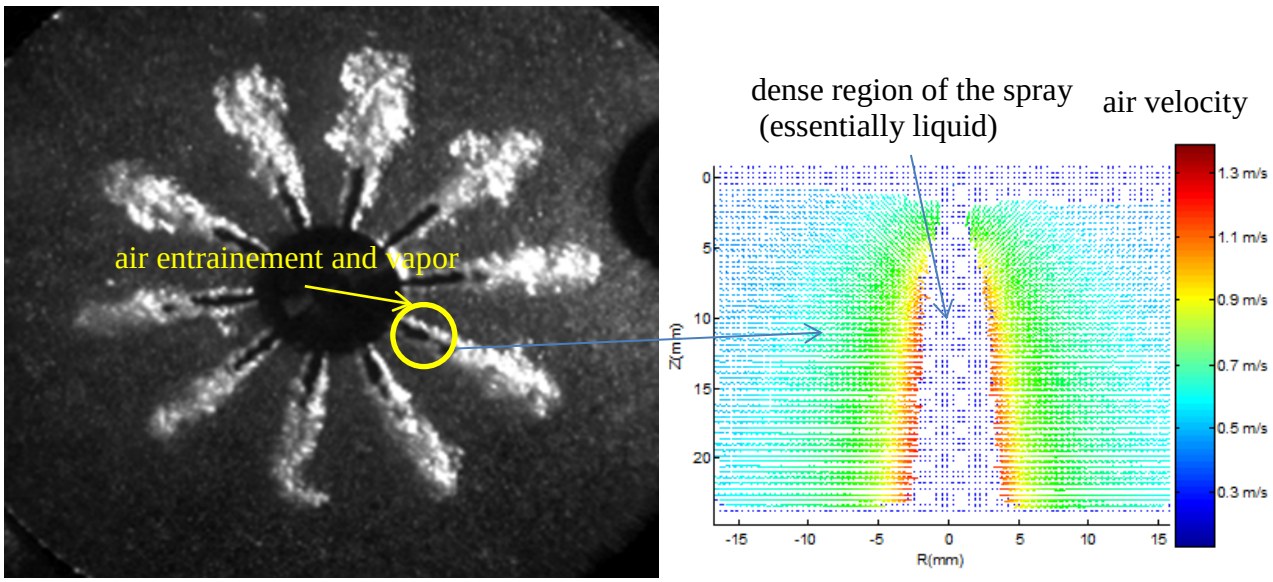

Figure 3-1b: air velocity field in the vicinity of a spray (Fluo-PIV) showing the air engulfment in the spray; z is the distance from the hole outlet, R is the distance from the spray axis

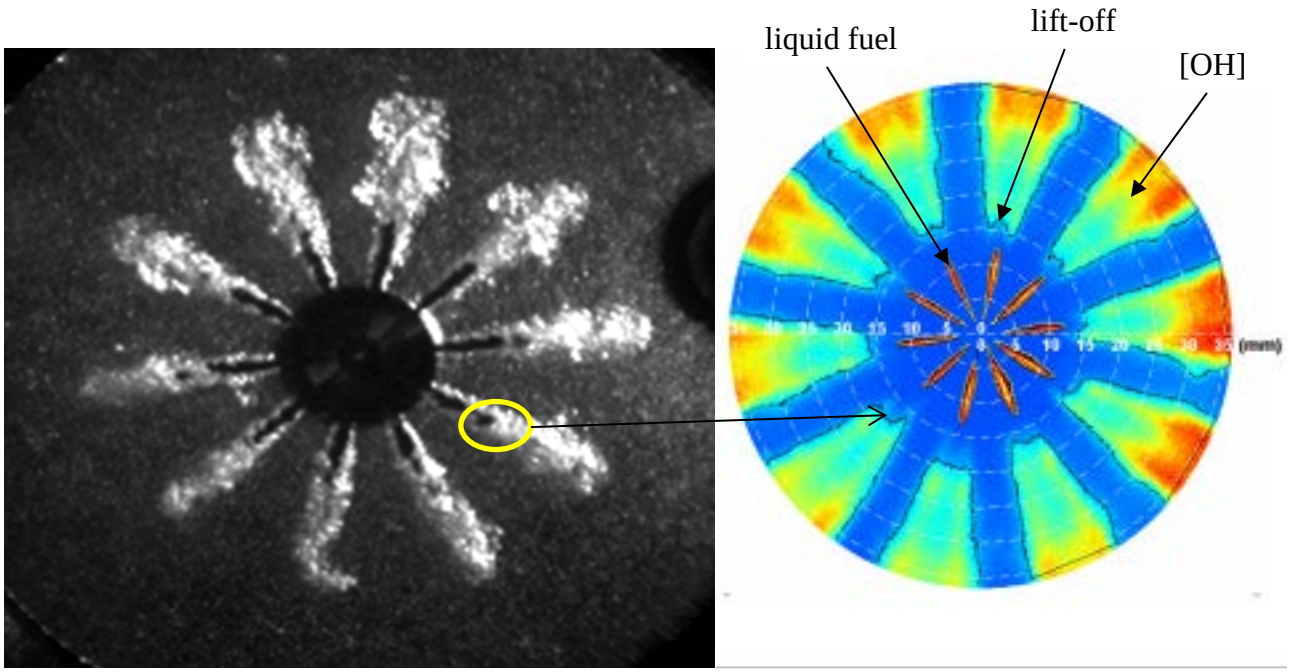

Figure 3-1c: lift-off length evaluation (LIF-OH); the different colors correspond to different OH concentrations (red the highest)

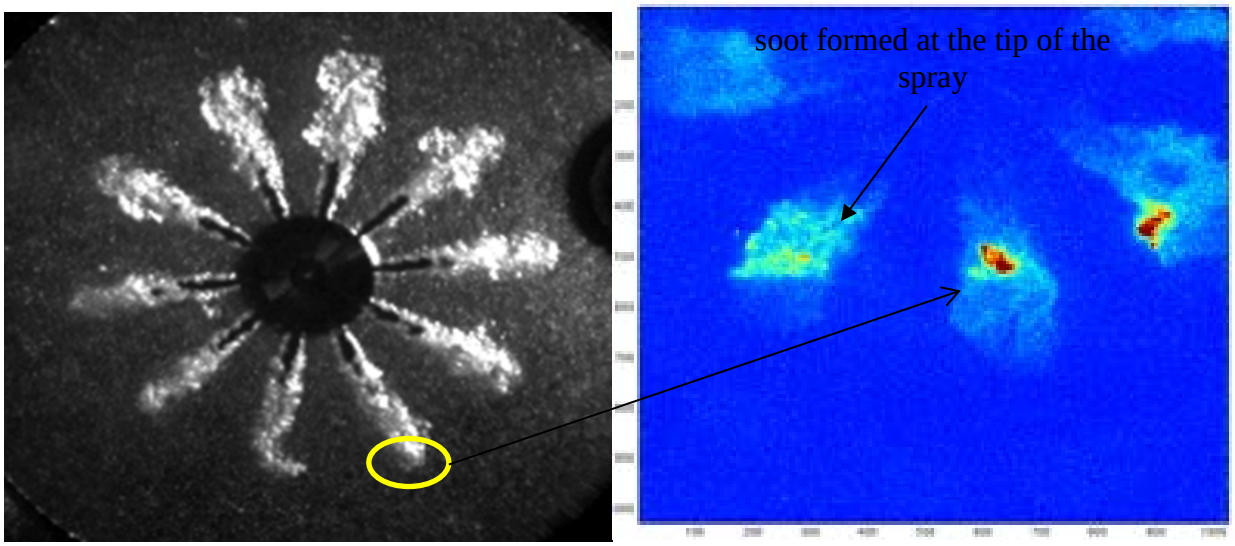

Figure 3-1d: soot visualization by LII; the different colors correspond to different LII intensities –eg roughly different soot concentrations.

3.3. **Detailed analysis for Diesel applications**.

3.3.1 Global structure of the spray.

The structure of the spray is a very complex item and, all along the years, a lot of hypothesis have been proposed to explain the evolution of the liquid core present at the hole outlet to the fuel vapor which will be mixed with the ambient gases.

At the same time the technologic progresses achieved by the injection suppliers drastically changed the boundary conditions of the flow; the pressure source increased from around the 600 bars usually used with single hole injectors dedicated to pre-chamber engines up to more than 2000 bars on the most up to date Common Rail systems. Physically, that means that the theoretic Bernouilli velocity significantly increased by a factor of nearly two and that the Weber number, which governs the single droplet atomization, by a factor higher than 3 close to the hole at constant orifice diameter. Meanwhile, this last dimension was divided by a factor of nearly 2 and, at a much smaller scale, the internal hole geometry was heavily optimized in order to increase the discharge coefficient; cylindrical shapes progressively disappeared to be replaced by conical designs, the hole inlet edges were rounded by the use of new finishing techniques like hydro-erosion ; there is also no doubt that the choice of this technique has a first order of importance concerning the hole roughness and the nature of the fluid and thermic boundary layers [3-3].

Figure 3-2 represents different models describing the spray atomization in the close vicinity of the nozzle [3-4].

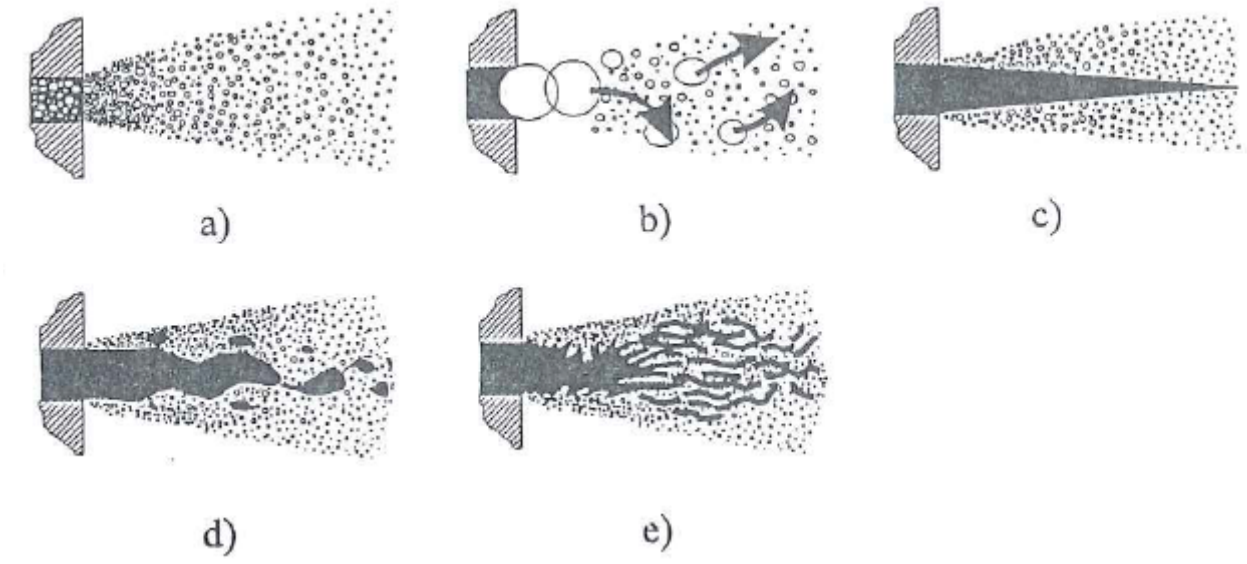

Figure 3-2: models of spray break-up in the atomization regime [3-4]

Models a and b are based on the hypothesis that the break-up occurs inside the hole; in Figure 3-2a, the fuel is already completely dispersed into droplets within the nozzle and the sizes of the droplets are smaller than the diameter of the nozzle –cf Huh and Gosman [3-5]. The model leading to Figure 3-2b is based on the assumption that individual droplets with diameters equal to the diameter of the nozzle hole are injected into the combustion chamber – cf Reitz and Diwakar [3-6].

Nevertheless, these theories can't be any more precisely applied to modern CR Diesel injectors as demonstrated for example by the X-Ray Radiography [3-7] shown Table 3-1 and Figure 3-3 where very high densities areas have been identified at the core of the spray. Models 3-2 c to e, which belong to the same family, are in good agreement with this visualization, with a compact column of

liquid leaving the hole without being perturbed until a certain distance from the nozzle [3-8], and being thereafter separated in many clusters. This column of liquid is clearly observed in Figure 3-3 but its dimensions heavily depend on both the experimental conditions and the nozzle definition.

Parameter	Case 1: [8] ◆	Case 2: [13] ■	Case 3: [13] ▲	Case 4: [7] ×	Case 5:[6] ●
Injection System	Caterpillar HEUI	Bosch Common Rail	Bosch Common Rail	Bosch Common Rail	Bosch Common Rail
Nozzle Type	Mini-Sac	Mini-Sac	Mini-Sac	VCO	Mini-Sac
Number of Orifices	6	1	1	3	3
Orifice Outlet Diameter [µm]	169	183	183	145	127*
Orifice Geometry	K 0	KS 0	KS 0	KS 1.5	KS 1.5
Included Angle [°]	126	0	0	160	120
Oil Rail Pressure [MPa]	17	---	---	---	---
Peak Injection Pressure [MPa]	112.2	100	100	80	130
Chamber Density [kg/m^3]	34.13	22.75	34.13	21.7	34.13
Chamber Pressure [MPa]	3	2	3	1.9	3

Table 3-1: characteristics of the injectors used for X-Ray investigation

At a higher distance from the nozzle, the spray plume always presents a radial expansion which reflects both the secondary atomization of the droplets and the mixing process with the surrounding air. Mechanisms d and e present some differences in the destruction of the liquid ligaments; as model d suggests a quite conventional secondary atomization, large droplets being atomized in smaller ones under the effect of the friction forces at the surface of the fuel, Figure e proposes the apparition of ligaments chaotically distributed across the spray and being submitted to pulsations like Kelvin Helmholtz instabilities.

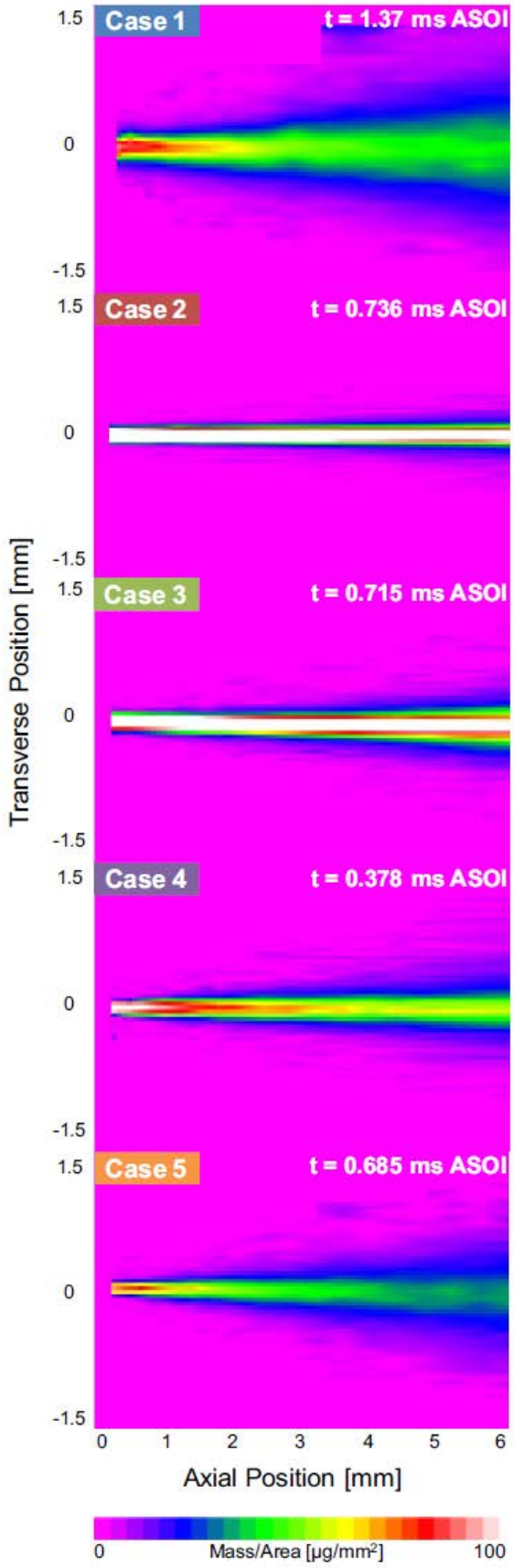

Figure 3-3: X-Ray radiography: projected mass density measured by X-Ray radiography at 50% of the injection duration; conditions are described in the table above.

3.3.2. Internal flow in the hole.

Numeric simulations and experimental techniques have recently confirmed that the fuel flow in the hole presents a significant physical complexity; besides its 3D structure, the flow is compressible in the range of pressures and temperatures really used on engines as illustrated by the results obtained at the Blaise Pascal University, see Figure 3-4 [3-9].

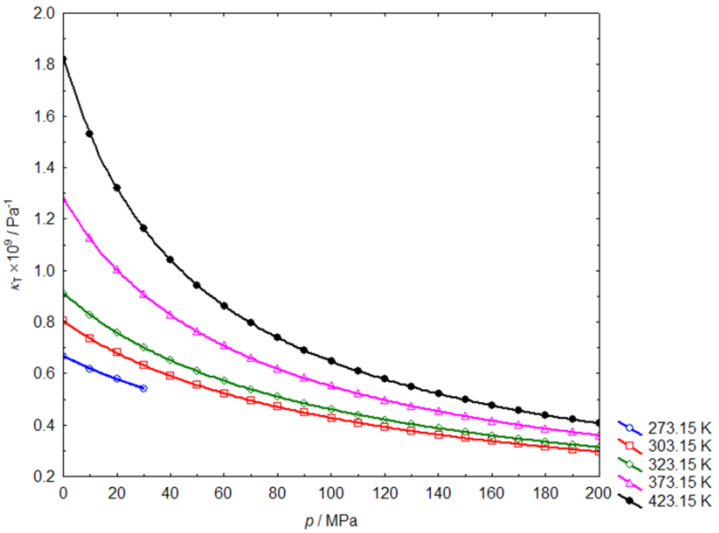

Figure 3-4: influence of pressure and temperature on the compressibility factor for a conventional B10 Diesel fuel [3-9]

The flow thereby presents 2 phases, one is liquid and the other is vapor due to cavitation, and it is unsteady, not only because of the needle lift motion but also at a smaller time scale because of the creation and the collapse of vapor bubbles –Figure 3-5.
In the late eighties, Arcoumanis [3-10] showed the importance of this cavitation, first on cylindrical enlarged transparent holes like for Figure 3-6, and thereafter on scale 1 models. On this figure, the effect of the cavitation number CN, roughly defined as the ratio between the injection pressure and the back pressure, is quite obvious; with the largest values of CN, the vapor is developed in the whole volume of the hole until the outlet. Even if the origin of the cavitation is not completely understood, the impact of the radius at the inlet of the hole, eventually near the sac according to the technology of the nozzle, the global shape of the nozzle –cylindrical or conical- and certainly the hole roughness play a key role [3-11].
This unsteady heterogeneous flow generates a dissymmetry in the velocity field just outside the nozzle as illustrated by Figure 3-5 with a VCO (Valve Covered Orifice) injector; in this case the hole is directly closed by the needle but the effect of the inlet radius is the same as with sac nozzles.

The other, and not negligible aspect, is related to the hole dimensions –eg a bit more than 100 µm for the diameter and a length of around 1 to 2 mm, which is hardly compatible with both conventional meshes and boundary layers laws.

The turbulence level occurring in the hole is thereafter dependent on the injection pressure, shifting from laminar at low Reynolds numbers to turbulent.

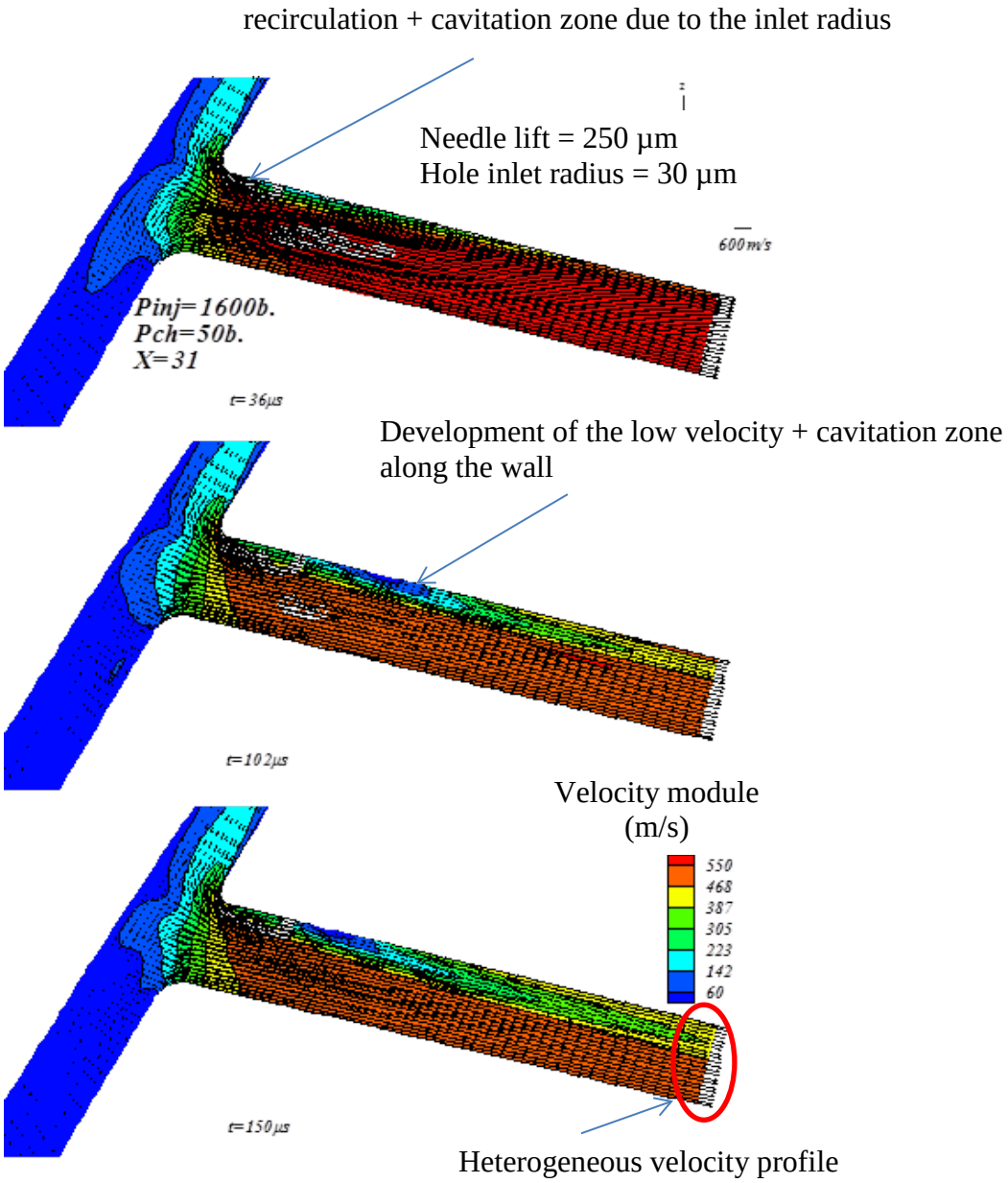

Figure 3-5: velocity field in the cylindrical hole of a VCO injector – simulation achieved with Eole at constant needle lift but at different timings

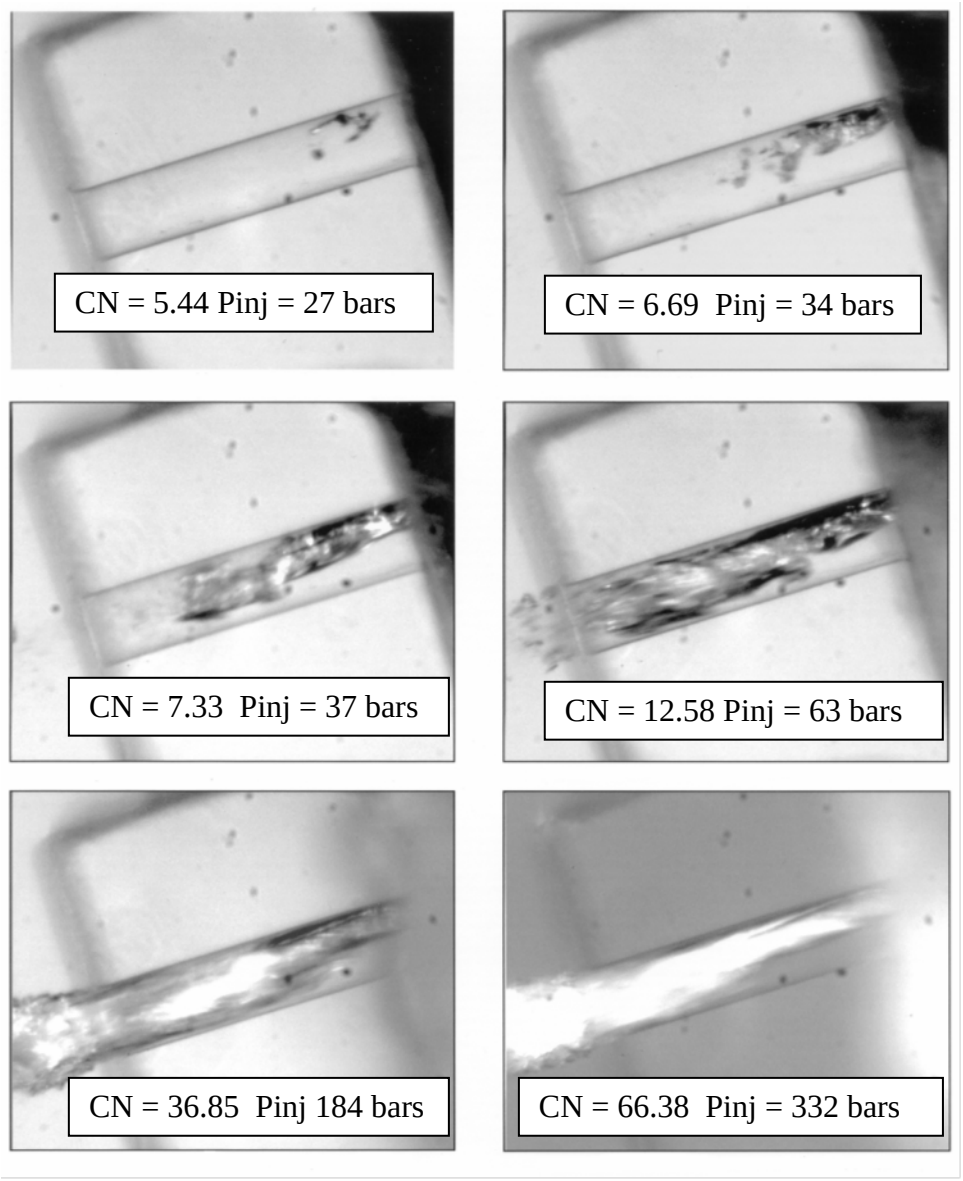

Figure 3-6: effect of the cavitation number CN through injection pressure Pinj (constant back pressure 5 bars) for a large scale transparent injector nozzle. Vapor appears in contrasted grey to white colors as liquid is transparent

3.3.3. Primary, secondary atomization and air entrainment.

The primary atomization, occurring within the very first millimeters after the hole outlet, is influenced by cavitation, as explained by Eifler [3-12] and later on confirmed by Desantes [3-13]; the implosion of the vapor bubbles in the hole is promoting a partial collapse of the liquid core and then enhancing the formation of liquid fragments or relatively big droplets. An important fact emphasized by Desantes is that this phenomenon can occur even for cavitation numbers where the hydraulic flow is not blocked.

At the same time, the liquid core is submitted to instability waves with a dedicated frequency as the X-Ray observation seems to highlight (Figure 3-7).

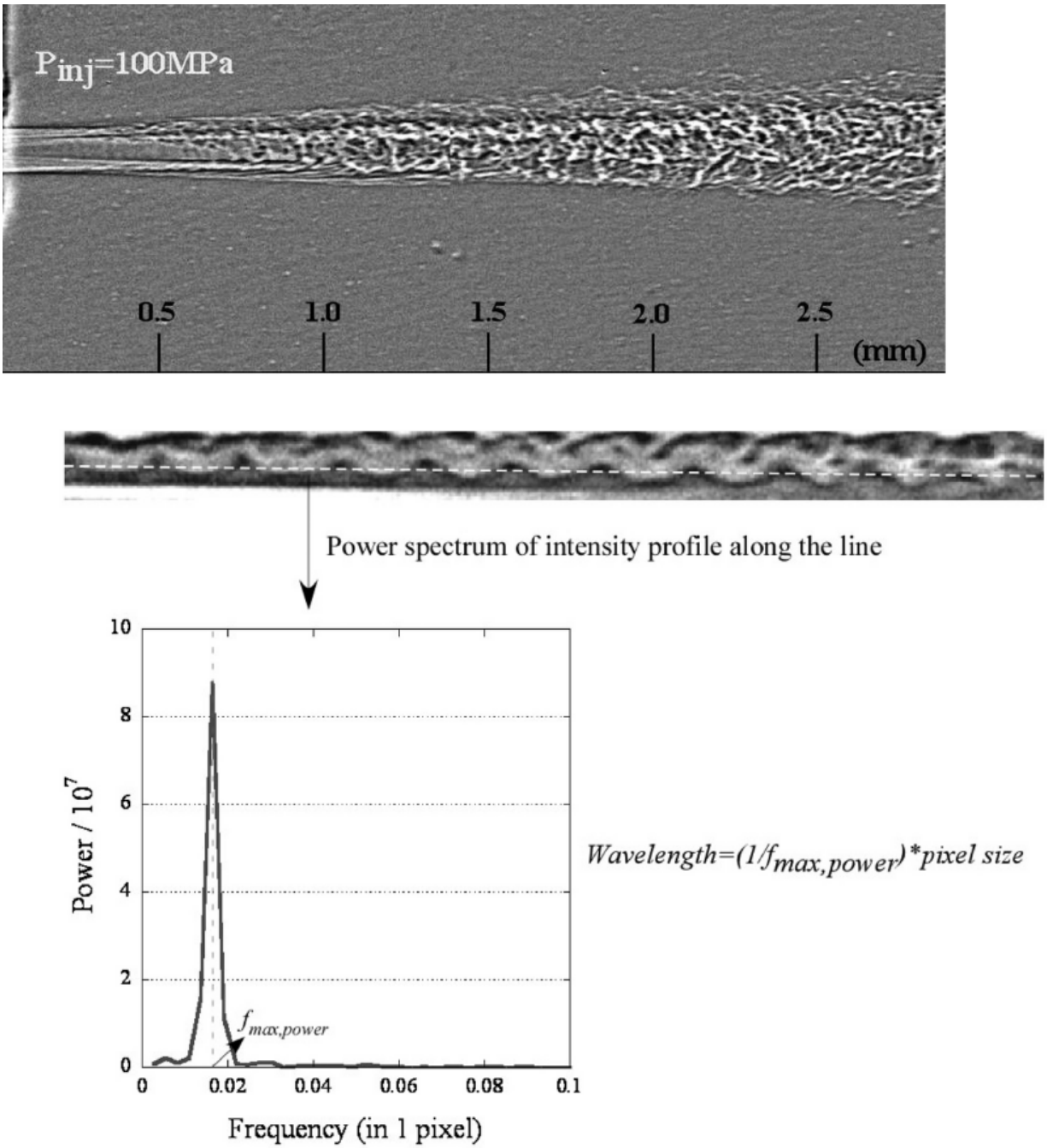

Figure 3-7: near-nozzle jet morphology of two-hole nozzle at 1000 bars 2.0 ms ASOI [3-7]

According to the author, these instabilities could be linked to the turbulence generated in the hole and both dependent upon the timing after SOI, the rail pressure and the hole geometry.
At the beginning of the needle lift, the flow is laminar and the waves only appear several millimeters from the exit; in steady state conditions, the flow becomes step by step more turbulent (the Reynolds number increases) until the waves reach back the orifice of the nozzle. The phenomenon is quite the same when the injection pressure is increased; the wavelength decreases and ligaments are step by step peeled from the jet core.

A very schematic representation of the primary atomization is provided by the 3D simulation results obtained with the Eole code developed by PRINCIPIA and illustrated in Figure 3-8.

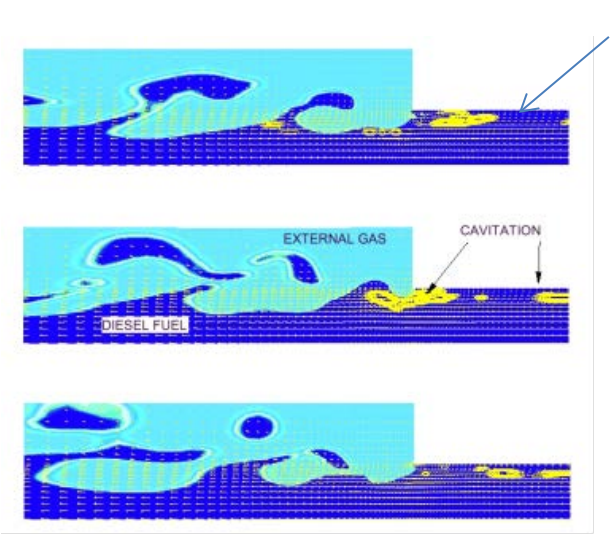

Figure 3-8: 3D simulation result obtained with the code Eole: schematic description of the primary atomization process

Nevertheless, current conical nozzles with large inlet radius present a very low level or no cavitation at all. In this case, the Kelvin Helmotz instabilities, and probably the turbulence induced by high rail pressures, seem to play a key role.

The secondary atomization, which occurs some millimeters after the nozzle exit, can't really been dissociated from the entrainment of the surrounding gases. As the already existing large droplets are broken in smaller ones due to the aerodynamic forces acting on their surface, the velocity gradient between the spray and the quite quiescent air in the chamber generates a high stress at the boundary of the spray, which itself promotes the apparition of vortices; these vortices promote an engulfment of the air in the spray and thereafter an exchange of momentum energy between the fuel and the gases. This phenomenon is responsible of both the rapid decrease of the spray velocity and of the increase of the vapor angle. For the forthcoming combustion, it will pilot the repartition of the air/fuel ratio.
An interesting point is concerning the fact that this air entrainment is increased by the momentum energy of the spray –eg the fuel exit velocity and the mass flow- as demonstrated by Ricou and Spalding [3-14] and more recently by Cossali [3-15].

3.3.4. Lift-off length.

During the steady state regime of the combustion, a turbulent lifted flame appears at a certain distance of the nozzle, separated by non- reactive gases. With other simple words, the lift-off length can be defined as the first occurrence of the combustion on the spray axis. Following the theory of Flynn, based on the combustion model from Dec [3-16], the volume between the

nozzle and the lift-off is the state of PAH formation (Poly-Aromatic Hydrocarbons) which are soot precursors.
In 2001, Higgins [3-17] emphasized the influence of the surrounding parameters like the injection pressure, the oxygen concentration or the ambient gas temperature and density on the position of this flame by measuring the OH concentration –see Figure 3-9.

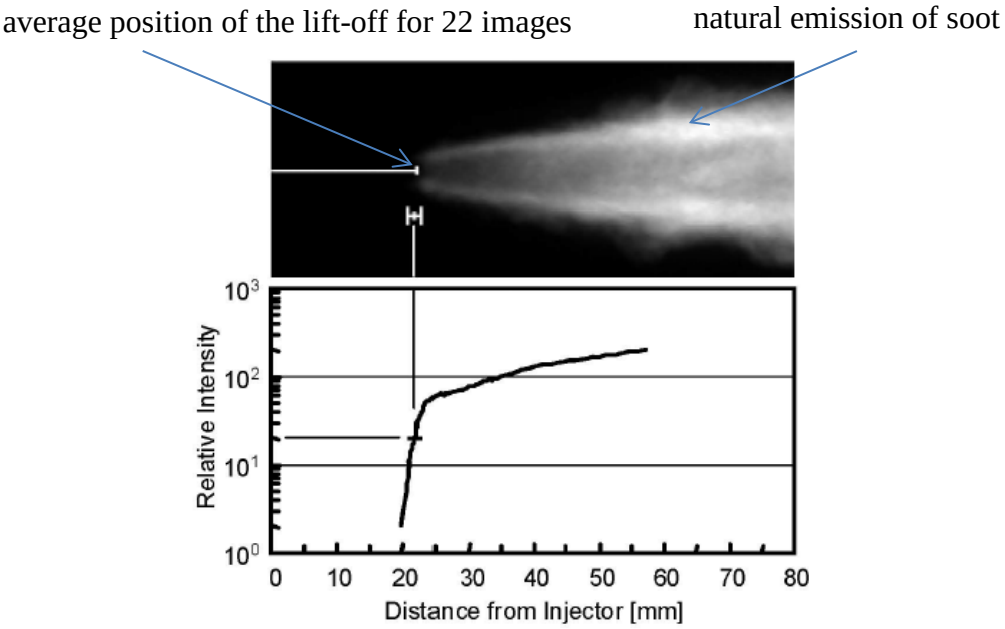

Figure 3-9: natural light emission at 310 nm from a burning Diesel spray (single hole injector, injection pressure 1380 bars, temperature 1000 K, ambient density 14.8 kg/m^3, 21% oxygen) [3-17]

The lift-off length has naturally a noticeable impact on the oxygen concentration at the beginning of the combustion –the longer it is the higher the amount of air entrained in the spray, reported to the amount of injected fuel, is. Thereby, the soot production, as demonstrated by Idicheria [3-18] or Siebers [3-19], see Figure 3-10, is lower with small orifices. In this last case a reduced diameter led to a quasi soot free combustion.

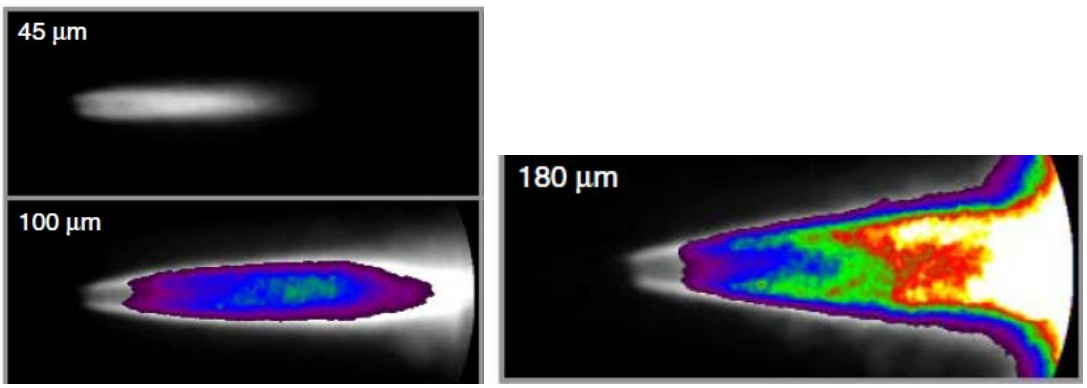

Figure 3-10: soot incandescence (false colors) and OH chemiluminiescence (white); injection in a constant volume vessel, rail pressure 1000 bars, air temperature 1000K, air density 14.8 kg/m^3 [3-19]

In the region situated downstream of the lift-off length and upstream of the first appearance of soot, particularly visible for the two largest diameters, rich reactions, promoting PAH, are occurring.

3.3.5. Pollutant formation.

The Sandia conceptual model, based on Dec combustion scheme [3-20], involved the different theories presented above. The soot is formed at the head of the spray and then partially oxidized at its periphery. The high temperature diffusion flame is surrounding the spray and is the source for thermal NOx –see Figure 3-11.

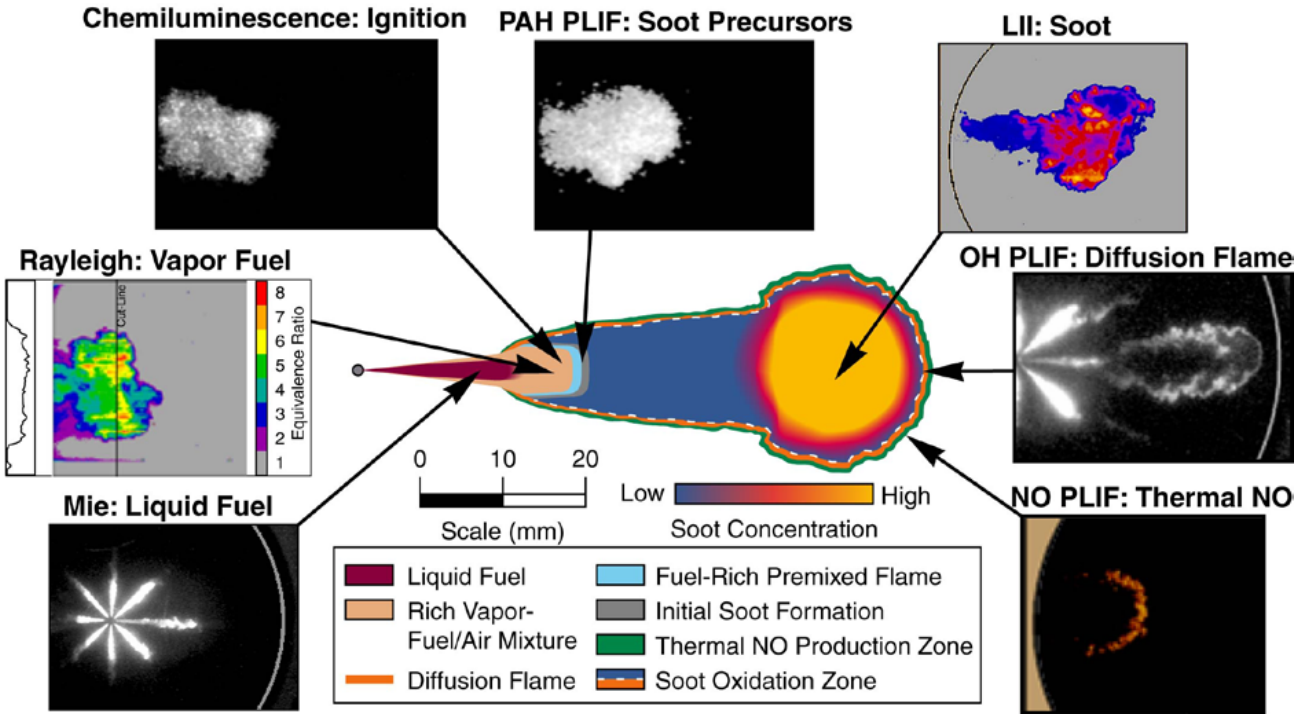

Figure 3-11: Sandia conceptual model of Diesel Combustion [3-20] and main optical techniques used for its characterization

During the expansion stroke, soot could be partially oxidized if a sufficient oxygen level and a sufficiently high temperature exist in the chamber. For this part of the combustion, the shape of the piston bowl has a first order of importance as the soot formed deep in the bowl has to be extracted early after the end of the combustion in the direction of the chamber center where fresh air is still present –see Figure 3-12.

The NOx emissions are obviously influenced by the equivalence ratio and the temperature as long as thermal NOx are considered as the sole player in an engine.

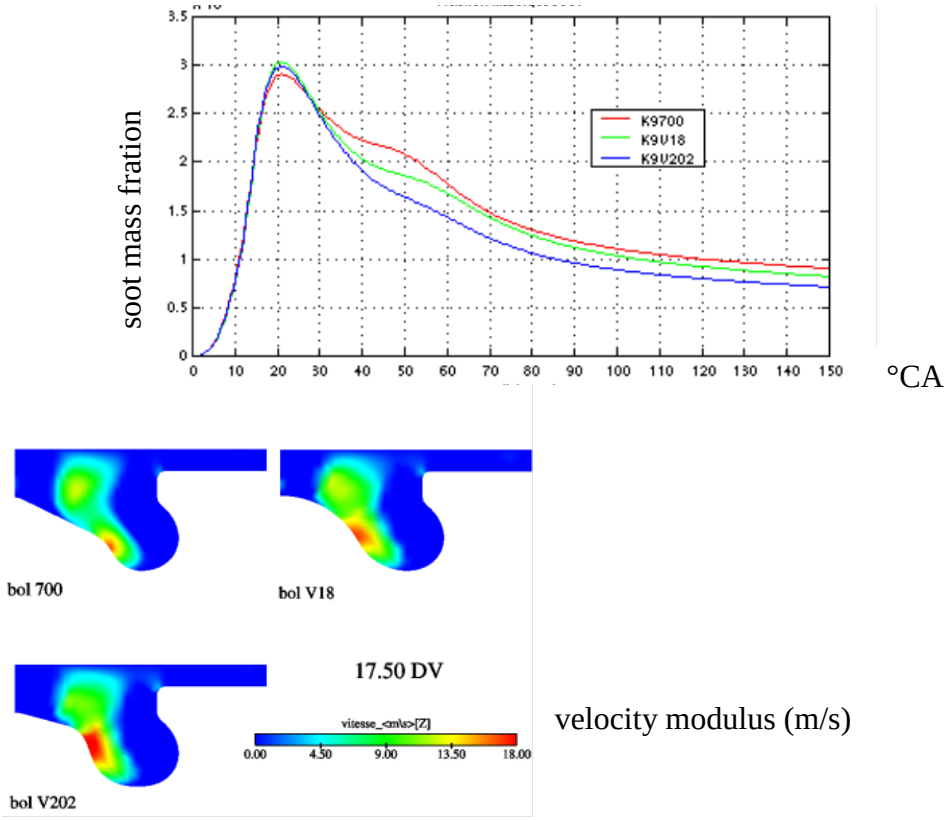

Figure 3-12: soot extraction phenomenon for 3 different bowl shapes – gas velocity modulus 17.5 °CA ATDC – and effect on the soot mass fraction in the chamber – KIVA simulation.

3.4. The high pressure gasoline injection.

The structure of the gasoline spray has not been as deeply investigated as for the Diesel applications, probably for three main reasons; the first one is historic because, apart some very few applications, this technology is quite new; the second one is linked to the large amount of technical solutions adopted since WWII (see chapter 2) and the third one is more linked to mixture preparation because the majority of the industrial applications are concerning engines operating in homogeneous mode.

Nevertheless, at the end of the last century, two main designs have been developed, the first one being based on an inwardly opening needle, with generally a swirl motion generated by the nozzle shape, and the second one with an outwardly opening needle. If both of them are generating a hollow cone spray, several significant differences have been outlined, highly dependent on the detailed structure of the injector.

3.4.1. The "inwardly opening needle"

In 1998 Shelby [3-21] confirmed that the spray develops according a hollow cone –Figure 3-13, with three main temporal phases described as follows:

- A solid jet or pre-spray phase with a poorly atomized stream of liquid at the very beginning of the injection, disappearing very quickly at high pressures;

- A wide hollow cone phase with the separation of the liquid jet into a hollow cone spray once sufficient tangential velocity has been established
- A fully developed spray, in which the spray cone angle is narrowed due to a low pressure zone at the center

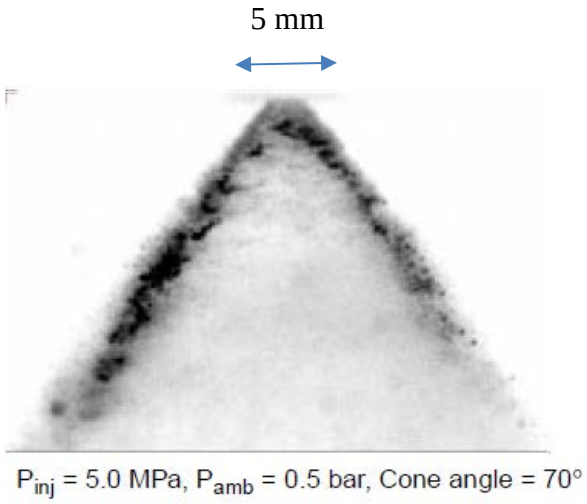

Figure 3-13: typical spray shape in the vicinity of the hole for swirl injector

The presence of the solid jet was not confirmed by Liu [3-22] using Xray Tomography but the two other phenomena were also observed by Arbeau [3-23] with the help of PIV measurements in the vicinity of the spray –see Figure 3-14.

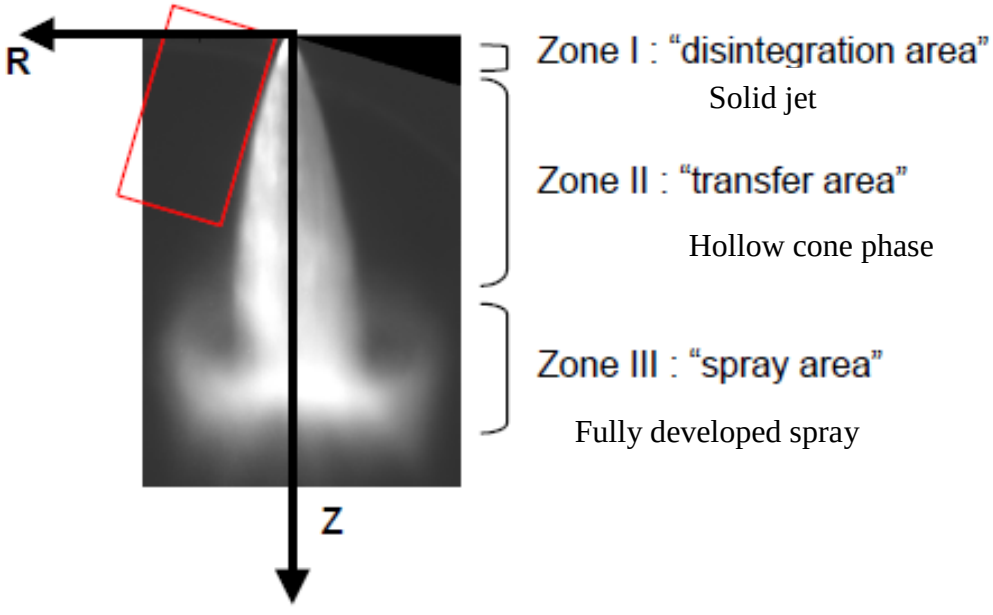

Figure 3-14: structure of a Direct Injection swirl injector spray; zone I is not clearly visible

The large recirculation zones at the spray tip (zone III in Figure 3-14) are constituted by the vortices due to air entrainment at the outside periphery of the

plume. They are forming a very interesting zone because the mixture formed is not too rich for ignition.

3.4.2. The “outwardly opening needle”.

In this case, the fuel is emerging from the nozzle as a hollow cone –Figure 3-15- composed of strings present from the very beginning of the injection – Figure 3-16; at the outer and inner edges of the hollow cone, droplets are sheared off and follow the air flow that is induced by the fuel [3-24].

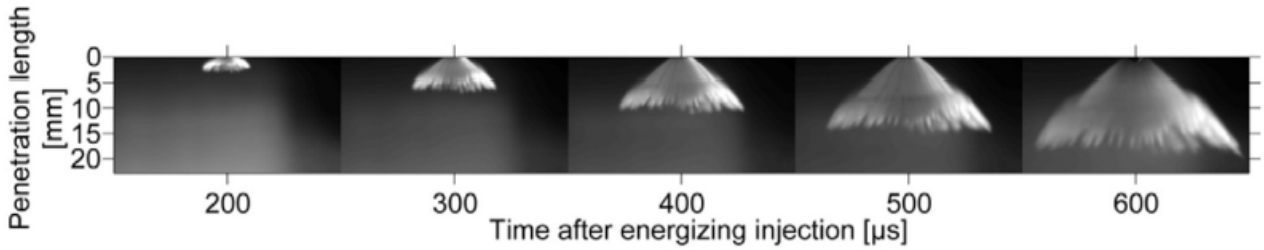

Figure 3-15: general shape of a spray issued from an outwardly opening needle injector [3-24]

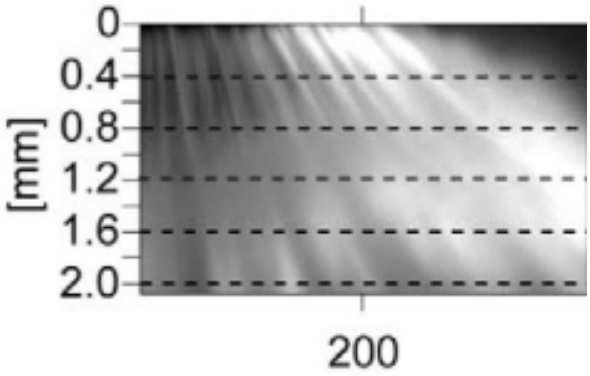

Figure 3-16: spray structure near the nozzle exist, 200µs ASOI [3-24]

Cordes [3-24] but also Liu [3-23] showed that the position of the ligaments only depends on the injection pressure and on the ambient conditions and are constant all along the injection or from one shot to the other. After a certain distance from the nozzle, they quite disappear as fuel is atomized. None of these authors suggest any explanation about the physical origin of these ligaments.

3.4.3. General remarks.

Despite a much lower rail pressure, cavitation is certainly playing a significant role in the GDI injector nozzles; a rapid calculation shows that the cavitation number for an injection during the intake stroke at WOT is around 80 for a rail pressure of 80 bars, compared to a number around 20 for a Diesel CR system injecting near TDC.

On a “microscopic” point of view, the interaction between air and fuel is qualitatively quite close to Diesel, led by the shear stress at the periphery of the plume; differences related to the physical properties of the fuels obviously play a key role concerning the quantitative rate of atomization –via the Weber number- and evaporation.
The mixing phenomena are leading to an Air/Fuel stratification which is thereafter governed by the spray/aerodynamics interaction.
Combustion is initiated by the spark and the flame propagation velocity, or the appearance of knock, are linked to the local equivalence ratio and temperature in the chamber. Even with stratified systems, there is no diffusion controlled flame even if soot can be produced in rich area.

3.5. Conclusion.

The aim of the work described in the following chapters was to optimize a technical definition of the combustion system respects to the fuel efficiency and / or the pollutant emissions. For each one, the physics of the mixture preparation was particular as well as its interaction with the flame. The results provided by the bibliography, mainly focused on the Diesel injector because it is probably the more complex, and presented above, are highlighting the reference mechanisms which link the spray to the heat release and to the soot and NOx formation. They clearly emphasize the importance of the knowledge of the boundary conditions around the nozzle hole and the necessity to have a good understanding of the performances of the injectors. This statement was the base to the methodology followed thereafter, which consisted in deeply investigating the spray behavior, eventually by developing new optical or numerical tools, before operating the complete combustion system on an engine.

Bibliography.

[3-1] DICO (Diffusive Combustion): rapport final à l'ANR
Paris 2012.

[3-2] DIAMANP (DIesel A Maitrise de l'Acoustique, des Nox et des Particules): rapport final à l'ADEME
Paris 2009

[3-3] J.Manin: Analysis of Mixing Processes in Liquid and Vaporized Diesel Sprays through LIF and Rayleigh Scattering Measurements.
PhD report – Valencia - 2011

[3-4] A.Fath, K.U.Münch, A.Leipertz: Spray Break-Up Process of Diesel Fuel Investigated Close to the Nozzle
ICLASS – Seoul – 1997

[3-5] K.Y.Huh, Y.D.Gosman: A phenomenological model of Diesel spray flow
International Conference on Multiphase flows – 1991.

[3-6] R.D.Reitz, R.Diwakar: Effect of drop breakup on fuel sprays
SAE 860469

[3-7] A.I.Ramirez, S.Som, S.K.Aggarwall, A.L.Kastengren, E.M.El Hannouny, D.E.Longman, C.F.Powell: Characterizing Spray Behavior of Diesel Injection Systems Using X-Ray Radiography
SAE 2009-01-0846

[3-8] J.M.Desantes, R.Payri, J.M.Garcia, F.J.Salvador: A Contribution to the Understanding of Isothermal Diesel Spray Dynamics
Fuel, vol. 86 - 2007.

[3-9] NADIA_bio (New Advanced Direct Injection Analysis for bio fuels): rapport final à l'ANR
Paris 2011

[3-10] C.Arcoumanis, M.Badami, H.Flora, M.Gavaises: Cavitation in Real-Size Multi-Hole Diesel Injector Nozzles
SAE 2000-01-1249

[3-11] C.Mauger: Cavitation dans un micro-canal, modèle d'injecteur Diesel: methods de visualization et influence de l'état de surface.
PhD report – Lyon 2012

[3-12] W.Eifler: Untersuchungen zur Struktur des instationären Dieselöleinspritzstrahles im Düsennahbereich mit der Methode der Hochfrequenz-Kinematografie
PhD report – Kaiserlautern - 1990

[3-13] J.M.Desantes, R.Payri, F.J.Salvador, J.de la Morena: Cavitation effects on Spray characteristics in the near nozzle field
SAE 2009-24-0037

[3-14] F.P.Ricou, D.B.Spalding: Measurements of entrainment by axisymmetric turbulent jets.
Journal of Fluid Mechanics -11 - 1960

[3-15] G.Cossali, G.Brunello, A.Coghe: LDV characterization of Air Entrainement in Transient Diesel Sprays
SAE 910178

[3-16] P.F.Flynn, R.P.Durrett, G.L.Hunter, A.O. zur Loye,O. C. Akinyemi, J.E.Dec, C.K.Westbrook: Diesel Combustion: An Integrated View Combining Laser Diagnostics, Chemical Kinetics, And Empirical Validation
SAE 99-01-0509

[3-17] B.Higgins, D.Siebers: Measurement of the Flame Lift-Off Location on DI Diesel Sprays Using OH Chemiluminescence
SAE 2001-01-0918

[3-18] C.A.Idicheria, L.M.Pickett: Soot Formation in Diesel Combustion under High-EGR Conditions
SAE 2005-01-3834

[3-19] D.Siebers, B.Higgins, L.Pickett: Flame Lift-Off on Direct-Injection Diesel Fuel Jets: Oxygen Concentration Effects
SAE 2002-01-0890

[3-20] M.P.B.Musculus: Heavy-Duty Low-Temperature and Diesel Combustion & Heavy-Duty Combustion Modeling
FY 2010 DOE Vehicle Technologies Program Annual Merit Review

[3-21] M.H.Shelby, B.A.VanDerWege, S.Hochgreb: Early Spray Development in Gasoline Direct-Injected Spark Ignition Engines
SAE 980160

[3-22] X.Liu, Kyoung-Su Lm, Y.Wang, J.Wang, M.W.Tate, A.Ercan, D. R. Schuette, S. M. Gruner: Ultrafast and Quantitative X-Tomography and Simulation of Hollow-Cone Gasoline Direct-Injection Sprays
SAE 2007-01-1847

[3-23] A.Arbeau, R.Bazile, G.Charnay, P.Gastaldi: A New Application of the Particle Image Velocimetry (PIV) to the Air Entrainment in Gasoline Direct Injection Sprays
SAE 2004-01-1948

[3-24] D.Cordes, P.Pischke, R.Kneer: Influence of Injection and Ambient Conditions on the Nozzle Exit Spray of an Outwardly Opening GDI Injector
SAE 2012-01-0396

Chapter 4

Tools and methodologies

4.1. Introduction.

As well as technologies used on gasoline and Diesel engines, investigation tools have been strongly improved all along the years. If the engine tests themselves remained quite conventional with the use of single cylinder engines for combustion investigation, visualization and simulation have been intensively developed, especially in the field of mixture preparation.
The tools capabilities progressively reproduced thermodynamics closer and closer to the real engine, for example for the spray diagnosis, with an evolution from an environment at atmospheric pressure and with neutral gas to fired combustion.

The main idea in this chapter is to focus on the description of the tools which were not currently used in the industry or whose application needed some innovative adaptations.

4.2. Engines tests.

4.2.1. Bench overview.

The single cylinder engine has been used for all the investigation described in the present document. Its advantages are well known concerning the hardware, as a high versatility versus the injection system, quite simple devices to get a variable air motion (tumble or swirl) or obviously very quick piston replacements.
Its other great interest is concerning charging and EGR, which can be independent of the engine itself, air pressure and temperature being generated and regulated by an electric compressor and an electric heater. The air mass flow is measured by a sonic tube. For the EGR, a manifold located on the exhaust system allows to regulate the mass flow.

Generally, the engine is conveniently linked to an electric motor/generator – most frequently synchronous for low size engines- for starting or for use without combustion, for instance during visualization tests. The torque is regularly observed for safety and reliability purposes, even if effective data concerning the tests are generally not used for the analysis for two main reasons: the measurement accuracy at low engine load is low –it is generally in the order of magnitude of 1% of the full sensor scale- and the friction level on a single cylinder engine is quite different from that on a full size one. Indicated data, preferably concerning the high pressure loop for combustion analysis, are therefore favored for detailed investigations.

The fuel consumption is directly measured in terms of weight with an AVL balance whose range is correctly fitted with the engine.
Conventional gas analyzers are used for measuring pollutant emissions and to evaluate the equivalence ratio; Infra-Red systems are well suited to CO and CO2 measurements, as Flame Ionization detectors for unburnt hydrocarbons HC and chemi-luminescence for NO and NO_2. Smoke on the Diesel engine is measured with a Bosch smoke-meter based on the gas opacity. Their technology has not changed very much during these late years, from the Beckman systems used in chapter 5 to the Pierburg devices for the other tests.
Several equivalence ratio comparisons have been achieved between exhaust gases analysis and fuel and air mass flow measurements.

4.2.2. Indicated values.

A piezo electric transducer is located in the cylinder head; for the earliest measurements described in Chapter 5, water cooled AVL 8 QP sensors were used and coupled with an AVL Indiscope which provided IMEP on line and could store around 100 cycles depending on the measurement rate –generally minimum 0.5 °CA- and the range –generally between -180 and +180°CA around the combustion TDC for high pressure cycle analysis. The system was particularly able to calculate the PV and LogP/LogV thermodynamic cycles; this last result was quite effective to secure the measurements because of the polytropic evolution of the gas between the inlet valve closure and the beginning of the injection; the LogP/Log V relation had therefore to be linear and a deviation could indicate some sensor drift.
The Indiscope also calculated the standard deviation of IMEP, which is the key parameter to characterize the combustion stability.

For further tests –Chapters 6 and 7- uncooled Kistler sensors were used together with an internally developed acquisition system integrated for all the single cylinder benches. The biggest advantage was concerning the amount of stored cycles but the analysis did not change very much.

4.2.3. Testing methodologies.

The easiest way to test a single cylinder engine is to operate at constant speed with a given injected fuel quantity. This allows to use a quite simple electronic control unit as, for high pressure injection systems, the mass flow is marginally influenced by the thermodynamic conditions in the chamber. This methodology, which was used for all the tests relevant to Chapter 5, has a sense on a thermodynamic point of view because the energy introduced for each cycle is constant. Nevertheless, the comparison between engines with different displacements or the use of the data to simulate the fuel consumption on a vehicle is a bit difficult.

For this last reason, tests achieved in the program described in Chapter 6 have followed another direction which consisted in operating the engine at constant

IMEP. This led to carefully optimize the injection duration while changing the engine tuning –for instance the throttle position-.

For the investigation on a Diesel engine, the problem is quite more complex because of the high interaction between emissions, combustion noise, fuel consumption and exhaust temperature on one side, and the number of parameters to be optimized such as EGR rate, boost pressure, injection pressure and timing on the other side. It is therefore important to fix some of these output data.
At full load the smoke level and the exhaust gas temperature are generally limited, the first one for environment reasons, the second one to keep the thermomecanic stress within acceptable values for the materials.
At part load, on each operating point, the noise level is fixed and the relation between NOx and soot or NOx and fuel consumption can be investigated. For conventional combustion, one way is to keep the heat release constant –for instance with the help of the CA50. This quite successful methodology has nevertheless the drawback of fixing the balance between premixed and diffusion controlled combustion and to forbid any investigation on new modes like those described in Chapter 7. That's the reason why usual EGR variations have been investigated for different boost pressures.

4.3. Visualization.

4.3.1. General overview.

Observing the physics of the combustion in an actual engine has always been a dream for all the automotive engineers, trying to understand very complex phenomena in a completely closed world.
During the late 80's, some laboratories and engine manufacturers began to develop "optical engines" to investigate the aerodynamics in motored conditions. Several years later, the MIT (Massachusetts Institute of Technology) [4-1] and the SNL (Sandia National Laboratory) paved the way with the first single cylinder gasoline engines operating in combustion, followed by many institutes and constructors like IFP (Institut Français du Pétrole) [4-2]. These engines were for a long time limited in terms of speed –below 2000 rpm- and load –below 6 bars IMEP.
In parallel, AVL proposed a quite simple visualization system based on two endoscopes located in the cylinder head; mainly used for Diesel applications -due to higher combustion pressures, the adaptation of quartz windows in the cylinder liner or in the piston was much more difficult than on a SI engine - , they also had a noticeable interest for Direct Injection Gasoline.
Another way was to develop dedicated systems like constant volume chambers and rapid compression machines, which "simulated" the engine conditions with very high peak pressures [4-3].

Besides the development of the adequate supports, optical techniques were intensively improved to provide the necessary information concerning mixture preparation, combustion…and pollutants. Three families could be identified [4-4] as thereafter described:

- The simplest one, based on the light emitted by the source itself like the flame or the soot; direct visualization, pyrometry, Infra Red thermography or emission spectroscopy belong to this family.
- Techniques based on the transmitted light: they need an external source (a lamp or a laser); the light emitted by the source is passing through the gases and modified in different ways. On the opposite side of the source, the light is collected, analyzed and compared with the emission. Absorption spectroscopy, extinction, holography, strioscopy (also called, Schlieren) are some examples of these methodologies.
- Diffusive light: in this case, the light emitted by an external source is not transmitted by the gas; it is diffused by the gas molecules themselves or by some tracers which have been introduced by external means. The Doppler anemometry, the Raman diffusion or the different fluorescence techniques are part of this family.

The aim of this chapter is obviously not to describe every available optical technique but only those which have been used during the different investigations described chapters 5 to 7.

4.3.2. Spray and combustion visualization for gasoline direct injection.

4.3.2.1. Free jet in atmospheric conditions.

- Description of the experimental system.

A very cheap and easy methodology consisted in taking photographs with a simple Nikon F301 24x36 camera using a 400 ASA color film [4-5]. The camera and the injector were located on the same micrometric table, carefully set in order to secure that the injector axis and the film were absolutely parallel. The column supporting the injector was designed in order to allow the rotation of the injector around its axis by steps of 30°.
The light was provided by a stroboscope triggered by the injection timing; different offset between the injection and the flash were possible in order to investigate opening, closure and steady state operations for the spray.
As an example, for an injection rate of 2000/min, the camera equipped with a Tamron 35-135 zoom set on 135 mm was located at 820 mm from the injector, with an exposure time of 1s and a diaphragm opened at 4.
The analysis of the photographs was carefully done with a Leitz projector equipped with a 90 mm objective and located at 1425 mm from the screen; it was checked that this configuration, with a screen perfectly parallel to the film, didn't introduce any geometric deformation.

A second step was achieved by using a high speed Hycam 16mm camera to visualize individual sprays and to compare them with the average data obtained with the Nikon. The same bench was used but the camera was located at 677 mm from the injector with an objective of 28 mm. A black and white 400 ASA film was used and the diaphragm was opened at 8. The biggest difficulty was to find a continuous light source sufficiently powerful relatively to the film speed which was generally set between 8 and

10.000 frames/second. Two HMI projectors –the same as used for movies in the cinematographic industry- of 2500 W each one were chosen and located as described in Figure 4-1.
The analysis was achieved by digitalizing the 16 mm film by the help of a NAC 160 F table linked to a PC via a NAC "Movias" software.

- Definition of the different parameters.

The definition of the spray characteristics –eg angle and penetration- has always been a difficult task because of different reasons:

- The lack of contrast at the boundary of the plume. Anyway, the use of a yellow filter has been very useful –see Figure 4-2 – to identify the different points used in this methodology.
- The presence of very small droplets issued from the secondary atomization in the vicinity and at the head of the spray
- The quite noticeable dispersion from one injection to the other
- The evolution of the angle during one injection

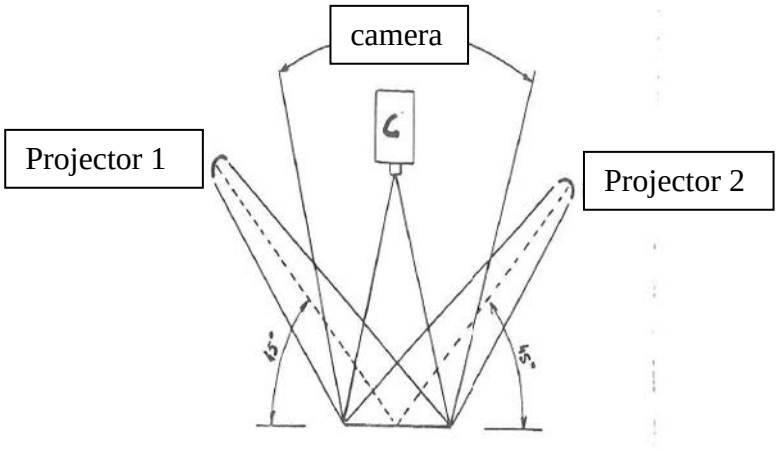

Figure 4-1: experimental set-up for high speed cinematography

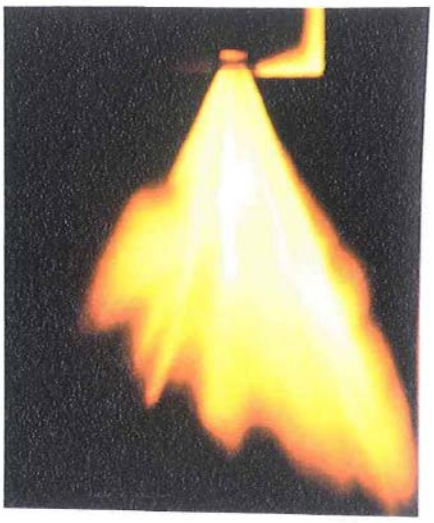

Figure 4-2: example of an image obtained with a yellow filter

The simplified drawing presented in Figure 4-3 shows how the different representative points have been chosen; index 1 to n represent the points directly defined on the photographs, n+1 to n+3 were calculated as explained below:

- Points 1 to 4 situated on the injector support were used to check the scale of the photographs; points n+1 and n+2 were located at the middle of segments 1-2 and 3-4 and defined the injector axis
- Point 5 was situated at the tip of the injector and defined the origin of the spray, independently of the vibrations during one injection; this point was mainly used for high speed cinematography
- Points 6 to 9 defined the edge of the spray; with point 5 they allowed to measure the spray angle; points 6,7 and n+1, 8,9 and n+2 defined the two spray half angles and gave an idea of its symmetry.
- Points 10 to n defined the penetration of the different ligaments forming the liquid sheet; point n+3 was their center of gravity and was defined as the spray penetration

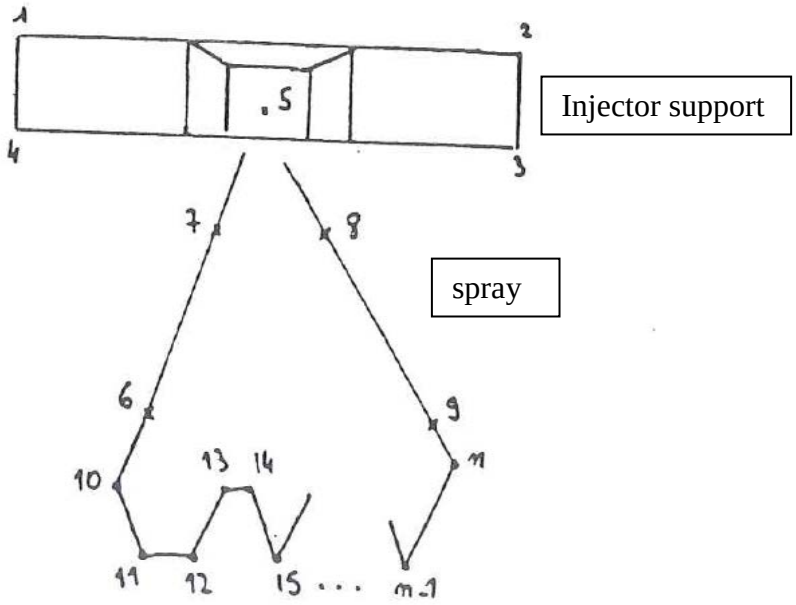

Figure 4-3: definition of the different points on the spray photograph

The penetration velocity was thereafter defined by using the derivative of the position of point n+3 versus time. Another methodology, based on the evaluation of the projected spray area, led to very similar results.

During one injection, the spray angle deviation was evaluated at 3.5°, obviously during the steady state phase (injection pressure 80 bars). The spray to spray deviation was recorded around 1.5° in the same conditions.

4.3.2.2. Jet in the motored engine.

The system provided by AVL can be described by Figure 4-4. Endoscope 1 was used to collect the image as Endoscope 2 was used for the flash lamp. The camera and the flash were triggered by an electronic control unit, the dwell time between the flash and the camera start was set by the user.

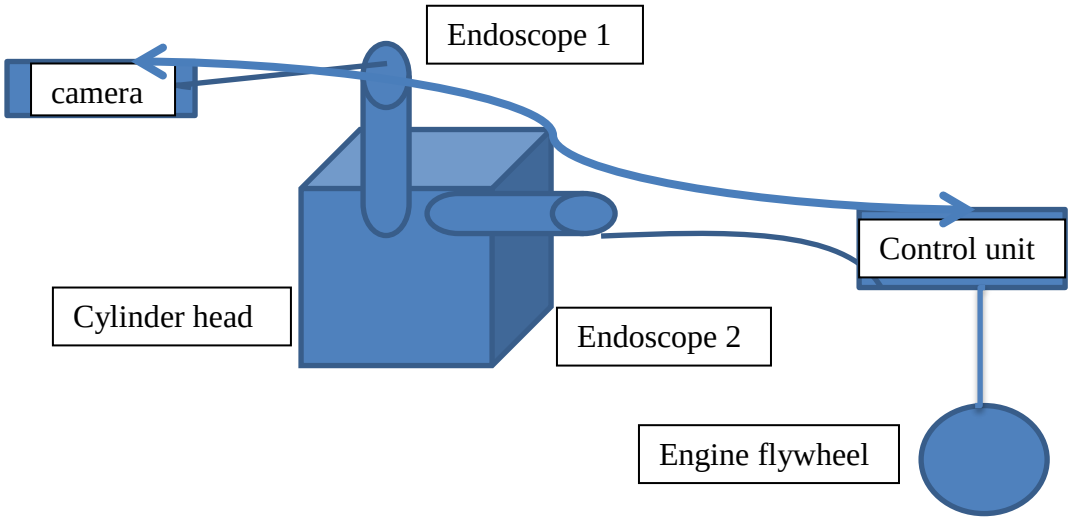

Figure 4-4: experimental setting for the endoscopic system

The control unit automatically took the film speed into account to be sure that the rate of photographs was constant during the selected period of time.
A crank angle signal was obviously provided to the control unit by a sensor located on the engine.

A careful optimization of all the parameters (location of the flash lamp in the endoscope, protrusion of the two endoscopes in the chamber …) was done for each operating point.

4.3.2.3. Visualization of the combustion.

The system, as described in Figure 4-4, was also used for combustion, at the exception of the flash lamp which was not useful any more. As well as on a Diesel engine, the soot formed during the combustion provided enough light for the high speed film. To enhance the sensitivity, especially at the very beginning of the combustion and at the end when the soot temperature decreased - the light intensity provided by the soot is proportional to T^4 where T is the temperature of the particles- a FUJI film 500 ASA pushed to 1000 or 1500 ASA during the treatment was used instead of the conventional KODAK 400 ASA.

4.3.3. Visualization of the mixture preparation for gasoline direct injection.

4.3.3.1. Background with homogeneous mixtures.

The knowledge of the equivalence ratio distribution in the combustion chamber of a SI engine takes a first order importance concerning efficiency, emissions and stability at low loads. This question was furthermore highlighted with the lean burn systems developed during the late 80's –see § 2.3.3. – in order to avoid misfiring and to secure a sufficient flame front velocity.
One basic idea to achieve this goal was to use the fluorescent properties of the fuels; when they are excited by an external source like a laser, the molecules emit photons at a different wavelength from the incident one. This phenomenon theoretically allows to evaluate the fuel concentration by measuring the intensity of the induced emission which can be separated from the incident one.
Among a lot of applications, the FARLIF –Fuel Air Ratio Laser Induced Fluorescence- developed at the CORIA in Rouen [4-6], [4-7] proposed a very powerful technique to provide a 2D analysis of the fuel distribution for MPI engines. Several tests were achieved on a single cylinder optical engine [4-8] by using a mixture of 95% isooctane and 5% toluene (tracer); an Excimer KrF laser at 248 nm provided the excitation source, while the fluorescence was recorded by an intensified CCD camera. The collected signal was corrected according to the temperature for each crank angle. Figure 4-5 shows an example of the correlation obtained for determining the equivalence ratio on a MPI engine operating in homogeneous mode; the FARLIF measurements were compared with conventional methodologies such as gas analysis, lambda sensor or fuel and air mass flows.

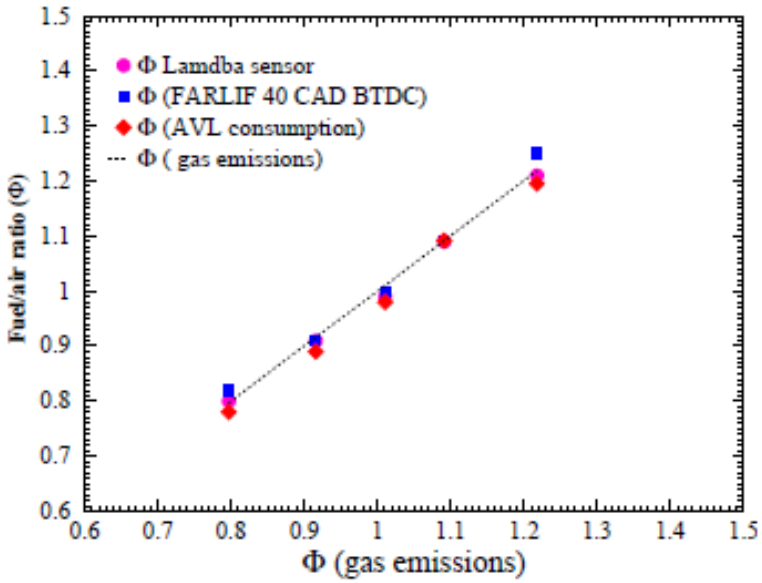

Figure 4-5: Fuel/air ratio measurements at 40°CA BTDC, engine speed 2000 rpm

4.3.3.2. Introduction of Direct Injection.

The ready to use FARLIF methodology was first successfully used with early injections during the intake stroke [4-8], highlighting fairly well mixed mixtures as seen in Figure 4-6, together with the start of combustion.
With later injections, and especially at the end of the compression stroke in stratified mode, the fuel evaporation was not complete and the fluorescence of the liquid phase was highly dominant versus the vapor. The evaluation of the equivalence ratio was therefore impossible and a second methodology had to be used: the LIEF –Laser Induced Exciplex Fluorescence.
Based on the separation of the two phases –liquid and vapor- by the use of two different tracers, LIEF was first developed by Melton in 1983 [4-9].

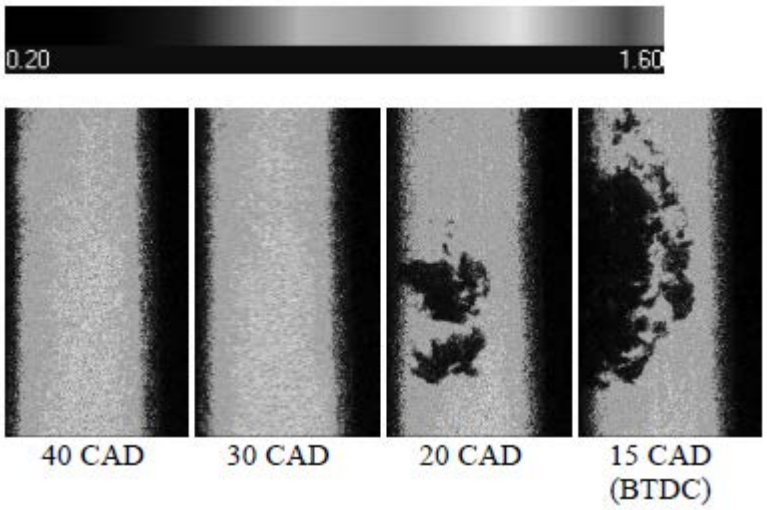

Figure 4-6: measurement of the fuel air ration with FARLIF, 1200 rpm, stoichiometric mixture; images taken in a diametral plan 3 mm below the plug; combustion is clearly visible at 20 and 15°CA BTDC.

A great job was thereafter achieved within the automotive industry and partners to define the best possible couple of seeds [4-10], [4-11]; very good results were obtained by Munch [4-12] with Benzene and Triethylamine (TEA). Munch found that the boiling point –and thereby the evaporation – of the tracers –see Table 4-1- as well as their mixing and stability with iso-octane were coherent; the fluorescence intensity of the corresponding mixture also depended on the fuel-air ratio since oxygen was the only quenching partner. Several works [4-13], [4-14] later on demonstrated the linear dependence of this Exciplex mixture with the fuel-air ratio.

The chamber was illuminated by a Nd-YAG Infinity Coherent laser sheet triggered at 266 nm. Figure 4-7 shows the result of both the careful optimization of the seed concentration and of the filter [4-15] used to separate the wavelengths emitted by the two tracers. Vapor and liquid are therefore correctly distinct.
This methodology was applied and provided realistic quantitative results as observed in Figure 4-8 with an evaluation of the equivalence ratio in the spark plug vicinity.

In comparison, the order of magnitude of the FARLIF results (Figure 4-9) were quantitatively out of scope due to the presence of liquid (Figure 4-10), even if the global phasing of the signal was correct.

.

Substance	Formula	Molecular weight	Boiling point
ISO-OCTANE 2,2,4 trimethylpentane, C8H18	$3(CH_3)$-C-CH_2-CH-$2(CH_3)$	114.23	99.2°C
TOLUENE Methylbenzene, C7H8	$C_6H_5CH_3$	92.14	110.6°C
BENZENE C6H6	aromatic ring	78.11	80.1°C
TEA Triethylamine, C6H15N	$3(C_2H_5)$-N	101.19	89°C

Table 4-1: seeds and fuel properties for LIEF [4-12]

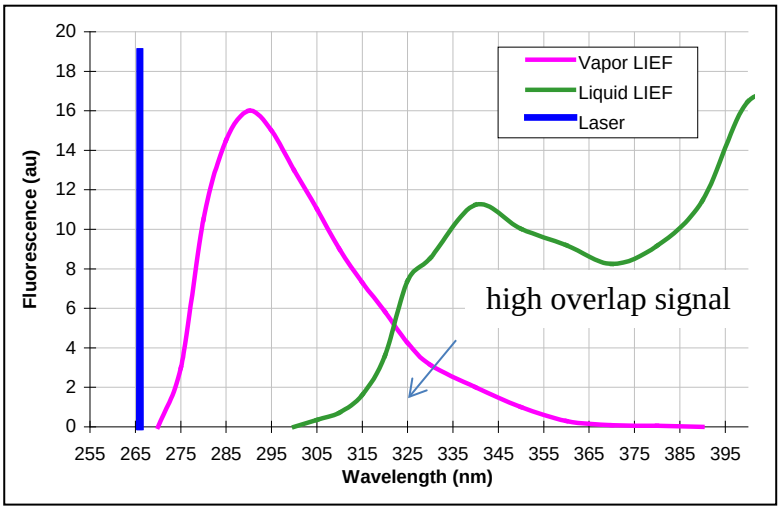

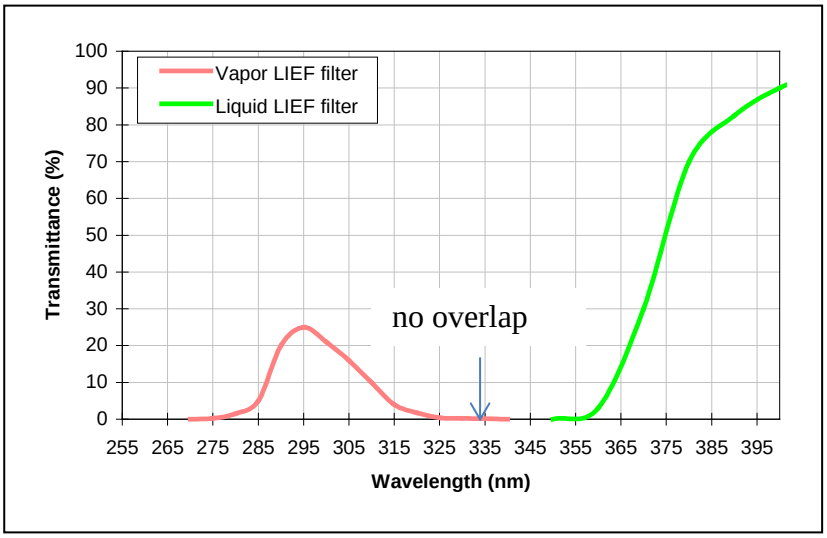

Figure 4-7: emitted wavelengths w (upper) and w/o (lower) filter

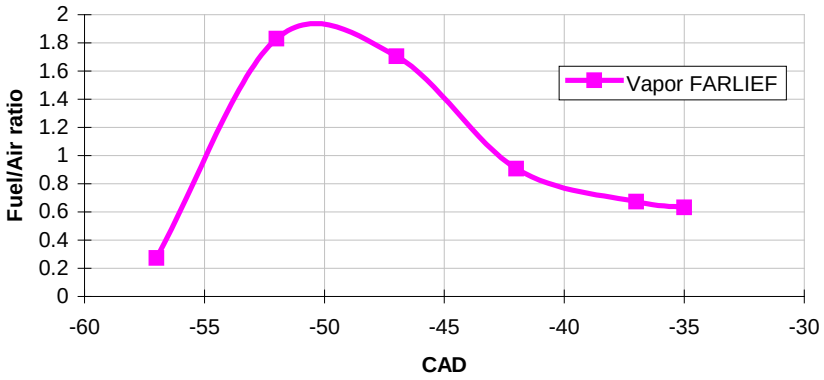

Figure 4-8: evaluation of the equivalence ratio near the spark plug - LIEF applied on a single cylinder optical engine – 1200 tr/min – WOT – 8.5 mg/stroke – EOI -56°CA

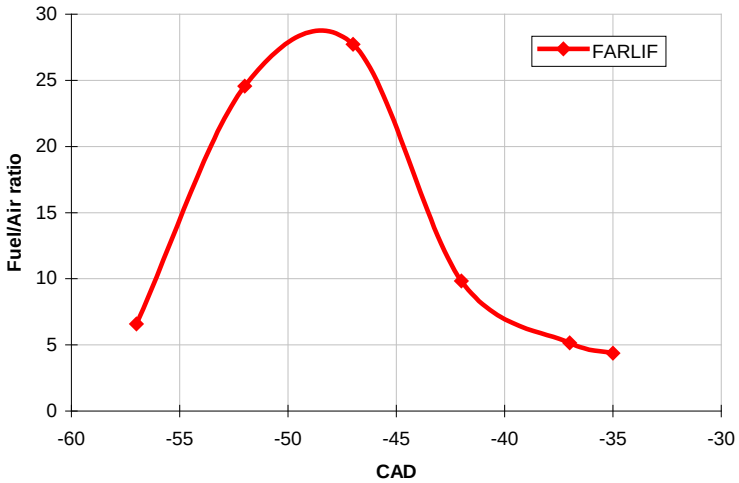

.

Figure 4-9: evaluation of the equivalence ratio near the spark plug with FARLIF– 1200 tr/min – WOT – 8.5 mg/stroke – EOI -56°CA

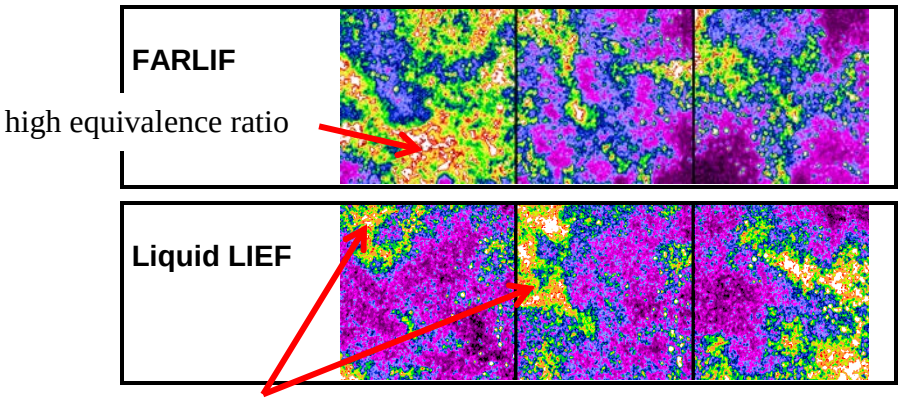

Figure 4-10: comparison of FARLIF and Liquid LIEF at -35°CA -1200 rpm, WOT – 8.5 mg/stroke – EOI -56°CA – individual cycles

One major improvement to the LIEF technique would have been to integrate a correction for the vapor signal, corresponding to the evolution of the temperature due to fuel evaporation, as well as it had been made for compression.

4.4. Simulation.

4.4.1. Historical background.

The need for some mathematical simulation describing the jet development began in the late 30's with phenomenological models; for instance Schweitzer [4-16] proposed a relation to calculate the quasi steady penetration for a free Diesel spray injected in the air. The models were later on improved all along the years as described by Hiroyasu [4-17].

In 1985, 3D simulation began to appear for combustion engines with the first public version of the US made code Kiva developed at Los Alamos National Laboratory. Very first industrial applications were related to Diesel engines, with Ricardo pre-chambers like for example [4-18], or with Direct Injection like [4-19]. These geometries didn't necessitate to simulate the intake flow; for the first example, the air motion was generated by the channel between cylinder and pre-chamber; for the second example, the high intensity swirl was correctly described as a solid movement.

The situation was a bit more difficult for SI engines because of the complexity of the relatively weak aerodynamics in the cylinder; in fact Kiva was based on a hexahedral structured mesh which was quite difficult to use with moving valves; that is the reason why IFP developed a modified version with a new unstructured solver called KIFP [4-20]. Other suppliers thereafter followed the same way, as for instance Star-CD from CD-Adapco.

4.4.2. Dedicated methodology for the aerodynamics simulation.

For GDI engines, a careful description of the air motion has a first order of importance on the mixture preparation and the combustion results.

The methodology described in Figure 4-11 therefore coupled simulation and experimental techniques [4-21].
The final design of the intake ports was finally tested on the flow bench to validate both the flow efficiency and the tumble level issued from CFD.
A motored optical engine associated to PIV measurements was as well used to validate the detailed flow field described by the Vectis code provided by Ricardo.

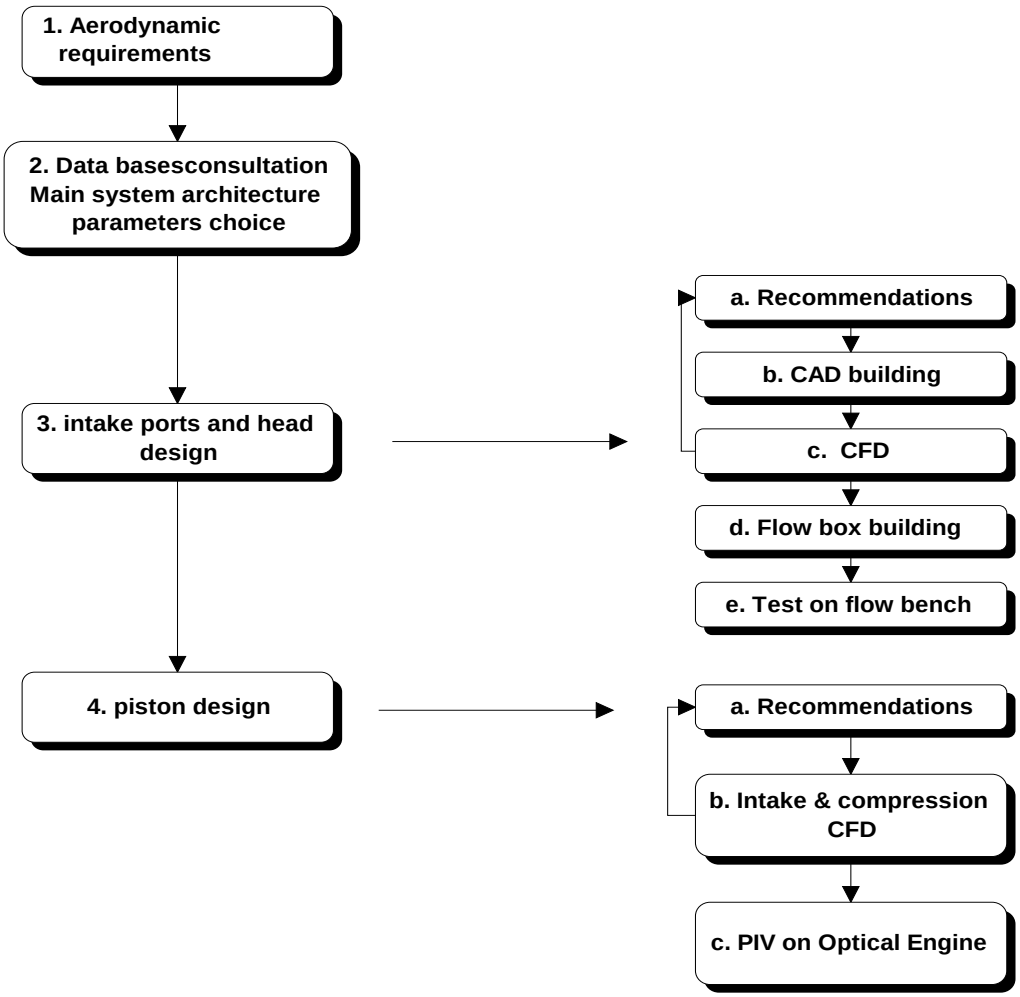

Figure 4-11: methodology followed to describe the aerodynamic motion in a GDI engine

4.4.3. Dedicated methodology for the Diesel spray simulation.

The 3D simulation of the Diesel spray is still a current topic for many investigations in the academic world and new advanced models have recently been proposed, like the ELSA (Euler Lagrangian spray atomization) which combined the Eulerian method for dense region and the Lagrangian method for the dispersed zone [4-22].

Nevertheless, more conservative models are generally used in commercial codes like Star CD, as Huh and Gosman [4-23] for the primary break-up and Reitz and Diwakar [4-24] for the secondary atomization. Their accuracy highly relies on several empiric coefficients, but also on a careful evaluation of the nozzle hole outlet velocity during the injection. This parameter shows a

high importance and the assumption of the Bernouilli value is rarely acceptable, even if quite often used because of the impossibility to have adequate measurements.

A quite simple methodology, based on the work of Wojdas [4-25], was well adapted to the industry because it only needed a conventional hydraulic characterization of the injector, providing the instantaneous mass flow during the needle movement, and a spray visualization in cold conditions.
The idea was to couple different hypothesis for the evolution of the effective hole diameter during the needle lift with the liquid penetration, as described in Figure 4-12.

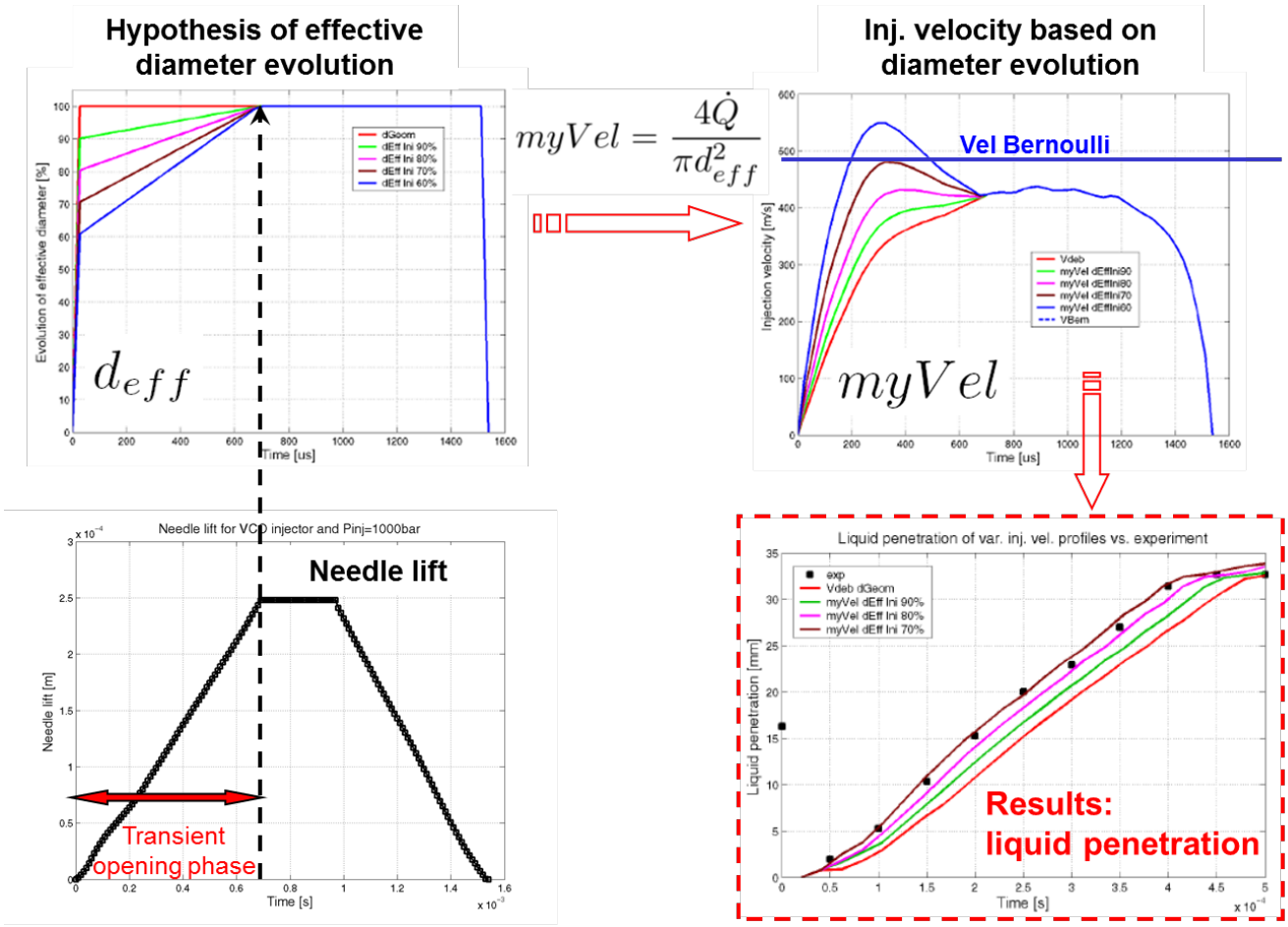

Figure 4-12: methodology for determining the nozzle outlet velocity during the injection

More advanced techniques, like the parallel use of mass flow and spray momentum measurements developed at CMT [4-26], can lead to a much better evaluation of the outlet velocity; moreover, new methods ([4-26],[4-27]) can allow to optimize the different model parameters but all of them need quite sophisticated experimental apparatus which are generally not available in the industry.

In order to measure the liquid spray penetration, a constant volume vessel operating at ambient temperature was chosen in the study; the back pressure could be regulated up to 80 bars. A CCD camera coupled to a stroboscopic light allowed to photograph the spray at different timing after SOI; the quality of the results obtained with this relatively cheap system obviously relied on a good shot to shot injection repeatability.

4.5. Conclusion.

During a research program or during the development of an industrial project, the choice of the most suitable tools takes a great importance. If the bibliography and the different publications provide a great help for the engineer, it is very often led by the availability, by the cost, and by the possibility to get results on time – with other words by the complexity- of the systems. The final decision is therefore a trade-off between all these parameters, securing the best possible answer to the initial question!

A second important aspect is concerning the complementarity between different tools; if the conventional single cylinder engine was and remains the core of any investigation concerning mixture preparation and combustion, because it is the unique system to both provide performances, fuel consumption and emissions, the engineer remains quite blind while facing to macroscopic results coming out of the bench, even with the help of thermodynamic analysis. The help can therefore come either from numeric simulations – up to now concerning only "averaged" data with the RANS methodologies, but providing detailed results in the whole chamber for almost all the physical parameters- or from optical techniques, sometimes able to provide instantaneous evolutions during one engine cycle, but in only dedicated area. Coupling all these tools allow to construct an accurate diagnosis concerning the problem to be solved.

The progress shown by lighting systems, like lasers or photo-diodes…, and cameras, especially with high speed and high sensitivity, is paving the way for a wider use of endoscopes which have the interest of quite moderate modifications in the cylinder head; they nevertheless are limited to a macroscopic understanding of the phenomena, like the spray behavior in the chamber for late injections.

Sophisticated fluorescence techniques can provide accurate quantitative results concerning the fuel repartition in the chamber or concerning the site of auto ignition. Coupling them with 3D simulation is very efficient to calibrate the numeric results and to investigate other operating points or chamber zone not accessible on an optical engine.

Bibliography.

[4-1] M.Namazian, S.Hanson, E.Lyford-Pike, J.Sanchez-Barsse, J.Heywood, J.Rife: Schlieren visualization of the flow and density fields in the cylinder of a spark-ignited engine.
SAE 800044

[4-2] P.Pinchon, R.Levesque: Visualisation de la combustion dans les moteurs
Rapport IFP/GSM n° 32732 – Rueil 1985

[4-3] R.Maly: Improved Otto cycle by enhancing the final phase of combustion
Contractors meeting on Combustion Research – Brussels 1988

[4-4] J.J.Marie: Diagnostics optiques: application à l'étude de la combustion dans les moteurs thermiques
Renault internal report n°0812/88/1205 – Rueil 1988

[4-5] P.Gastaldi, T.Soler: Visualisation des jets d'injection sur et hors moteur
Renault internal report n° 17/91 – Rueil 1991.

[4-6] J.Reboux, D.Puechberty, F.Dionnet: A new approach of Planar Laser Induced Fluorescence applied to Fuel/Air ratio measurement in the compression stroke of an optical SI engine
SAE 941988

[4-7] J.Reboux, D.Puechberty, F.Dionnet: Study of mixture inhomogeneities and combustion development in a SI engine using a new approach of Laser Induced Fluorescence (FARLIF)
SAE 961205

[4-8] J.C.Sacadura, L.Robin, F.Dionnet, D.Gervais, P.Gastaldi, A.Ahmed: Experimental Investigation of an Optical Direct Injection S.I. Engine using Fuel Air Ratio Laser Induced Fluorescence
SAE 2000-01-1794

[4-9] L.A.Melton : Applied Optics
1983

[4-10] M.Knapp, P.Andresen, A.Luczak, V.Beushausen, W.Hentschel : Vapor/Liquid Visualization with Laser Induced Exciplex Fluorescence in an S.I.Engine for Different Fuel Injection timings
SAE 961122

[4-11] J.U.Kim, B.Golding, D.G.Nocera, H.J.Schock, P.Keller : Exciplex Fluorescence Visualization Systems for Pre-Combustion Diagnosis for an Automotive Gasoline Engine
SAE 960826

[4-12] K.U.Munch, H.Kramer, A.Leipertz: Investigation of Fuel Evaporation Inside the Intake of a SA Engine Using Laser Induced Exciplex Fluorescence with a New Seed
SAE 961930

[4-13] G.Ortolan, B.Deschamps: Separate Vapor-Liquid Visualization with Laser Induced Exciplex Fluorescence Applied to Gasoline Direct Injection Engines
10th Gordon Research Conference on Laser Diagnostics (Poster) – Ciocco – 1999

[4-14] A.P. Fröba, F.Rabenstein, K.U.Munch, A.Leipertz: Mixture of TEA and Benzene as a new seeding material for the quantitative two-dimensional LIEF Imaging of Vapor and Liquid Fuel inside SI Engines
Combustion and Flame - 1998

[4-15] P.Gastaldi, D.Gervais: Application of various Laser Induced Fluorescence techniques as tools for developping a new air guided Direct Injection SI combustion chamber.
Esslingen – 2000

[4-16] P.H. Schweitzer: Penetration of Oil Spray
Pennsylvania State College Bulletin – 1937

[4-17] H.Hiroyasu: Diesel Engine Combustion and its Modeling
University of Hiroshima – 1982

[4-18] M.Zellat, T.Rolland, F.Poplow: Three Dimensional Modelling of Combustion and Soot Formation in an Indirect Injection Diesel Engine
SAE 900254

[4-19] K.C.Tsao, Y.Dong, Y.Xu: Investigation of Flow Spray and Flow Field in a Direct Injection Diesel Engine via Kiva II Program
SAE 901616

[4-20] M.Solver, D.Klahr, A.Torres: An Unstructured Parallel Solver for Engine Intake and Combustion Stroke Simulation
SAE 2002-01-1120

[4-21] A.Dupont, A.Floch, X.Baby: In-cylinder flow investigation in a GDI 4 valve engine : bowl shape piston effects on swirl and tumble motions
FISITA 1998

[4-22] R.Lebas, G.Blokkeel, P.A.Beau, F.X.Demoulin : Coupling Vaporization Model with the Eulerian-Lagrangian Spray Atomization Model (ELSA) in Diesel Engine Conditions
SAE 2005-01-0213

[4-23] K.Y. Huh, A.D. Gosman: Phenomenological Model of Diesel spray atomisation.
International Conference on Multiphase Flows – Tsukuba – 1991

[4-24] R.D.Reitz, R.Diwakar: Structure of High Pressure Fuel Sprays
SAE 870598

[4-25] O.Wojdas : Numerical simulation for the Diesel engine development
PhD report – INSA Lyon – 2010

[4-26] J.M.Desantes, R.Payri, F.J.Salvador, J.Gimeno : Prediction of Spray Penetration by Means of Spray Momentum Flux
SAE 2006-01-1387

[4-27] X.Margot, R.Payri, A.Gil, M.Chavez, A.Pinzello : Combined CFD-Phenomenological Approach to the Analysis of Diesel Sprays under Non-Evaporative Conditions
SAE 2008-0-0962

Chapter 5

The MID3S spray guided stratified engine

5.1. Introduction.

Historically, on gasoline carbureted or port injected engines, the development of a cylinder head began by designing the combustion chamber; the carburetor (s) or the injectors were thereafter adapted to the intake system, and mixture preparation effects were eventually investigated on the full size prototype, especially to secure fuel repartition between the cylinders and cold start ability.

With direct injection, this methodology was not changed a lot as combustion was still the heart of the problem, for power oriented applications with homogeneous mixtures as well as for fuel economy purposes with stratification. It was true that, even some early work had been successfully achieved during the Second World War on aircraft engines, the existing theoretical knowledge concerning the in-cylinder mixture preparation and the quasi simultaneous burn was quite poor.

Meanwhile, injectors for GDI applications were at the state of prototypes, hardly available, and generally issued from Diesel systems. The question was therefore not to define any specification concerning the spray properties but only to procure a sufficient number of different samples for the tests. The current methodology, based on the prior design of the combustion chamber, was thereby not so surprising even if it looked quite close to “test and failure”.

The work achieved on the MID3S combustion system, even if conducted so, was nevertheless not a “race in the dark”; the possibility to have a quasi “green field” project was really a chance to introduce some new scientific methods like in situ visualization. The different optimizations concerning the chamber design and the injector characteristics, as far as its technology allowed it, were based on the best possible understanding of the physical phenomena occurring during mixture preparation and combustion. Based on the experience acquired step by step along the project, the “spray guided” concept, even if this denomination was not defined at this time, was characterized as the sum of the interactions between the spray, the chamber walls, the air motion and the spark.

The development and the adaptation of the visualization techniques on a real size combustion chamber, and in actual thermodynamic conditions –not in a constant volume vessel or in an optical engine operating at very low loads and speeds- constituted a significant part of the work; the importance of the results obtained during these tests, in parallel with the quite conventional cylinder pressure analysis, proved that it had to be considered as essential for the project and not as some extra work done in parallel.

5.2. General design and patents.

5.2.1 Specifications and requirements.

The aim of the investigation conducted on a four stroke direct injection gasoline engine was to strongly reduce the fuel consumption of the current all-aluminum 2.0 liter block whose main characteristics are summarized Table 5-1 .

Cylinder displacement cm^3	Stroke mm	Bore mm	Compression ratio	Number of valves	aerodynamics
498	82	88	9 to 1	2 or 3	none

Table 5-1: basic characteristics of the J6/7R engine

This engine largely equipped C and D segment limousines and mini vans for the European market in carbureted J6 (rated power 105 hp) and MPI J7 (120 hp) versions with or without an after-treatment system; some applications were dedicated to the USA with a 3 way catalyst.

The performance requirement for the Direct Injection was to keep the rated power unchanged –eg around 50 hp/l or 37 kW/l-; the NOx emissions level had to be low enough to cope with the forthcoming regulation as CO and HC were to be treated by an oxidation catalyst. Soot was as usual not concerned by the regulation for gasoline automobiles.

Concerning the industrial tool, cylinder block, connecting rod and crankshaft had to remain unchanged while piston, cylinder head, valve train, injection and ignition systems were completely free.

5.2.2. General design origins and description.

5.2.2.1. Thermodynamic roots.

As a breakthrough in fuel efficiency was the most challenging topic of the research program, a brief analysis of the losses breakdown in a conventional gasoline engine was led following the methodology described by Equation (1).
Generally the engine effective efficiency ηeff (1) –eg the ratio between the mechanical work available on the crankshaft and the energy provided by the injected fuel- is split as [5-1]:

$$\eta eff = \eta comb.\ \eta theo.\ \eta cycle\ \ \eta mech \qquad (1)$$

where:

- ηcomb. is the combustion efficiency (related to uncompleted combustion)

- ηtheo. is the theoretical thermodynamic cycle efficiency (of the high pressure loop)
- ηcycle is the form efficiency (including the low pressure loop and the heat losses)
- ηmech is the mechanical efficiency (including friction)

At partial load, and particularly in urban use and on ECE cycle, large SI engines are penalized by the throttling (pumping) losses –eg by the low pressure loop and so the form efficiency. The obvious solution to improve this situation is to operate the engine at wide open throttle (WOT) even at very low load and at idle; this requirement leads to stratify the fuel around the spark plug in order to secure ignition; the combustion is therefore globally lean with an acceptable stoichiometric or slightly rich mixture in the plug vicinity.

Concerning the heat losses, the ratio between the chamber volume and the wall surface has to be maximized; geometrically the hemispherical chamber was known as optimum for long years.

Nevertheless, even if the reduction of the pumping losses was commonly presented to explain the interest of the stratified combustion, several other arguments were generally omitted.

The first one was concerning the influence of the polytropic exponents, γc during the compression stroke and γe during the expansion stroke. The work W provided or obtained during these phases can be evaluated by Equation (2)

$$W = (P'V' - PV)/(\gamma-1) \qquad (2)$$

where P and V represent pressure and volume at the end (') and at the beginning of the transformation

The direct meaning of Equation (2) clearly shows that:

- a high value of the polytropic coefficient, obtained with a very lean mixture or with pure air with a late injection, at low temperature, decreases the compression work
- a low value, obtained with a hot mixture (generated by a quick combustion), increases the expansion work

The evolution of the polytropic coefficient is clearly illustrated in Figure 5-1 [5-1].

The second argument was linked to a cooling effect of the late injection, therefore reducing the knock sensitivity and allowing a higher compression ratio.

All these improvements in efficiency have been evaluated as a 20 to 30% improvement in fuel consumption at very low loads and especially in FTP or ECE+EUDC [5-2] cycles –see Figure 5-2.

From the thermodynamic analysis, the requirements for the combustion system were summarized as follows:

- a capability to stratify the mixture around the spark plug, even at WOT and idle, with a late fuel injection
- a capability to secure a quick combustion around TDC
- a high chamber volume to wall surface ratio
- a high compression ratio

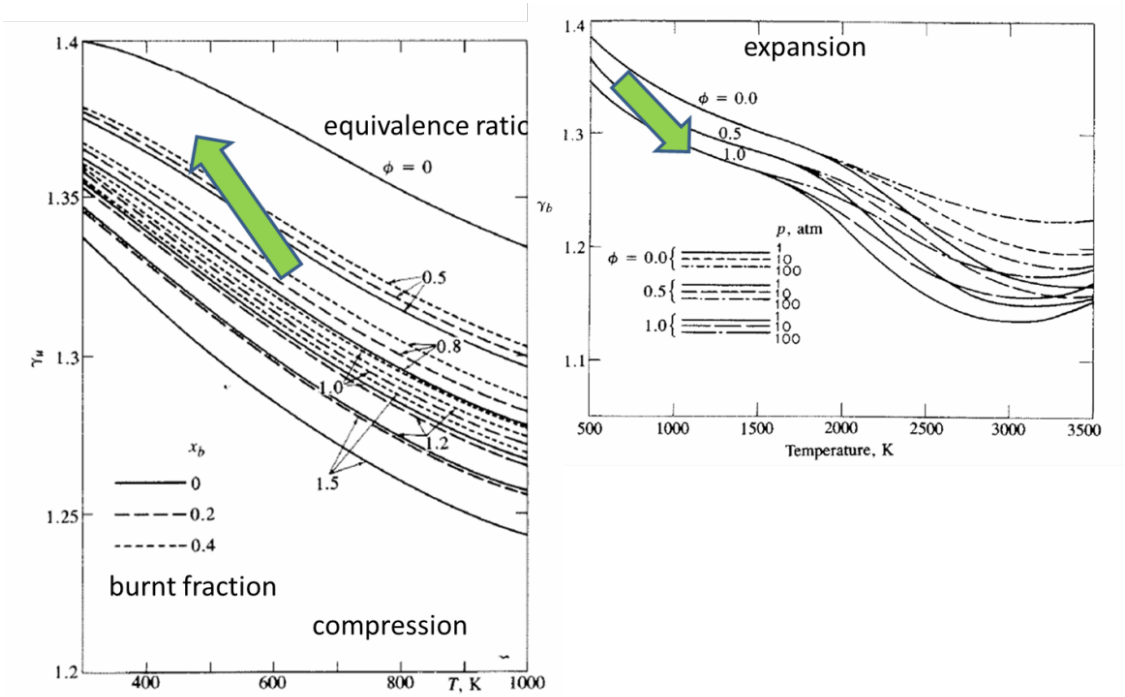

Figure 5-1: evolution of the polytropic coefficient during compression and expansion

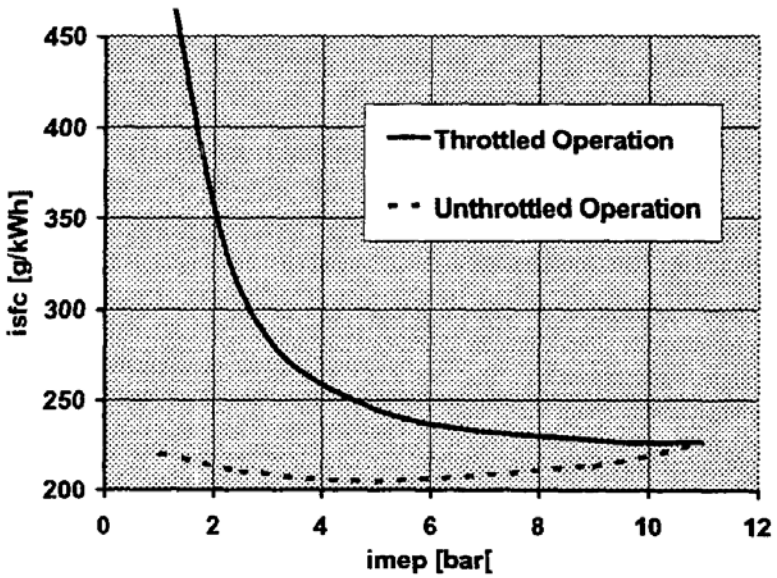

Figure 5-2: comparison of throttled and un-throttled indicated fuel consumption according to the load, constant speed 2000 rpm [5-2]

5.2.2.2. State of the art.

As mentioned in Chapter 2, very few applications had been developed since the end of the war. Only one effectively came into production, the L6 engine which equipped the Mercedes 300 SL, or the L8 for the marginal racing car SLR. The Ford PROCO concept was thereafter used on several V8 powertrains in experimental fleet as the VW Futura and the Porsche DEO were only presented as research investigations.

- The Mercedes concept.

The production L6 engine was first presented in New York in 1954; clearly oriented towards high performances and racing applications, its peak power at 5800 rpm varied between 158 kW for street versions up to 170 kW [5-3]. The main geometric characteristics are summarized Table 5-2; despite its destination, it is interesting to note that a slightly long stroke was chosen by the engineers, probably to enhance low end torque, but finally with a positive impact on fuel consumption.

Cylinder displacement cm^3	Stroke mm	Bore mm	Compression ratio	Number of valves	aerodynamics
499	88	85	8.5 to 9.5	2	squish

Table 5-2: basic characteristics of the Mercedes 300 SL engine

General arrangement [5-4].
The two valves per cylinder were operated by a single camshaft located on the engine side; two ignition plugs were installed approximately in the vicinity of the center of the chamber in order to accelerate the combustion at high engine speeds and to reduce the relatively high knocking sensitivity due to the large bore.
The fuel injector was positioned on the side of the chamber, allowing a fine accessibility for maintenance.
A particularity of this design concerned the “main” combustion chamber which was partially located in the cylinder block.
This global arrangement was finally quite close to conventional engines –do not forget carburetors versions were existing in parallel with the Direct Injection- and belonged to the “open chamber” family.

Aerodynamics.
A large squish area located under the valves promoted a high and stable turbulence level around TDC. The intake port was optimized only for air filling.

Injection system.
The injection system designed and manufactured by Bosch was constituted by an in line 6 pistons mechanically driven pump and multi holes injectors. The fuel quantity was governed by the pump and based on intake pressure, throttle position and air temperature.

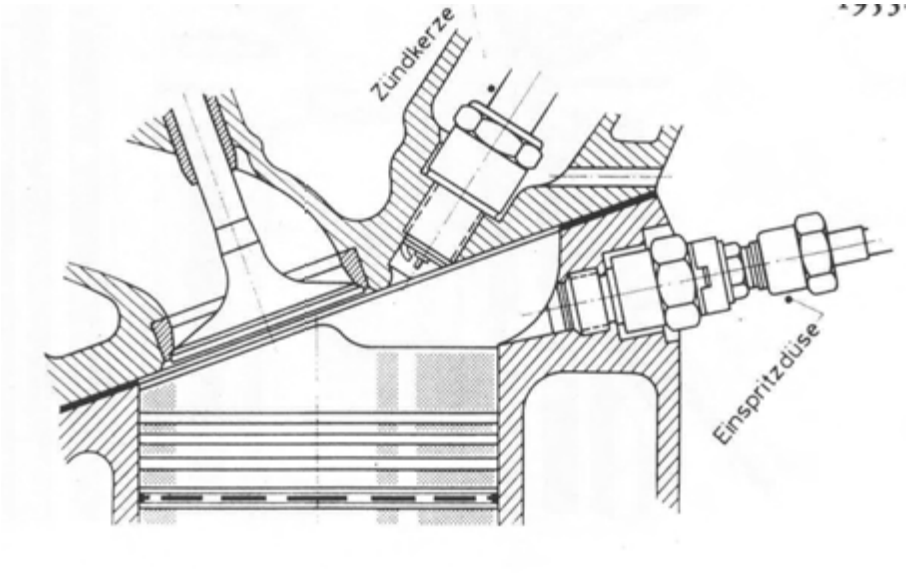

Figure 5-3: Mercedes 300 SL combustion chamber [5-3]
(Zündkerze = ignition plug; Einspritzdüse = injector)

Injection and combustion strategy.
The fuel was injected during the intake stroke in order to form the most possible homogeneous mixture at ignition as well as to use almost all of the air trapped during the intake stroke. Meanwhile, the injection began just after the intake valve closure and therefore allowed a quite wide overlap which directly benefited to high rev power.

Performances and benefits.
Compared to the original carbureted version, the Direct Injection engine offered more than 50% extra power and a much lower fuel consumption. Knock resistance was quite good, even in warm countries like Mexico. The main drawback, apart from cost and complexity, was reliability; even if the injector inclination avoided a direct wetting of the cylinder liner, during stop phases, the fuel was still injected after ignition cut-off due to the mechanically driven pump and the hydraulically activated injectors. The unburned gasoline was therefore mixed with oil, leading to both a quite large sump volume and very short oil service intervals.

- Ford, Volkswagen and Porsche concepts.

The Ford PROCO [5-5] – PROCO meant “PROgrammed COmbustion” - has been developed in the USA during the 70’s in order to reduce the gap in energy efficiency which existed between gasoline and Diesel engines. The basic idea was therefore to stratify mixture at TDC and so to operate the engine without throttling, even at part load.

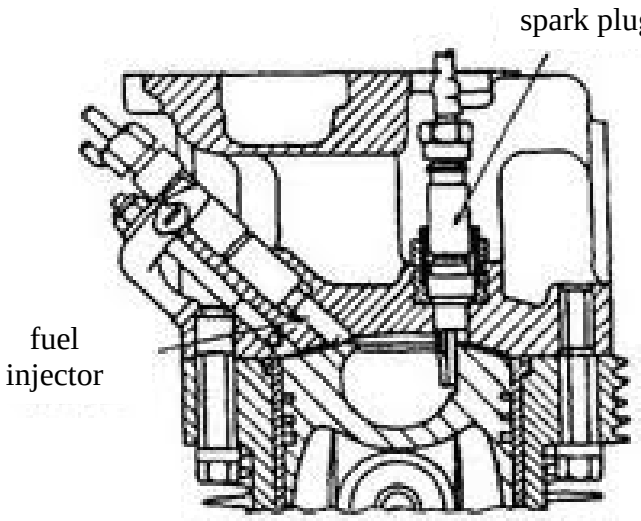

Figure 5-4: Ford PROCO combustion chamber [5-5]

Roughly ten years after, Volkswagen developed the "Futura" concept [5-6], which was primarily focused on achieving a "3 liter/100 km vehicle" coping with the US emission standard and avoiding the soot emissions inherent to Diesel.

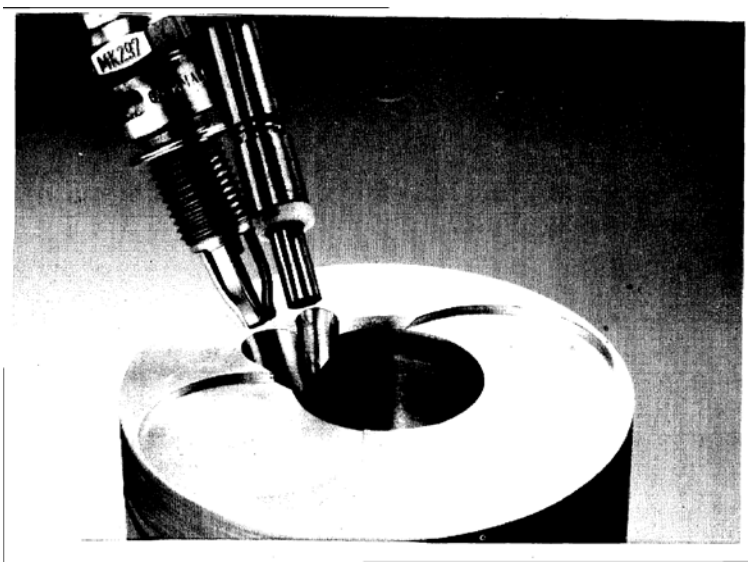

Figure 5-5: VW Futura combustion chamber [5-6]

During the late 80^{ies}, Porsche investigated different ways to optimize the efficiency of gasoline engines compared to Diesel. One of them was Direct Injection [5-7]

As these three last concepts were finally quite similar, and in order to avoid too many redundancies, their description has been gathered in the same following paragraph.

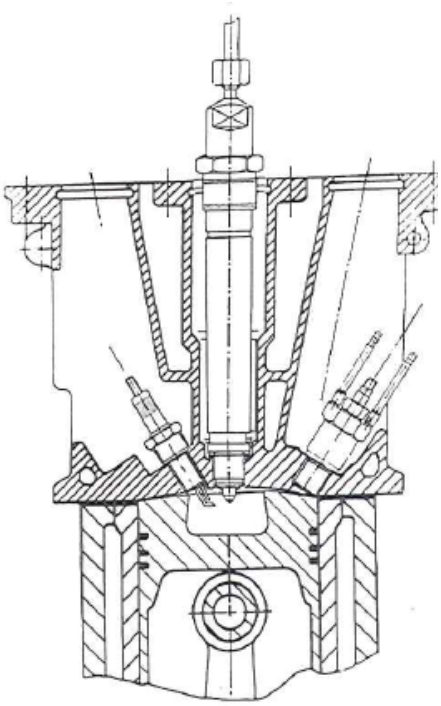

Figure 5-6: Porsche DEO (Direkt Einspriztung Ottomotor – Direct Injection Engine) combustion chamber [5-7]

Basic characteristics.

	Cylinder displacement cm^3	Stroke mm	Bore mm	Compression ratio	Number of valves	aerodynamics
Porsche	430	79.5	83	13 to 15	4	Swirl + squish
VW	425	86.4	79.5	16	2	

Table 5-3: basic characteristics of the Porsche DEO and VW Futura

General arrangement

The general concepts illustrated in Figures 5-4 to 5-6 were basically issued from the Diesel technology –eg with a bowl in the piston and a quite flat cylinder head with 2 or 4 valves.

The spark plug and the injector were very close one from the other on the VW and Porsche engines, probably to secure stratification at part load. With Porsche the injector was located at the center of the chamber and its tip was on the bowl side for VW.

On both concepts, elongated plugs were used.

Aerodynamics.

A swirl motion was generated by the intake port, in order to enhance the mixture at middle and high engine loads. According to VW, by the mean of the intensification factor linked to the reduced bowl diameter, this aerodynamics helped to mix the air with the fuel film coating the piston wall.

In order to reduce the intake pressure loss due to this design, VW choose to use a mechanically driven air compressor G40 for obtaining a reasonable level of performances.
Porsche used swirl at low and middle engine loads for combustion stability criteria, but its effect at high loads was quite negative, probably because of too high thermal losses at the walls.
Even if it had not been explicitly underlined by the manufacturers, the two designs presented a noticeable and quite symmetric squish area creating high turbulence levels around TDC by direct and then reverse air motion between the cylinder head and the piston.

Injection systems.
Both of them were based on Diesel units.
The VW one was designed and manufactured by Stanadyne; constituted by a distributor pump with dedicated ceramic parts in order to support the very poor lubricity of gasoline, it provided a maximum pressure of 450 bars. The pintle needle injector was particularly interesting because:

- the choice of an inwardly opening needle was led by spray stability criteria; outwardly opening needles were said to generate spray angles which were very sensitive to back pressure. This last drawback was said to be at the origin of misfiring at part load as the fuel plume was located too far from the plugs.
- A two steps valve lift was piloted by and roughly proportional to the injection pressure –see Figure 5-7.

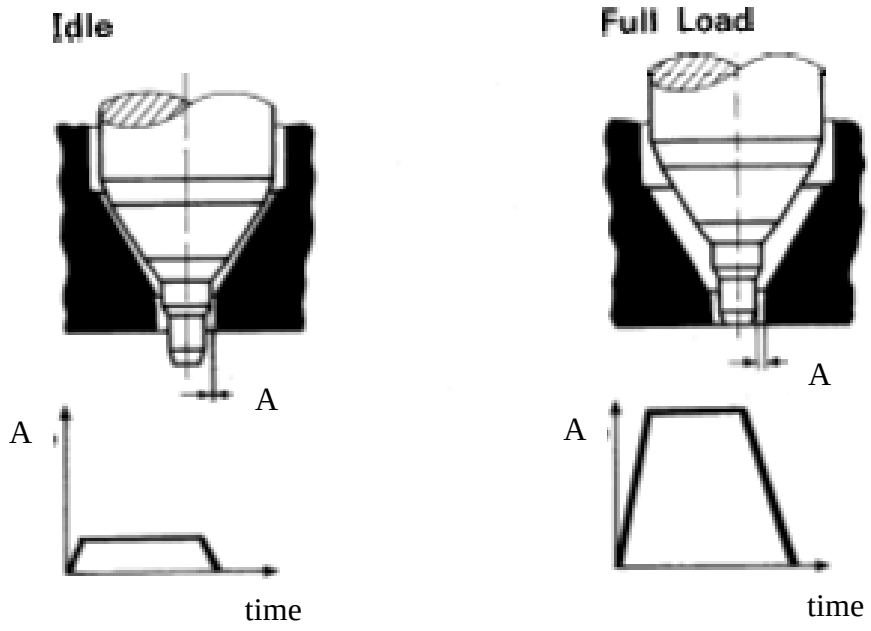

Figure 5-7: stroke curve of the Stanadyne injector used by VW [5-6]

Porsche used a system provided by Bosch with a maximum pressure of 120 bars. Preliminary tests showed that multi holes nozzles led to a poor combustion quality and stability. They therefore shifted to a pintle needle injector with different cone angles.

Injection and combustion strategy.
At high and full loads, on the VW engine, fuel was always injected late during compression in order to prevent knock and soot formation at low Air/Fuel ratio. The strong swirl generated a highly turbulent mixture in the bowl and the lean mixture could burn easily. The injector needle lift was set to the "high" position to reduce the injection duration and to improve the spray penetration in the cylinder, facilitating the use of all the air admitted during the intake stroke.
On the Porsche engine, the injection was set during the intake stroke and the mixture was roughly stoichiometric.

At part loads and at idle, the short needle lift and the low injection pressures generated short penetration sprays and highly stratified mixtures around the plug on the VW engine, probably without throttling.
On the Porsche engine, the best results in fuel consumption were obtained without throttling but stability was not satisfactory. The different arrangements of spark plug and spray cone angle failed to solve the problem, even if at idle an ignition phased during the injection period was the best solution. In this case the spark probably occurred in the spray and fouling was certainly at the origin of unstable cycles.

One main difficulty for these concepts was due to the hydraulically piloted injectors which limited the optimization of the injection timing, especially for transient and car applications.

Performances and benefits.
The Futura presented a peak power of 60 kW – eg 35 kW/l wich was a quite low value for a supercharged engine. The minimum specific fuel consumption was around 240 g/kWh at full load, with a great benefit of lean burn operation. Simulated NOx emissions were low enough to cope with the current US regulation of 0.8 g/mile.
Figure 5-8 presents results obtained on the Porsche engine.

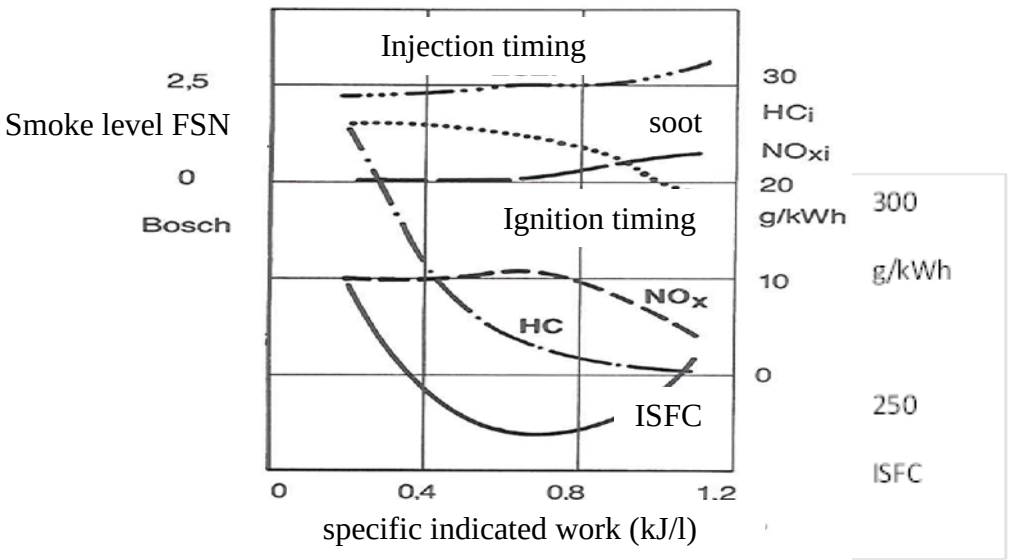

Figure 5-8: combustion results on the Porsche engine at 2000 rpm [5-7]
Injection and ignition timing are only for indication

A quite good ISFC of 220 g/kWh has been obtained at around 7 bars IMEP but the full load seemed to be limited around 11 bars; the throttling effect and the rapid increase of HC emissions above 4 bars explained the relatively disappointing efficiency in this area.

- Conclusion of the "state of the art" analysis.

The first point is concerning the achievement of a maximum power density of 37 kW/l. The three observed concepts derived from Diesel systems failed to procure this performance level, mainly because of a poor mixture preparation at high loads, leading to a limited equivalence ratio. The other origin was due to the intake port arrangement, designed for swirl and not for air filling.
On the contrary, the old Mercedes design completely fulfilled the goal at full load and even exceeded it while, of course, being completely unable to stratify at part load.
The second point is linked to the efficiency at part load; even if precise results were not very numerous, unthrottled operations were achieved successfully on the VW and Porsche engines but both with stability problems. Nevertheless the chosen arrangement of closed ignition plug and injector seemed to operate on both systems.
For air motion, squish was common and Porsche showed that swirl was not mandatory with a quite "open" chamber.

5.2.2.3. Choice of the general design.

The basic idea was to start from a completely open chamber like on the Mercedes engine in order to secure the peak power target.
Then, the question was how to fulfill the thermodynamic requirements for a good efficiency at part load as identified § 5.2.2.1:

- a capability to stratify the mixture around the spark plug, even at WOT and idle, with a late fuel injection
- a capability to secure a quick combustion around TDC
- a high chamber volume to wall surface ratio
- a high compression ratio

The second idea was thereby to locate the injector and the ignition plug as close as possible in the chamber, taking into account the spray angle sensitivity to ambient conditions and the spray angle dispersion according to the injector technology.
Finally the question of combustion velocity and turbulence was solved by retaining a large squish area like on all the previous engines.
The bibliographic investigation was furthermore pushed in the direction of lean burn solutions which were intensively developed during the 80's in order to reduce fuel consumption without introducing new technologies such as direct injection.

- The May Fireball concept.

The strategy developed by the Swiss engineer Michael May [5-8] was to promote lean burn conditions with a high compression ratio; Figure 5-9 shows the basic

arrangement with the combustion chamber located in the cylinder head, just under the exhaust valve, and with a very large squish area under the intake valve. The main advantages could be summarized as follows:

- the promoted squish generated a high and stable turbulence intensity in the chamber, promoting a quick and safe initial combustion phase
- the major quantity of the end gases were trapped under the exhaust valve and easily pushed out of the chamber during the exhaust cycle, reducing the amount of residuals.
- the mixture located in the large squish area hardly ignited due to a very low volume to surface ratio; these two last characteristics retarded the knock limit at very high load even if some concern could be noticed related to the plug positioned in a very hot zone which would be probably difficult to cool down.
- the exhaust valve heated the lean mixture and facilitated its ignition at low load.
- the flat piston was very reliable and cheap to manufacture

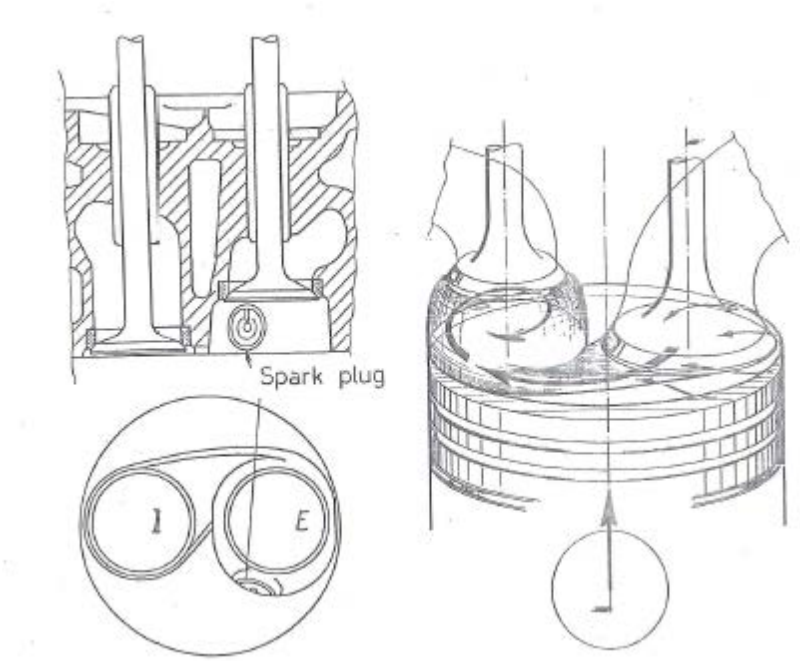

Figure 5-9: arrangement of the May Fireball combustion chamber [5-9]

With a RON 97 leaded gasoline, a May engine with a CR higher than 14 provided some good results in lean burn mode as shown in Figure 5-10. The comparison had been made on the same engine equipped with a conventional “Heron” chamber with CR 9. The advantage in efficiency at part load (1500 rpm and ~3.6 bars BMEP) is noticeable for A/F higher than 17; at the stoichiometry, the comparison was reversed, probably indicating some potential problems at full load. The NOx emissions were higher due to the CR.

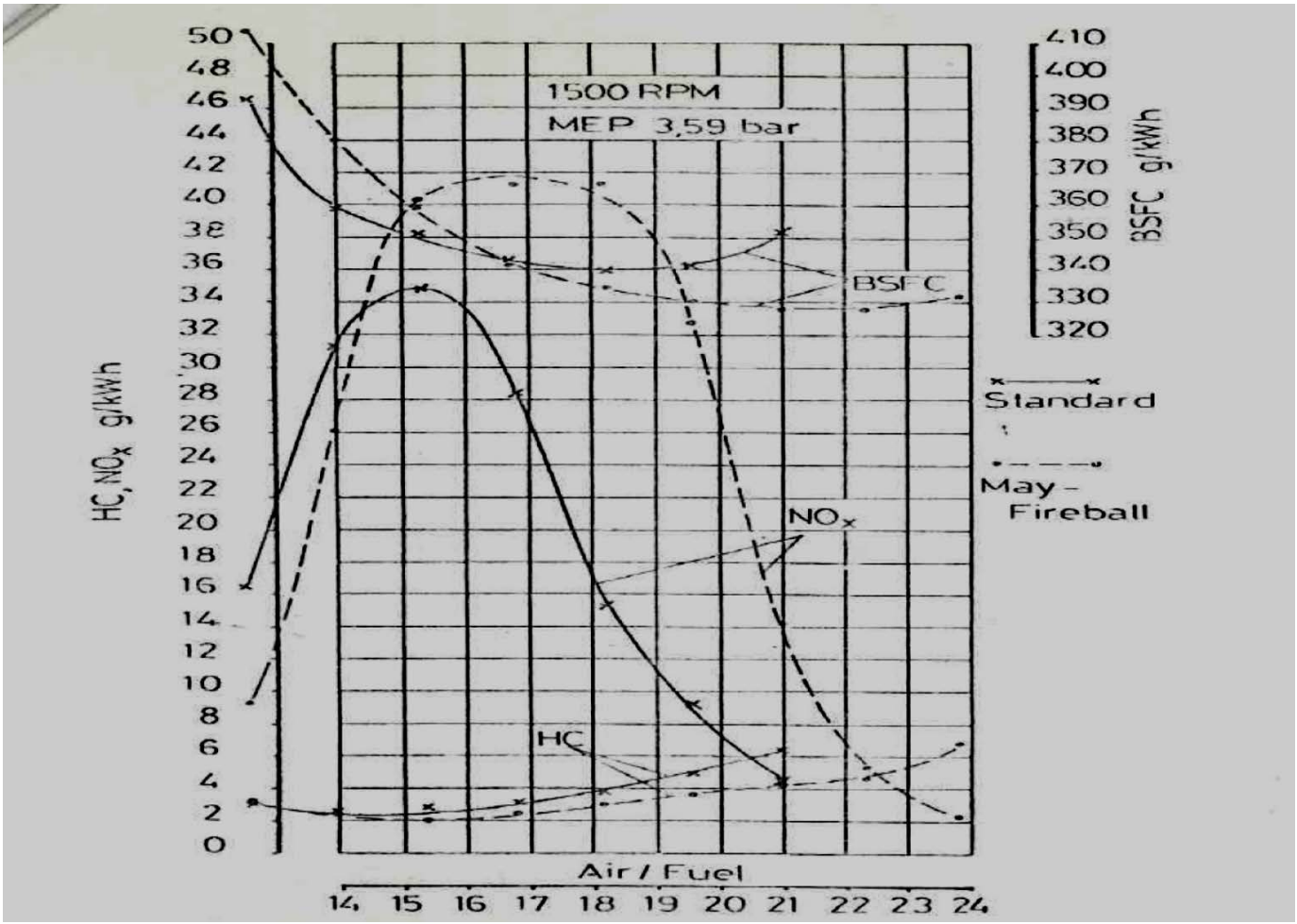

Figure 5-10: comparison of Heron (standard) and May chambers on a 620 cc single cylinder engine [5-9]

The May chamber has been applied in serial production on V12 and L6 engines by the English manufacturer Jaguar. The L6, which appeared on the market in 1988, presented a power density of 42 kW/l but operated only in stoichiometric mode with a three way catalyst; this choice, inherent to the small production volumes of Jaguar, was mainly due to the need of standardization between US and European markets and unfortunately prevented to get the benefits of the improved lean-burn capabilities.

Cylinder displacement cm^3	Stroke mm	Bore mm	Compression ratio	Number of valves	aerodynamics
486.5	74.8	91	12.6	2	squish

Table 5-4: characteristics of the Jaguar L6 engine with a May Fireball chamber [5-9]

- The MID3S concept.

Following the previously described investigation, the May Fireball arrangement was adopted, but with a direct injection –the MID acronym meaning in French “May Injection Directe”.
The large flat area available on the cylinder head allowed to install two intake valves for an improved air filling –eg “3S” meant “3 soupapes” (valves). The combustion chamber was entirely located in the cylinder head and the piston was completely flat.
The CR was controlled by changing the volume of the chamber; values between 12 and 14 were easily achievable.
The squish intensity was set at its maximum possible level with a squish height between piston and cylinder head of 0.8mm, which was the minimum value due to industrial dispersions.

Figure 5-11 describes the basic arrangement protected by the French patent 89-10440 [5-12].

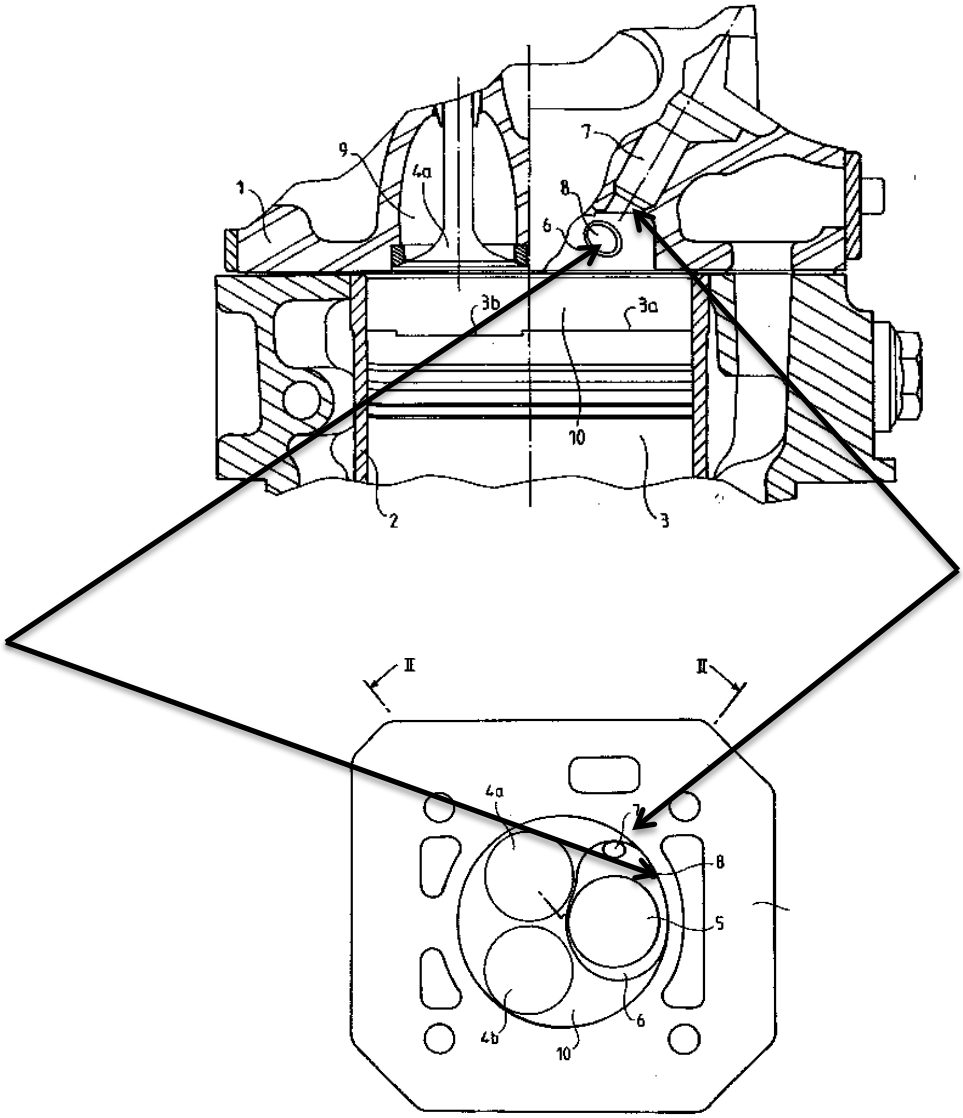

Figure 5-11: MID3S design [5-11]

One originality of the single cylinder development engine was the introduction of two endoscope locations –one for the flash light and the other for the film- directly in the cylinder head; these could be or not machined according to the tests. They were arranged in order to look at the mixture preparation and the combustion in the vicinity of the plug electrodes.

5.3. **Ignition and injection systems**.

5.3.1. The ignition system.

The initially chosen ignition plug had a diameter of 10 mm due to installation criteria and lack of available volume for the water chamber. Different manufacturers and models were tested, coming from the motorcycle industry or from previous Formula 1 engines. The best results have been obtained with the Champion G63 plug which equipped the Volkswagen Golf 16S Oettinger and the NGK C7E which equipped the Husqvarna 510 cm^3. Unfortunately, their too low thermal index often led to fouling and to misfire at part load where the combustion temperature was relatively low, which was specially the case in stratified operation mode.
The choice finally came to a BANTAM plug which was the adaptation of a 14mm plug to a 10 mm seat, like the Champion RC 12 YC.

5.3.2. The injection system.

5.3.2.1. Design and hydraulic performances.

As the potential of direct injection was clearly reduced by the use of inappropriate injectors adapted from currently available Diesel systems, a dedicated system developed for both 2 and 4 stroke gasoline engines was used [5-13] for the MID3S.

The main idea was to design a solenoid controlled injector completely independent of the pump and allowing the full possible range of injection timings. The maximum pressure was theoretically set to around 150 bars and multi holes nozzles were avoided according to the previously described competitor experiences.
At rest, the moving elements of the injector were hydrostatically balanced and only submitted to the mechanical force of spring B –see Figure 5-12. At the same time the outwardly opening needle was submitted to both the fuel pressure at its seat and the differential force of springs A and B. This solution was sufficient to secure sealing.
When the electric current was generated in the coil, the moving element and thereafter the spring A support were attracted by the magnetic circuit and the hydraulic force due to fuel forced the needle to open.

This arrangement allowed an opening velocity represented in Figure 5-13 by the maximum needle lift Y, quasi proportional to the fuel pressure, and a very short closure time Z, quasi-independent, as can be seen in Figure 5-13. At 90 bars the mobile train and the needle approximately have synchronous motions as $X_3=Y_3$.

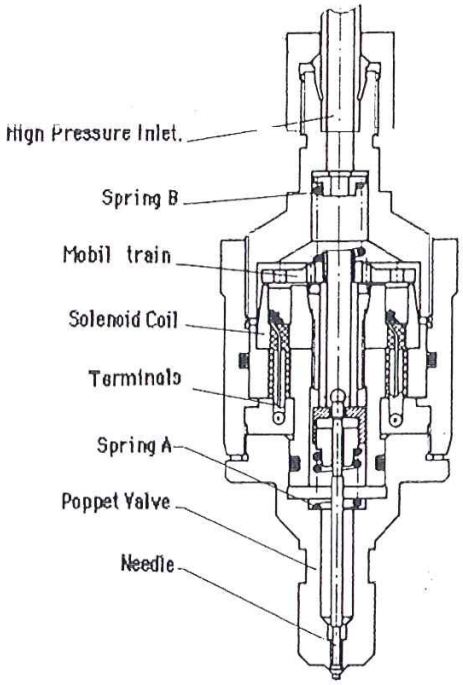

Figure 5-12: solenoid injector for Direct Injection applications [5-13]

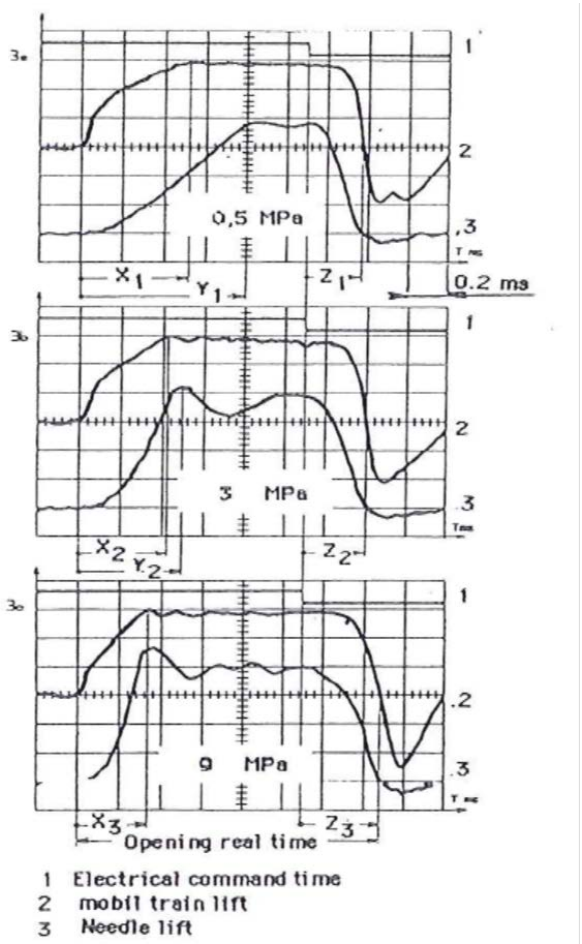

Figure 5-13: needle lift response versus electrical command time
at different fuel pressures from 5 to 90 bars [5-13]

5.3.2.2. Spray behavior.

The optimization of both combustion chamber design and injection/ignition tuning requires a good understanding of the spray behavior, primarily defined by:

- Spray structure.
- Cone angle
- Penetration

The use of the injection and visualization bench described §4.3.2 allowed to evaluate the spray sheet quality and properties such as its cone angle and its penetration according time. Unfortunately, these measurements were achieved at the atmosphere and with White Spirit for security reasons. In these conditions only the liquid part of the spray could be observed. The high speed cinematography was set at 8000 frames/s [5-14].
Several investigations, particularly obtained with an endoscope located under the injector, established that the spray had the structure of a hollow cone, the fuel being located in a sheet at the periphery of the cone. This hypothesis was comforted by observing the significant decrease of the spray cone angle during the injection –see Figure 5-14. If the first measurement at the very beginning of the injection was ignored due to very few points available to calculate the angle, the cone regularly got closer and closer until the end of the injection, from 48° down to 44°. This phenomenon was due to the air entrainment inside the hollow cone, reducing the pressure in this semi closed volume and therefore leading to a collapse of the spray angle.

Figure 5-15 presents photographs obtained by high speed cinematography. The qualitative analysis of the Mie scattering effects showed that the fuel sheet was not homogeneous, with many “fuel ligaments” which penetrated quite independently one from the others. Several photographs taken at the same timing after Start of Injection demonstrated that the fuel ligaments were located at the same position whatever the chosen spray was; this indicated that their origin could be linked to different pressure losses at the needle seat, losses probably due to machining defaults.

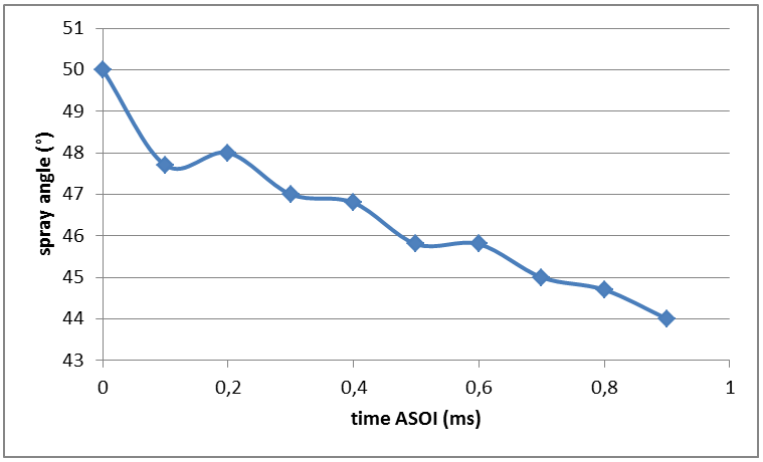

Figure 5-14: collapse of the spray angle according to the time after SOI (electric signal) [5-14]

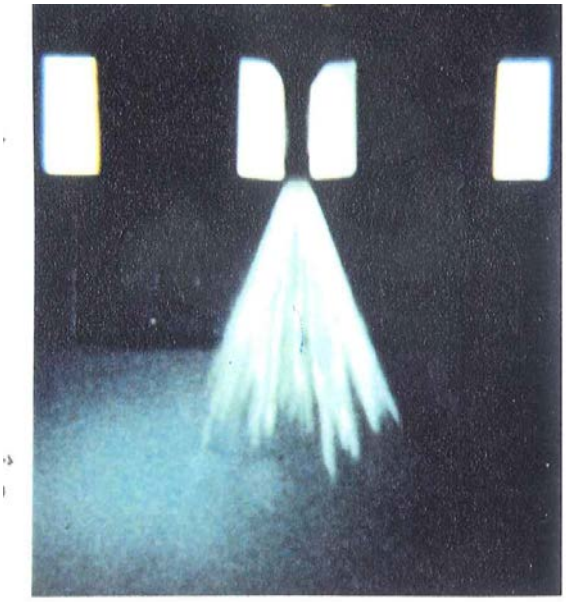

Figure 5-15: macroscopic structure of the spray (80 bars injection pressure, atmospheric conditions). Pphotograph obtained with high speed cinematography (8000 frames/s) [5-14]

This last observation could also be linked to the different sheet cone angle measured when rotating the injector around its axis. With always the same photographic method, results presented Figure 5-16 showed a variability difference of 5° - between 41 and 46°- according to the injector position for a theoretic value of 50° issue from the needle seat design.

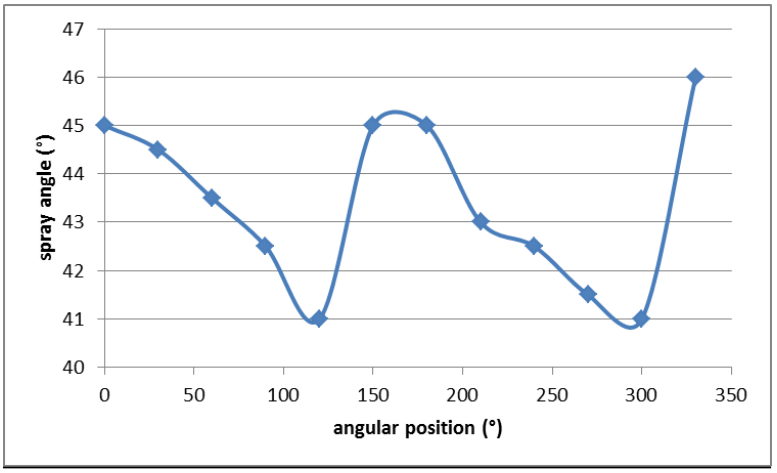

Figure 5-16: variation of the spray angle versus the injector angular position around its axis – Injection Pressure 80 bars, atmospheric conditions [5-14]

This default led to carefully set the injector in the cylinder head in order to secure – as much as it was possible- a reproducible spray distance versus the plug.

Finally some investigation had been achieved to get a first rough evaluation of the spray velocity. Using the methodology based on the evolution of the spray gravity center described §4.3.2.1, a value of 75 m/s was obtained just after the beginning of the needle lift, value decreasing to 20 m/s after the end of injection –see Figure 5-17- for an injection pressure of 100 bars. The comparison with the Bernouilli velocity, calculated at 160 m/s, was quite coherent with the theory.

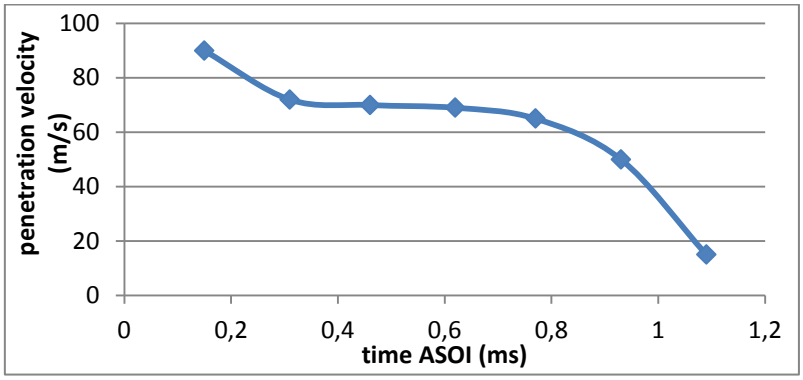

Figure 5-17: spray tip velocity versus time after SOI – injection pressure 100 bars [5-14]

5.3.2.3. spray atomization.

A tentative for qualifying the spray atomization and the droplet size was achieved at the Institut Saint Louis with a laser micro-holography technique –see Figure 5-18.

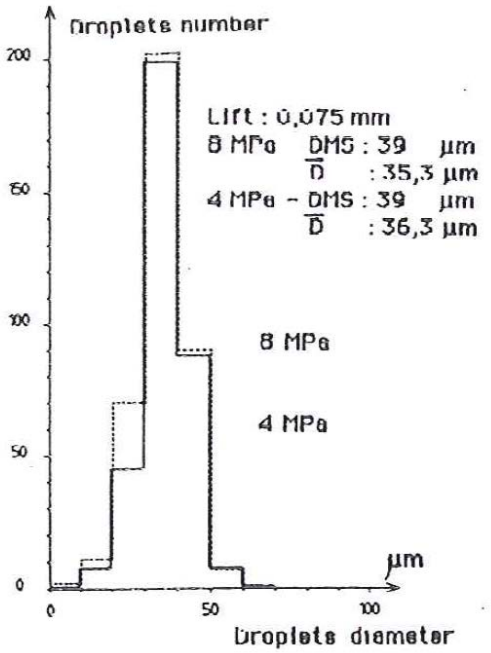

Figure 5-18: droplet repartition for two different injection pressures (40 and 80 bars); atmospheric conditions (DMS = SMD) [5-13]

The injection pressure –eg 40 and 80 bars- showed a little effect on the Sauter Mean Diameter SMD while the distribution was quite narrow with no diameter higher than 60 µm. Nevertheless the accuracy of the technique and the use of White Spirit to avoid explosion hazards could be in question.

5.4. **Mixture preparation**.

Several tentative for using 3D simulation on the MID3S combustion system unfortunately failed to provide acceptable results; a lot of time has been spent for carefully calibrating the spray model but the sensitivity to the back pressure was never correctly predicted, probably because these models had been developed for Diesel injectors and not GDI. As mixture preparation effects were of first order importance for describing the stratification process and as the spray behavior was highly dependent on the ambient conditions which varied during the compression stroke, it was decided to focus the activity on experimental optical techniques. In-cylinder visualizations with endoscopes were therefore intensively used to qualitatively describe mixture preparation and combustion.

5.4.1. Experimental set-up.

The optical techniques used for this task have already been described in §4.3.2.2; this item is therefore focused on the set-up dedicated to the MID3S combustion chamber. Figure 5-19 describes the general arrangement of the injector, spark plug, flash lamp and endoscope, both of them being protected by a quartz window. The endoscope was linked to a HYCAM high speed camera operating between 3 and 8000 frames/second.

Flash lamp and endoscope were oriented in order to visualize the spray in the vicinity of the injector and of the ignition plug. That is to say that this work mainly concerned the stratification capabilities of the system.

A yellow filter was used before the camera to enhance the contrast between the droplets and the wall and to avoid a too high light intensity.
Some very simple optical corrections were used to take the geometric orientation of the endoscope into account.
During tests concerning mixture preparation, the engine was motored to avoid any fouling of the quartz windows with combustion products and especially soot deposits.
Limitations of this methodology concerned a reduced evaporation rate of the fuel, even if a current gasoline RON 95 was used; some effects due to a lower wall temperature and a slightly reduced compression ratio due to short test duration with the firing engine could be the source of this deviation, but probably remained of second order of importance relatively to the physics of the phenomena.

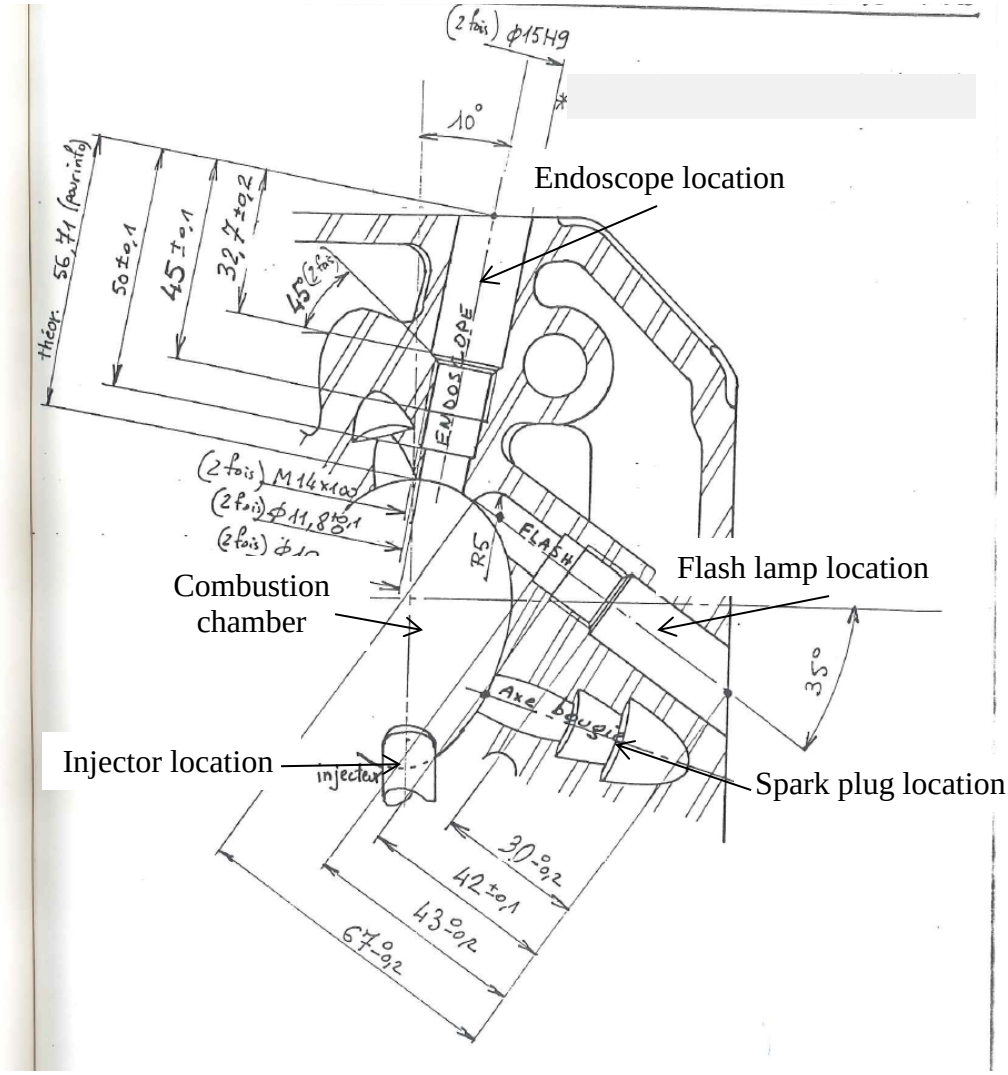

Figure 5-19: general arrangement of the visualization system adapted to MID3S chamber. “bougie” = ignition plug [5-13]

5.4.2. Mixture preparation results.

The single cylinder engine operating point was set at 2000 rpm with an injected fuel quantity of 15.5 mg/stroke, which roughly corresponded to 3 bars BMEP according to the efficiency. The focus was made on the stratified mode.

The injector spray presented a cone angle of 45° measured in atmospheric conditions.

The –mainly- qualitative criteria used for the comparison of different tunings were wall wetting by the fuel, spray plume behavior in the vicinity of the ignition plug and estimated “stratification” in the chamber.

The investigated parameters were injection pressure, injector nominal sheet angle, intake pressure –throttling- and injection timing.

5.4.2.1. Macroscopic observation of the films.

- Effect of the injection pressure.

For all the tests, the engine was operated at WOT with a fixed injection timing of 60°CA BTDC; two injection pressures -30 and 100 bars- were investigated.

Photographs obtained at 30 bars are presented in Figure 5-20.
The droplet penetration was very low with a maximum value which was reached very quickly after SOI; this was due to both a quite low initial droplet velocity at 30 bars and a rapid increase of the gas pressure due to the high compression ratio. At the same time, the spray got larger and larger with an apparent initial cone angle increasing from 57° just after SOI up to more than 80° only 9°CA after.
Due to the strong squish motion and the relatively low droplet momentum, the liquid part of the spray was deviated towards the spark plug and the chamber wall, as the fuel cone became asymmetric; all these effects led to a high stratification level with a presence of liquid around the spark plug (see the red circle on the picture).

The situation was quite different for an injection pressure of 100 bars as can be seen in Figure 5-21. The spray remained much more symmetrical versus its axis and was marginally influenced by the squish motion, remaining at a noticeable distance from the chamber wall. As soon as the injection was finished, the liquid phase disappeared but a significant amount of fuel vapor certainly remained in the vicinity of the plug.

- Effect of the intake pressure

The idea was to have a better understanding of the effect of a slight throttling in stratified mode. For all the tests, the engine was operated at 100 bars injection pressure and with an injection timing at 51°CA before TDC; two different relative intake pressures, 0 and -60 mbars, were used.

Even if the influence was quite moderate, the reduced pressure in the chamber led to a slightly lower initial spray angle; the angle difference was 10° at SOI and 15° at 8°CA after. The apparent plume area was also a bit higher with the low intake pressure, leading to a lower stratification and less wetting risks around the spark plug.

- Effect of the injection timing

For all the tests, the injection pressure was set at 100 bars with WOT.
The film was very much helpful to visualize the spray deformation when the injection timing was reduced; as the squish motion increased when the piston was coming closer to TDC, the interaction between the spray and the air became stronger and the fuel plume was more and more disturbed; the spray shape was less and less conical and droplets were transported towards the chamber wall, especially after 30°CA BTDC, leading to a higher stratification.

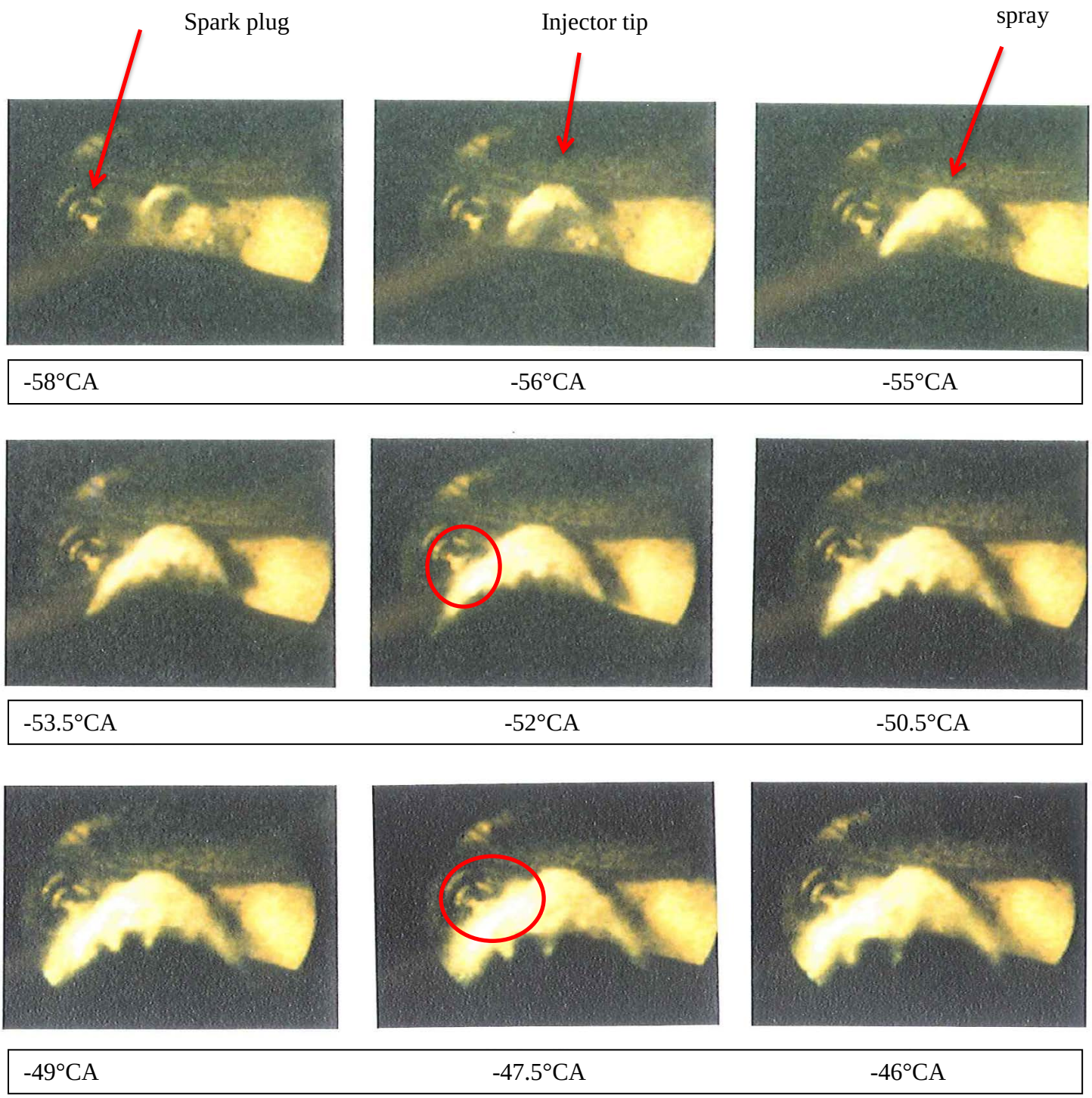

Figure 5-20: spray visualization in motored mode – 2000 rpm WOT- Injection Pressure 30 bars – 15.5 mg/stroke – SOI 60°CA BTDC – photographs taken at different °CA after SOI [5-14]

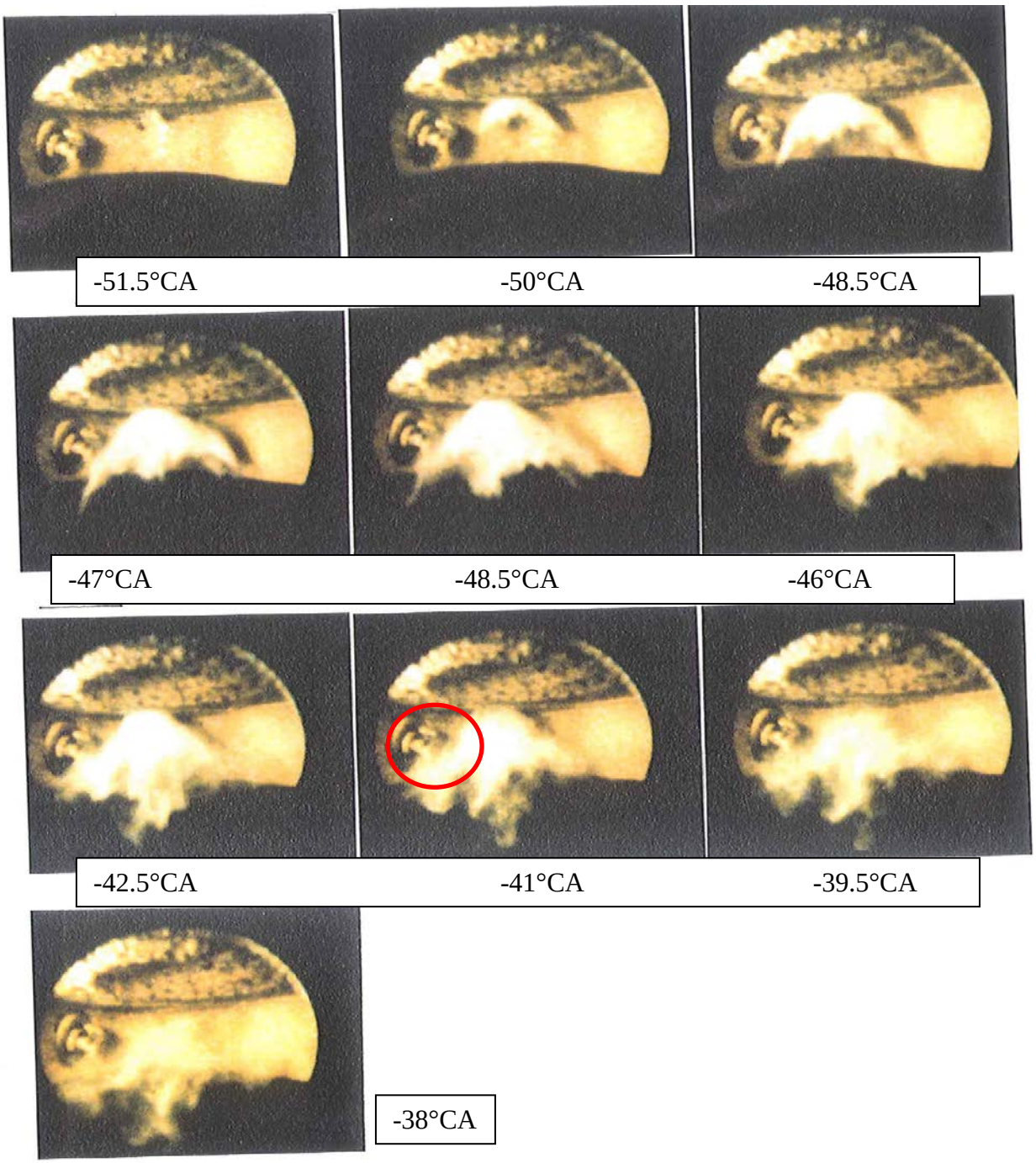

Figure 5-21: spray visualization in motored mode – 2000 rpm WOT- Inj.Pressure 100 bars – 15.5 mg/stroke – SOI 60°CA BTDC – photographs taken after SOI [5-14]

5.4.2.2 Explanation of the physics

Figure 5.22 represents the evolution of penetration, angle and apparent surface of the plume during the injection. SOI of the 30 bars injection pressure conditions has been chosen as the time origin in order to secure the same ambient conditions at each CA.

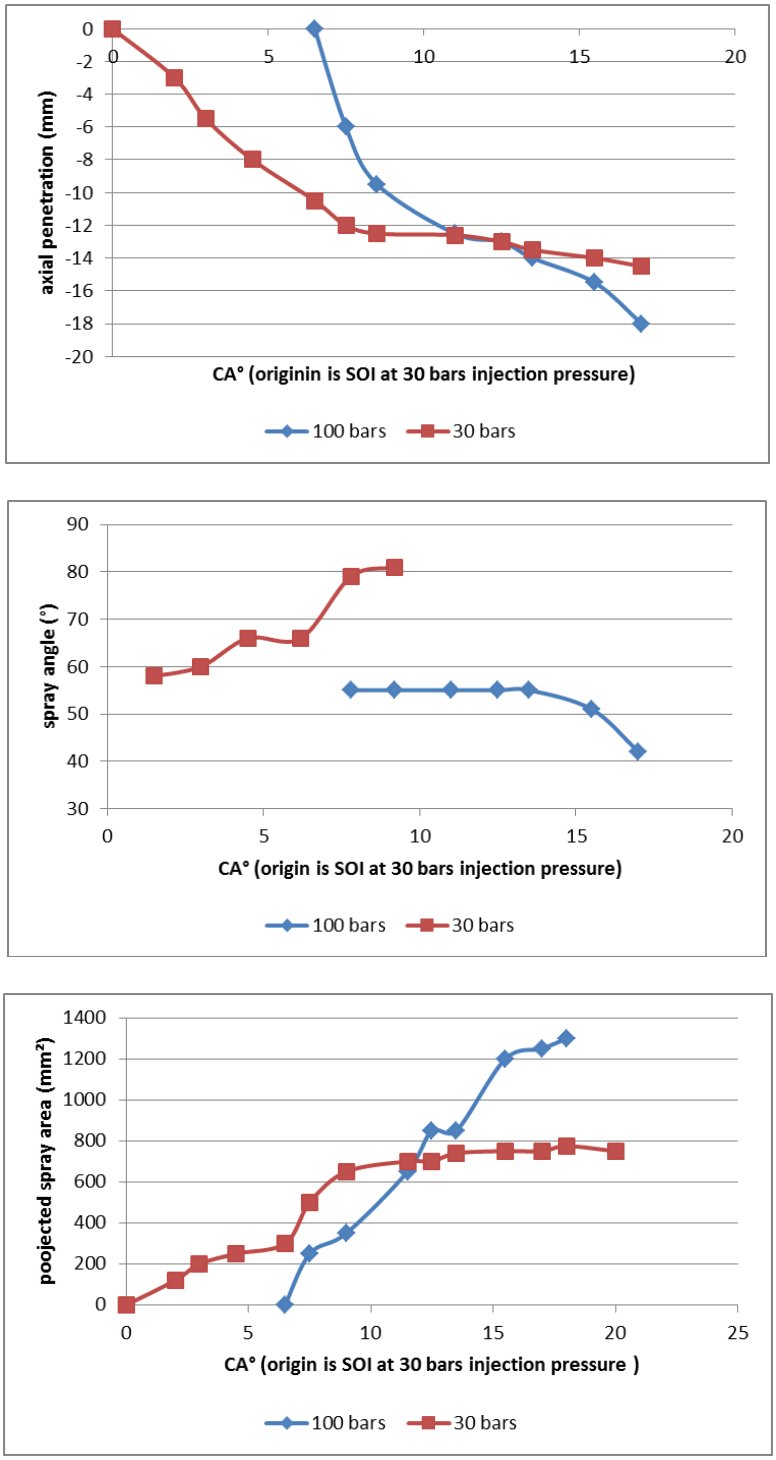

Figure 5-22: effect of the injection pressure [5-14]

Figure 5-23 represents the influence of the injection timing at constant injection pressure 100 bars and WOT.

.

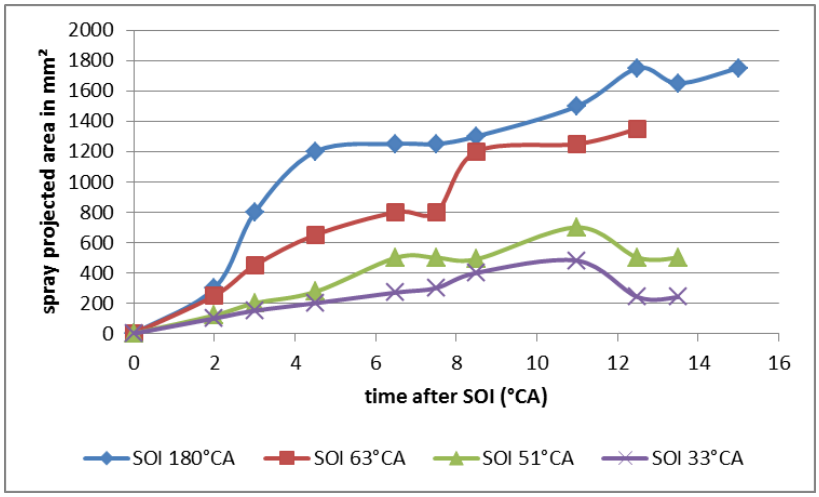

Figure 5-23: effect of the injection timing on the projected area of the spray plume [5-14]

Concerning the penetration velocity, the explanation seemed to be quite easy because of the direct link with the droplet momentum; at 30 bars injection pressure, they were very early stopped due to the increase of the back pressure and the ascendant air motion.

This last factor was also influencing the spray angle but was coupled with the effect of the air entrainment outside and inside the hollow cone:

- At 30 bars injection pressure, compared to 100 bars, the air entrainment was weaker and the superposed air and droplet velocities led to a higher angle. At 100 bars the two phenomena were balanced because the air entrainment inside the spray was higher.
- With a lower back pressure, the air entrainment was lower, so the pressure drop inside the cone was smaller, but few droplets were diffused at the periphery of the jet, generating an optically lower apparent angle.
- When the injection timing was decreased, the back pressure increased at SOI, with thereby an increased pressure drop inside the cone due to the air entrainment and a more important collapse of the cone angle.

The projected area of the plumes was the direct consequence of the evolution of the penetration and the angle.

It was nevertheless difficult, without a sophisticated 3D simulation tool, to quantify these effects.

5.4.3. Conclusion.

The different visualizations showed that a fine stratification could be achieved at a quite high injection pressure ~100 bars and a late injection timing; the reduced

spray penetration associated to the high squish effect pushed the fuel in the vicinity of the spark plug.
Nevertheless, due to its hollow cone structure, the spray was very sensitive to the ambient conditions –eg the chamber back pressure and the aerodynamics- which could lead to wall or plug electrodes wetting and which could also lead to important cycle to cycle variations in the Fuel/Air ratio in the ignition area.

5.5. Combustion.

Several operating points had been chosen to illustrate the NEDC –New European Driving Cycle- used to homologate fuel consumption and pollutant emissions on a medium size sedan – Renault R21- equipped with a 2.0 liter engine:

- 1000 rpm and low injected quantity to represent idle conditions
- 2000 rpm and 15.5 mg/stroke as injected quantity
- 2000 rpm and 8.5 mg/stroke

all representative of the urban part of the cycle

- 2500 rpm and 25 mg/stroke

representative of the "high speed" cycle –acceleration until 120 km/h.

A full load WOT trace at different engine speeds was of course achieved to evaluate the performance capabilities.

In some cases, a comparison with conventional port injected single cylinder engines called "Mono J6R" (2 valves) and "J12S" (3 valves) with the same displacement was achieved to have a better idea of the effect of the direct injection and of the stratification.

The same single cylinder engine equipped with dedicated cylinder heads (endoscope locations were or not machined) was used for both combustion and visualization tests.

A regular R0N 95 unleaded fuel was used.

5.5.1. Full load results.

5.5.1.1. Global results.

All the tests have been achieved with a constant equivalence ratio of 1.10 [5-15]; the ignition and injection timing were chosen to obtain the best possible torque at the knock limit. The injection pressure was set at 80 bars.

Figure 5-24 presents the IMEP and ISFC obtained between 1000 and 4250 rpm – the two limits were linked to the single cylinder engine and to the test bench capabilities. The corresponding ignition and injection timings are illustrated in Figure 5-25.

Two different regions were observed:

- At 1000 rpm where ignition had to be set 10°CA after TDC to avoid knock, explaining poor IMEP and ISFC.
- Between 1500 and 4250 rpm where the IMEP remained quite constant and where the ISFC was reduced as engine speed was increasing.

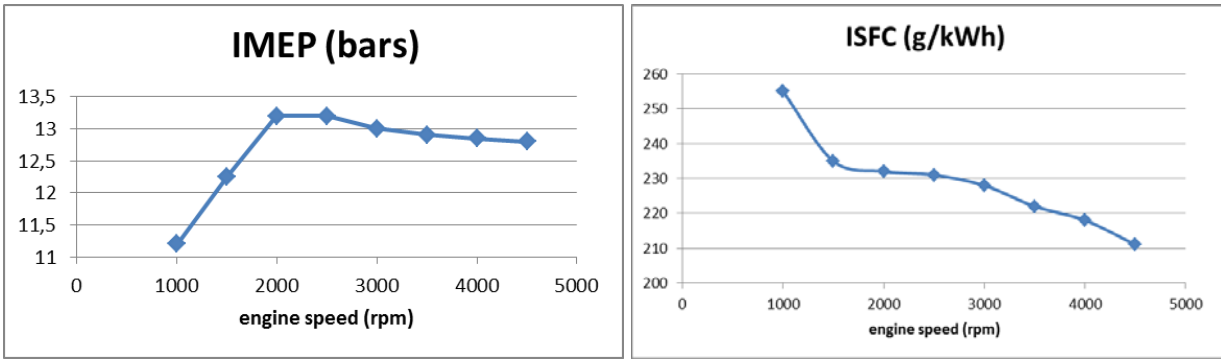

Figure 5-24: full load WOT engine response – equivalence ratio 1.10 [5-15]

5.5.1.2. Injection timing.

Two phenomena were at the origin of the chosen tuning:

- The necessity to evaporate all the fuel before ignition, which led to inject as early as possible.
- The interest of injecting later during intake and compression strokes in order to obtain a better cooling effect when fuel was evaporated in the cylinder, effect which was positive for reducing the compression work (higher polytropic coefficient –see § 5.2.2.1) and for reducing the knock sensitivity.

These two requirements explained that the injection began as early as possible at 4500 rpm because of the short time available in ms and that the ignition was delayed as the engine speed was reduced.

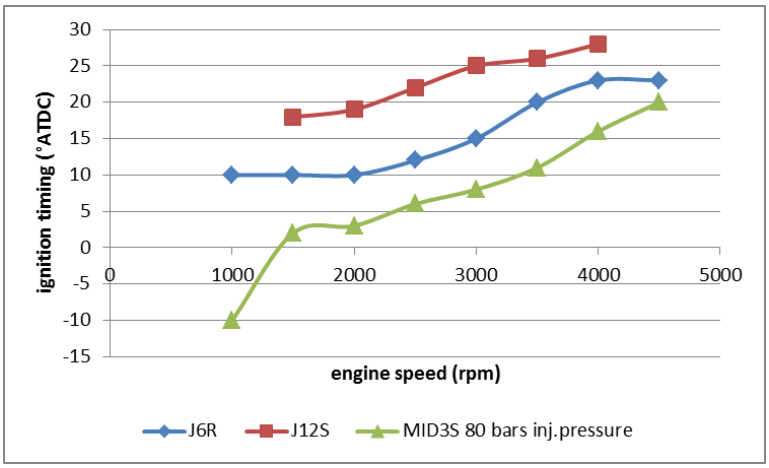

Figure 5-25a: ignition timing at full load (all the data are concerning single cylinder engines) [5-15]

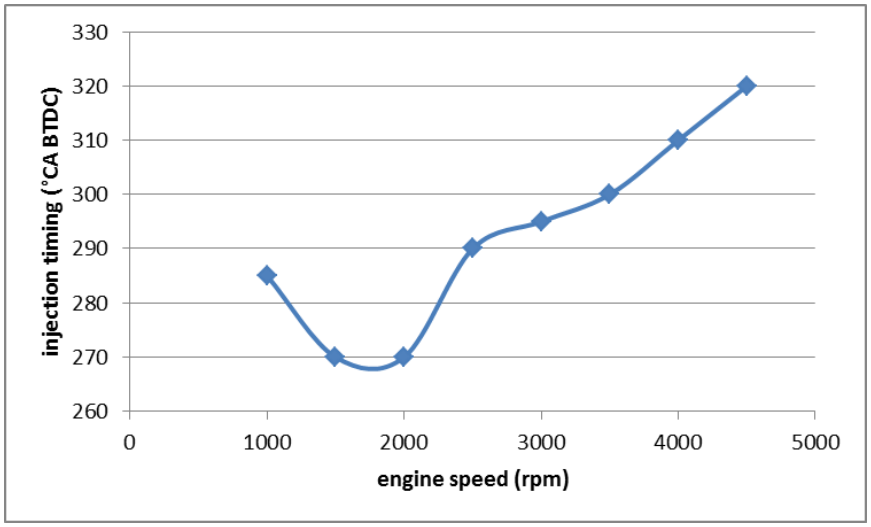

Figure 5-25b: injection timing at full load (all the data are concerning single cylinder engines) [5-15]

Nevertheless, at 1000 rpm, the general trend observed at higher speeds would have led to retard the injection around 240-250°CA BTDC to take full benefit of the cooling effect during the fuel evaporation. Unfortunately, the air motion was probably not sufficient to enhance the fuel/air mixing and time had to be added to achieve a correct homogenization.

5.5.1.3. Ignition timing.

The effect of the high CR was quite obvious with a global difference of about 7°CA with the J6R at speeds higher than 1000 rpm; the high CR on the MID3S engine was probably partially compensated by the cooling effect due to a late fuel evaporation with direct injection. The evolution of the ignition timing with the engine speed followed the same trend as on the port injected engines, probably proving the similarity between the two combustions.

At 1000 rpm, an ignition after TDC was necessary to avoid knock; the combustion was very brutal and occurred too late during the expansion stroke. A low level of turbulence was probably the main root for this behavior.

5.5.1.4. Effect of the injection pressure.

At 30 bars, performance strongly decreased and fuel consumption increased compared to 80 bars. As, according to § 5.3.2.3., the atomization seemed to be quite comparable, this lack of torque was probably due to a lower spray penetration and therefore a bad mixture preparation as the air was not completely used.

5.5.2. Part load results.

5.5.2.1. Choice of the injection pressure.

For all the tests the injection pressure was set at 80 bars as the engine refused to run properly at 30 bars due to a too high instability. This result was easily explained by visualization –see §5.4.2.1. A very high quantity of fuel was deflected towards the spark plug with a too high and too early stratification, leading to wetting, fouling and thereby no ignition. On the contrary high injection pressures lead to a quite nice stratification in this area.

5.5.2.2 Choice of the ignition timing.

According to mixture preparation tests, the ignition timing was set at the end of the injection command determined by the electric signal provided to the injector; at 2000 rpm, this corresponded to an ignition around 10°CA after the actual SOI measured on the films; at this timing fuel vapor and/or fine droplets were entrained towards the plug by the squish motion as shown Figure 5-26.

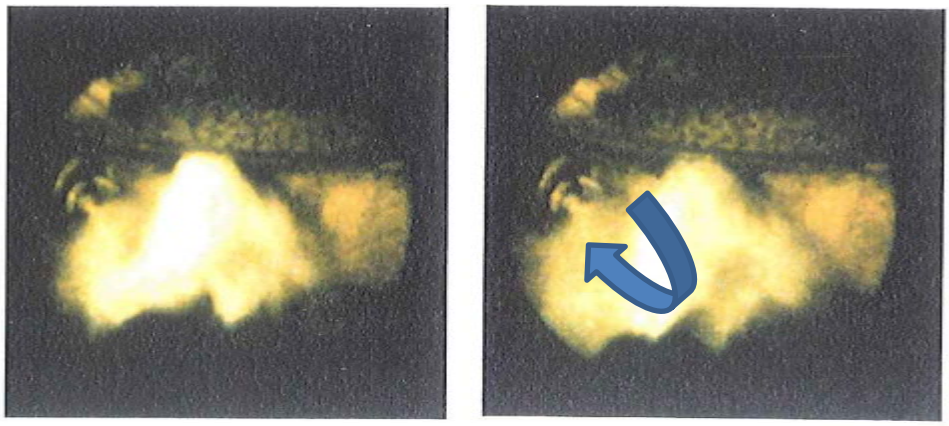

Figure 5-26: spray visualization in motored mode – 2000 rpm WOT- Inj.Pressure 100 bars – 15.5 mg/stroke – SOI 60°CA BTDC – photographs taken 10 and 12°CA after real SOI [5-14]

This resulted in a quite fine stratification with moderate Fuel/Air ratio.

5.5.2.3. Optimization of the injection timing.

The aim of the trade-off was to optimize both fuel consumption and NOx emissions while securing an acceptable combustion stability. For all the part load operating points considered during the tests, the best compromise was to start the injection as late as possible during the compression stroke. For injected quantities of 15.5 and 8.5 mg/stroke, this setting corresponded to an injection timing of respectively 60 and 55°CA before TDC.

For earlier settings, NOx emissions linearly increased with timing; for later settings, the stability became unacceptable; an interesting point was related to the fuel

consumption whose variation was quite moderate. Figure 5-27 illustrates results obtained at 2000 rpm and 8.5 mg/stroke for two different equivalence ratios (equivalence ratio 0.28 corresponded to WOT).

The effect of injection –and automatically ignition- timing on NOx emissions was well known on all SI engines because of the sensitivity of this pollutant to the residence time at high temperatures.

The effect on engine stability could be explained by the spray behavior as seen §5.4.2.1. For very late timings, despite a high injection pressure, the spray was too much deviated by the strong squish motion, with a very low penetration due to the back pressure; these two phenomena led to a very high stratification, high Fuel/Air ratio near the plug and possible fouling effects as seen after examination of the plug.

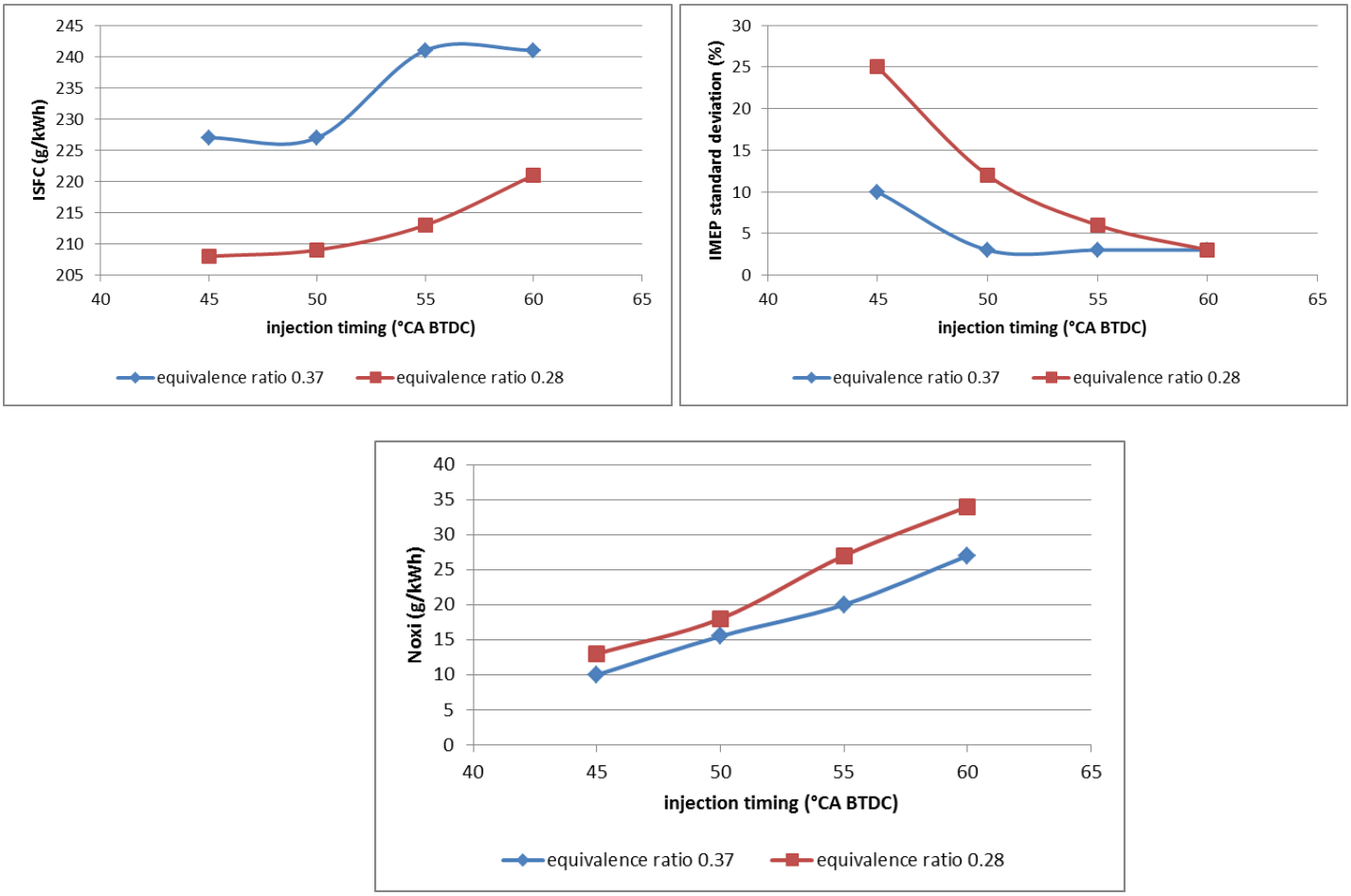

Figure 5-27: single cylinder engine results – 2000 rpm 8.5 mg/stroke – [5-15]

5.5.2.4. Influence of the equivalence ratio.

- Results analysis.

During these tests, the engine was operated with different intake pressures modified by the throttle position. The minimum equivalence ratio was obviously obtained at WOT. Injection and ignition timing were kept constant.
All the results obtained at 2000 rpm and 15.5 mg/stroke are illustrated in Figure 5-28.

The first key point was to check the coherence between MID3S and J6R results; even if combustion chamber and CR were a bit different –CR of the J6R was 9.5 with a 2 valve cylinder head and a "hemispherical" chamber - results with neighbored equivalence ratios might not be too different in terms of stability, ISFC and air filling. This important item was realized for equivalence ratios of 0.7 and 0.8.

Concerning combustion stability, a standard deviation of IMEP was accepted until 3 or 4% for this operating point. This was achieved until 0.8 for the J6R engine and until 0.55 for the MID3S in stratified mode. This level increased very much for leaner mixtures and reached 9% at 0.45 at WOT. As the fuel consumption continued to decrease until this value, it was particularly interesting to understand the origin of the instabilities. This item will be analyzed § 5.5.2.4.

The equivalence ratio decrease was obtained by opening the throttle valve and thereby increasing the amount of air in the chamber; the air filling increased from 0.55 up to 0.85 and this high dilution was followed by a linear reduction of the exhaust temperature from 510 down to 320°C. Meanwhile the indicated NOx emissions strongly increased from 10 up to 22 g/kWh, pointing out that the combustion probably occurred with a local equivalence ratio closer to 0.9, as this value is generally admitted to correspond to the maximum production rate for NOx; this last remark was confirmed by the evolution of the same pollutant on the J6R engine.

On the contrary, the good new was provided by the quite moderate levels of HC and CO showing that, either the local equivalence ratio was never too high in the chamber, either the temperature was sufficient to oxidize them.

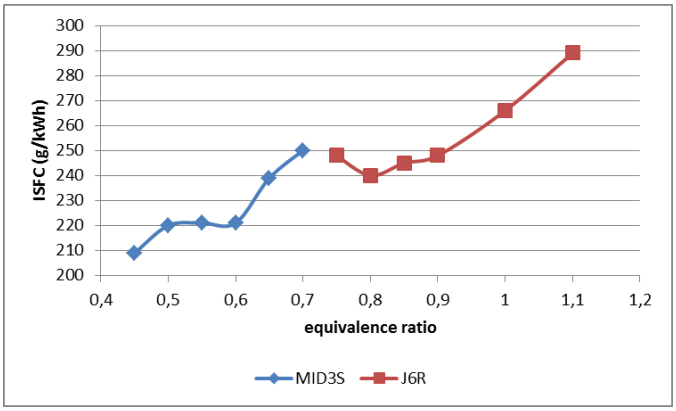

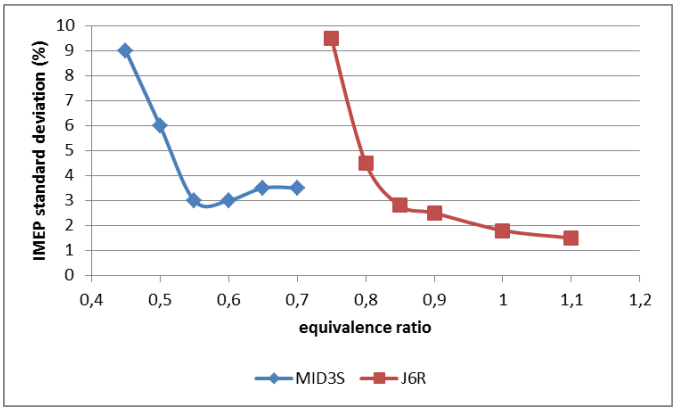

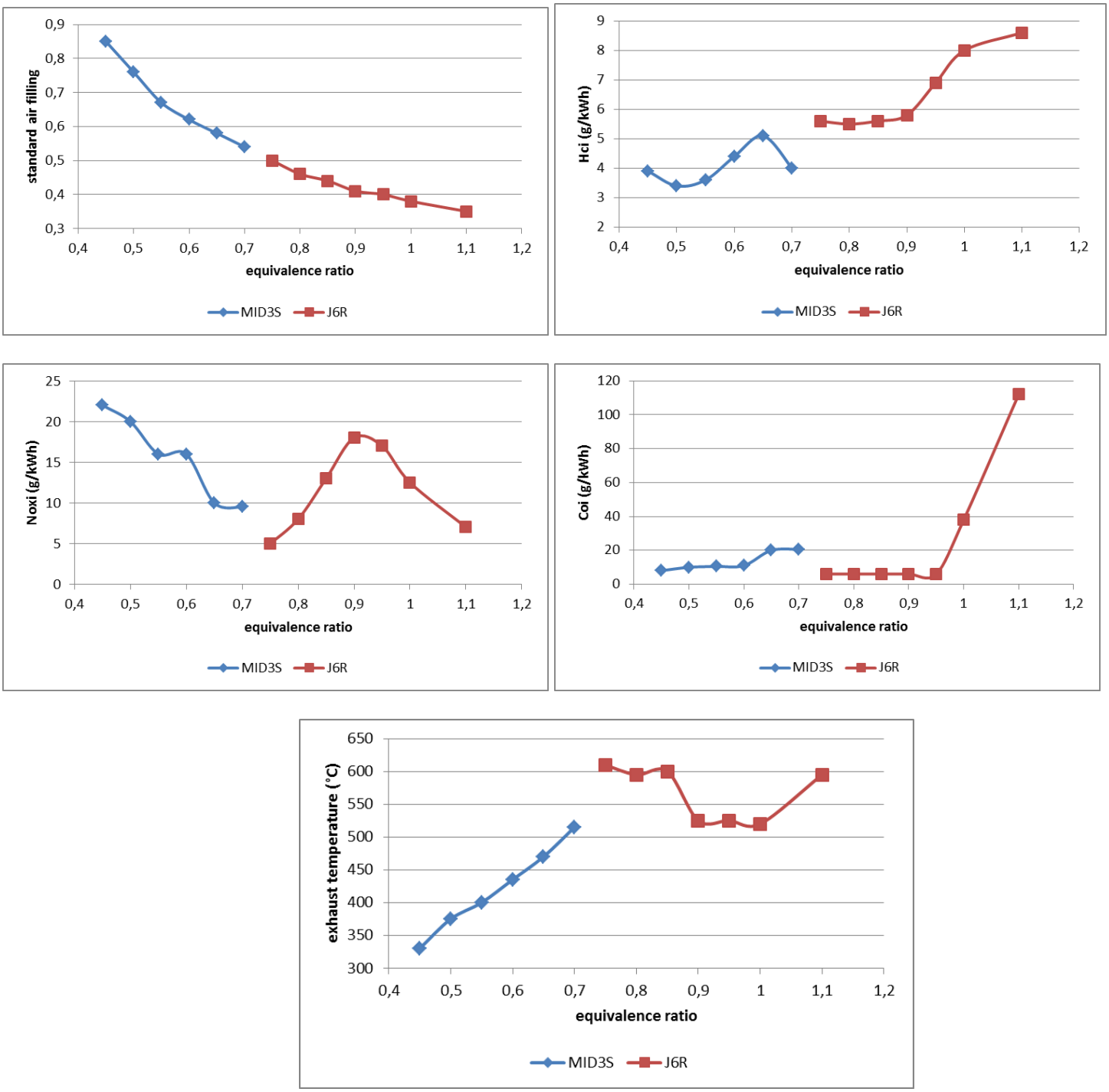

Figure 5-28: single cylinder engine tests results at 2000 rpm – 15.5 mg/stroke [5-15]

- Combustion analysis.

For equivalence ratios between 0.7 and 0.45, around 57% of the injected fuel was burned at TDC; this behavior was known as not optimal for fuel efficiency because a bit too early in the cycle.

The detailed analysis based on the first principle of thermodynamics clearly stated four different steps during the combustion event:

- A very sharp energy release between -35 and -10°CA with a maximum rate around 0.05/°CA and a noticeable noise level on the bench (Ph1)
- A rapid decrease of this combustion velocity to very low values around TDC (Ph2)
- A third phase occurring between 5 and 25°CA as if combustion was starting again (Ph3)
- A quite long end of combustion after 30°CA which made an early ignition mandatory and thereby explained a decrease of the efficiency (Ph4).

This global scenario was reproduced for each equivalence ratio from 0.7 to 0.45, with only minor changes as it is presented Figure 5-29. This was probably linked to the aerodynamic system and thereby the induced turbulence level: the squish motion is efficient on both sides of TDC, collapses at TDC –piston is not moving- and is very much reduced during the expansion phase.

Concerning the effect of the equivalence ratio, Phase 1 of the heat release showed the greatest sensitivity; at 0.7 –upper Figure 5-29 -, with the same injection and injection timings, the combustion started later during the cycle than for the leaner case at WOT; the other phases remained quite unchanged.

The explanation was probably linked to the local equivalence ratio in the vicinity of the plug. In §5.4.2.2, it was established that the lower intake pressure lead to a lower stratification and a leaner mixture near the plug than at WOT. With the lower global equivalence ratio, the mixture was probably very rich near the plug.

The second and third phases, as they occurred at the beginning of the expansion stroke, were probably representative of the combustion of a very lean mixture, enriched by the aspiration of the fuel initially located near the piston surface to the squish area.

The high speed cinematography used on this operating point could provide similar information: the first illumination on the film appeared roughly 10°CA after ignition (40°CA BTDC), with a yellow zone developing quite quickly from the plug to the chamber –see Figures 5-30 for the images and 5-31 for the evolution of the projected “yellow surface” versus time. This apparent velocity was almost constant during 15°CA; this period has always been observed before TDC, which is coherent with the heat release analysis. As this yellow color is due to soot emissions at high temperature, the hypothesis of a high equivalence ratio near the plug seemed to be comforted.
A second phase was also detected on the film, occurring until 35 to 40°CA after TDC, with the yellow intensity decreasing more or less rapidly with time.

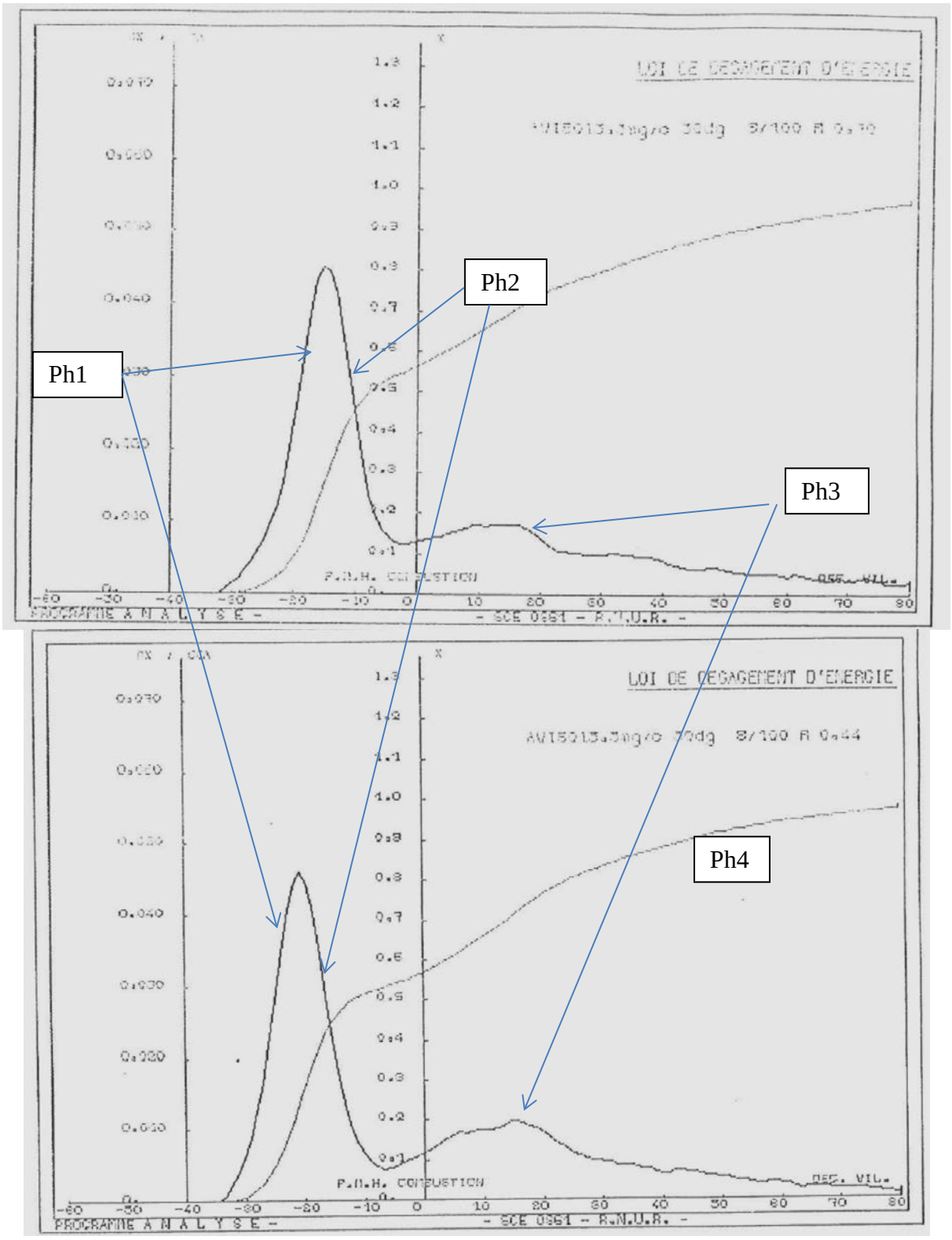

Figure 5-29: heat release rate at two different equivalence ratios: 0.7 (upper Figure) and 0.45 (lower Figure) [5-15]

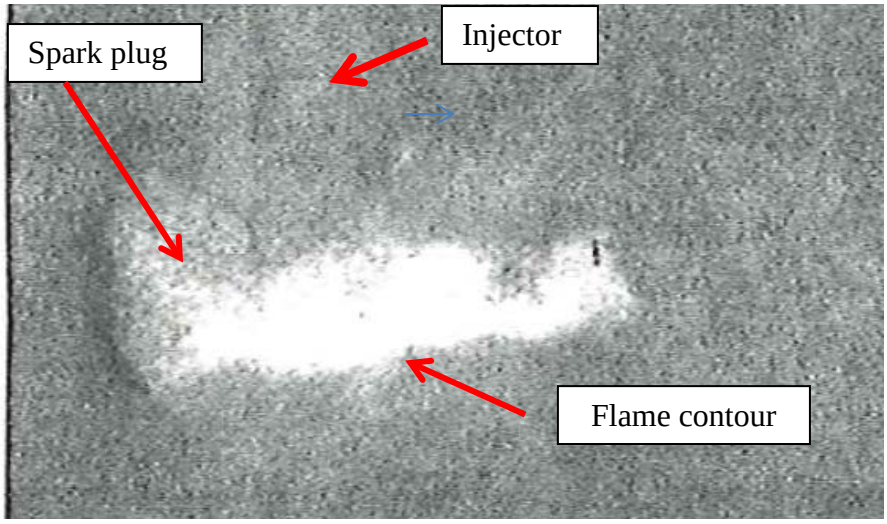

Figure 5-30: high speed image of the combustion phase – 2000 rpm 15.5 mg/stroke - Inj. Pressure 80 bars – SOI 60°CA BTDC – Ignition timing 50°CA BTDC [5-14] Photograph at 35°CA BTDC

An impact of the fuel spray on the piston head was clearly visible on the films and deposits confirmed this observation. As the HC emissions were quite acceptable, a quick evaporation of the fuel impinging the hot surface of the piston was assumed.

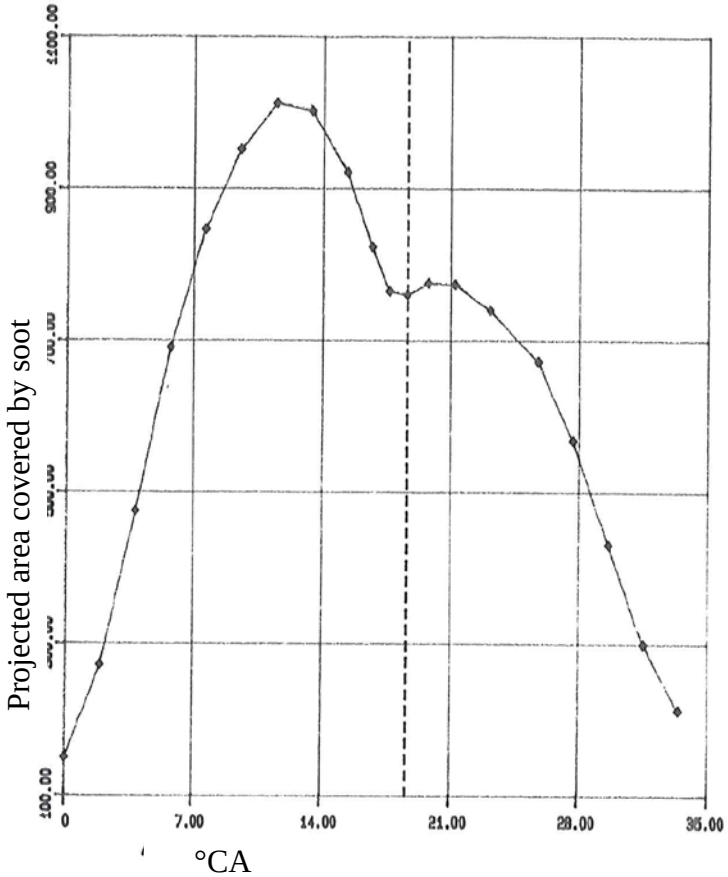

Figure 5-31: evolution of the projected surface occupied by soot. 2000 rpm 15.5 mg/stroke - Inj. Pressure 80 bars – SOI 60°CA BTDC – Ignition timing 50°CA BTDC [5-14]

- Origin of the instabilities.

The key difference between MID3S and J6R concerned the exhaust temperature which increased as the IMEP deviation increased on J6R operating with leaner and leaner mixtures; on the contrary, this temperature went on decreasing on the stratified engine as the throttle was opened, even with a higher level of instabilities. This phenomenon could be linked to different origins of the cycle to cycle variations: on the J6R, a longer combustion duration occurred in lean homogeneous mode, with high cycle to cycle differences in IMEP; on the contrary, the stratified mode was affected by unburned cycles which have a large contribution to the standard deviation.
A slight increase of the spray angle was noticed (§5.4.2.2) as the throttle was opened; this related globally well with the appearance of deposits on the exhaust valve as the engine was operated a sufficient time; these deposits probably meant that fuel was impinging the periphery of the valve, deflecting the spray and significantly changing the equivalence ratio near the plug.

5.5.3. Conclusions.

At the end of the single cylinder tests, several important facts were pointed out, leading to modify the full size engine:

a. The full load performances were acceptable but limited by a severe knock, especially at low engine speed; decreasing the CR down to 12 could be interesting. Increasing the injection pressure over 80 bars could allow to inject later during the intake stroke with the same mixture homogeneity.
b. At part load, the efficiency was quite good while operating the engine at nearly WOT and ultra- lean mixture. Nevertheless, the turbulence during the expansion stroke was probably too low and was unable to maintain a sufficient combustion velocity.
c. The NOx emissions were not acceptable; reducing the injection/ignition timing was probably the best solution besides shutting the throttle or using EGR but a too low maximum injection pressure and a high spray angle sensitivity to the back pressure prevented to use late tunings.
d. HC and CO emissions were acceptable, emphasizing a sufficient temperature in the chamber for oxidation but soot was formed during combustion and after the spray impact on the piston head as could be illustrated by the yellow flames.
e. Deposits appeared on the exhaust valve and lead to unburned cycles while they deflect the spray.

The overall conclusion enhanced the importance of mixture preparation and pointed out the negative impacts of the outwardly opening injector needle. This potential drawback had been already emphasized by VW –see § 5.2.2.2.

5.6. Conclusions.

5.6.1. Methodologies and tools.

This research program was essentially based on single cylinder engine tests and combustion analysis. Nevertheless, if the bibliographic study greatly inspired a primary design of the combustion system, potential difficulties of the stratified operation mode as the control of the air fuel ratio around the spark plug electrodes were also pointed out.

Standard spray visualizations in atmospheric conditions were therefore not sufficient to analyze engine results because of the strong sensitivity of penetration and plume angle to the cylinder back pressure. Instead of developing a constant volume vessel to test the injectors at high back pressure, it was decided to integrate endoscope locations in the cylinder head directly during the design of the single cylinder engine. All the leakage problems linked to additional holes machined on an already existing casted part were thereby avoided. Criticism could of course been made concerning the induced modification of the internal water jacket and thereby of the heat transfers from the combustion chamber to water but it was really of second order of importance compared to the information we got about mixture preparation.
Another important point was the necessity to visualize the dynamic behavior of the spray during the compression stroke and its interaction with the strong squish motion; the use of a high speed camera associated with a flash lighting allowed to catch the spray evolution during some °CA during one cycle; this was absolutely necessary to avoid possible misunderstanding due to the high cycle to cycle variations.
Results obtained with simple and easy to use optical diagnosis as the direct visualization were quickly integrated in the project and contributed to define step by step improvements in tuning and design.

In the future, the advances achieved with high speed video cameras and lasers would optimize the diagnosis and perhaps allow some semi-quantitative results concerning the air fuel ratio in the chamber, for instance by LIF. The development of more accurate 3D simulation tools might not preserve from checking the accuracy of the spray models and their ability to reflect the plume behavior in different ambient conditions.

5.6.2. Physics.

The work achieved on the MID3S as well as other published investigations have particularly shown that the technology of the injector –eg inwardly our outwardly opening needle- could completely modify the combustion behavior, from a spray angle collapse to a spray angle increase as the back pressure changed. It is obvious that this phenomenon is of prior importance in late injection during compression stroke for stratified operation.

Concerning more dedicated engineering aspects, the MID3S allowed to validate the interest of a “spray guided” stratification system associated to a combustion

chamber aerodynamics based on squish. Advantages in fuel consumption, partially due to throttle-less operation, were quite aggressive even if the NOx emissions were not low enough to secure an industrial application. The necessity to achieve higher injection pressures, in order to reduce the injection and ignition timings, was at the same time highlighted.

On the other side, the sensitivity of the system was linked to spray dispersions, not only from one stroke to the other because this problem didn't prevent from obtaining very good combustion results, but merely from one injector to the other; this was clearly the weak point of the concept and explained difficulties encountered later on with a full size four cylinder engine.

Bibliography.

[5-1] E.F.Obert : Internal Combustion Engines and Air Pollution
Harper and Row

[5-2] G.K.Fraidl, W.F.Piock, M.Wirth: Gasoline Direct Injection: Actual Trends and Future Strategies for Injection and Combustion Systems
SAE 960465

[5-3] H. Scherenberg : Der Erfolg der Benzin Einspritzung bei Daimler-Benz" - MTZ 07/61 pp. 241 -245

[5-4] H-C Graff Seherr-Stoss: Die Brennstoffzuführung bei schnelllaufenden Verbrennungsmotoren
Kultur und Technik – 1/1987

[5-5] Scussel, AO.Simko, W.R.Wade : The Ford PROCO Engine Update
SAE 780699

[5-6] H.Schäppertons, K.D.Emmenthal, H.J.Grabe, W.Oppermann: VW's Gasoline Direct Injection (GDI) Research Engine
SAE 910054

[5-7] Dr.Tech.W.Wurster: Grundsatzuntersuchungen am Ottomotor mit direkter Einspritzung (Porsche AG)
Technische Akademie Wuppertal – 09/1989

[5-8] M.G.May, F.Spinnler: Betriebserfahrungen mit hochverdichteten Ottomotoren nach dem May Fireball-Verfahren
MTZ 06/78

[5-9] M.G.May: The High Compression Lean Burn Spark Ignited 4-Stroke Engine
Journal of I-Mech 1979

[5-10] Zwei neue Motoren von Jaguar
MTZ 5/1988

[5-11] P.Gastaldi: Présentation de la culasse MID3S
Renault internal report n°126 – 01/89

[5-12] P.Gastaldi, F.Clivillé: Moteur multicylindre à injection d'essence, comportant 3 soupapes par cylinder
French Patent n°89/10440, European Patent n° EP0412009

[5-13] JP.Jourde, B.Hauet: Development of a Pressure-Time type Electromagnetic Injector for Direct Injection in a 2-Stroke Spark Ignition Engine
SAE 885132

[5-14] P.Gastaldi, T.Soler: Visualisation des jets d'injection sur et hors moteur – Renault internal report n° 17 – 02/91

[5-15] P.Gastaldi: Compte rendu des essais sur culasse MID3S
Renault internal report n°26 – 02/90

Chapter 6

The K5M air guided stratified engine

6.1. Introduction.

The development of early spray guided, direct injection stratified engines, mainly relied on the geometric optimization of the chamber design, with a quite moderate work on the injector. The thereby encountered difficulties, as the need for high injection pressures-typically over 80 bars-, injector and/or plug fouling, or deposits on the valve, like for the MID3S concept, led manufacturers to find other ways to achieve a proper stratification. Wall guided systems, relying on the interaction of the spray with the chamber wall, and air guided engines, relying on the interaction between the air motion and the spray, have therefore been developed to overcome these difficulties with injectors fitted for mass production. Possibilities to modify and adapt spray properties were quite limited because of the necessity for suppliers to provide the same technology to all the customers and to secure sufficient volumes. This parameter constitutes one of the main differences between research and industrial projects.

As predicted by its name, the Air Guided system relied upon the use of the aerodynamic field for achieving stratification. The interaction between the spray and the air were of first order of importance, with a control of the equivalence ratio in the ignition plug vicinity. This quantitative requirement could not be handled by simple 0D simulations or by direct visualization as done for the MID3S engine. For this reason, 3D models and sophisticated optical techniques, like PIV for the air motion and LIF for mixture preparation, were developed and used on dedicated optical engines.

During the development of the K5M system, visualization methodologies were evaluated and optimized in parallel of CFD calculations and tests on conventional single cylinder engines. The focus was pointed on the repartition of the fuel in the chamber and on the ability to lead the droplets towards the plug by an adaption of the piston geometry and the tumble level; modifications on the injector were quite limited even if the chosen technology was firstly dedicated to wall guided engines.

The parallel use of these three tools, on a system which quite fully relied on mixture preparation and not combustion, was a key for the success of the development. Even if, as it will be explained later on, the K5M itself came not on the market, the production of the Audi FSI engine proved that the concept was globally viable; it was thereafter a question of overall production cost, including quality control, and risks acceptance for the manufacturer. That was one time again what differences research and industrial projects.

6.2. General design and patents.

6.2.1. Specifications and requirements.

During the late 90's, the development of gasoline direct injection stratified charge engines was pushed by all the automotive manufacturers. The aim was to strongly reduce the fuel consumption compared to conventional lambda 1.0 solutions while avoiding the complex and costly NOx after-treatment systems which were still at the advanced research stage.

The following program was achieved on a Renault four cylinder all-aluminum 1.6l engine whose main characteristics are summarized in Table 6-1.

Cylinder displacement cm^3	Stroke mm	Bore mm	Compression ratio	Number of valves	aerodynamics
400	79.5	80.5	10 to 1	4	tumble

Table 6-1: basic characteristics of the K5M engine

The basis K4M block largely equipped B and C segment limousines for the European market with a conventional port injection and a three way catalyst.

The performance requirement for the Direct Injection was to keep the rated power unchanged –eg around 80 kW-; the NOx emissions level had to be low enough to cope with the forthcoming regulation as CO and HC were to be treated by an oxidation catalyst. Soot was not considered during the program.

Concerning the industrial tool, cylinder block, connecting rod, crankshaft as well as cylinder head and valve train global arrangements had to remain unchanged; the injector had to be ready for industrialization as well as the ignition system and the spark plug; only the piston shape was completely free.

6.2.2. General design origins and description.

6.2.2.1. Thermodynamic roots.

As described in chapter 5, the advantage in fuel consumption was awaited through a throttle-less stratified operation at part load, and especially during the ECE cycle.

6.2.2.2. State of the art.

After the emergence of a large variety of gasoline direct injection research engines at the end of the 80's, based on stratified spray guided systems, the work has been focused on conventional port injected lambda 1.0 engines during almost one decade. The first information concerning a "new age" for direct injection was provided in

1992 by the Japanese manufacturers Mitsubishi [6-1],[6-2], Toyota [6-3] and Nissan. Mitsubishi was the first to come on the market with a 1.8 l four cylinder engine in 1996 but all the systems were using a "wall guided" mixture preparation.

For some time, the "spray guided" configuration was forgiven because of the lack of robustness of the spray in industrial production, as evocated in chapter 5, leading to misfiring and injector fouling. At the same time, the injection system specialist Siemens announced the development of a new solenoid injector with a maximum injection pressure of 130 bars as Bosch chose a hydraulically governed system derived from Diesel and limited at 300 bars but integrating a spark plug [6-4].

- The Reverse Tumble concept.

The engine was derived from a conventional MPI powertrain dedicated to family limousines and mini vans in Europe. Its main characteristics are summarized in Table 6-2 [6-5]. It is interesting to note that GDI is a trade mark protected by Mitsubishi, even if this acronym has been widely used in the common language and in publications.
The combustion system was designed to operate both in stratified lean mode and at lambda 1.0 with a homogeneous mixture. EGR was used to reduce NOx emissions but a Lean NOx trap (LNT) was necessary to cope with current European, US and Japanese regulation.

Cylinder displacement cm^3	Stroke mm	Bore mm	Compression ratio	Number of valves	aerodynamics
458	89	81	12	4	tumble

Table 6-2: basic characteristics of the Mitsubishi GDI engine [6-5]

General arrangement.
The four valves were operated by two camshafts located on each side of the conventional pent roof combustion chamber. The spark plug was approximately at the center of the chamber and the high pressure injector on the intake side, below the ports. The piston integrated a spherical cavity which formed a bowl on the intake side.

Mixture preparation and combustion strategy.
Figure 6-1 describes how the injected fuel was transported to the spark plug vicinity by mean of a reverse tumble motion.
The fuel was injected towards the piston cavity and thereafter deflected by a wall in the direction of the spark plug; the reverse tumble entrained the vapor and the remaining droplets in the same direction.
The spark plug was located at the periphery of the chamber formed by the bowl; the large squish area formed by the piston on the exhaust side helped to concentrate the fuel in the vicinity of the plug, but was also favorable to the flame propagation towards the center of the spherical bowl where oxygen was still present at the end of the compression stroke. During the expansion stroke, the remaining reverse tumble

and the reverse squish helped to direct the burnt gases in the direction of the exhaust valves.

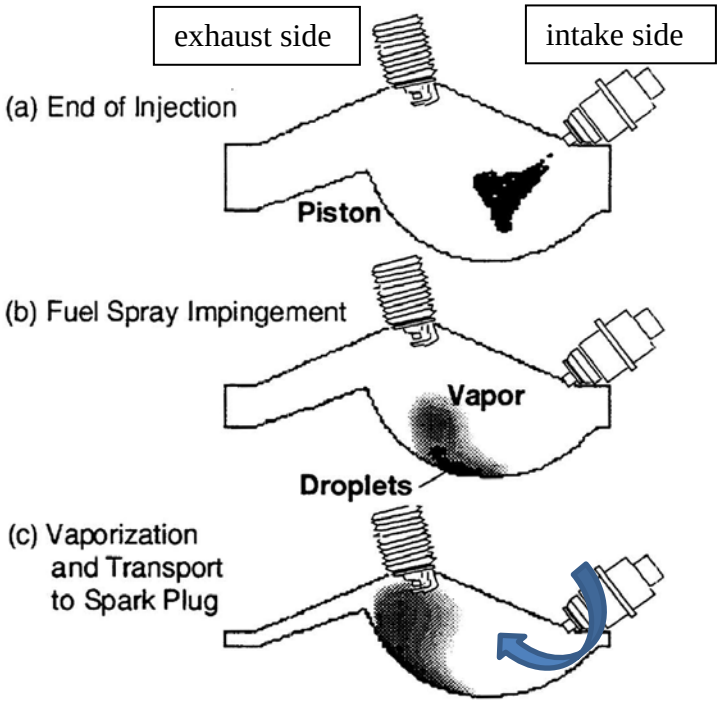

Figure 6-1: mixture preparation strategy [6-5]
The blue arrow represents the reverse tumble motion

Intake port definition.
A straight vertical intake port has been designed to generate the desired reverse tumble, as explains by Figure 6-2.
The air flow was deflected in the direction of the outer part of the valve, along the cylinder liner; a reverse tumble intensity of 1.8 was obtained with such an arrangement, with a claimed permeability increased by 10% compared to the conventional MPI horizontal port [6-5].

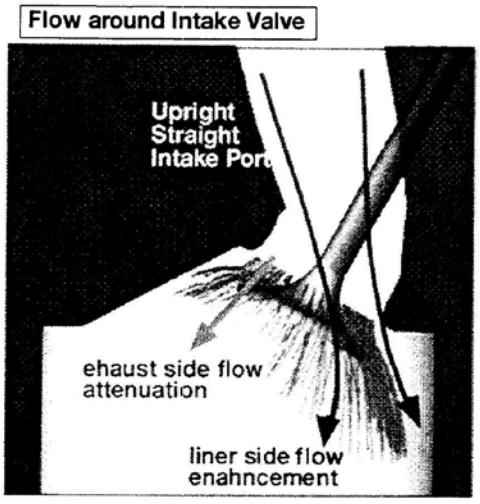

Figure 6-2: design of the intake port [6-5]

Injection system.
For pump reliability, cost and friction work, the maximum injection pressure was limited to 50 bars.
The injector has been designed in order to fulfill both high load homogeneous and part load stratified operations:

- In case of early injection a wide angle and low penetration spray was required to avoid piston wall and cylinder liner wetting
- In case of late injection, a compact spray was necessary to secure a sufficient momentum to reach the spark plug after splashing on the cavity wall. The importance of the tumble was undoubtedly high because of the low droplet velocity after the impact on the wall.

According to these requirements, a swirl injector manufactured by Mitsubishi Electric has been chosen. Its principle is described in Figure 6-3.

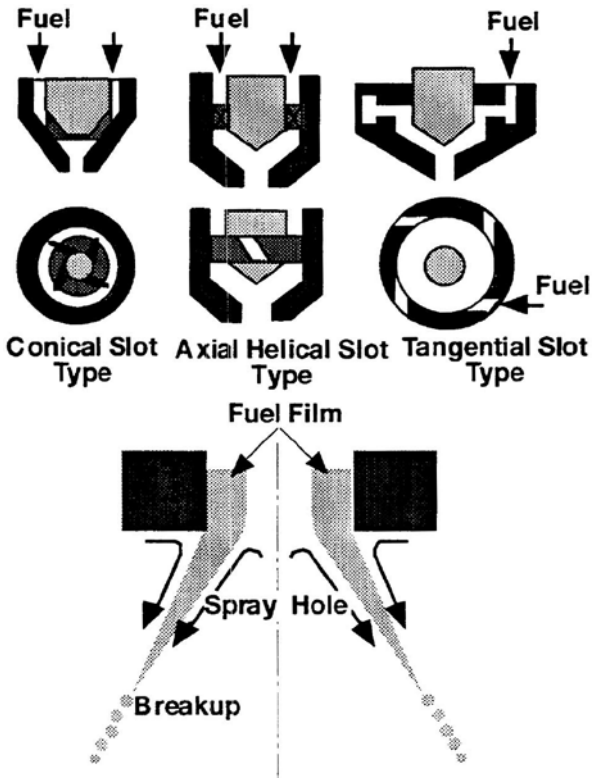

Figure 6-3: basic principle of the swirl nozzle (6-5); right hand solution was adopted

The structure of the spray was a hollow cone with quite large recirculation zones near its front edge.
The optimization of the "swirler" tip located at the upstream of the injector hole allowed to choose spray angle and penetration; as the induced swirl motion increased, penetration was reduced and the spray cone angle increased as shown in Figure 6-4.

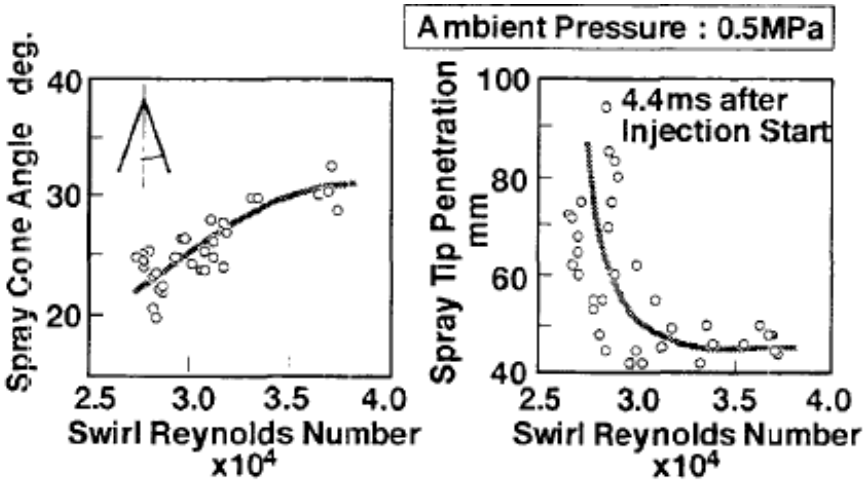

Figure 6-4: dependence of spray cone angle and penetration on swirl Reynolds Number [6-5]

The swirl Reynolds Number was defined as the product of the velocity in the swirling grooves, multiplied by the swirling radius and divided by the fuel viscosity. With this arrangement, the spray axial velocity decreased very quickly above 20 m/s at a distance of 40 mm from the tip in ambient conditions.

The influence of the chamber back pressure is illustrated in Figure 6-5; the spray cone angle significantly collapsed as the back pressure was increased. The above mentioned qualitative requirements for homogeneous (ambient pressure 1 bar) and stratified (ambient pressure typically around 5 bars) seemed therefore to be fulfilled.

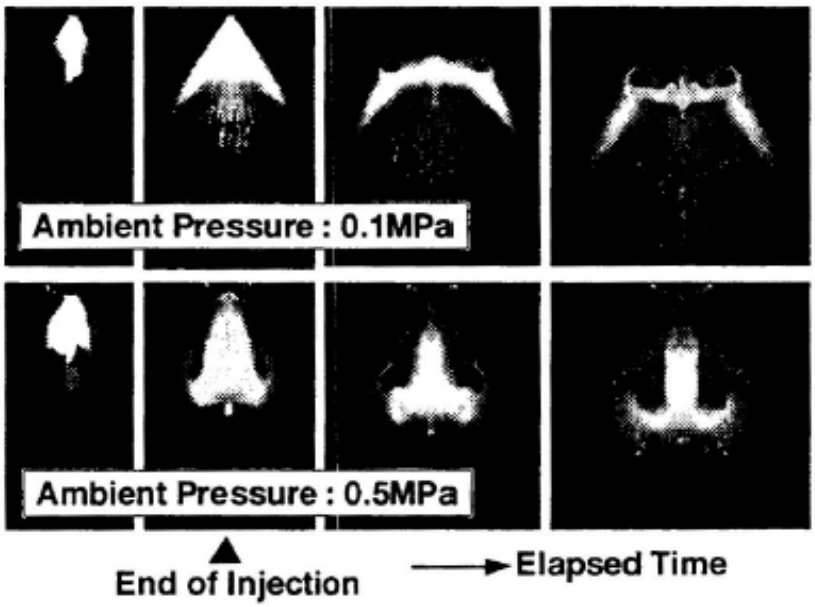

Figure 6-5: effect of the back pressure on the spray shape and angle

This “swirl” based technology was used by all the injector manufacturers in the following decade.

Performances and benefits.

Figure 6-6 presents an example of the strategy chosen for mixing homogeneous and stratified modes. Please note that the claimed advantages of the GDI vehicles (right hand side graph) were not only due to the combustion system but also to other improvements made on the engine and on the car, like another gear box, low friction mechanical parts, or tires with a reduced rolling resistance. Some tests achieved by independent laboratories have shown much lower gains, mostly due to high heat losses at the chamber wall or high HC and CO emissions at part load or in cold conditions. This late observation was quite consistent with the impingement of fuel on the piston.

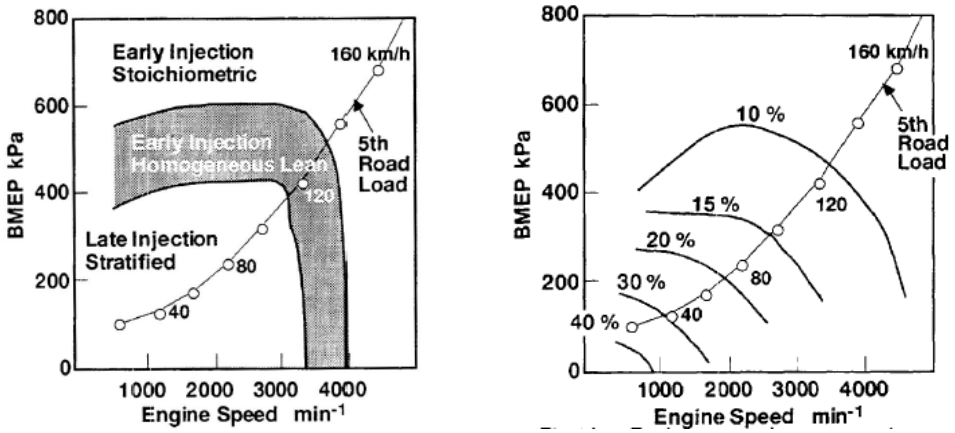

Figure 6-6: strategy (left) and fuel consumption reduction obtained by the GDI engine compared to the conventional MPI system [6-5]

- The Swirl concept.

In 1997, Nissan introduced another concept, also belonging to the family of the "wall guided" systems, where the stratification was obtained via a swirl motion [6-6] associated to a "casting net" injector developed by Hitachi and whose spray was deflected.

Characteristics of the V6 engine are given in Table 6-3.

Cylinder displacement cm^3	Stroke mm	Bore mm	Compression ratio	Number of valves	aerodynamics
498	73.3	93	11	4	swirl

Table 6-3: basic characteristics of the Nissan V6 [6-6]

General arrangement.

The four valves were operated by two camshafts located on each side of the conventional pent roof combustion chamber. The spark plug was approximately at the center of the chamber and the high pressure injector on the intake side, below

the ports. The piston integrated a shallow bowl of moderate depth on the intake side.

Mixture preparation and combustion strategy.
The initial idea was the same as for the Reverse Tumble engine: the bowl wall was used to lead the spray towards the plug but, in this case, a swirl motion initiated by the intake port contributed to entrain the fuel. 3D simulation results presented in Figure 6-7 explain the mechanism.

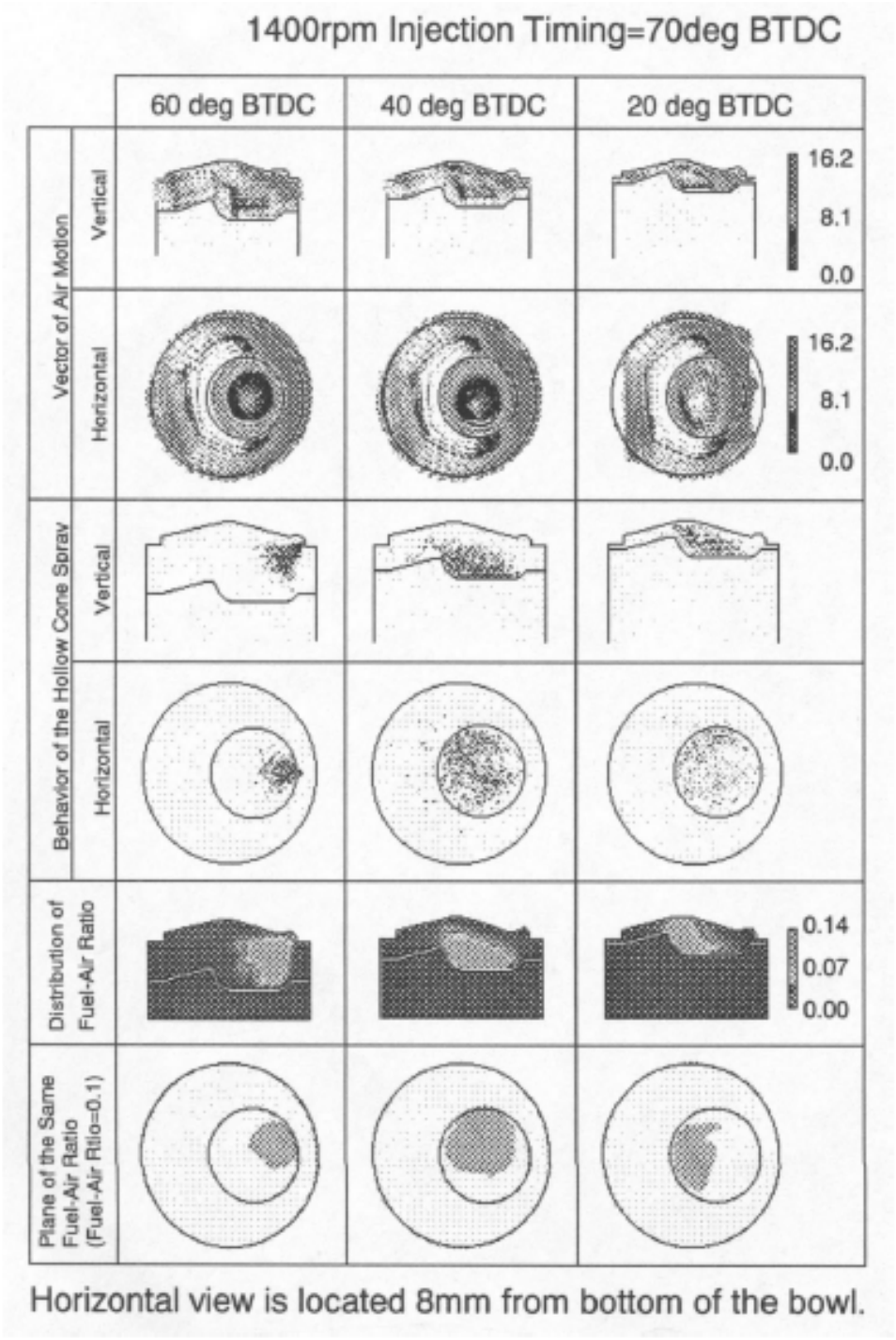

Figure 6-7: swirl stratification system [6-6]

The fuel was injected towards the piston bowl wall and then transported by the swirl motion to the spark plug. The upward flow created from the edge of the bowl to the center of the chamber –the Lift up swirl- allowed to avoid a too high protrusion of the plug electrodes [6-7].
The robustness of the induced swirl motion secured few cycle to cycle variations of the equivalence ratio in the vicinity of the plug.

Injection system.
The technology of the injector was the same for both reverse tumble and swirl systems –eg a solenoid activated swirl valve- but its maximum operating pressure was increased up to 90 bars.

- The Direct Tumble concept

In 1997, the German engineering laboratory FEV proposed a quite new design [6-8], keeping the general arrangement of a conventional MPI 4 valve pent roof chamber with a centrally located spark plug and an injector below the intake ports- but relying on an "air guided" mixture preparation.

Mixture preparation strategy.
A 0.5 l single cylinder engine was equipped with a variable direct tumble system. The piston presented a slight shallow bowl at its center; the fuel spray was deflected by the air motion only and then transported to the plug –see Figure 6-8. Thanks to very few dead volumes generating a quick and complete combustion, the piston was favorable to full load performances.

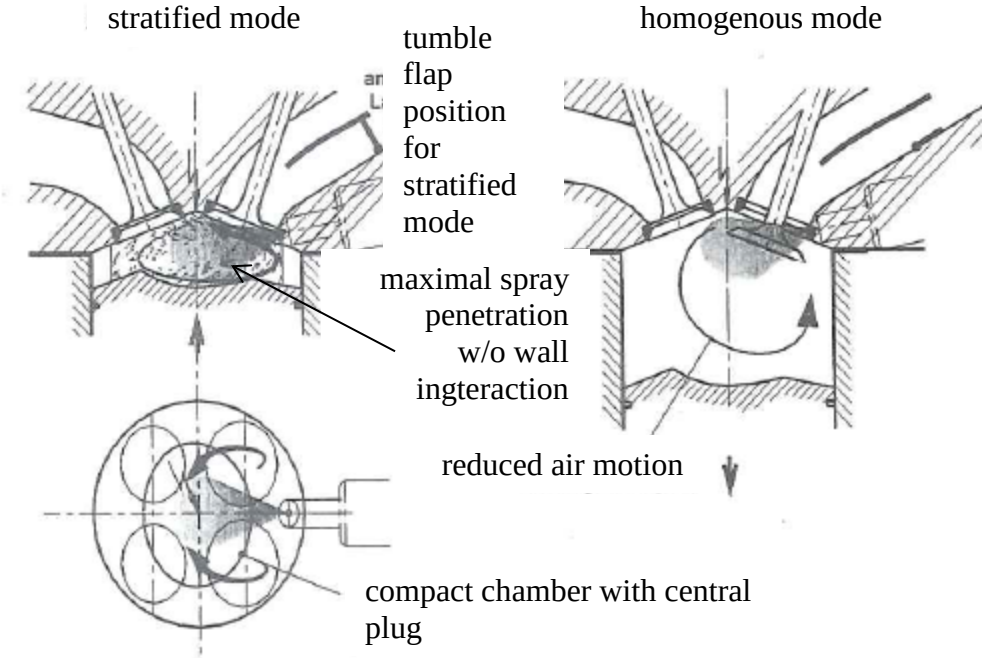

Figure 6-8: FEV DISI combustion system arrangement [6-8]

The spray was directed towards the plug but a relatively strong direct tumble motion prevented the droplets to directly impinge it in stratified mode. On the contrary, due

to a flap located in the intake port, a reduced air motion was used in homogeneous mode. The basic target was to preserve full load performances while letting the general arrangement quite unchanged compared to conventional systems and avoiding fuel impacts on the wall as with the previous "wall guided" solutions.
The physical principle of this solution was obviously relying on the balance between the tumble and the spray momenta; a carefully optimized and industrially robust air system was therefore required to secure an acceptable cycle to cycle dispersion in stratified mode.

Injection system.
A swirl injector was used during the presented tests.

Comparison with the other systems.
An interesting comparison with "wall guided" and "spray guided" systems was presented in [6-8] and is illustrated in Table 6-4.

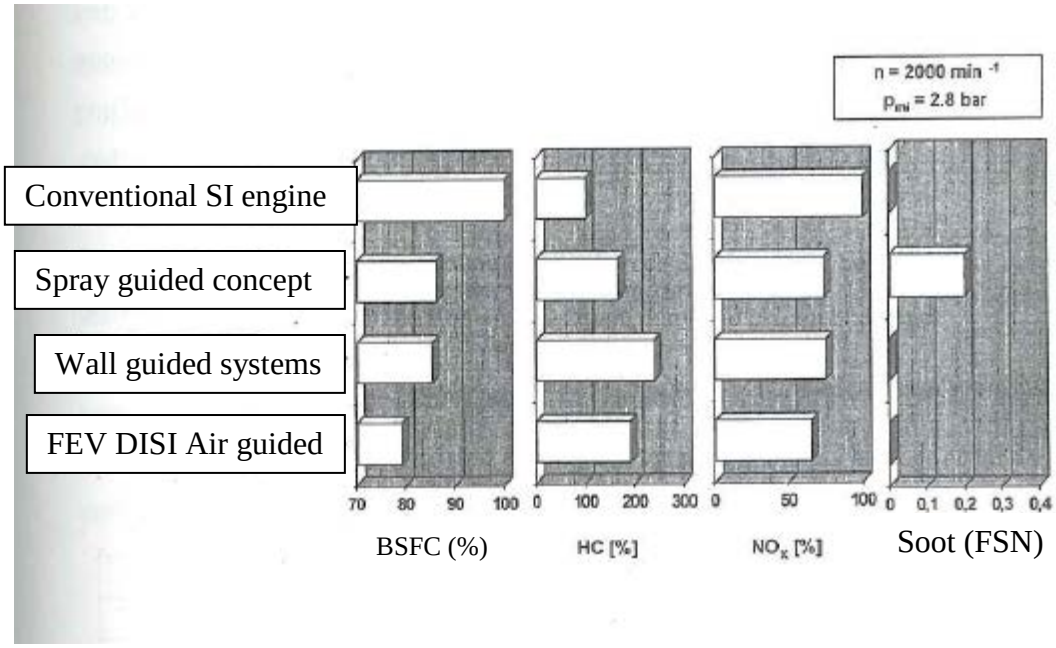

Table 6-4: comparison of the DISI and other direct injection systems versus the standard lambda 1.0 definition [6-8]. Operating point was 2000 rpm and 2.8 bars IMEP.

Compared to the others, the DISI engine provided a 10% fuel consumption benefit on the chosen operating point, partially due to a reduction of the unburned HC and mainly to a reduction of the heat wall losses.

Performances.
One example of the single cylinder test results was provided in Figure 6-9. The effect of the tumble level was quite sensible on both operating points, and especially for the highest load. A quite fine and robust tumble zone seemed to exist for both points, leading the authors to underline that a two steps flap would be sufficient instead of the continuously variable tool used during the experiments.
Nevertheless, even if the reached indicated efficiency seemed to be fair, the hydrocarbon levels –eg more than 10 g/kWh- were clearly important. This was

probably due to a too high fuel dispersion in the chamber leading to over-mixing with some very lean zones.

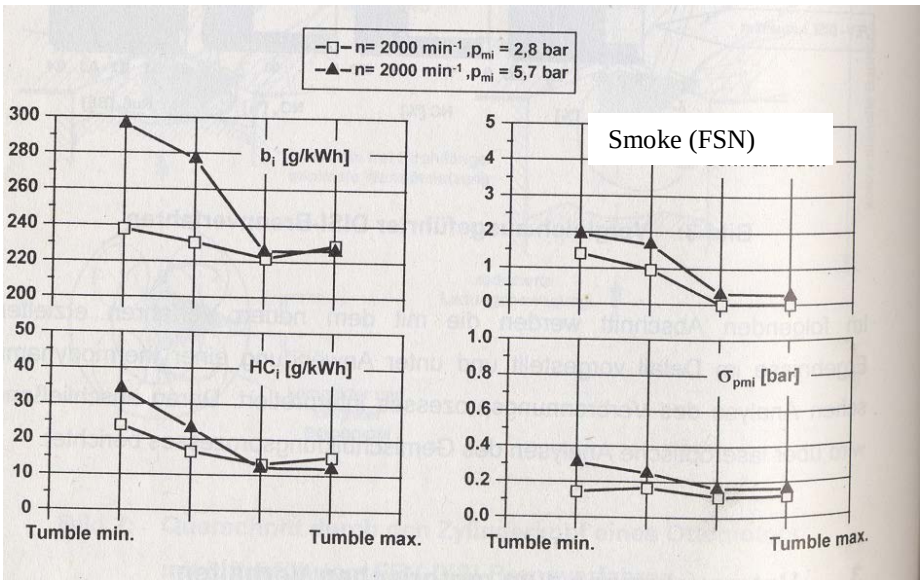

Figure 6-9: DISI results on two operating points, engine speed 2000 rpm, IMEP 2.8 and 5.7 bars [6-8]

- Conclusion of the state of the art analysis.

Several points were quite clear following the relatively short analysis of the previous and current realizations:

- The necessity to maintain the maximum peak power of the basic MPI engine led to keep the general design of the combustion chamber unchanged and to avoid too sophisticated pistons with large "dead" zones where knock would occur.
- Only swirl injectors were industrially available, whatever the manufacturer; the corresponding sprays were characterized by quite a small penetration and a large sensitivity of the angle to the back pressure which clearly forbid a "spray guided" strategy in stratified mode.
- The "wall guided" option, especially if associated to a robust swirl motion, presented the advantage of a quite low cycle to cycle dispersion and also a good robustness for mass production; several drawbacks concerning heat losses, unburned emissions and therefore efficiency were nevertheless existing.
- The "air guided" solution seemed to be the best one relatively to fuel efficiency but its success probably relied on the optimization and on the robustness of the air motion, securing the right balance between air and spray momenta.

In conclusion, the idea was to develop a new "air guided" system, quite close to the DISI proposed by FEV, where the fuel would have been transported to the plug by a direct tumble motion generated by the intake port. A great attention would have to be paid to the understanding of the interaction between air and spray.

6.2.2.3. The K5M engine.

The basic idea was to use the K4M cylinder head without changing valve arrangement and spark plug location, but with modifying the inlet ports and locating a swirl injector below them.
On the contrary, the piston shape was carefully redesigned and the whole system was protected by several European patents [6-9].

Compared to the DISI system, the K5M design was proposing a new arrangement for the interaction between the spray and the tumble as illustrated in Figure 6-10; a convergent ramp was machined in the piston head and located between the spark plug and the injection tip; the idea was to deflect the spray at a certain distance from the tip, where the fuel droplets already had lost a part of their momentum. Several piston bowl configurations –a and b are two examples- were protected.

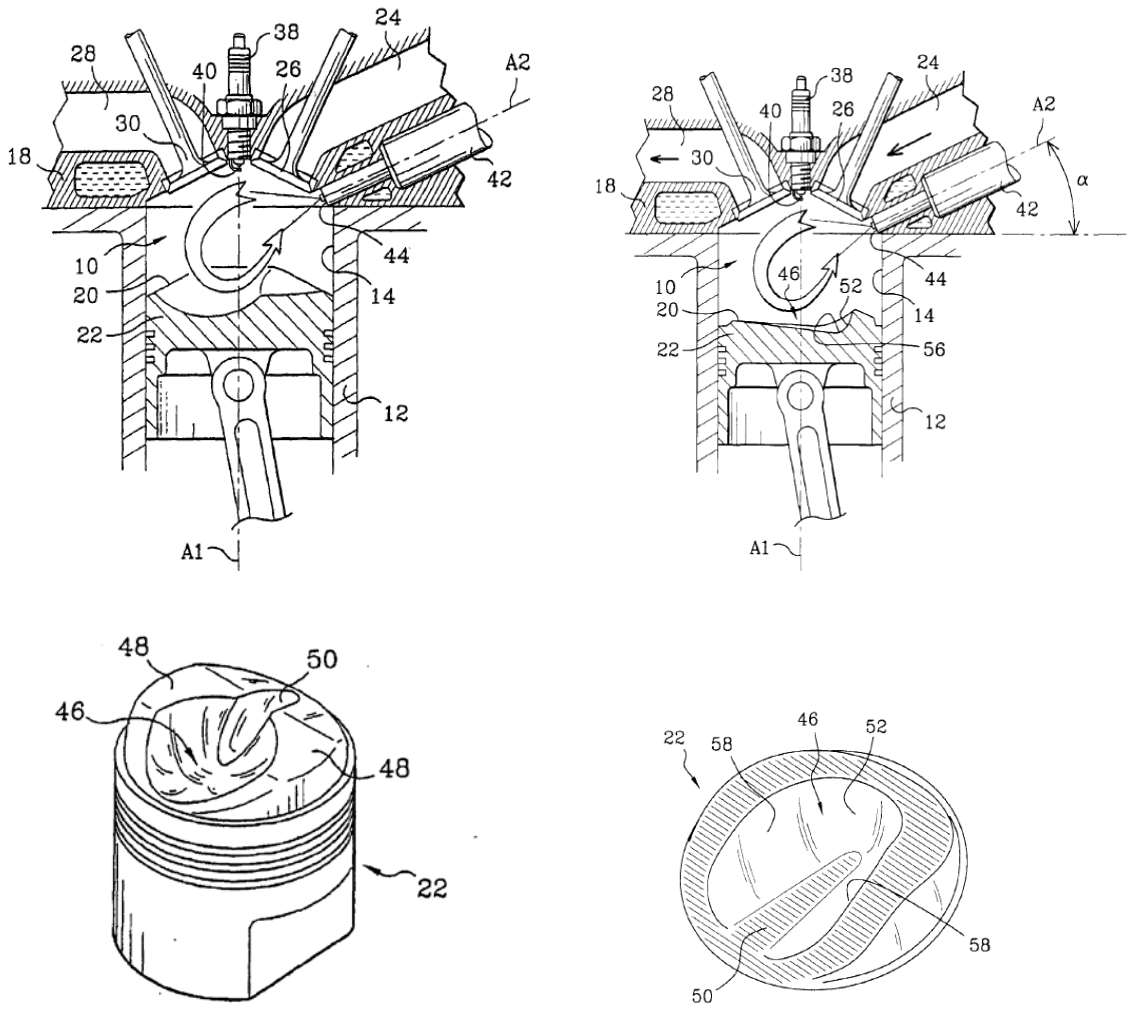

Figure 6-10: main concepts for the K5M engine (left figure a, right figure b)

6.3. Ignition and injection systems.

6.3.1. The ignition system.

The ignition plug had a standard diameter of 12 mm and the same thermal index as the one used on the stock K4M engine; several plug protrusions were tested in order to optimize the combustion stability in stratified mode.

6.3.2. The injection system.

A standard commercially available swirl injector was provided by Siemens [6-10]. The maximum injection pressure was set to 80 bars; above this value the injector could not be opened because of the needle moving inward.

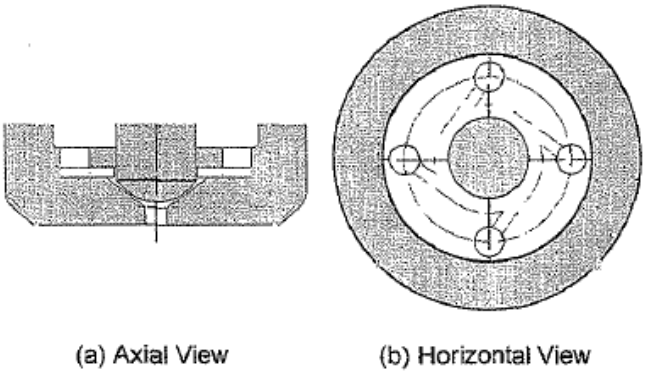

Figure 6-11: Schematics of the Swirl Generator inside the injector [6-10]

Because of this architecture, the penetration of the spray issued from the swirl generator was quite low compared to more conventional outwardly opening injectors. The momentum energy was converted in both an axial but also a radial and a tangential velocity as described in Figure 6-12. These data, obtained by calculation, revealed that the spray plum presented a quantifiable thickness, depending upon the swirler inlet dimensions [6-10].

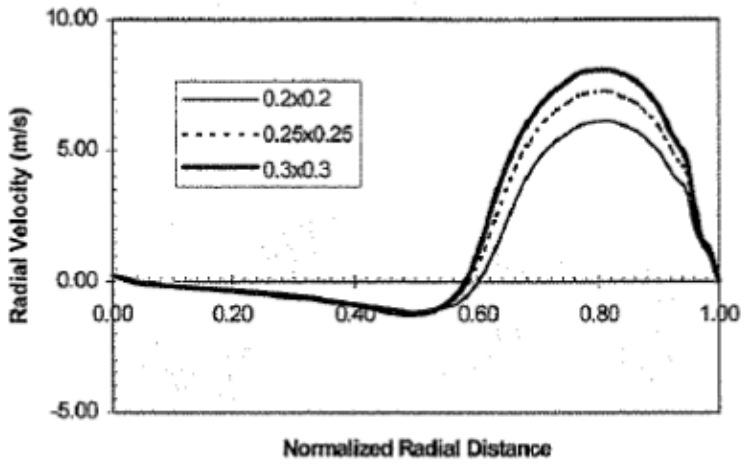

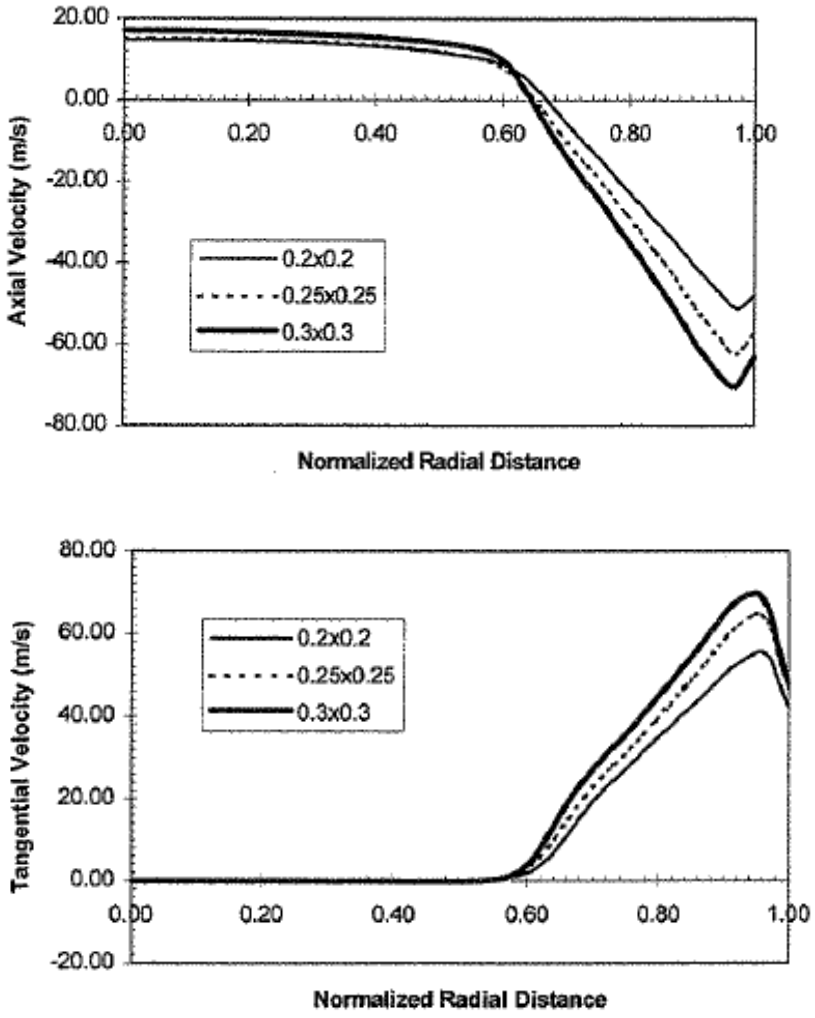

Figure 6-12: velocity exit profile for different swirler inlet dimensions – injection 70 bars

6.4. Optimization of the mixture preparation.

6.4.1. Methodology.

The optimization of both detailed combustion chamber design, aerodynamics and injection parameters required a good understanding of the physics of each phenomenon. The followed methodology is described in Table 6-5 [6-11].

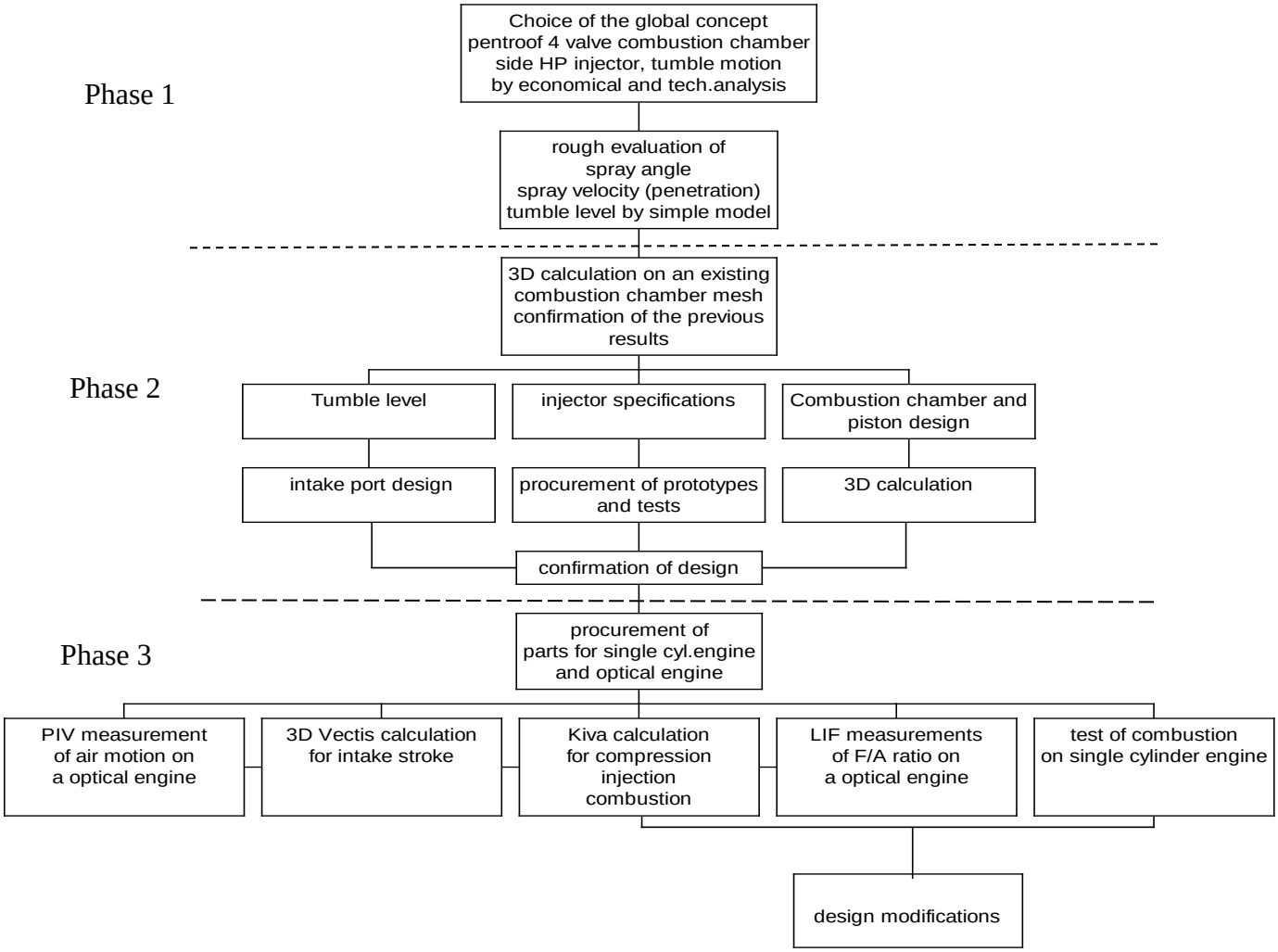

Table 6-5: methodology followed for the development of the K5M engine

Three phases could be defined:

- A quick and rough evaluation of the desired injector and aerodynamic characteristics, mainly based on experience and simple 0D/1D tools, to check feasibility and to define the most important design parameters (Phase1)
- An refined design based on 3D simulation for both the injector characteristics and the aerodynamics (Phase 2)
- An optimization phase using all the available tools like 3D simulation, visualization and tests on a single cylinder engine, particularly to secure the A/F ratio in the spark plug vicinity (Phase 3)

6.4.2. First estimation of the spray and tumble characteristics.

The need of simple, quick and easy to use 0D simulation tools was obvious during the first steps of the pre-development phase; for this task, a model has internally been developed under Excel to simulate the deviation of single droplets by a tumble flow. On the example given thereafter, the droplets had a Sauter Mean Diameter of

40µm, which corresponded to the standard data provided by Siemens, an initial velocity of 80 m/s as the surrounding pressure and temperature corresponded to a late injection for a stratified operating point. The frontal and transverse aerodynamic forces interacting with the droplets were taken into account.

Figures 6-13 to 6-15 clearly show the influence of the tumble center position on the spray upper edge deviation; the x axis was corresponding to a bore diameter, the y axis was corresponding to the cylinder axis. The injector tip was located quite close to the cylinder liner and the cylinder head gasket, at respectively x=0 and y = 0 mm, with an inclination of 10° versus the cylinder head base. The electrode gap of the spark plug was located at x= 40 mm at the chamber center and approximately y = 15 mm, height which could be optimized during the tests (see the blue circle on the pictures).
The tumble motion was assumed as a perfect solid body motion with a velocity decreasing with the radial position.

Figure 6-13 corresponds to a natural tumble and a flat piston; a fine behavior of the droplets which were dramatically deviated towards a possible position of the spark plug is shown; the supposed flow field was perfectly centered in the chamber with a strong velocity of around 25 m/s at the injector tip. The spray deviation became sensible for x higher than 20 mm and droplets arrived in the plug zone with a low velocity of 5 m/s.

Figure 6-14 shows another field with the same tumble velocity at the tip but with a bulk air motion centered at x = 20 mm –eg a tumble offset of 20 mm- and still a flat piston; the effect on the spray was quite low, pointing out the difficulty to deviate droplets just at the nozzle outlet as they still have a high velocity; Figures 6-13 and 6-14 could represent the cycle to cycle variation of the tumble center and show some misfiring risk in the situation presented in Figure 14.

Figure 6-15 clearly shows the interest of a deflector on the intake side of the upper part of the piston, at x=20 mm, associated to a moderate and realistic tumble level. The deflector helped to center the tumble in the center and to promote an interaction between spray and aerodynamics where the droplet momentum is weak enough to be balanced by the tumble.

This simple tool allowed to precise the range of acceptable tumble levels to be generated by the intake port design.

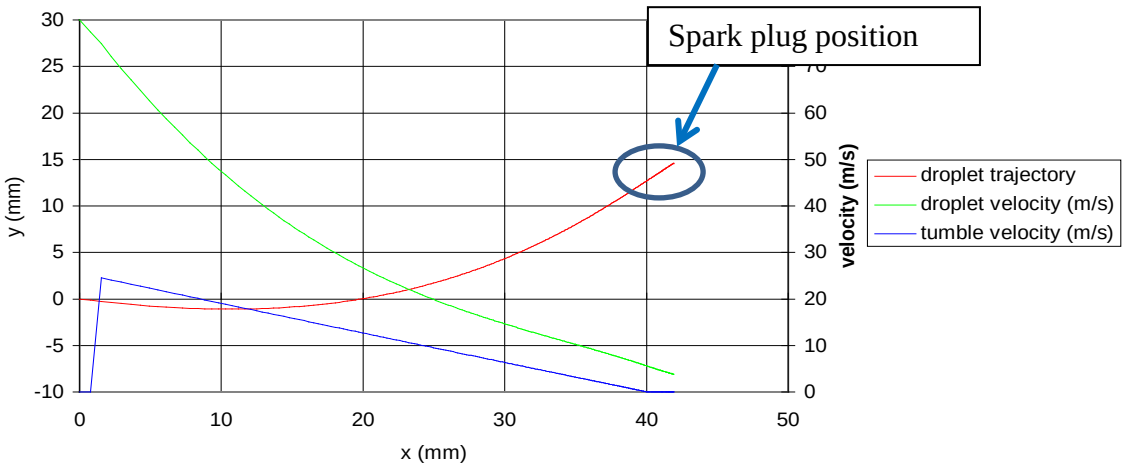

Figure 6-13: effect of a natural tumble on the spray velocity and on the droplet trajectory (flat piston) – centered tumble and flat piston

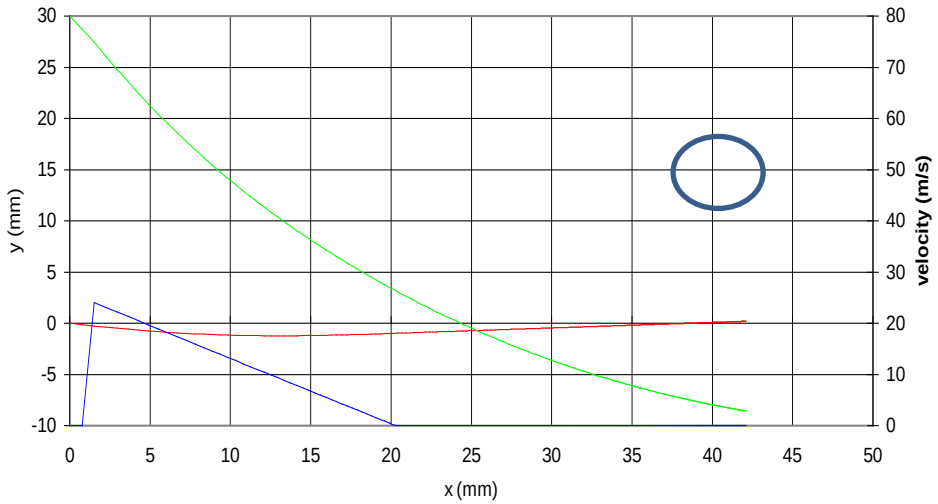

Figure 6-14: effect of a non centered tumble on the spray velocity and on the droplet trajectory (flat piston) – tumble offset of 20 mm and flat piston

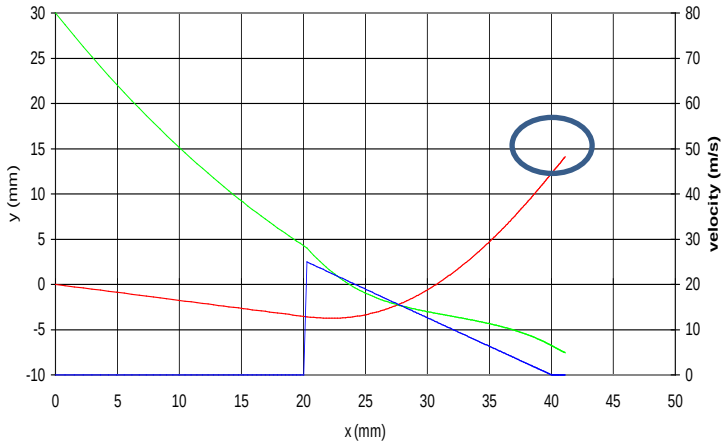

Figure 6-15: effect of a piston deflector (x=20 mm) on the spray velocity and on the droplet trajectory – piston with deflector

6.4.3. Aerodynamics optimization.

6.4.3.1. Choice of the system.

In order to generate the adequate tumble level, a rotary valve was fitted in the intake port as described in Figure 6-16.

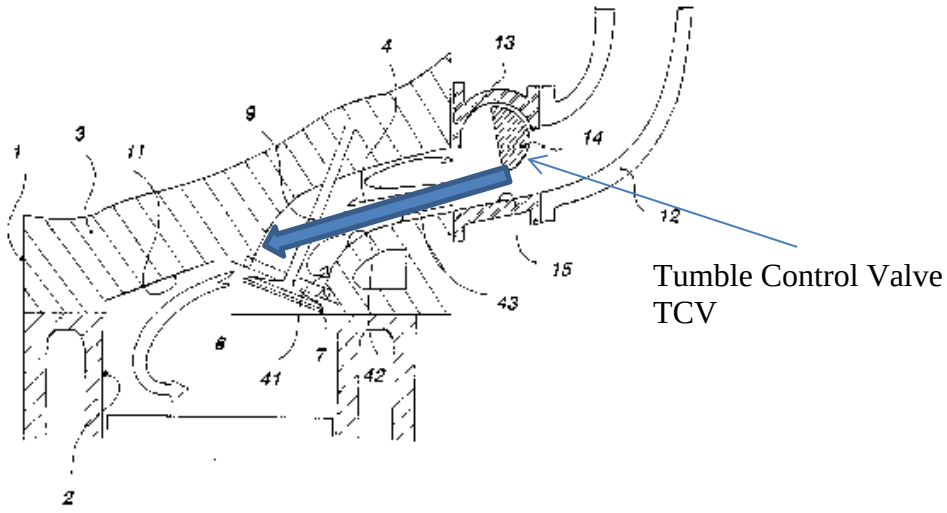

Figure 6-16: intake port arrangement and tumble generation

A tumble control valve (TCV, 14) has been introduced inside the ports to generate the aerodynamic motion:

- When the valve was shut down, no aerodynamic motion was generated and the flow coefficient was at its maximum level, as necessary for full load operation.
- When the valve was open, the air velocity increased at the tumble control valve, leading to a flow take off at the port/throat diameter junction. No flow was induced at the rear part of the valve; the major part of the flow (blue arrow) was transferred at the front part of the valve, leading to the formation of a tumble motion inside the cylinder.

The system allowed a continuously variable tumble motion, whose intensity was depending on the TCV geometry and position, with the possibility to adjust the level from 0° (valve closed) to 90° (valve completely open).

Figure 6-17 presents a CFD simulation of the air flow with the two different TCV positions and an optimized intake port.

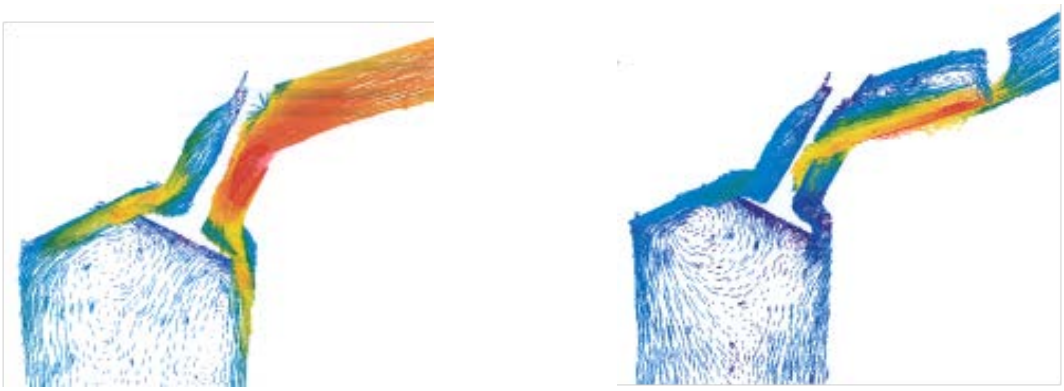

Figure 6-17: variation of air flow according to the TCV position (left: TCV wide open, right TCV completely close)

The simulation achieved with the code Vectis provided by Ricardo confirmed the basis hypothesis of Figure 6-16.

Compared to other potential solutions, for instance with two independent flaps in the intake ports –see Figure 6-18-, this architecture had the advantage to be quite simple to manage for tuning the engine, with the TCV position as the only parameter to be set.

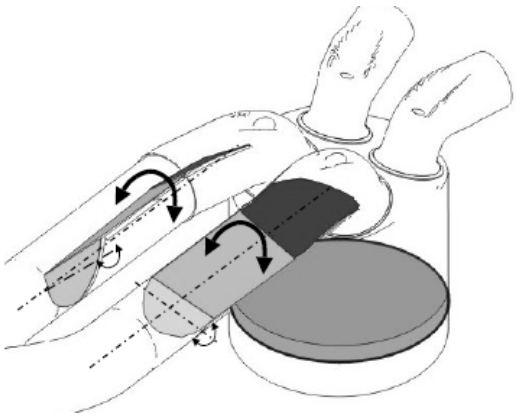

Figure 6-18: two flaps tumble generator [6-13]

6.4.3.2. Detailed flow analysis: CFD.

As the TCV potential was confirmed, the second development step consisted in checking the velocity level in the vicinity of the injector tip as preliminary defined in § 6.4.2. For this task, a detailed 3D simulation associated to PIV measurements was conducted.

Figure 6-19 is presenting results obtained at 1200 rpm with a TCV position fixed at 30° and providing the maximum tumble level.
On the left hand side of the Figure, the represented aerodynamic field concerns a diametric plane passing by the injector tip; on the right hand side, the flow field in

the intake valve plane is represented. Origin of the °CA was chosen at the overlap TDC (combustion TDC was therefore at 360°CA).

At 60 and 90 °CA, the tumble motion was formed as scheduled § 6.4.3.1 and the piston shape had no noticeable influence; the flow take-off at the TCV was quite obvious. The situation completely changed around BDC (180°CA) with a strong upward motion enhanced by the piston ramp. The tumble was globally centered in the cylinder.

At 270°CA (90°CA BTDC), the flow was much weaker but the maximum air velocity area was correctly positioned respects to the injector tip. At 300°CA the velocities one time again decreased and a maximum value of 12 m/s was obtained in the vicinity of the injector tip.

Even if the global motion was corresponding to the mixture preparation requirements, this value was significantly lower than scheduled and some optimization of the spray properties and/or the latest possible injection angle in stratified mode were clearly necessary. At this stage of the work, the necessity of a very low spray momentum –eg a low injection pressure and/or a low penetration- was quite obvious.

6.4.3.3. Detailed flow analysis: PIV

PIV measurements achieved on an optical single cylinder engine (Figure 6-20) were used to confirm CFD results, concerning both the global aerodynamics behavior but also the quantitative values of the air velocities.

2D flow fields were acquired with a real time on-line vector processing. Predominant results were concerning CA 120, 180 and 270 (Figure 6-21) and could be compared to CFD results presented § 6.4.3.2.

The flow acceleration due to the convergent shape of the piston and the re-direction of the flow towards the cylinder head have been correctly predicted by the simulation and confirmed the strong importance of the piston geometry.
At CA 270, the same amplitude of air velocity near the injector tip was measured.

Figure 6-19: air flow simulation at 1200 rpm, TCV angle 30°, maximum tumble level
The red arrows represent a velocity of 20 m/s

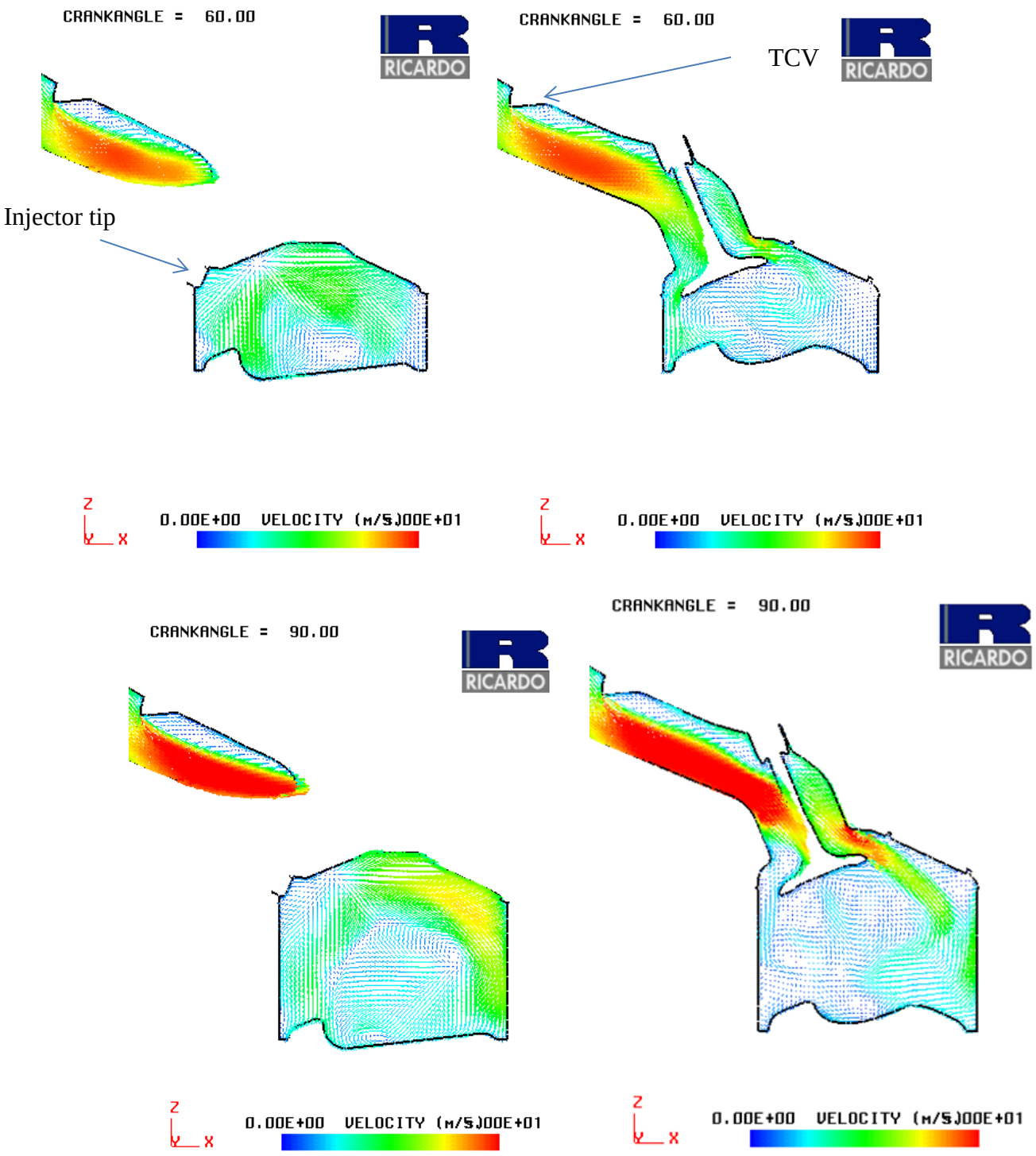

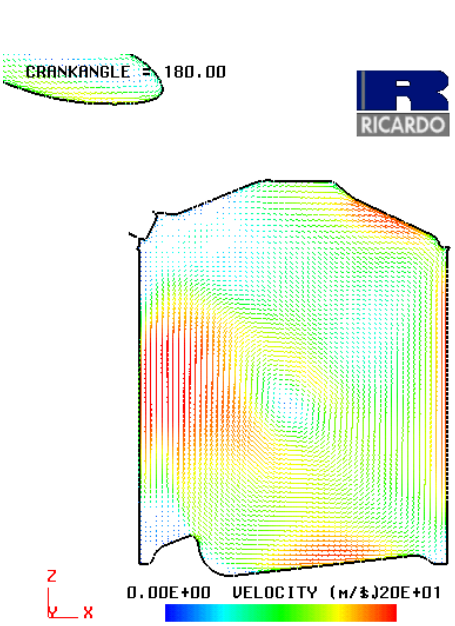

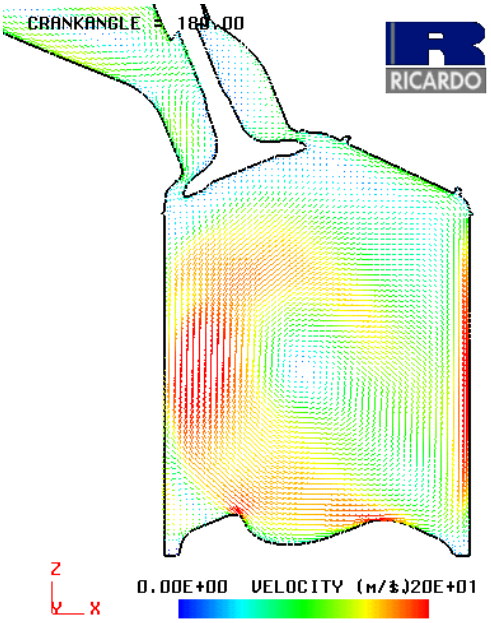

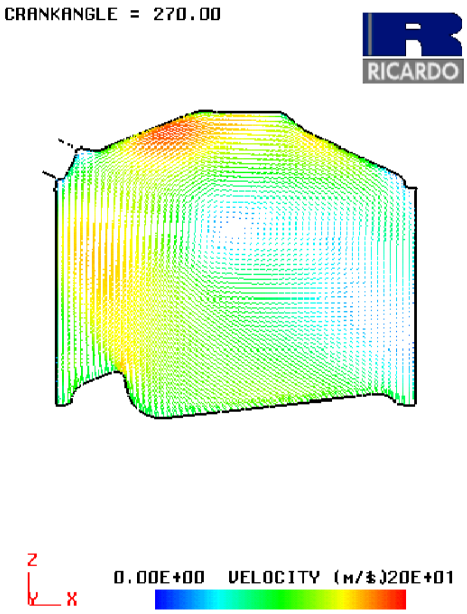

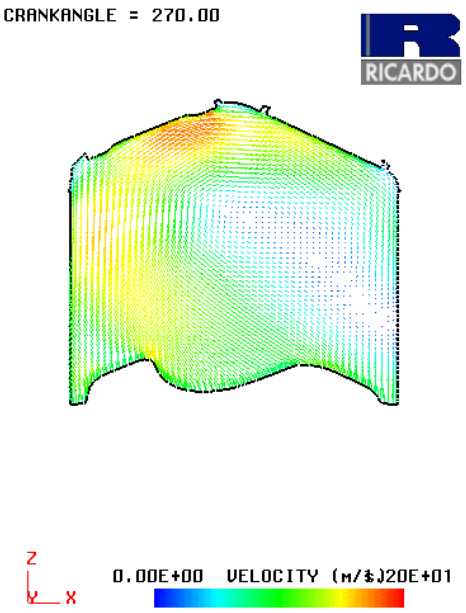

CRANK ANGLE = 300

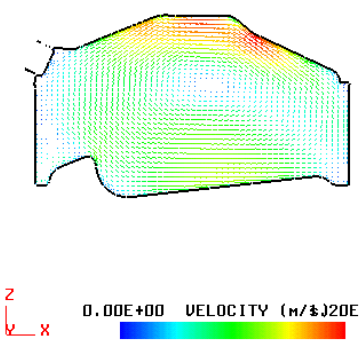

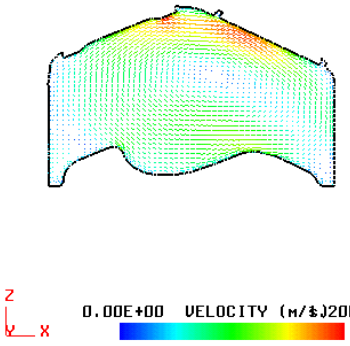

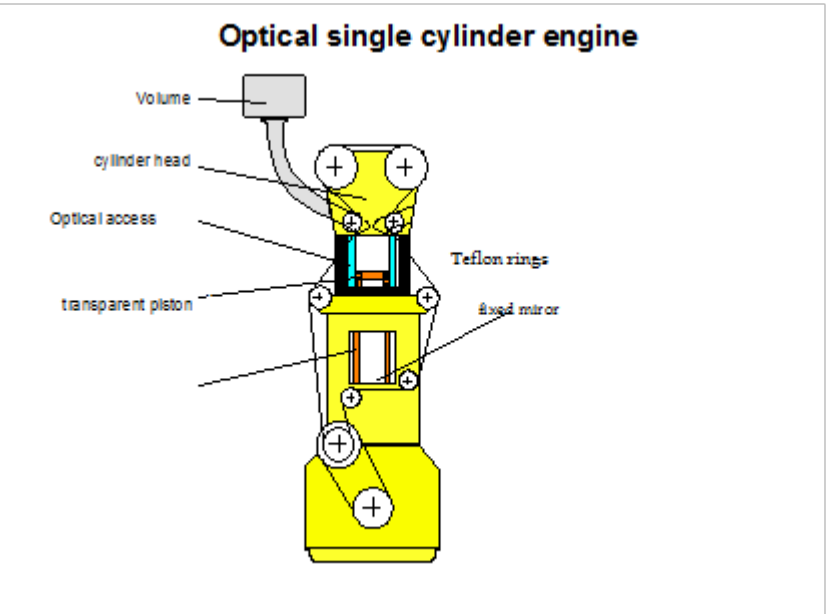

Figure 6-20: optical single cylinder engine used for PIV measurements [6-14]

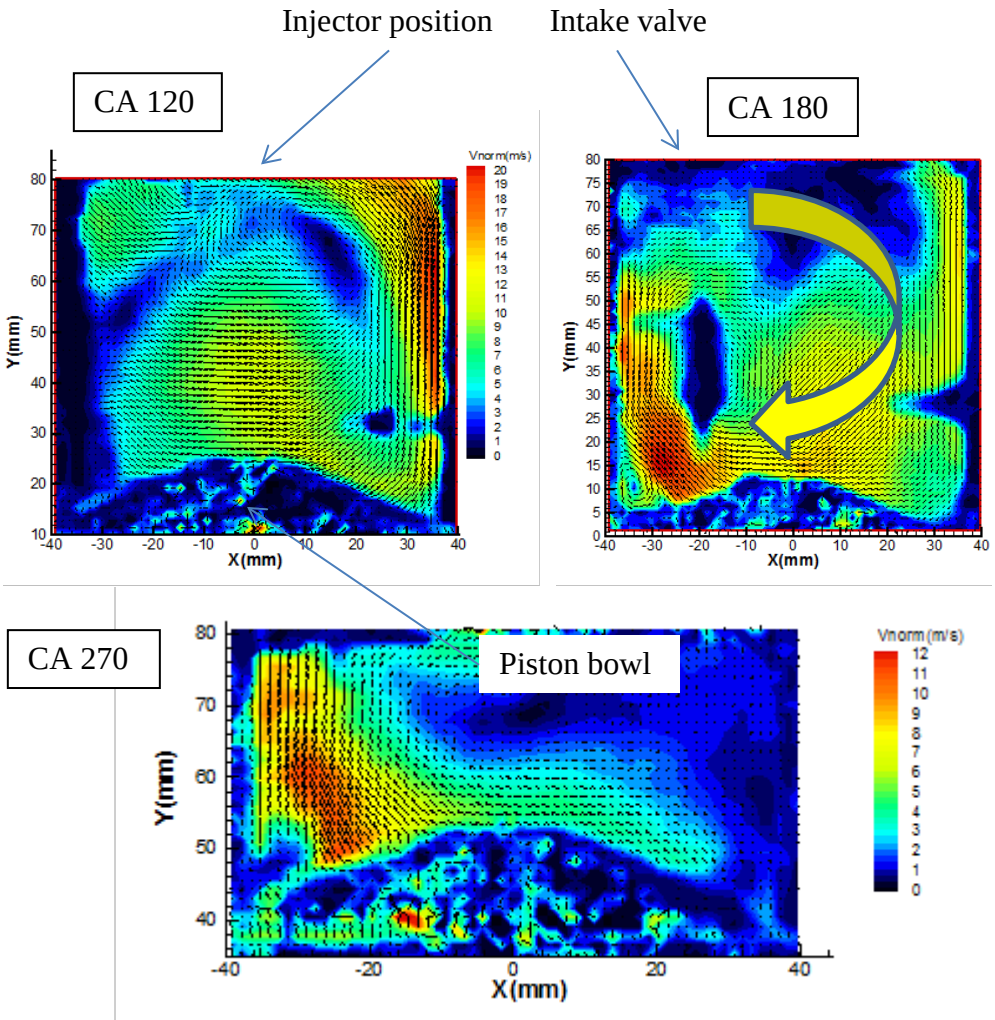

Figure 6-21: PIV measurements in a diametric plan passing by the injector tip. Engine speed 1200 rpm, TCV position 30°.

6.4.4. Mixture preparation.

6.4.4.1. Spray parameters setting.

The calibration of the spray model parameters was based on Mie visualization in a constant volume vessel, with variable injection and back pressure but at an ambient temperature around 20°C. Main advantage of the Mie technique was to visualize all the droplets existing in the spray, even the smallest which could be observed in the recirculation zones.

The criteria necessary to compare tests and calculations were not the usual spray angle, whose definition is not clear for narrow angles or highly collapsed jets, but preferably the spray width measured at different distances from the injector nozzle - eg 15 and 25 mm - and different timings after beginning of injection. Comparison on penetration and global view of the spray, especially concerning recirculation, were also of great interest. Figure 6-22 provides an example for one swirl injector tested during this program. For safety reasons, White Spirit was used instead of gasoline.

Figure 6-23 presents a comparison between the 3D model result obtained with the code Kiva GSM (Groupement Scientifique Moteur) and the visualization; simulated fuel was iso-octane; for the spray, the Wave Fipa model was used, taking into account primary and secondary atomization. The aerodynamic field generated during the intake stroke was provided by Vectis results and plugged in Kiva mesh after the valve closure.
Two different criteria concerning the plume penetration were used, one taking 100% of the injected fuel into account –eg involving the smallest droplets-, the second taking only 90%.

The global result was quite satisfactory even if the calibration parameters of the model had to be modified for each operating condition. The relative position of the experimental results versus the 100 and 90% traces was also correct.

The major drawback of this methodology concerned the absence of evaporation in hot conditions. This fact enhanced the necessity to achieve some LIF measurements in an optical engine besides 3D simulation

6.4.4.2. Mixture preparation analysis.

Calculations with Kiva were run on the basis of the actual optical engine used for LIF (Laser Induced Fluorescence) and combustion analysis. Due to a too high level of liquid, it was not possible to use the quantitative FARLIF [6-15] and measurements were therefore qualitative [6-16], [6-17]; nevertheless, the liquid phase could clearly be seen using Mie scattering.

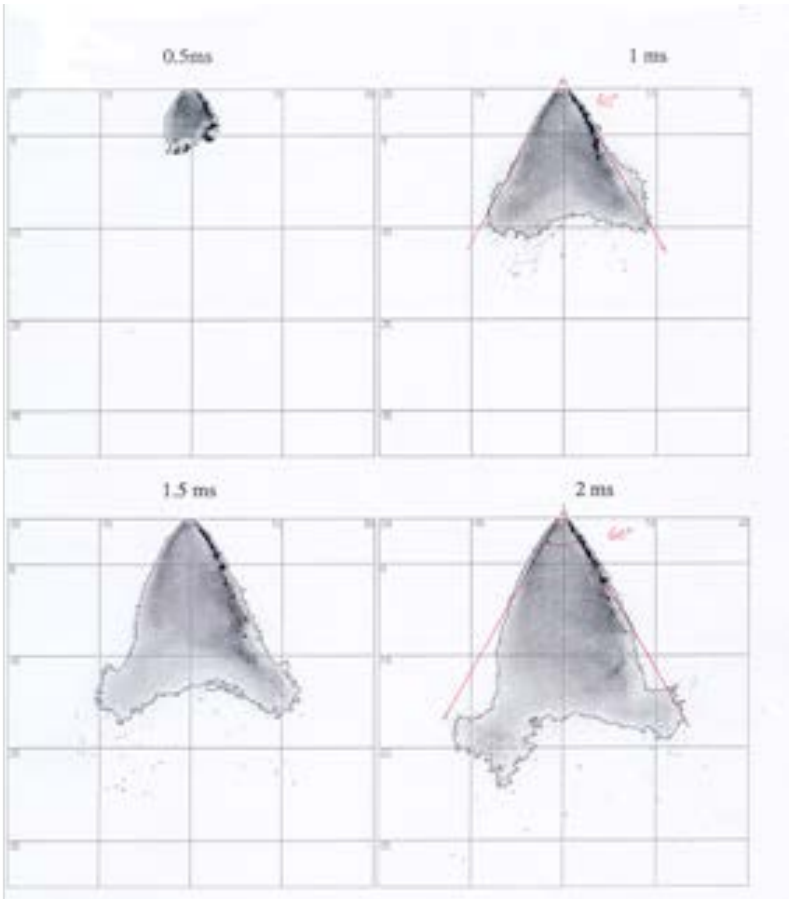

Figure 6-22: Mie visualization of a spray – injection pressure was 30 bars, back pressure 2.5 bars, ambient temperature – reference time ASOI (first visible droplets)

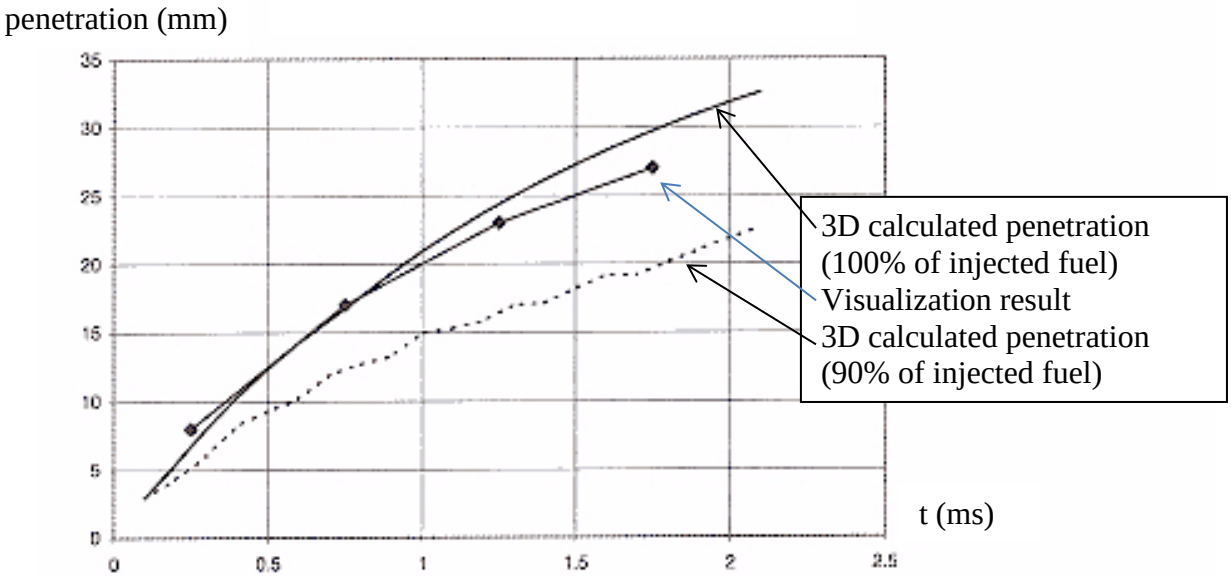

Figure 6-23: comparison between calculation and visualization - injection pressure was 30 bars, back pressure 2.5 bars, ambient temperature – reference time t ASOI (first visible droplets)

- Experimental set-up

Figure 6-24 presents the single cylinder engine as Figure 6-25 shows the cylinder head and piston design; a quartz window was located in the piston to allow visualization from the bottom of the engine as a Ne-Yag laser sheet was going through the cylinder head about 1.5 mm under the spark plug (protrusion between 5 and 10 mm in the combustion chamber). The measured compression ratio was 8.6 which is a rather low value for modern SI engines but does not lead to unrealistic combustions. The actual combustion chamber was meshed (CR was 8.7) and compression only pressure calculation at TDC was in very good agreement with experiments.

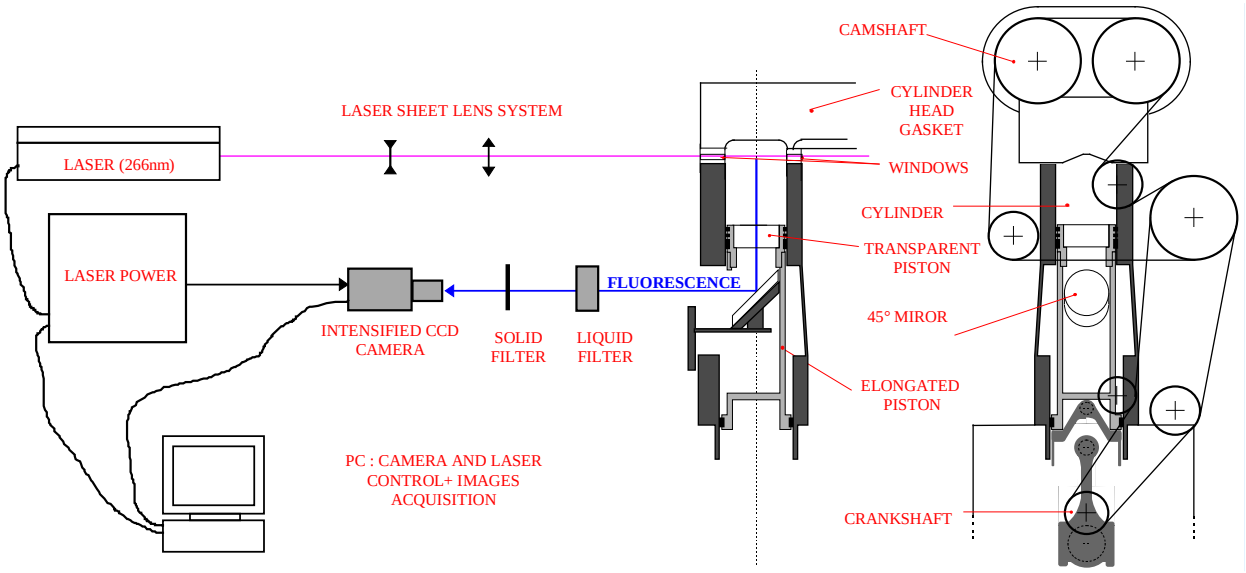

Figure 6-24: definition of the LIF optical set-up and arrangement of the optical single cylinder engine

The same fuel - eg iso-octane- was used for both tests and calculations with the injector spray described above, the 1% toluene used for fluorescence having no influence. The flow field at BDC was issued from previous Vectis calculations - see §4.4.3.2 - and used by Kiva as boundary condition.

- Results at 2000 rpm.

Figure 6-26 shows the situation at WOT, part load; the tumble motion had clearly two main effects: in the upper part of the chamber, the air and droplet velocities had the same direction, so the tumble contributed to the fuel motion towards the chamber roof and the spark plug; in the lower part, these velocities had opposite directions, the tumble braked the spray and so prevented too much fuel to impinge on the piston. In this region, the higher relative velocity of the droplets versus the air accelerated the vaporization, 95% of the isooctane being vaporized at TDC.

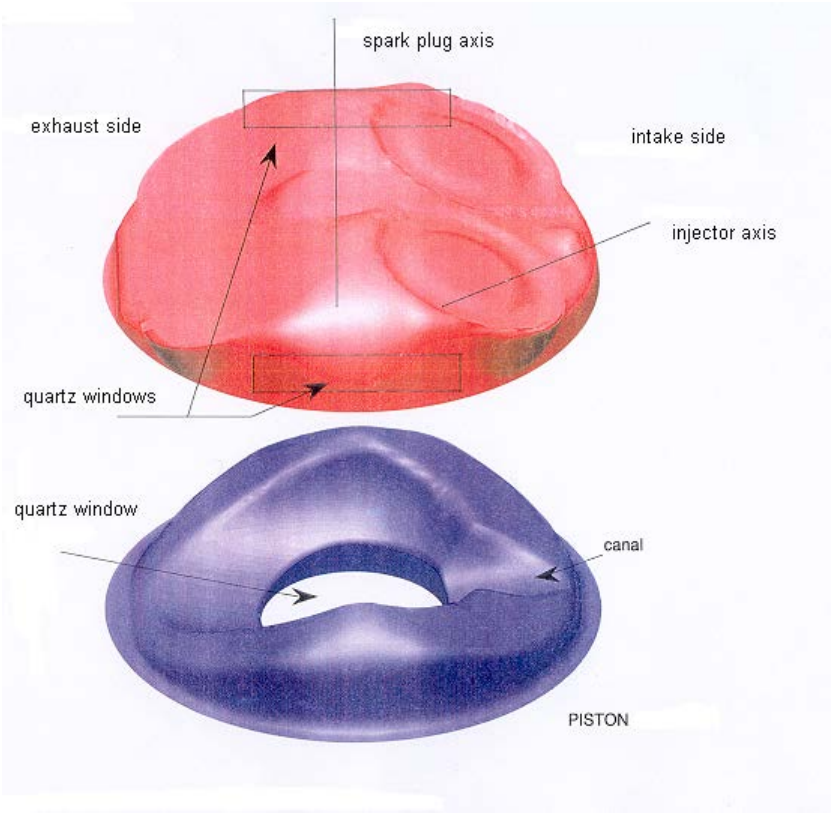

Figure 6-25: cylinder head and piston bowl definition

Figure 6-27 represents the spatial evolution of the zone with an equivalence ratio of 0.8 versus time; this cloud moved vertically and a large region of flameable mixture was present between 5 and 10 mm from the chamber roof at ignition timing, around 35°CA BTDC, with some liquid droplets; this behavior explained the quite acceptable ignitability with protruded electrodes and a tendency to misfire with standard ones whose ignition point was at around 5 mm from the roof. Piston wall wetting was avoided as no droplet impingement appeared on the pictures.

Figure 6-28 presents a comparison between the above Kiva simulation, with an equivalence ratio map in the diametric plan situated 10 mm under the chamber roof, and a qualitative visualization on the optical engine at the same location. These data confirmed the quite good –but not complete as seen with the Mie pictures- fuel evaporation at - 35°CA with both high spatial and temporal equivalence ratio gradients; the other aspect is concerning the absolute value of the equivalence ratio at ignition timing, around the spark plug. The lean value, between 0.7 and 1.0, contributed to some risks concerning cylinder to cylinder or industrial dispersions but also concerning NOx emissions, whose peak is around 0.90.

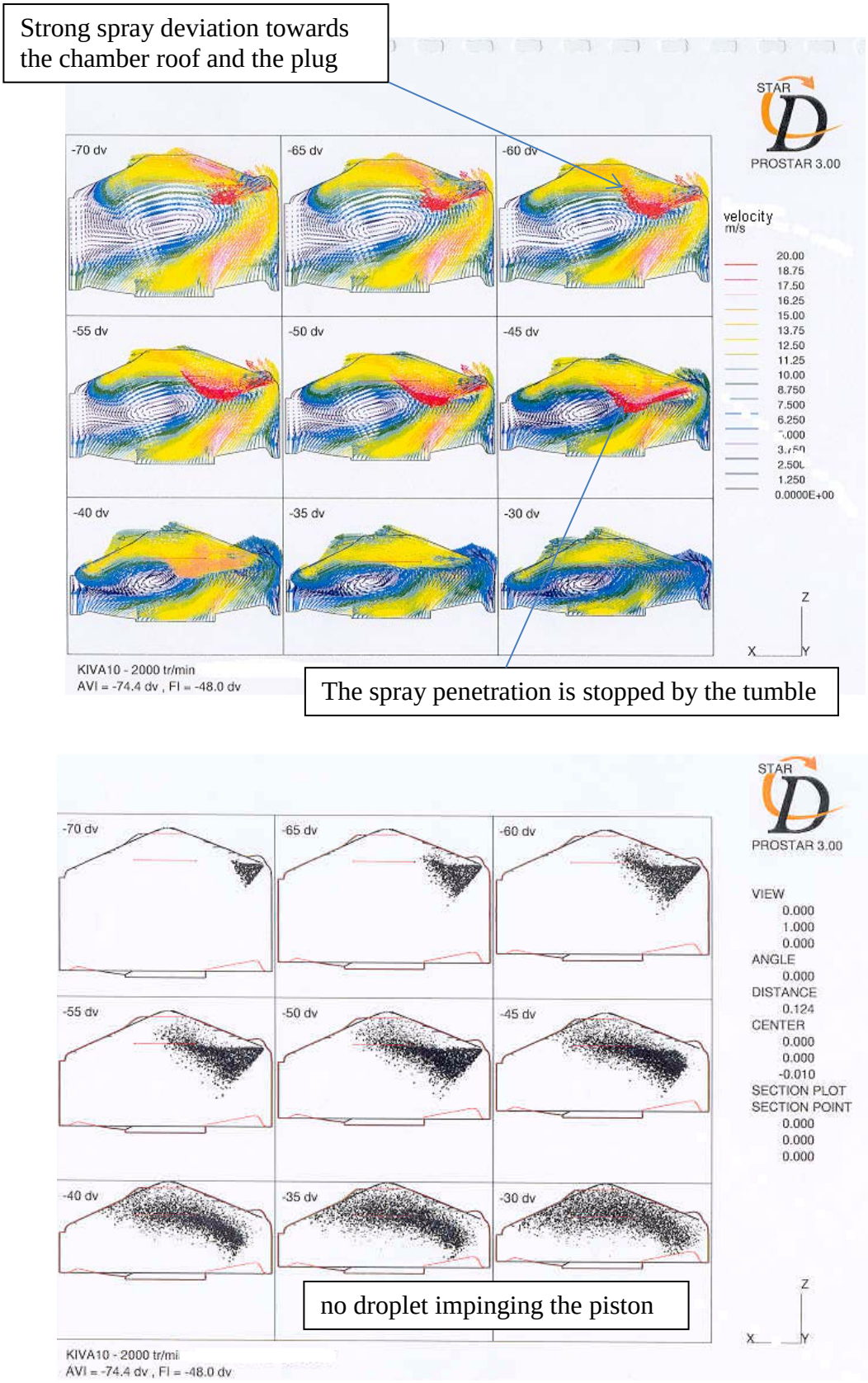

Figure 6-26: 3D simulation with Kiva – engine speed 2000 rpm – WOT – SOI at 74.4°CA, end of injection 48°CA BTDC – upper figure: air and droplet velocities field – lower figure: droplet position

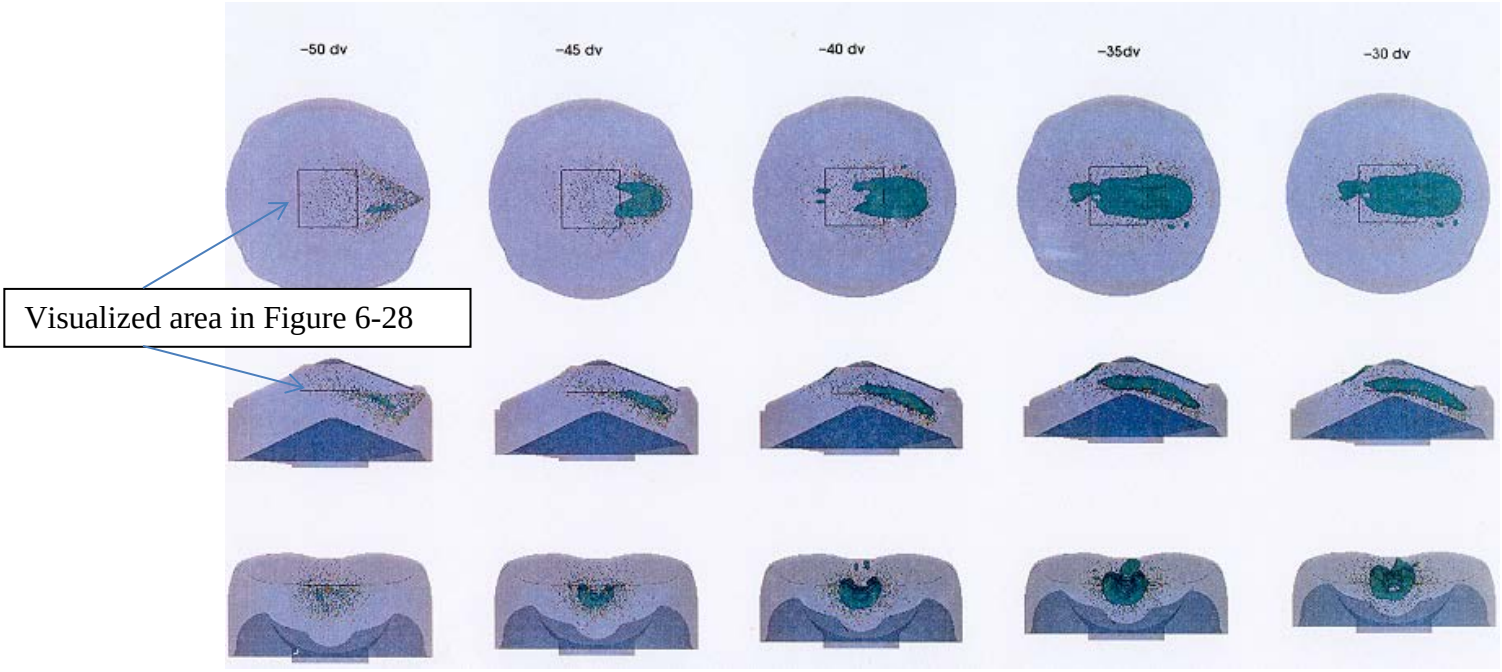

Figure 6-27: evolution of the equivalence ratio 0.8 area versus CA – engine speed 2000 rpm – WOT – SOI at 74.4°CA, end of injection 48°CA BTDC – ignition timing 35°CA

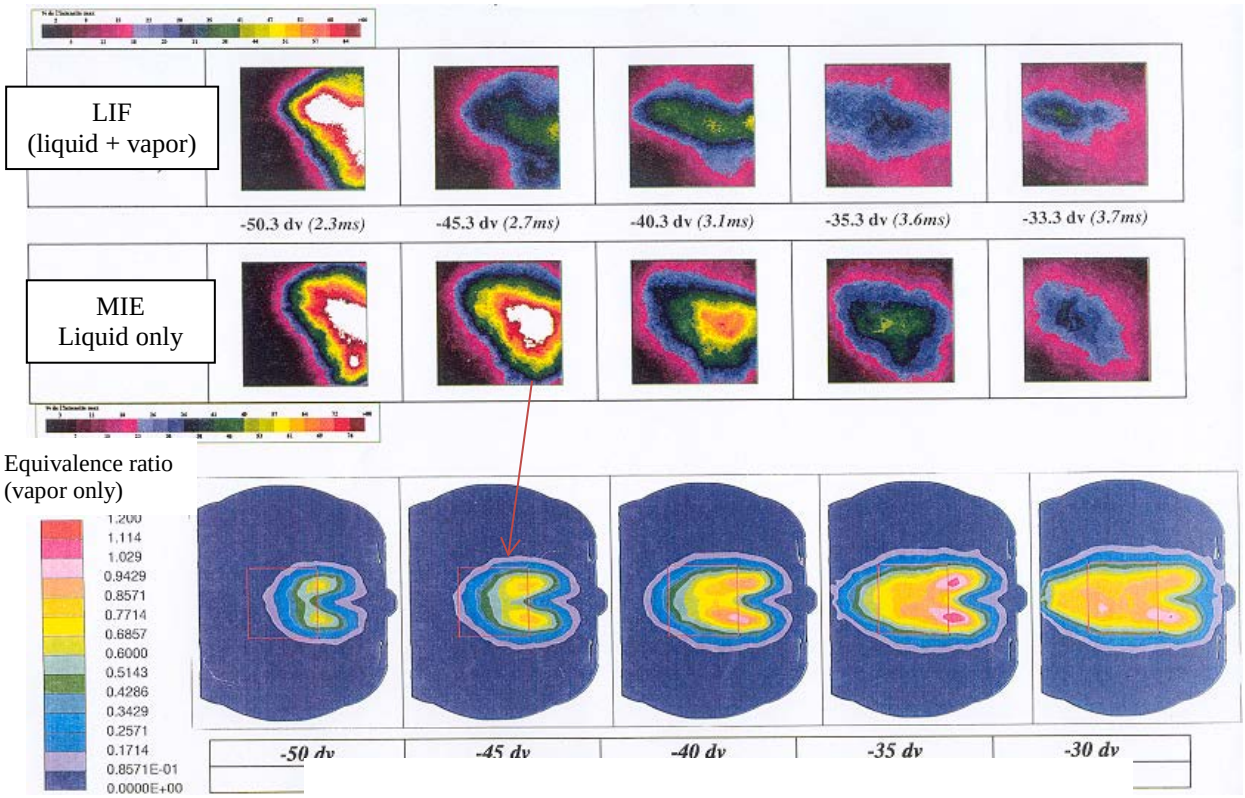

Figure 6-28: comparison between LIF/Mie visualization (upper figure) and Kiva simulation (lower figure) : engine speed 2000 rpm – WOT – SOI at 74.4°CA, end of injection 48°CA BTDC – ignition timing 35°CA – the visualized area is represented by the red square and situated 10 mm below the chamber roof

- Results at 1200 rpm.

At 1200 rpm, the situation was slightly more difficult; as the tumble motion was naturally weaker than at 2000 rpm, the spray penetrated more deeply in the combustion chamber at constant injection pressure – see Figure 6-29. The equivalence ratio gradient was steeper in the vicinity of the spark plug and the rich cloud was situated under the exhaust valve at ignition timing. To come back to the previous situation, a reduction of the injection pressure would have been necessary but the induced poor atomization below approximately 30 bars forbid this solution.

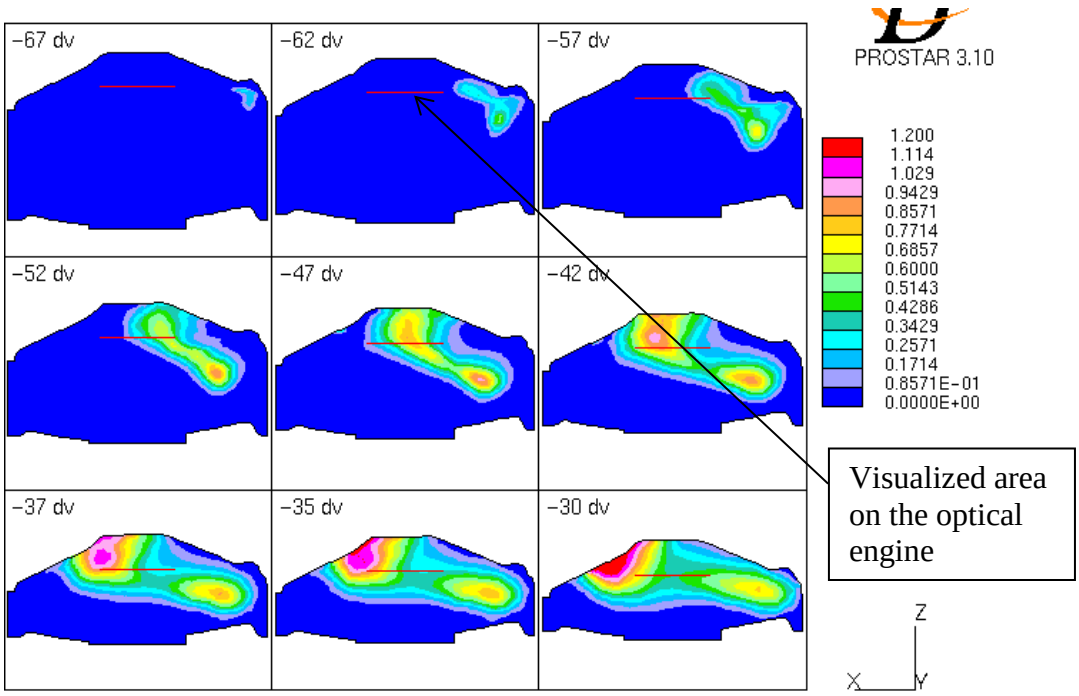

Figure 6-29: equivalence ratio map versus time in a vertical plane passing by the cylinder axis and integrating spark plug and injector tip – engine speed 1200 rpm – WOT – SOI - 69°CA, EOI – 56°CA – the black horizontal segment represents the visualized area on the optical engine and is situated 10 mm below the chamber roof

A deeper analysis illustrated by Figure 6-30 shows the formation of two vortices around the hollow cone spray which moved towards the chamber roof and the exhaust valves; at such a low engine speed, they had enough time to move and grow; this phenomenon led to a high fuel concentration within the vortices and a very low amount of fuel within the cylinder center as shown with the U shape of the « equivalence ratio =0.8 » in Figure 6-31. The region with a high equivalence ratio was therefore located under the exhaust valves at ignition timing, with a lean mixture in the vicinity of the spark plug. This result was very well correlated to the bad stability obtained on this operating point. Figure 6-31 also shows the good agreement between Kiva results and Mie/LIF measurements for both liquid and vapor. The visualized area was situated 10 mm above the chamber roof.

These physical phenomena as well as the order of magnitude of the optimum injection timings were completely in agreement with the work published later on by

Kakuho [6-18] –Figure 6-32. The quite late injection timing –at least compared to the wall guided system- were explained by the necessity to keep a sufficiently powerful tumble level, tumble level which tends to collapse in the vicinity of the TDC.

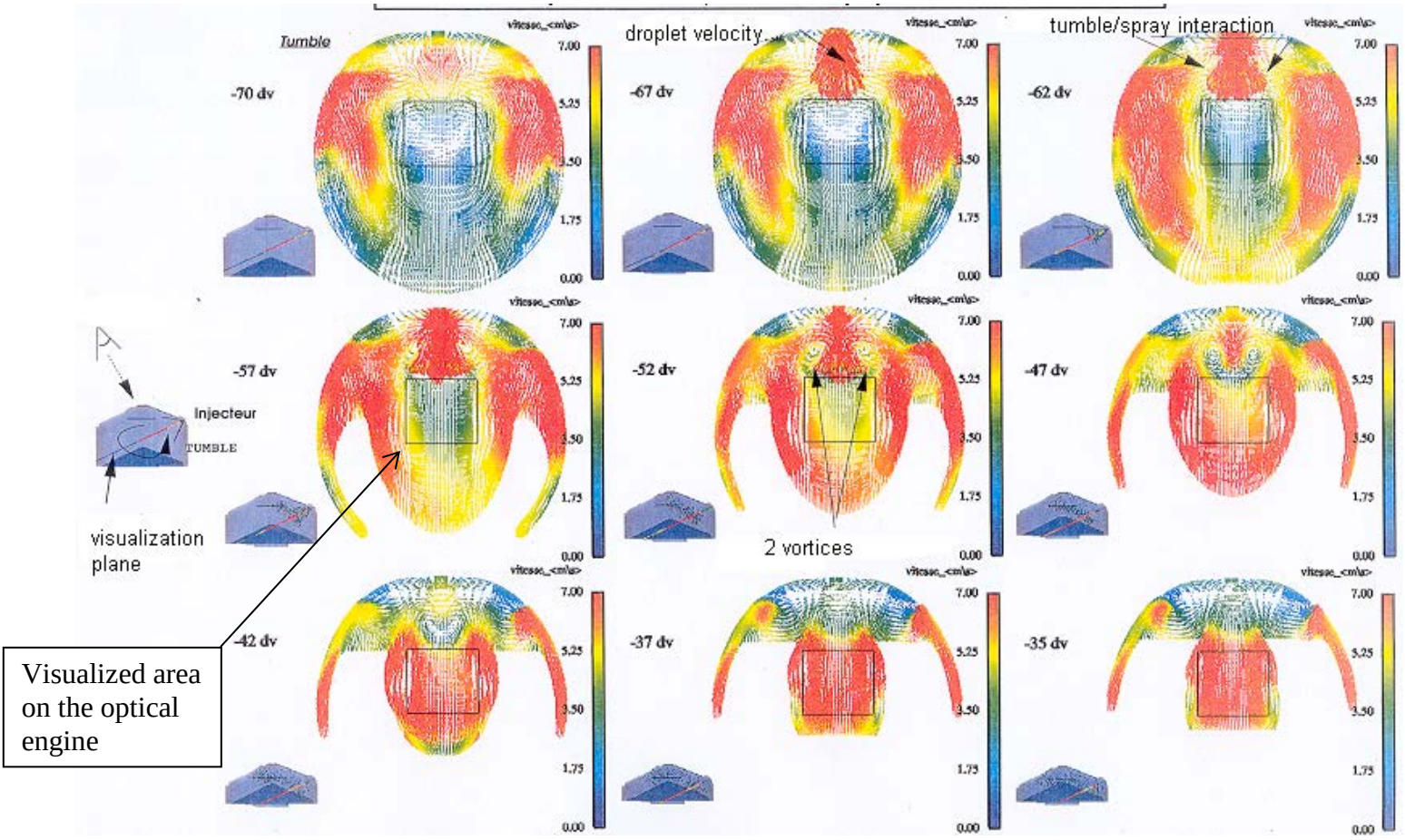

Figure 6-30: velocity field in a plane defined by the injector axis (see drawing on the left hand side of the picture); engine speed 1200 rpm – WOT – SOI - 69°CA, EOI – 56°CA

A focus on the cycle to cycle variation has been achieved by the help of the LIEF technique [6-14]. Figure 6-33 presents results from both the vapor and the liquid phases between -42 and -35°CA and at the same location as for the other visualizations.

The quite low equivalence ratio, especially at 37 and 35°CA BTDC when the average value is around 0.6, was confirmed but also the fact that the standard deviation of this ratio was nearly at the same order of magnitude than the average value (around 0.3 at 37°CA). The same situation exists with the liquid, showing that the vapor but also the droplets are submitted to the aerodynamics fluctuations.

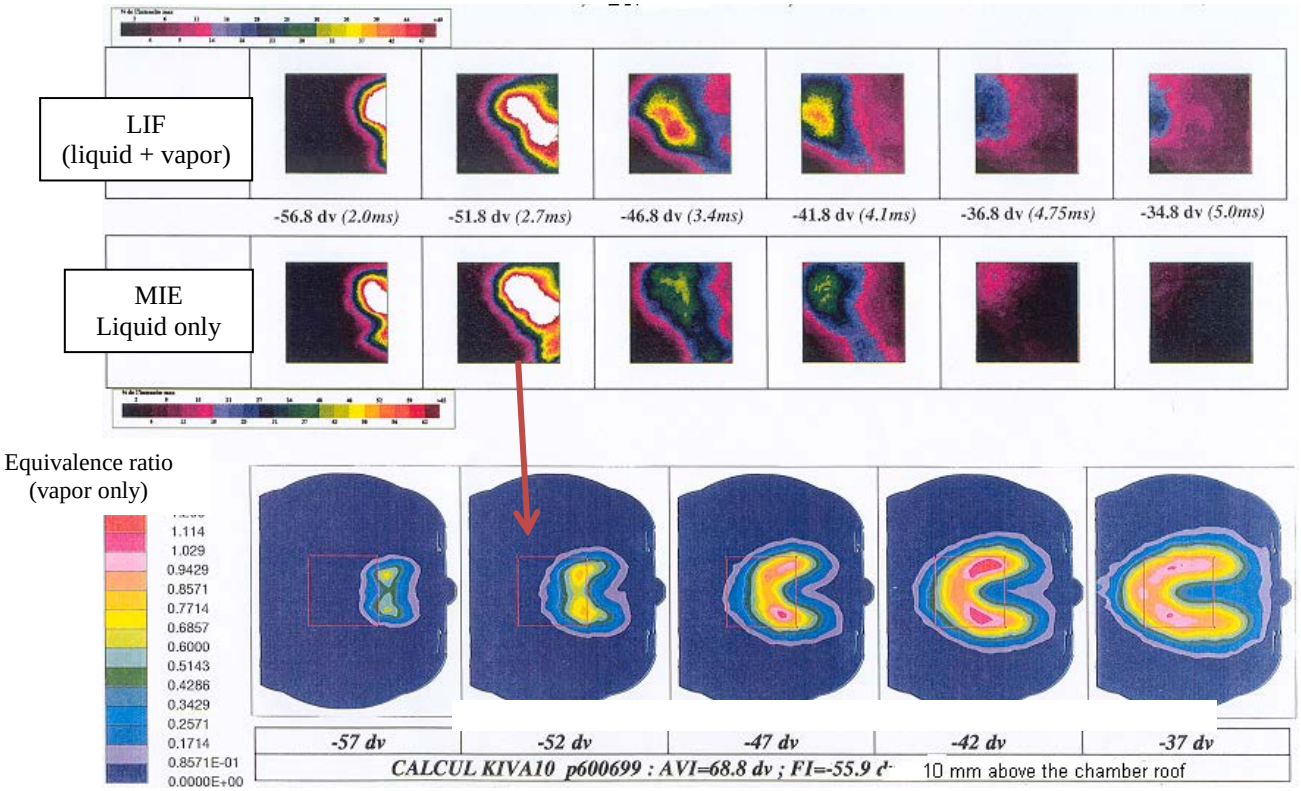

Figure 6-31: comparison between LIF/Mie visualization (upper figure) and Kiva simulation (lower figure): engine speed 1200 rpm – WOT – SOI at 69°CA, end of injection 56°CA BTDC – ignition timing 33°CA BTDC

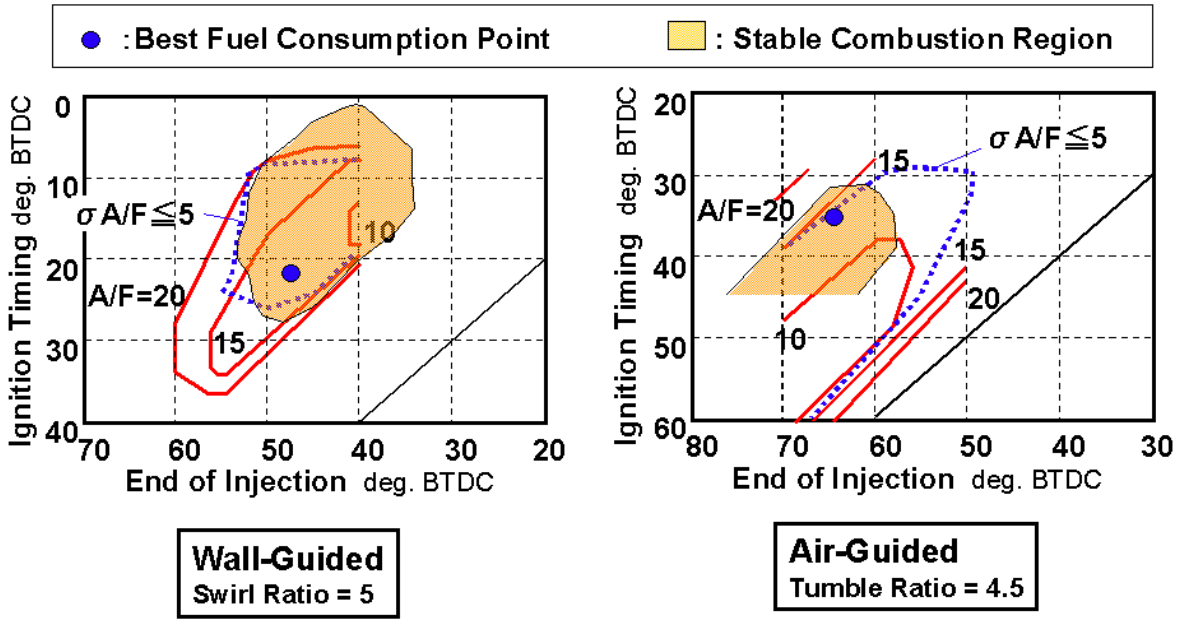

Figure 6-32: best tuning for both wall guided and air guided systems at 1400 rpm 3bars IMEP

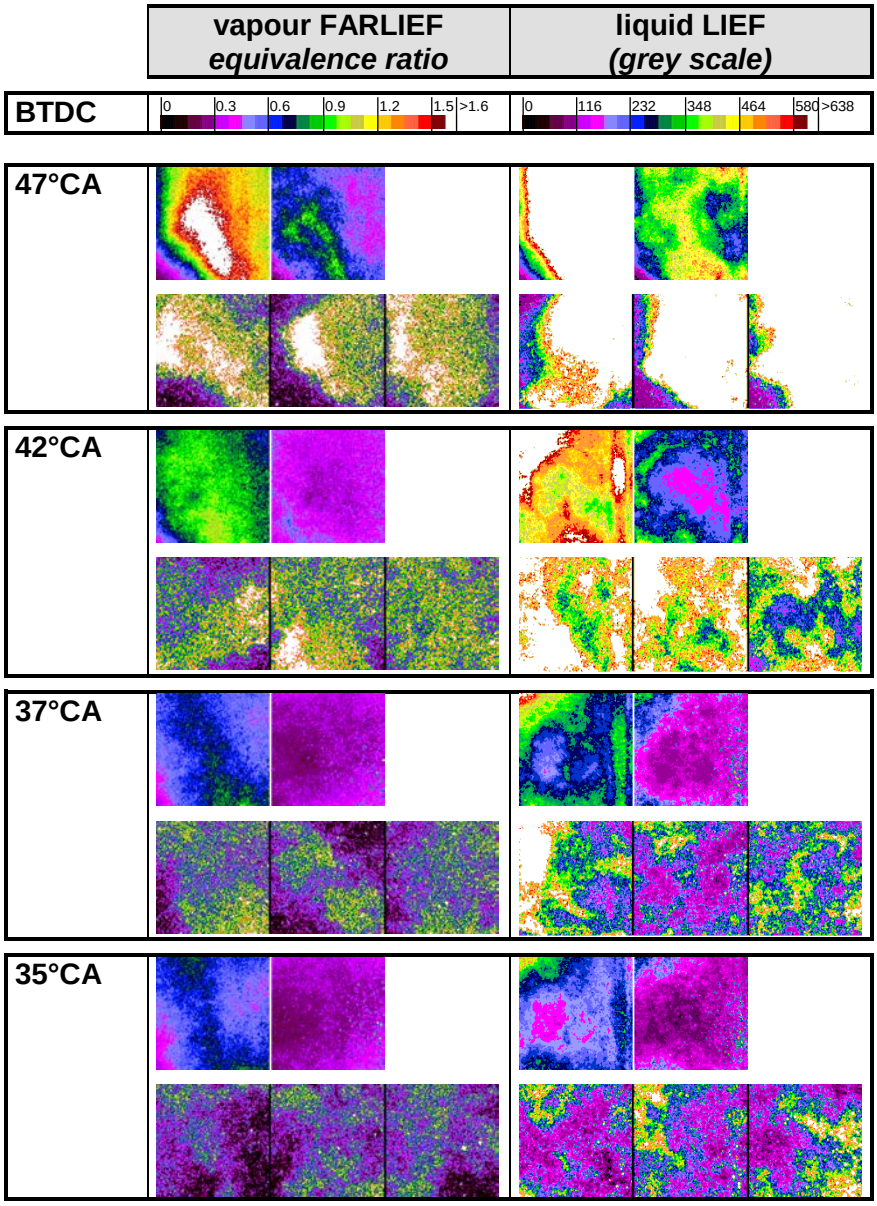

Figure 6-33: vapor and liquid maps obtained by LIEF at 1200 rpm, WOT. At each CA the two upper photos respectively represent the average field and the standard deviation, as the three lower photos represent individual cycles

6.4.5. Combustion at 2000 rpm.

As the Air Fuel repartition within the combustion chamber obtained with Kiva seemed to be quite accurate, it really was interesting to go on with combustion; therefore, the ECFM model (Coherent Flame Model for Gasoline engines) developed by the GSM has been used as well as the Diwakar model for heat transfers, even if this latest one generally overestimates the wall losses, especially during the expansion stroke.

First test was to compare the vaporized fraction of fuel during the cycle, with and without combustion. The calculation established that less than 2% of the fuel vapor was due to the combustion, the very great majority of this vapor being created by

the compression; this could be explained by the fact that the liquid droplets which had not been vaporized were situated out of the combustion region and were therefore not affected by the temperature rise - see droplets position at 2000 rpm in Figure 6-27.

A first rough calculation without residual gases –this hypothesis was coherent with the WOT operation- led to compare Kiva result with the average and min/max of 60 cycles measured on test bench –see Figure 6-34.
The experimental results showed a significant dispersion during the first half of the combustion, associated to low or high peak pressures (+/- 4 bars); this dispersion was not due to misfiring because of the peak pressure location but to significantly different combustion velocities at the beginning of the combustion. A cycle to cycle evolution of the Air Fuel ratio and/or the turbulence level could explain this behavior.

The cycle predicted by Kiva was quite close to the average experimental one, with a slightly lower peak pressure but a good phasing versus TDC. The rate of fuel consumption is presented in Figure 6-35 and showed a quick combustion beginning until 5°CA BTDC and then a quite slow propagation.

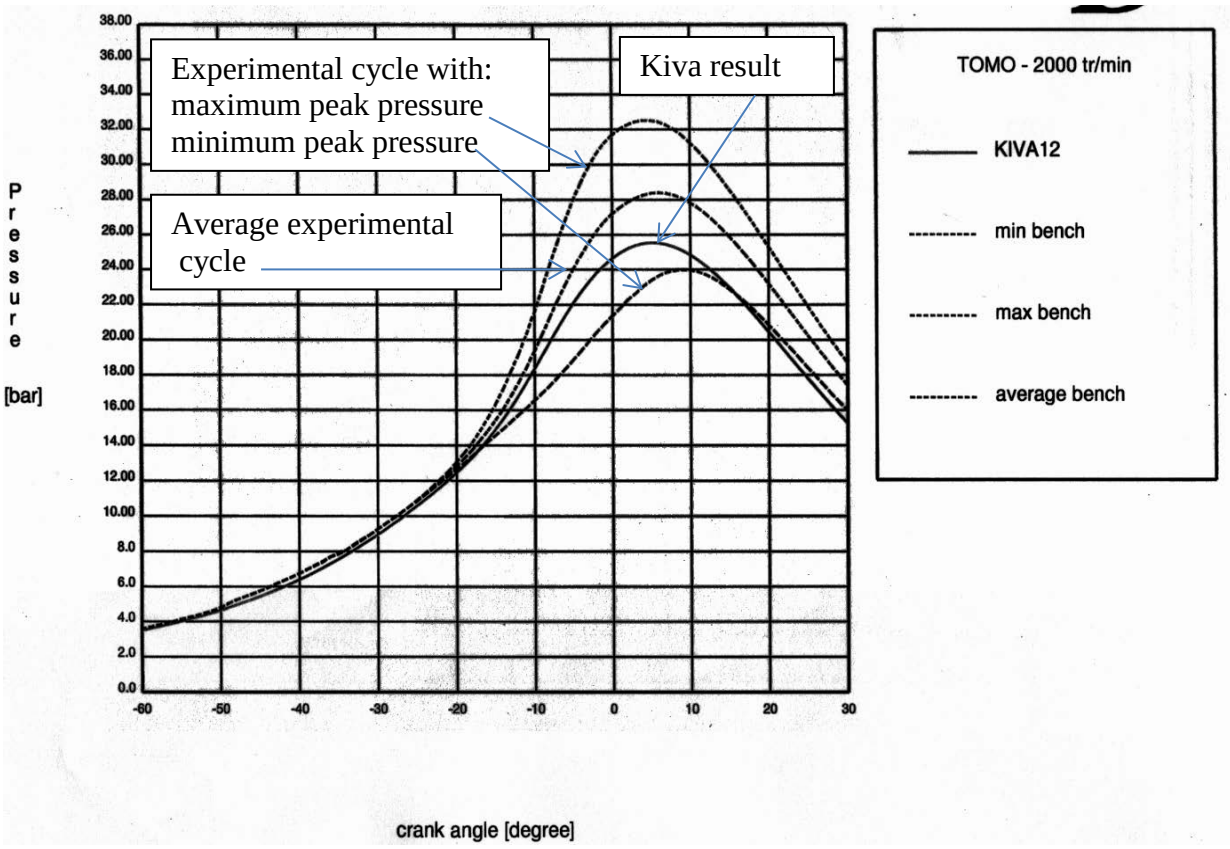

Figure 6-34: combustion pressure comparison between Kiva simulation and single cylinder engine tests – engine speed 2000 rpm – WOT – ignition timing 30°CA BTDC

.

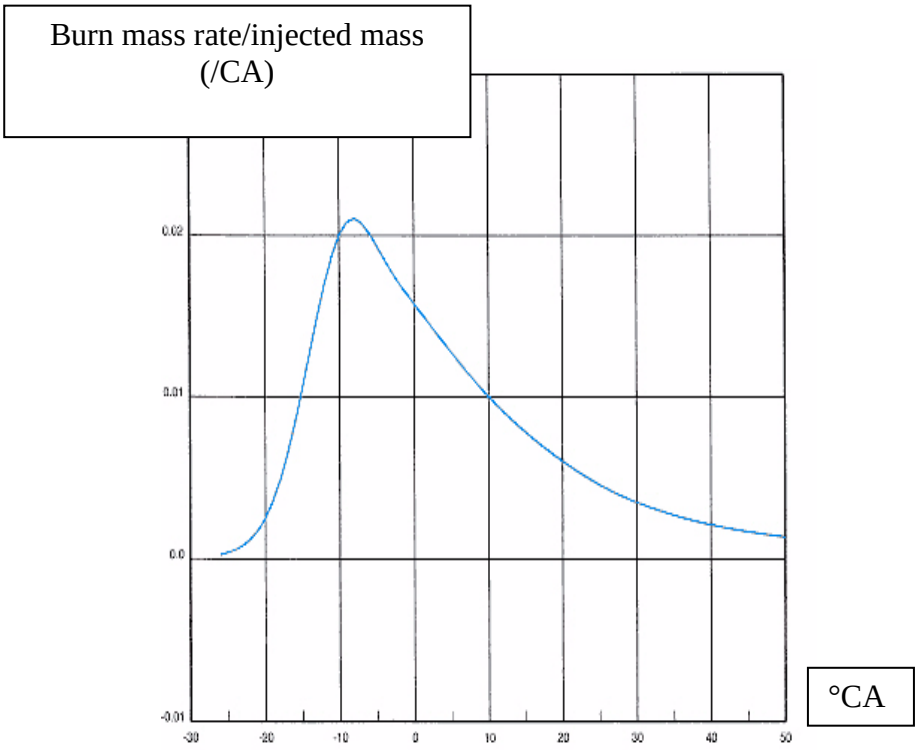

Figure 6-35: ratio of burn mass rate / injected fuel mass versus timing - engine speed 2000 rpm – WOT – ignition timing 30°CA BTDC – Kiva result

The 3D visualization of the equivalence ratio is presented in Figure 6-36 and the calculated reaction rate in Figure 6-37; the vapor repartition clearly explained that the flame initiated at the spark plug propagated quite quickly towards the chamber roof on the exhaust side until 5°CA BTDC (355°CA on the pictures) where the equivalence ratio was higher than 1.0, and then significantly slowed down as observed in Figure 6-37; some late burning zones appeared on the intake side where the equivalence ratio was lower than 0.8, near the injector nozzle, just beyond the chamber roof and in a quenching volume on the exhaust side. A slow reaction rate was also noticeable on the piston even if combustion seemed to be completed here. Remaining quite rich zones after 25°CA ATDC could lead to HC emissions, which generally was a drawback for Gasoline Direct Injection SI engines.

One time again, the high gradient in fuel repartition, in the vicinity of the plug was quite noticeable and could explain that, in some conditions, the flame velocity could be quite low at the beginning of the combustion as illustrated by Figure 6-34.

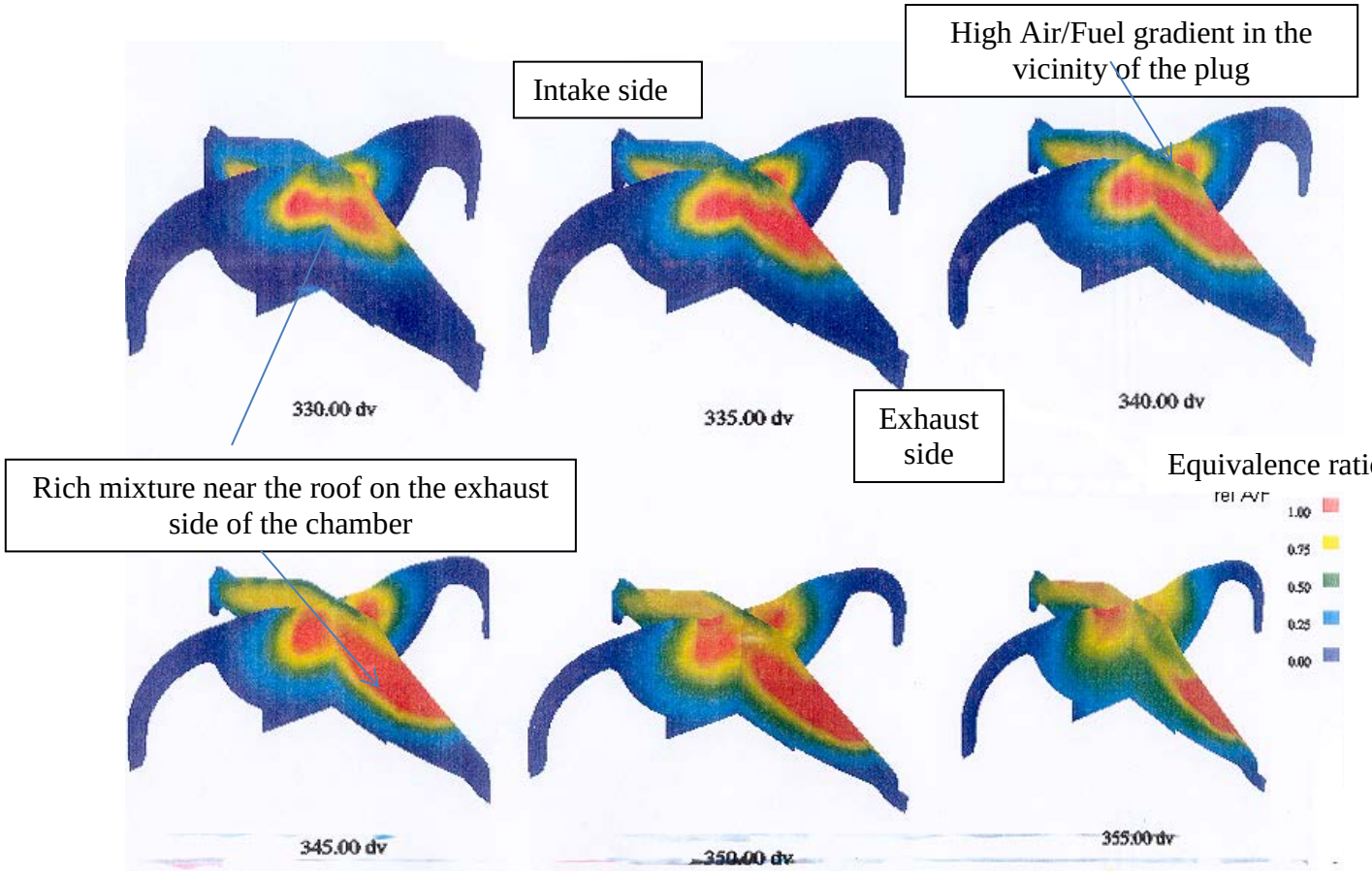

Figure 6-36: equivalence ratio repartition (upper figure) at 2000 rpm WOT

Figure 6-37: reaction rate (lower figure) at 2000 rpm, WOT – Kiva results

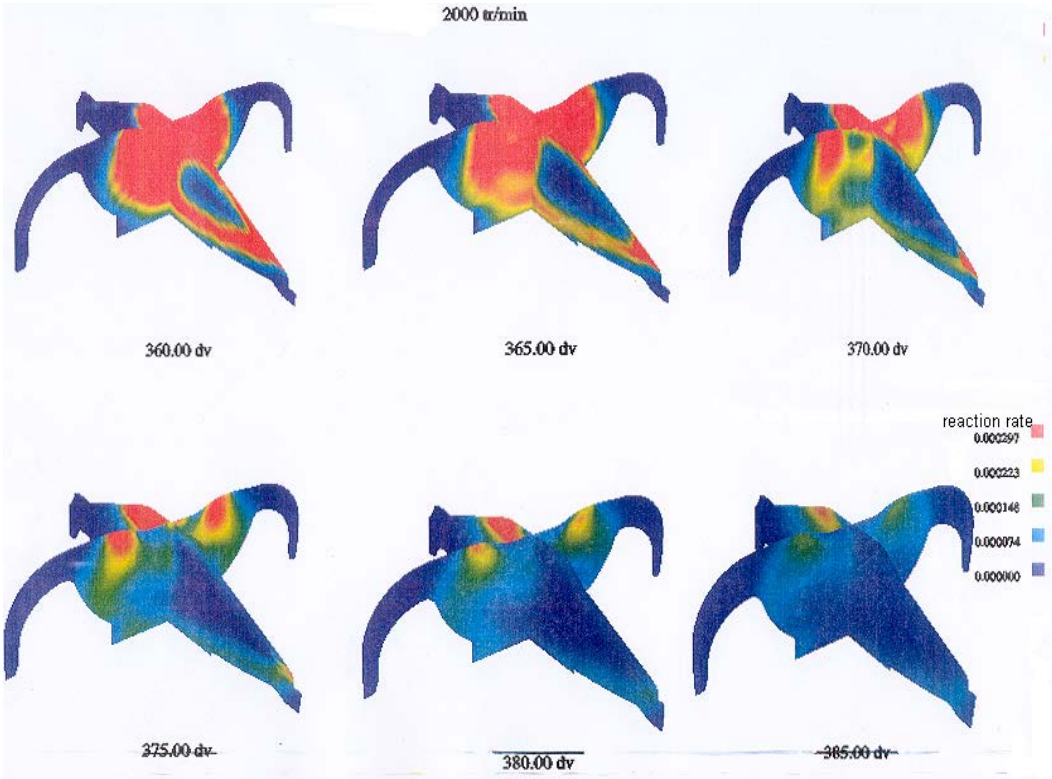

6.4.6. Conclusion.

The difficulty to obtain an acceptable cycle to cycle dispersion avoiding misfiring was due to a high equivalence ratio gradient in the vicinity of the spark plug, especially at low engine load and WOT; the problem could be avoided by the use of protruding electrodes but some remaining reliability risks didn't allow the industrialization of the system; the second problem was due to the engine to engine dispersion for the tumble level generated by the ports and the sensitivity to the TCV position.
These risks had been clearly identified during the development phase described above.
Nevertheless a quite close concept, called FSI, was mass-produced for the European market and adapted on a 2.0 l engine [6-19] –see Figure 6-37. A specific on line control of the tumble level was set up on the engine assembly line, probably to avoid the previous difficulties previously described. Nevertheless a very few number of cars were produced.

Figure 6-37: FSI concept – description of the stratified mode [6-19]

6.5 Conclusion.

6.5.1. Methodologies and tools.

Despite the fact that this program was focused on combustion in stratified mode, a great part of the activity has been dedicated to precisely understand the interaction between the aerodynamic field and the injector spray.

If the heart of the problem –eg securing the Air/Fuel ratio in the vicinity of the ignition plugs- was the same for both the MID3S described in Chapter 5 and the K5M, the corresponding physics was completely different. For the MID3S the mixture formation was primarily governed by the spray pattern; direct visualization and qualitative diagnosis of the fuel evolution in a reduced volume of the chamber, where plugs and injector tip were located, were therefore quite sufficient to establish a precise diagnosis of the mixture. For this purpose, endoscopes carefully oriented in the chamber completely satisfied the needs. On the other hand, the use of a high speed film camera fitted very well with the observation of the most interesting events occurring during one cycle –the injection and the combustion.

For the Air Guided system, the situation was quite different because the complete chamber had to be visualized; the interaction between the air and the spray spatially began at the injector outlet, under the intake ports, and had to be followed until the interaction with the piston bowl and thereafter until the chamber roof and the plug. On a temporal scale, the development of the direct tumble motion had to be investigated from the beginning of the intake stroke until the injection. Local diagnosis as they were used for the MID3S engine were clearly not sufficient to provide efficient results and it was therefore necessary to develop advanced optical techniques, adapted to an optical engine, to provide the largest possible field of vision in the chamber. Techniques such as Particles Image Velocimetry PIV for a detailed description of the flow field and Laser Induced Fluorescence LIF or Exciplex LIF to follow both the liquid and the fuel vapor had to be developed for Direct Injection applications. The use of an intensified CCD camera didn't allow to monitor a complete cycle and cumulative sampling techniques had to be used to have an idea of the cycle to cycle dispersion, especially of the Air/Fuel ratio at the plugs.

Last but not least, the 3D CFD has been intensively used to compare different design solutions, for both the tumble intensity and the piston shape.

For the future, optical and numeric tools might be improved to have a better understanding of the aerodynamic instabilities and the misfire events which mainly prevented the use of this solution for an industrial application.

6.5.2. Physics.

A very few work has been achieved on the injector because it was an entry data for our problem; the swirl technology has been imposed by the suppliers because this injector had already been industrialized for "Wall guided" systems and seemed to be able to cover the wide range of customers. Spray momentum and penetration, which

are key factors in the compliance with the tumble level, were therefore marginally modified during the project to be matched with the quite weak available air velocities. This optimization was clearly not sufficient, especially at low engine speed where the tumble level was naturally low.
The correlative question would concern the ability to improve the spray atomization as the injection pressure was reduced; with the prototypes used during this program, it would have been necessary to use an injection pressure lower than 30 bars in these last conditions. This was not possible because the fuel droplets became too big, leading to a poor evaporation and to a high fuel dispersion in the chamber.

Bibliography.

[6-1] MMC close to a production DI gasoline 4-stroke
RD's Engine and Vehicle Technology Update – 02/1992

[6-2] Mitsubishi Motors Begins Research on In-cylinder Injection Technology of Gasoline Engine
EGIS "The Japan Automobile Letter" – 05/1992

[6-3] Toyota plans DI gasoline engine in 1993
Ward's Engine Update – 10/1992

[6-4] Closeup: Gasoline DI could make waves soon
Ward's Engine Update – 03/1992

[6-5] Y.Iwamoto, K.Noma, O.Nakayama, T.Yamauchi, H.Ando: Development of Gasoline Direct Injection Engine
SAE 970541

[6-6] H.Tatsuta, M.Matsumura, J.Yajima, H.Nishide: Mixture Formation and Combustion Performance in a new Direct-Injection SI V6 engine
SAE 981435

[6-7] A.Kakuhou, T.Urushihara, I.Itoh, Y.Takagi: Characteristics of Mixture Formation in a Direct Injection SI Engine with Optimized In-Cylinder Swirl Air Motion
SAE 99010505

[6-8] P.Wolters, M.Grigo, P.Walzer: Betriebsverhalten eines direkteinspritzenden Ottomotors mit luftgeführter Gemischbildung
6.Aachener Kolloquium 1997

[6-9] European Patents:
a) R.Leboeuf, P.Gastaldi, C.Voisin : EP 0997622
b) A.Floch, P.Gastaldi, JC.Lucas, D.Stéphan : EP 1068433

[6-10] W.Ren, J.Shen, JF.Nally: Geometrical Effects Flow Characteristics of a Gasoline High Pressure Swirl Injector
SAE 971641

[6-11] A.Ahmed, A.Dupont, P.Gastaldi, D.Stéphan: Entwicklung eines neuen Brennraums für einen luftgeführten DI-Otto Motor mittels neuster experimenteller und computergestüzter Entwicklungstools.
9.Aachener Kolloquium 2000

[6-12] P.Gastaldi, C.Préterre: Entwicklung neuer Methoden zur Analyse von direkteinspritzenden Ottomotoren
8.Aachener Kolloquium, 1999

[6-13] J.Fischer, M.Kettner, A.Nauwerck, J.Pfeil, U.Spicher: Influence of an Adjustable Tumble System on In-Cylinder Air Motion and Stratification in a Gasoline Direct Injection Engine
SAE 2002-01-1645

[6-14] A.Dupont, A.Floch, X.Baby: In-cylinder flow investigation in a GDI 4 valve engine : bowl shape piston effects on swirl and tumble motions
FISITA 1998

[6-15] JC.Saccadura, L.Robin, F.Dionnet, D.Gervais, P.Gastaldi, A.Ahmed: Experimental Investigation of an Optical Direct Injection S.I. Engine using Fuel-Air Ratio Laser Induced Fluorescence
SAE 00FL-221

[6-16] P.Gastaldi, D.Gervais: Application of various Laser Induced Fluorescence techniques as tools for developing a new air guided direct injection SI combustion chamber
Haus der Technik Essen – Esslingen - 2000

[6-17] D.Gervais, P.Gastaldi: a comparison of two quantitative Laser Induced Fluorescence Techniques applied to a new air guided direct injection SI engine
SAE 2002-01-750

[6-18] A.Kakuho, K.Yamaguchi, Y.Hashizume, T.Urushihara, T.Itoh, E.Tomita: A Study of Air Fuel Mixture Formation in Direct Injection SI Engines
SAE 2004-01-1946

[6-19] Audi France – press book on the FSI system presented at the Paris Motor Show Paris - September 2001.

Chapter 7

The Lifted Flame Diffusion Controlled (LFDC) combustion

7.1. Introduction.

Since its birth, and except for the pre-chamber IDI design only dedicated to small displacement engines, the Diesel combustion system has remained quite unchanged until now, with a more or less central injector, a flat cylinder head and a bowl-in piston. The evolutions have clearly been led by the injection improvements such as the increase of the number of holes in the nozzle, from 5 to 8 or more, the higher pressures, from 800 to 2400 bars, and the shift from hydraulically to solenoid or piezo driven injectors. This trend is clearly explained by the fact that mixture preparation between fuel and air in the diffusion mode is generated by the spray, just because of the ratio of the momentum energies between the droplets and the air motion.

Differences in swirl level or bowl shape are directly related to the modifications of the fuel spray, such as penetration or plume angle versus time and back pressure. Optimizing a Diesel engine must thereby clearly begin by a good understanding of the injector behavior and then by the interaction between the environment and the plume.

For all these physical reasons, this chapter is different from the two previous ones. It is based on a dramatic evolution of the nozzle holes diameter, paving the way to a possible new combustion mode. As well as the work on GDI engines was either focused on more or less “global” interactions between air and fuel, this investigation was clearly driven by the local interferences at the boundary and inside the spray plume. The greatest part of the work has therefore been allocated to understand the behavior differences between currently available and innovative nozzles concerning mixture preparation and combustion. Some minor adaptations have been allocated to the swirl and to the piston shape as it is usual for Diesel.

It is nevertheless following the same methodology which consisted in identifying the key phenomena occurring in mixture preparation, choosing the most adequate optical or numerical diagnosis to capture them, and using the results to interpret conventional tests. In this chapter, the area of interest was situated from the vicinity of the plume until auto ignition and soot formation in the diffusion flame. Main parameters of the engine tuning, as the EGR rate and the boost pressure (or the oxygen content) were identified and estimated in more “academic” conditions than the conventional single cylinder engine to be sure to correctly understand the physics.

7.2. General design.

7.2.1. Specifications and requirements.

The trend for more and more stringent regulations concerning Diesel exhaust pollutants has led and currently leads to investigate new combustion modes, with the aim to reduce engine out emissions and to reduce the cost of the after-treatment system.
This challenge was particularly difficult for down-sized engines equipping quite heavy passenger cars or light duty vehicles, as an example is illustrated in Table 7-1 for the H9M engine which was the base of the current LFDC research program.

Cylinder displacement cm^3	Stroke mm	Bore mm	Compression ratio	Number of valves	aerodynamics
402	80	80	15 to 1	4	Variable swirl

Table 7-1: basic characteristics of the H9M engine

The performance requirement was to achieve a power density of at least 60 kW/l while maintaining both conventional levels of fuel consumption and a moderate combustion noise, this last item taking a great importance for passenger car applications.

Concerning the industrial tool, cylinder block, connecting rod and crankshaft had to remain unchanged while piston and injection systems were completely free.

7.2.2. Background of low emissions concepts.

7.2.2.1. Physics of the Diesel combustion.

As presented in Figure 7-1, the traditional Diesel combustion is generally composed of two phases of heat release; the first one is the “premixed burn” and the second one is the “mixing controlled burn”. The balance between the two phases depends upon thermodynamic and injection conditions like fuel quantity and timing.

During the phase 1 of the diagram, the fuel is premixed with the air prior to auto-ignition. It has therefore enough time to be mixed with the gases present in the chamber, generating lean or dilute mixtures for which the flame temperature is too low –typically under 2200 K- for a significant NOx formation, and the fuel-air ratio too lean –typically lower than 2- for soot formation (phase 2 on the diagram).

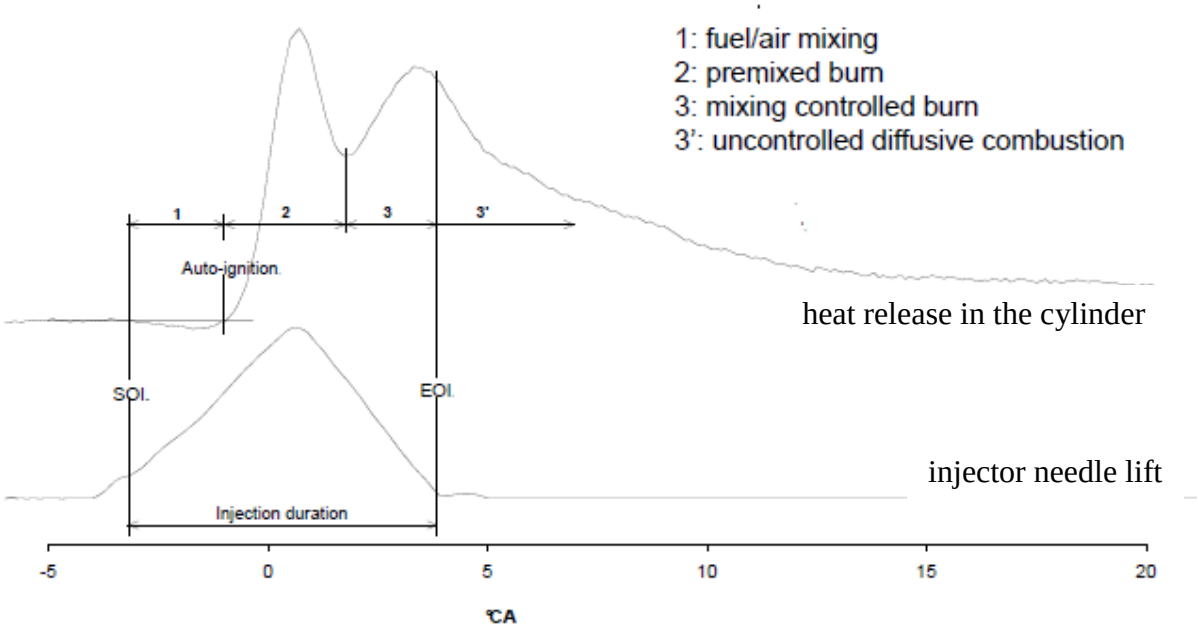

Figure 7-1: traditional shape of the Diesel heat release

During the mixing controlled phase (phase 3), the fuel is on the contrary progressively burning as it is introduced in the chamber. The heat release is generally limited by the rate of mixing of fuel with the surrounding air. As a diffusion flame is formed at near stoichiometric fuel-air mixtures, NOx formation is high due to the important level of the diffusion flame temperature at typical Diesel operating conditions, exceeding 2600 K. Soot formation occurs inside the envelope of the diffusion flame in the fuel-rich regions of the jet after some standoff distance from the injector as explained by the model proposed by Dec –see Figure 7-2 [7-1]. This mechanism is not only led by the injection strategy but also by the spray behaviour in the chamber –that is to say by the nozzle internal flow whose properties are hardly obtained, even with sophisticated simulation tools.

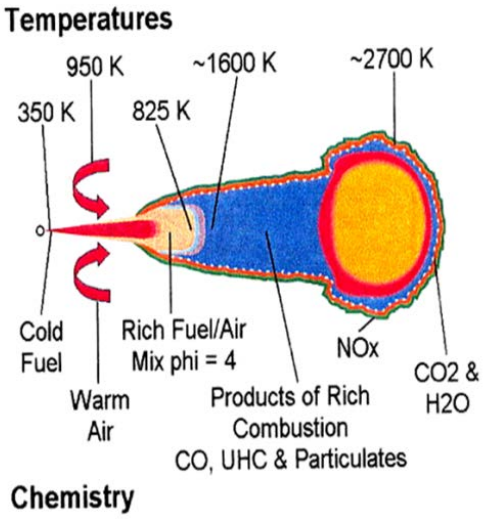

Figure 7-2: conceptual model of the diffusive combustion proposed by Dec [7-1]

During the expansion stroke, an uncontrolled combustion occurs after the injection has stopped (phase 3'). Soot can be oxidized if the temperature remains over 1500 K and if a sufficient amount of OH and oxygen is available.

The existence of these two main combustion phases, whose repartition depends upon the engine load and the injection tuning, leads to the emission chart first presented by Kamimoto in 1988 and illustrated in Figure 7-3 [7-2]. The interaction of the "mixing controlled zone" with both NOx and soot peninsula is pointed out with the red circle.

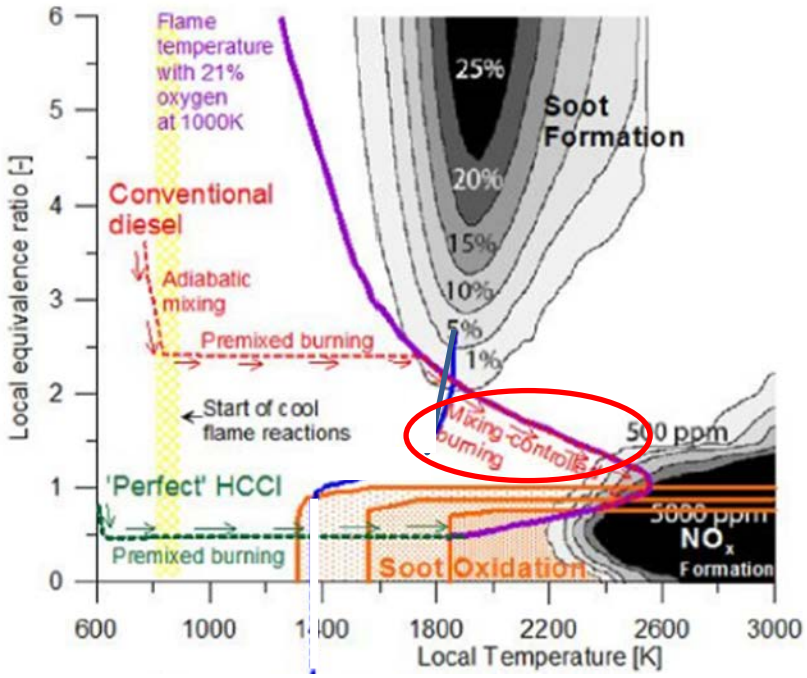

Figure 7-3: generic NOx and soot Kamimoto chart for Diesel combustion [7-2]

As the very high temperature / rich zone in the right upper part of the above diagram is not very realist for industrial applications, all the efforts have therefore been focused on the low temperature zone; this clearly led to the development of Low Temperature Combustion strategies (LTC).

A first limitation to the LTC concept clearly appears in the chart with the "soot oxidation" area which necessitates both temperatures higher than 1400 K and a sufficient level of residual oxygen.

The second important problem, quite unknown by Diesel specialists until the first LTC investigations, is concerning hydrocarbon and carbon monoxide emissions. The possibility to oxidize them as well as soot during the expansion stroke has to be taken into account. Miles showed that a minimum temperature of 1200 K is necessary for HC and of 1400 K for CO [7-3] –see Figure 7-4.

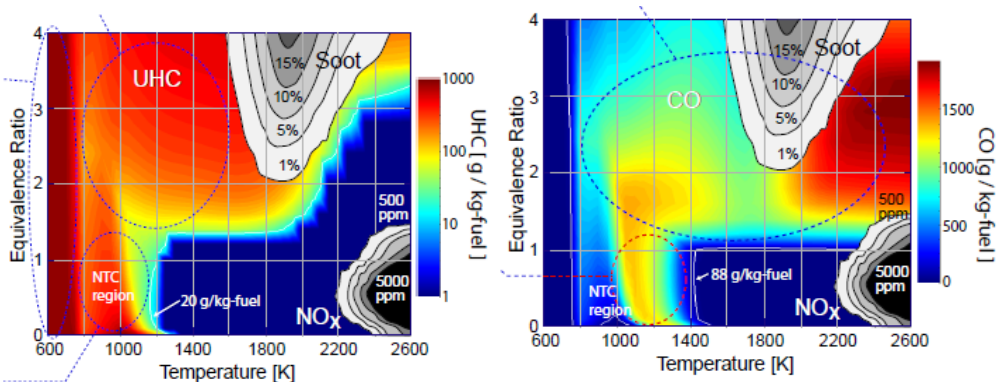

Figure 7-4: HC (left) and CO (right) production chart in Kamimoto diagram [7-3]

That is to say that the really available area for LTC is very much restricted compared to the theoretical zone only defined by the NOx and soot peninsula.

Last but not least, the noise level, which is very important for passenger car applications at low and medium engine speeds, is proportional to the intensity of the heat release rate. The higher the fuel quantity burns in premixed mode –eg the higher the load is-, the higher the noise level is. On the contrary, the heat release in diffusive combustion is mainly governed by the injection rate; in this case, the noise intensity is much smoother and, for a given nozzle hydraulic flow, can be modulated by the injection pressure.

7.2.2.2. Emergence of HCCI

At the beginning of the 21st century, solutions to achieve a proper LTC were very well identified, proposing the reduction of the compression ratio and the intensive use of EGR, but two alternatives remained open concerning the tuning of the air fuel ratio:

- The first one consisted to operate the engine in lean mode –eg to favour a premixed combustion located in the left lower part of the Kamimoto diagram as proposed by Kimura [7-4]
- The second one consisted to operate the engine in rich mode, –eg to favour diffusive combustion – see Sasaki [7-5]-, in the left upper part of the chart.

The choice was mainly linked to the complexity of the two solutions.

For the lean premixed mode, the burn is mainly governed by the physical parameters interacting with the delay, mostly the A/F ratio, regulated by the EGR and air mass flows, and the surrounding gas temperature and pressure; concerning the hardware, a reduction of the compression ratio from around 17 down to 15 or 14 was very often proposed to naturally generate a long delay, for instance with the NADI [7-6] or the MK ([7-4] and [7-7]) concepts; thereafter, for each operating point, a high EGR level associated to advanced injection timings was used to govern combustion; the association of theoretically homogeneous mixtures and low temperatures obtained with a

high EGR rate was very often called HCCI for “Homogeneous Combustion Compression Ignition”.

For the rich mode, which relied on the diffusive combustion process, the way the fuel is injected in the chamber –eg the mass rate and the rail pressure - had to be optimized for each operating point. Unfortunately, the spray plume and the mixing between fuel and air or EGR also depend on the flow pattern in the injector nozzle, whose detailed geometry and surface roughness have a highly significant influence. The great difficulty to manage this mixing mechanism, even with sophisticated simulation tools, led researchers and manufacturers to firstly develop the lean mode strategy for prior LTC investigations.

7.2.2.3. HCCI concepts

If many acronyms have been used to avoid the generic HCCI name, all the strategies were based on a highly diluted premixed combustion. The most important differences concerned the injection timing as illustrated in Figure 7-5 and thereby the way the fuel was injected.

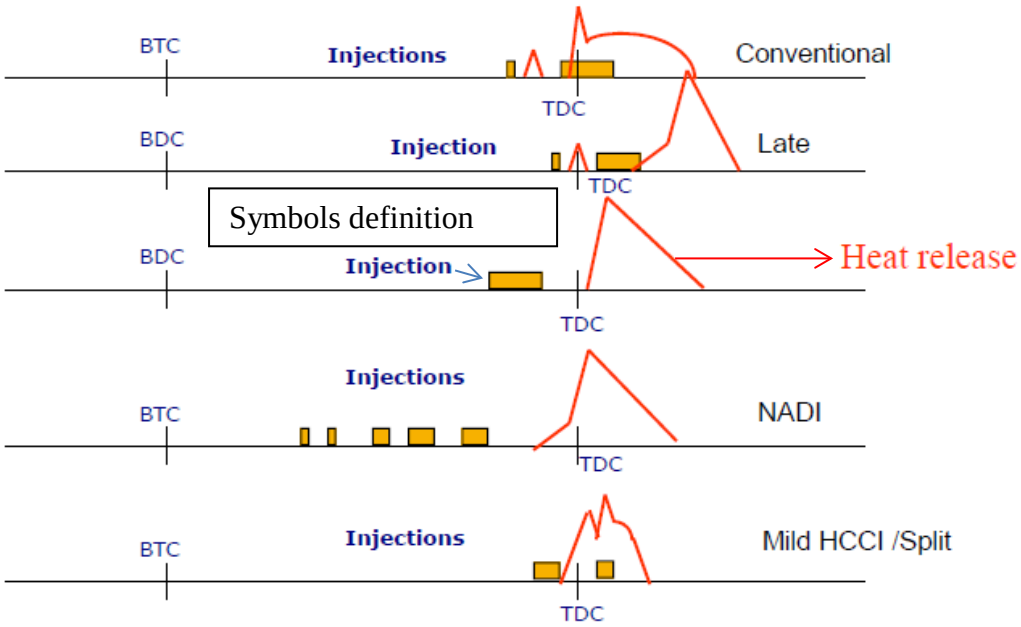

Figure 7-5: injection strategies to achieve a homogeneous combustion at part load

At part load, for conventional combustion strategies, a two or a three injection schedule, with one or two “pilots”, is generally used to manage the combustion noise.

A first quite natural solution to burn in premixed mode at low temperature was to retard the injection as much as possible in order to take advantage of the natural temperature decrease during the expansion stroke; the benefit was clear concerning NOx and soot production, but the crank angle window for securing a sufficient oxidation of the particles was clearly limited in order to secure the

1400 K boundary seen §7.2.2.1. Meanwhile, the thermodynamic efficiency was very much reduced because of the late heat release.

A second solution consisted in injecting very early in the compression phase while securing that all the fuel was introduced before auto ignition occurred; the difficulty was first to achieve a fair mixture homogeneity while avoiding the impact of the liquid spray on the cylinder liner, and to manage noise as all the fuel was burning in premixed mode.
One of the most interesting and advanced concept, proposed by IFP and called NADI ([7-6] and [7-8]) for Narrow Angle Direct Injection, has been intensively developed and tested by manufacturers for car and trucks applications. The basic idea was to inject very early during the compression stroke to secure a lean homogeneous mixture at TDC. To achieve this task and to avoid an intense wetting of the cylinder liner, a dedicated piston bowl shape associated to a quite narrow spray sheet angle were necessary as illustrated in Figure 7-6. The split injection helped both to reduce the spray penetration but also secured some time for a proper mixing, as far as the fuel quantities remained moderates.
Huge amount of EGR associated to a much reduced CR around 14 contributed to obtain a temperature low enough to retard auto-ignition for the majority of the operating points.
Figure 7-7 clearly shows the unconventional route followed by the liquid in the piston bowl. Nevertheless, a dedicated optimization of both the spray sheet angle and the piston bowl shape allowed to obtain an acceptable power density above 60 kW/l with a smoke level comparable to conventional engines [7-9].

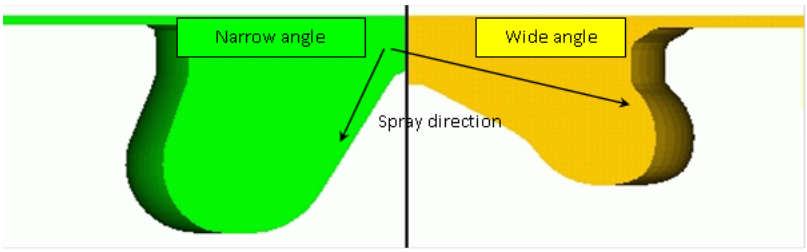

Figure 7-6: piston bowl shape for NADI (left) and conventional (right) combustion systems

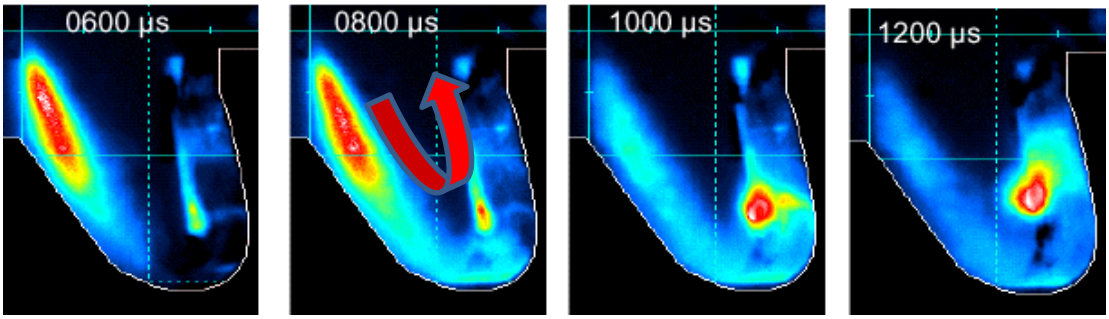

Figure 7-7: development of the liquid fuel phase in the piston bowl of a NADI engine – visualization by LIF technique- at different time after SOI

At part load, soot and NOx emissions were very much reduced in comparison with conventional combustion but two main difficulties remained unfortunately unsolved:

- The presence of high levels of HC and CO at very low IMEP, due to both the over-mixing effects linked to the very early injections and to the very low temperature during the expansion stoke which froze the oxidation reactions–see §7.2.2.1.
- The noise level which was unacceptable over 6 bars IMEP because of the premixed combustion.

The relative failure of these first systems led to develop a new concept called Mild HCCI and inspired from the NADI ([7-10] and [7-11]).

7.2.2.4. Mild HCCI combustion

To overcome several drawbacks of the NADI concept, the following solutions were implemented on the Mild HCCI design [7-12]:

- A come back to a conventional chamber arrangement –spray sheet angle and bowl design- to secure an acceptable mixing controlled combustion at high and full loads for power density, but also to avoid any design problem with a very deep bowl.
- A compression ratio reduced to 15 –eg 1 to 2 points lower than for conventional Diesel applications- but higher than the value of 14 used on the NADI; this choice was led by the necessity to govern HC and CO emissions at very low engine load, when the oxidation catalyst is not operating, and to secure cold start.
- A quite conventional injection timing phased at the end of the compression stroke in order to avoid fuel over-mixing and thereby high HC and CO emissions.

The new idea was thereafter to implement two injections, with comparable fuel quantities, in the vicinity of TDC, with a small time interval –the dwell- between them. This tuning has been called “split main injection” by some authors. Fuel introduced before TDC during the first injection period has sufficient time to be mixed with the surrounding gases before auto-ignition; the second injection occurs after this ignition and during the combustion of a part of this fuel; the evaporation of the fuel introduced during the second injection cools down the chamber and therefore slows down the combustion, limits the heat release, and thereby the noise as observed in Figure 7-8.

The influence of the dwell between first and second injection and the existence of an optimum value of around 5°CA are clearly highlighted with the heat release traces. With a dwell of 3°CA, the first injection has not burnt enough when the second injection is occurring; the fuel injected during the second one is mixed with the previously formed mixture and there is only one “fully premixed” and noisy combustion; with a dwell of 7°CA, the second combustion occurs too late as the first one is almost finished and burns in the expansion stroke with a poor efficiency and a high soot level.

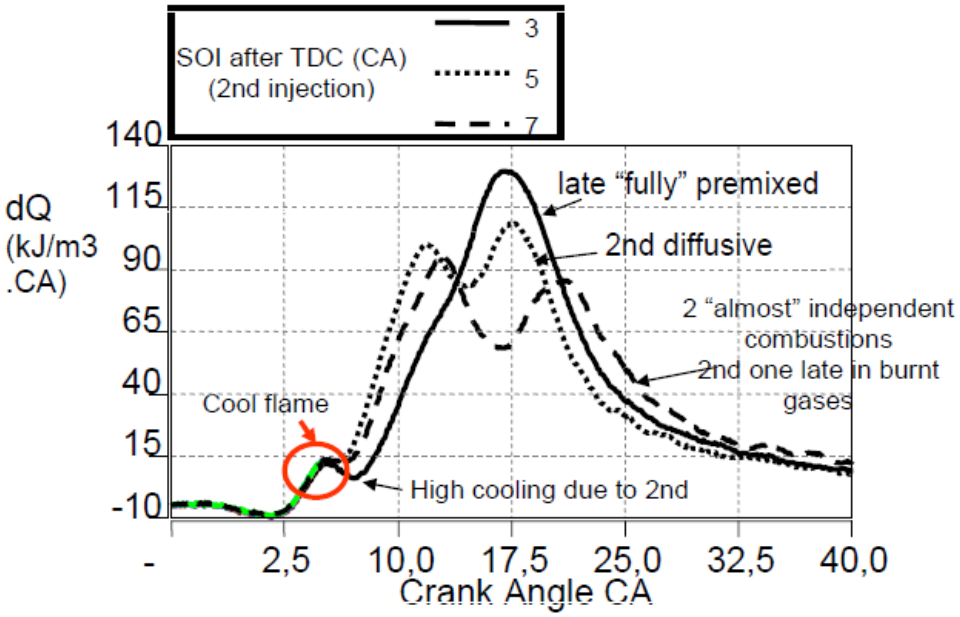

Figure 7-8: heat release rate for Mild HCCI combustion
2000 rpm – 6 bars IMEP

The comparison between results obtained with the NADI "early injection" and the Mild HCCI / split strategy are described in Figure 7-9a and b. The tests were achieved with a NADI hardware (injection, nozzle, piston bowl…) and only the injection tuning changed.

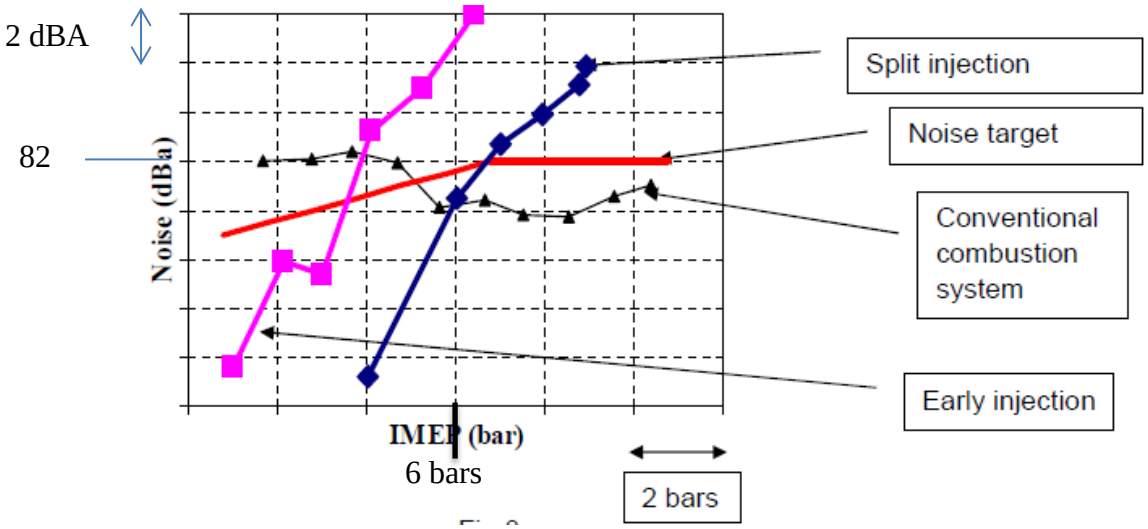

Figure 7-9a: effect of the injection strategy on the noise level at 2000 rpm, constant NOx emissions at a fixed IMEP.

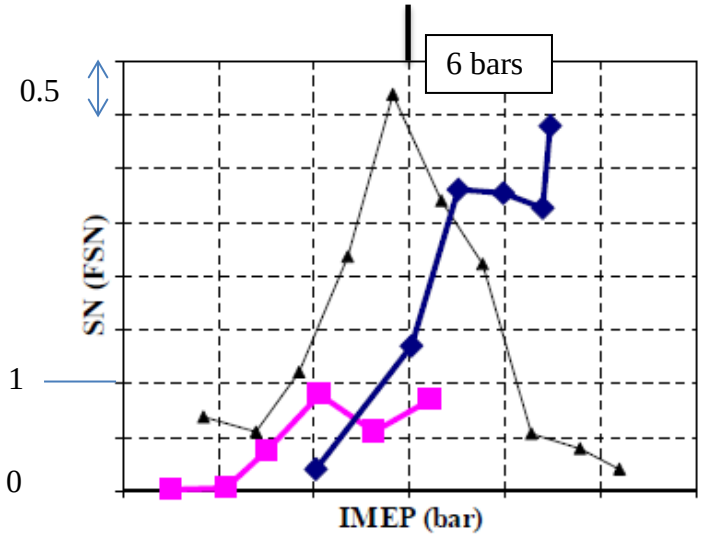

Figure 7-9 b: effect of the injection strategy on the smoke level at 2000 rpm – constant NOx emissions at a fixed IMEP

The advantage obtained with the split injection can be summarized by a reduction of around 6 dBA at same IMEP with a fairly low and acceptable soot level.
Nevertheless it was obvious that even the Mild HCCI was not able to cope with the noise target above 8 bars IMEP, limiting its use to the lower part of the engine map, especially for heavy vehicles.

7.2.3. Proposal for an improved diffusion controlled combustion.

Following the evidence that systems based on homogeneous burn were limited to light or medium engine loads, the necessity to improve diffusive combustion at high engine torques became obvious, especially for heavy applications.
It is then not surprising that the first proposal came from an industrial and trucks engines manufacturer, Cummins. In 2008, Stanton [7-13] proposed therefore to develop a combustion system which would allow both premixed (PCCI for Premixed Combustion Compression Ignition) and improved diffusive burns - see Figure 7-10.

The basic statement was to replace the conventional Diffusion Controlled combustion by the Lifted Flame Diffusion Controlled LFDC one whose principle had been demonstrated by Siebers in 2001 [7-14] in a constant volume reactor.

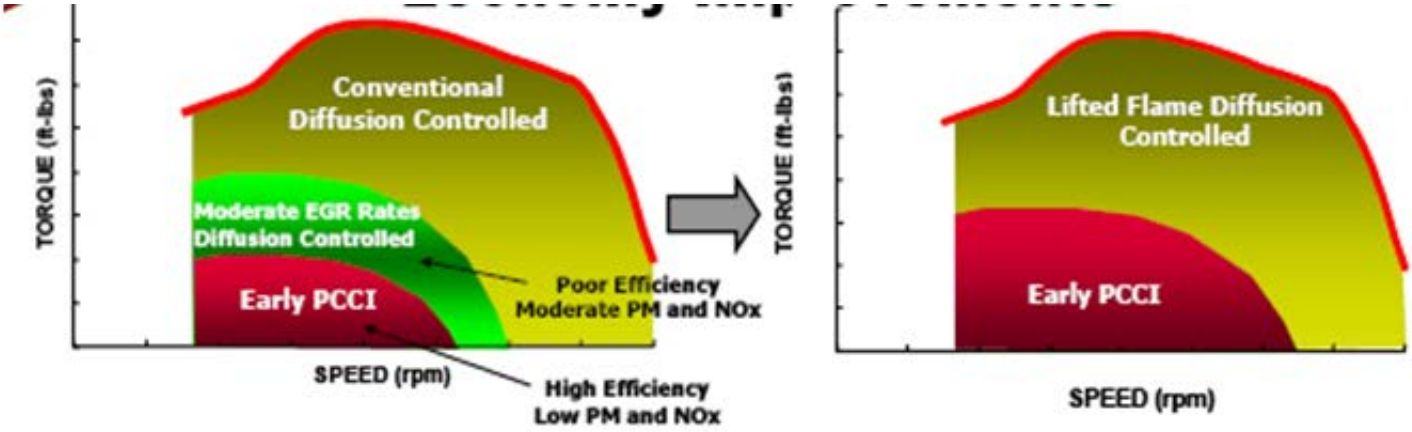

Figure 7-10: evolution of the combustion strategy proposed by Stanton (Cummins) [7-13]

7.2.4. Basis of the Lifted Flame Diffusion Controlled (LFDC) combustion.

7.2.4.1. Lift-off length definition and soot formation mechanism.

During its development, the free Diesel jet entrains warm gases present in the chamber –see §7.2.2.1 Figure 7-2 and Figure 7-11 [7-15]. These gases contribute on one hand to the fuel evaporation, by providing heat to the liquid spray and therefore by reducing the amount of liquid droplets, and on the other hand, to the reduction of the equivalence ratio in the plume.

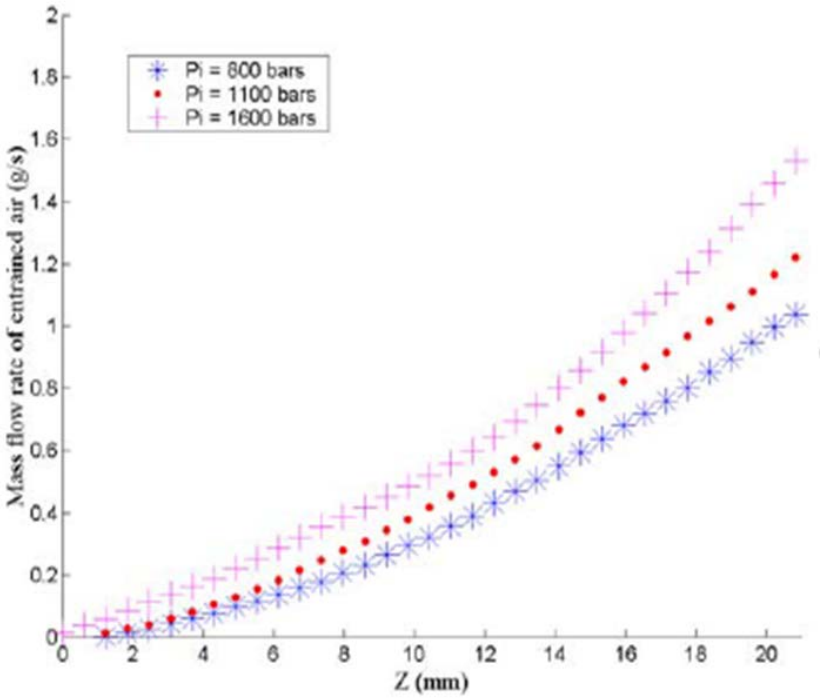

Figure 7-11: air mass flow rate entrained by the spray in a constant volume vessel at ambient temperature and in stationary conditions, for different injection pressures Pi [7-15]

In a heated vessel or in an engine, the auto-ignition is generally characterized by the formation of the radical OH. The distance between the nozzle hole orifice and the location of the first appearance of this specie, considered as the origin of the combustion, defines the lift-off length.

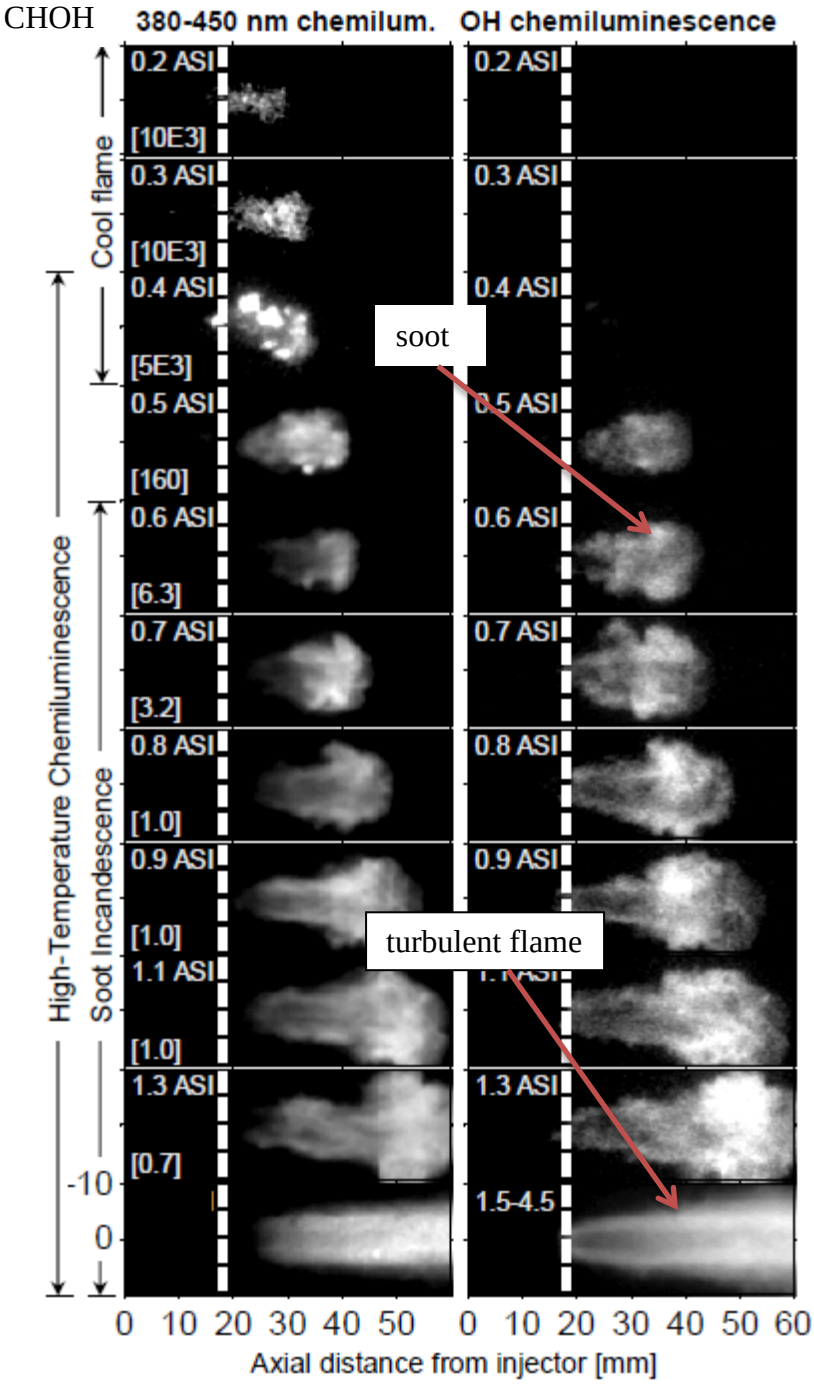

Figure 7-12: Chemiluminescence time sequence after start of injection ASOI. Experimental conditions: 100 μm nozzle orifice, 1380 bars pressure, ambient temperature, density, and oxygen concentration respectively 1000 K, 14.8 kg/m3, and 21%. [7-16].

In 2005 Pickett [7-16] nevertheless demonstrated –Figure 7-12- the existence of a cool flame characterized by the chemiluminescence signal due to formaldehyde CHOH (left column on the figure) upstream the first visualization of OH at 0.5 ms after start of injection.

The turbulent flame initiated at the lift-off length, 0.6 ms ASOI, rapidly stabilized upstream and then propagated downstream, symmetrically around the spray as illustrated by the high intensity line on the last picture of the right column in Figure 7-12. The dotted line on the picture represents the lift-off length. After 0.6 ms ASOI, a strong signal is seen on both left and right images downstream of the spray; correlations with LII measurements showed that this high intensity was linked to soot production.

An area between the lift-off length and the first occurrence of soot is filled with high temperature gases coming from the diffusion flame at the periphery of the spray and mixing with the fresh rich mixture coming from the injector. The presence of formaldehyde in this region, downstream of the lift-off, and the absence of OH signal, was a sign for the absence of any combustion; due to their high temperature and high equivalence ratio, these gases form the "fuel" for the remaining combustion process, downstream with soot precursors as schematically represented in Figure 7-13. Soot is therefore located near the spray axis and oxidation occurred in the region around the flame where oxygen is still present.

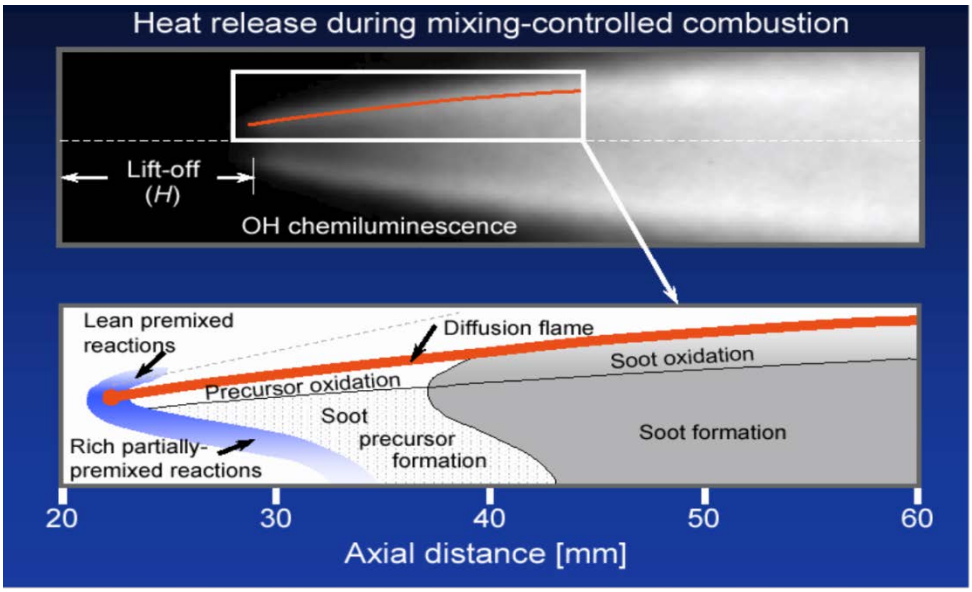

Figure 7-13: soot formation mechanism in a diffusion controlled flame [7-17]

7.2.4.2. First strategy contributing to a low soot formation.

One understanding of the above mechanisms is that the "rich partially-premixed reactions" zone illustrated in Figure 7-13 must be reduced as much

as possible to limit soot production in the spray. That is to say that the mixing between air and fuel must be enhanced upstream of the lift-off length and anyway that the presence of liquid must be avoided or, with other words, the mixture at lift-off must be lean enough.

This therefore results in a kind of competition between the increase of the lift-off length and the reduction of the spray liquid penetration.

- Relation between the lift-off length and the soot formation.

The impact of the lift-off length on the soot formation is illustrated by the results of quite elementary investigations in a constant volume vessel led by Siebers in 2001[7-14] –see Figure 7-14. For all the tested configurations, with different ambient densities and nozzle hole diameters, a quite linear reduction of the soot incandescence –assimilated at the first order to the amount of soot formed- was checked as the lift-off length was increased.

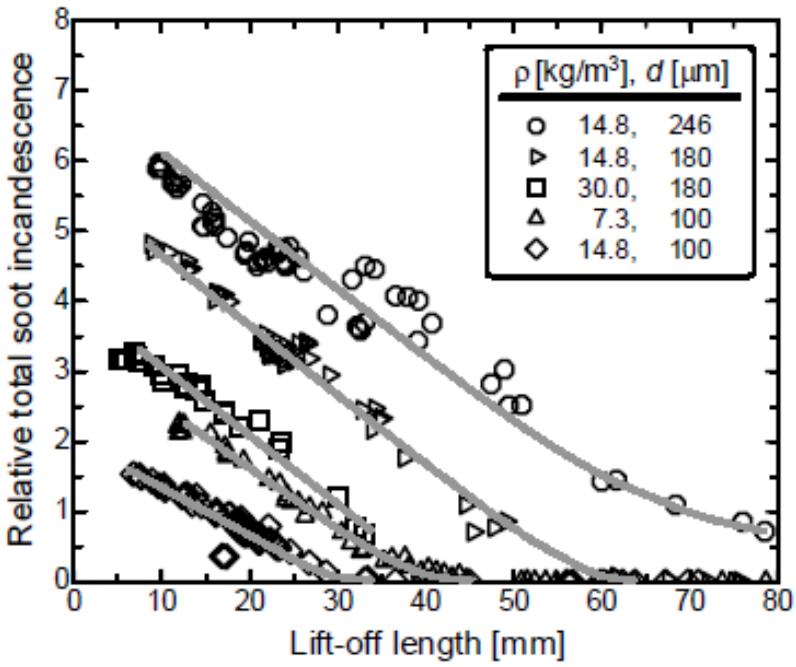

Figure 7-14: influence of the lift-off length on the soot formation by Siebers at constant injection pressure 1380 bars [7-14]

The second observation is concerning the effect of the air density, whose increase generates a reduction of the soot incandescence level at constant nozzle hole diameter 180 µm and lift-off length. Parallel investigations led by Arbeau [7-15] and Sepret [7-18] showed that increasing the ambient air density leads to a higher amount of air mass flow entrained by the spray and therefore a reduced equivalence ratio in the plume.
The third point is concerning the effect of the hole diameter: shifting its value from 246 µm down to 180 or from 180 to 100 at constant air density allows to reduce the incandescence signal at constant lift-off length.

These two remarks qualitatively confirm the importance of the "rich partially premixed reactions" zone on the soot formation –eg the local air fuel ratio and the presence of liquid droplets- quite independently of the lift-off length.

- Evolution of the lift-off length.

In 2005 Pickett [7-16] proposed a relatively simple formulation of the lift-off length *H* (mm) described by Equation (1):

$$(1)\ H = C\, Ta^{-3.74} \rho a^{-0.85}\, d^{0.34}\, U\, \zeta st^{-1}$$

where *C* is a proportionality constant, *Ta* [K] is the ambient gas temperature, ρ*a* [kg/m3] is the ambient gas density, *d* [μm] is the injector-tip orifice diameter, *U* [m/s] is the injection velocity, and ζst is the stoichiometric mixture fraction. The mixture fraction ζ is defined as the oxygen mass divided by the mixture mass.

Experiments in a constant volume vessel [7-14] established the influence of the diverse engine parameters on *H* –see Figure 7-15 and 7-16-, influence which is coherent with Equation (1) as:

- the effect of the injection velocity is linear
- the reduction of the lift-off length at constant injection velocity is quite moderate when the hole diameter is decreased, which is coherent with the 0.34 exponent in equation.
- the effect of the air density is strong as its increase leads to a decrease of the lift-off length
- the effect of the air temperature is coherent with the -3.74 exponent in the equation.

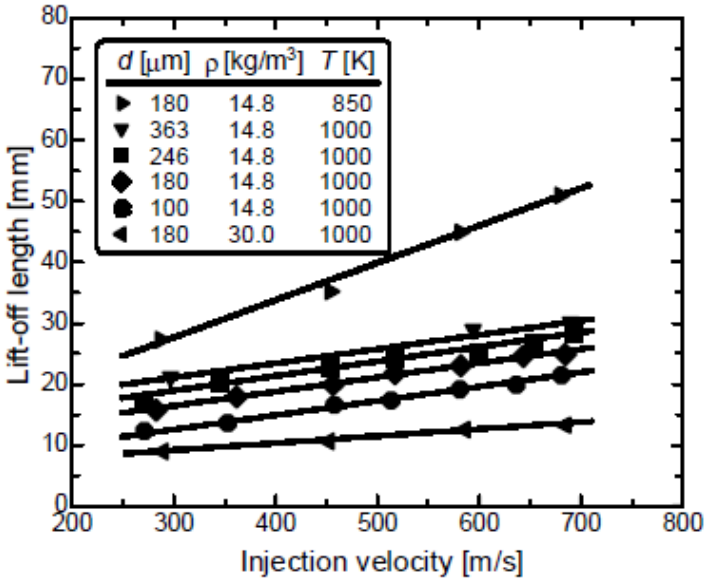

Figure 7-15: influence of injection velocity on *H*, for different air densities, holes diameters and temperatures [7-14]

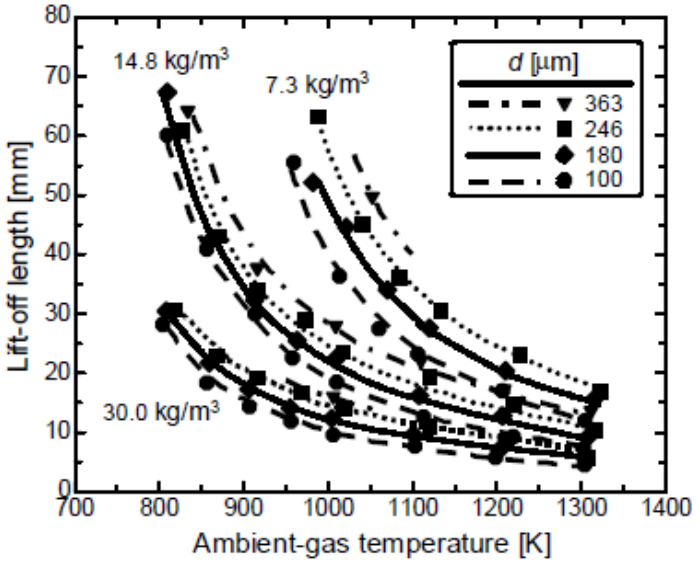

Figure 7-16: influence of ambient gas temperature on *H*, for different air densities and holes diameters [7-14]

- Air entrainment.

The clear influence of ζst%, percentage of the air mass necessary to burn the injected fuel entrained by the spray in stoichiometric conditions, on the amount of soot formed was clearly illustrated by Figure 7-17.

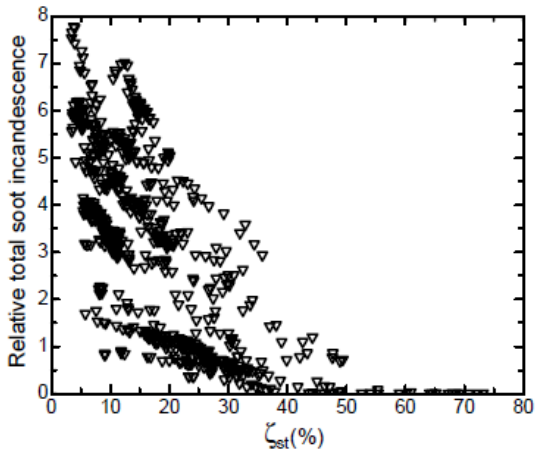

Figure 7-17: influence of ζst% on the soot level [7-14]

A low hole diameter and a high injection pressure were identified by both Siebers [7-14] and Arbeau [7-15] as first order parameters enhancing the air entrainment and thereby ζst% as presented by Figure 7-18. It is particularly interesting to notice that the effect of the injection pressure on ζst% is significantly emphasized by reduced nozzle holes, especially at 100 µm

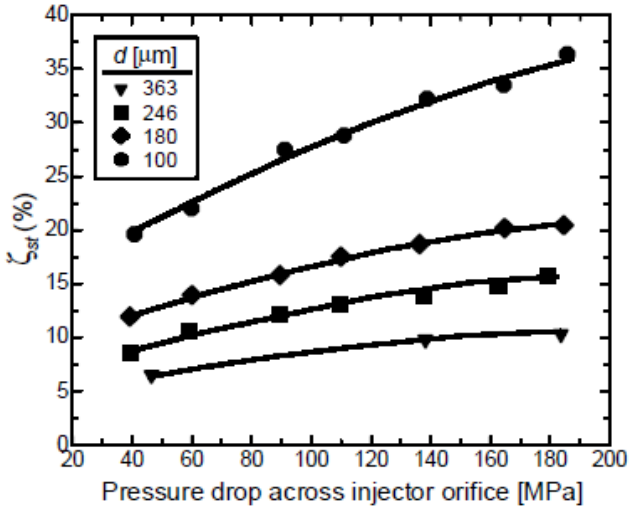

Figure 7-18: influence of injection pressure and hole diameter on ζst% (ambient temperature was 1000K, air density 14.8 kg/m3) [7-14]

As well, a reduced ambient temperature retards the auto ignition and thereby leads to a higher lift-off length, which allows more distance for mixing air and fuel –see Figure 7-19.

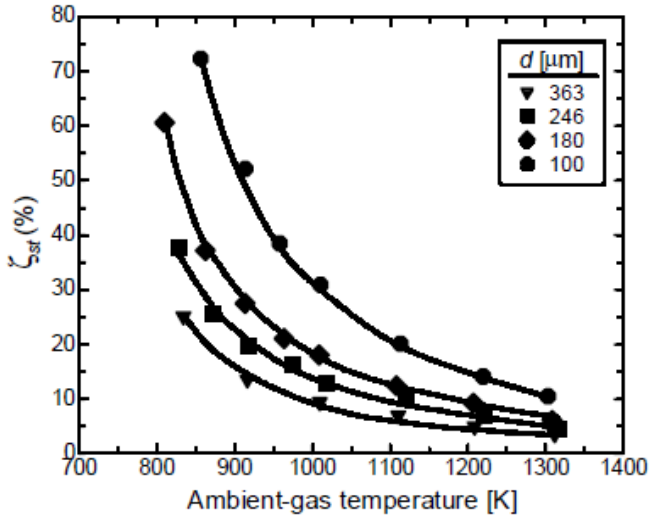

Figure 7-19: influence of the ambient temperature on ζst% (air density was 14.8 kg/m3 and injection pressure 1380 bars) [7-14]

- Liquid penetration.

In 1999, Siebers proposed to simulate the liquid length L(mm) by Equation (2):

$$(2)\ L = k \left(\frac{\rho f}{\rho a}\right)^{0.5} d$$

where k depends upon spray angle, ambient pressure and temperature, fuel temperature. It can be noticed that L is independent of the injection pressure.

The comparison between Equation (1) and Equation (2) provides the following relation (3) for a constant ambient temperature:

$$(3)\ \frac{H}{L} = C\ \rho a^{-0.35}\ d^{-0.66}\ U\ \zeta st^{-1}$$

where C is a constant depending upon the ambient temperature.

The use of Equation (3) allows to establish that the lift-off length increases quicker than the liquid penetration when the ambient air density decreases, where the orifice diameter decreases and when the injection pressure increases.
For a given air density and a given injector nozzle, Siebers [7-14] experimentally showed that the influence of the ambient temperature is much lower for liquid penetration –by evaporation effects- than for the lift-off length –via a high influence on the auto-ignition –see Figure 7-20; the lower the ambient temperature is, the greater the difference between the two lengths is. On the other hand, the higher the air density is, the lower the temperature where the two curves cross is –see the dotted line in Figure 7-20. Physically the amount of oxygen entrained by the spray at high air density generates a shorter lift-off length as the liquid penetration remains unchanged.

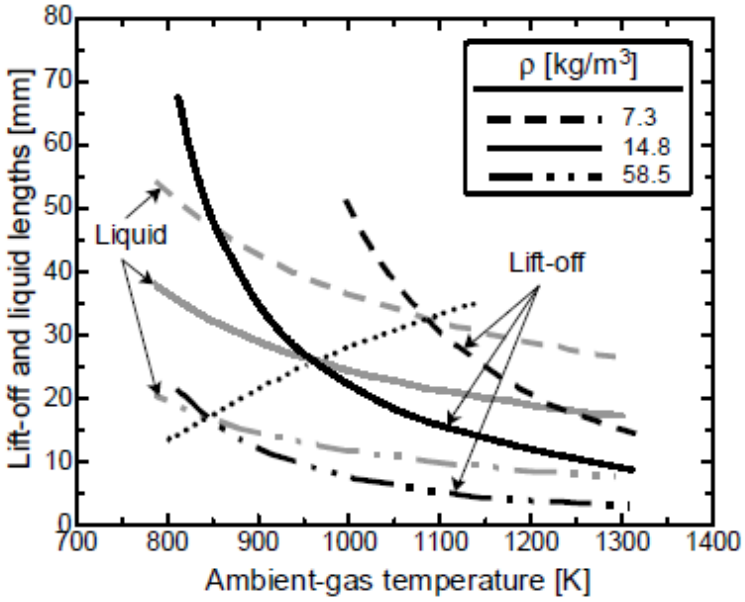

Figure 7-20: comparison of lift-off (black curve) and liquid lengths (gray line) as a function of the ambient temperature for different air densities. The pressure drop across the injector orifice was 1380 bars [7-14]

This conclusion is confirmed by Figure 7-21 with the influence of the oxygen content in the air. A rough approach can be summarized by the fact that *H* is inversely proportional to ζst%, or, more physically, that a low oxygen content retards auto-ignition.

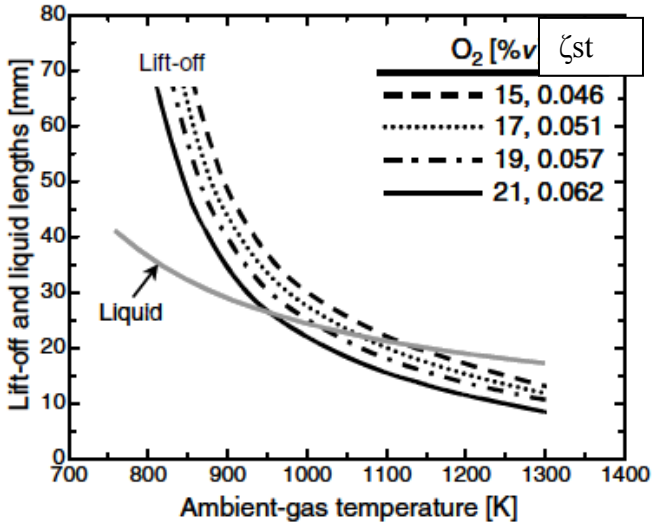

Figure 7-21: comparison of lift-off and liquid lengths as a function of the ambient temperature for different oxygen contents ζst% . The pressure drop across the injector orifice was 1380 bars, the orifice diameter was fixed [7-19]

The investigation concerning the influence of the nozzle hole diameter illustrated in Figure 7-22 points out that the liquid penetration linearly decreases much quicker than the lift-off length with small orifices, which confirms the conclusion obtained with Equation (3). In these operating conditions, the interest of a hole diameter smaller than 150 µm was clearly emphasized.

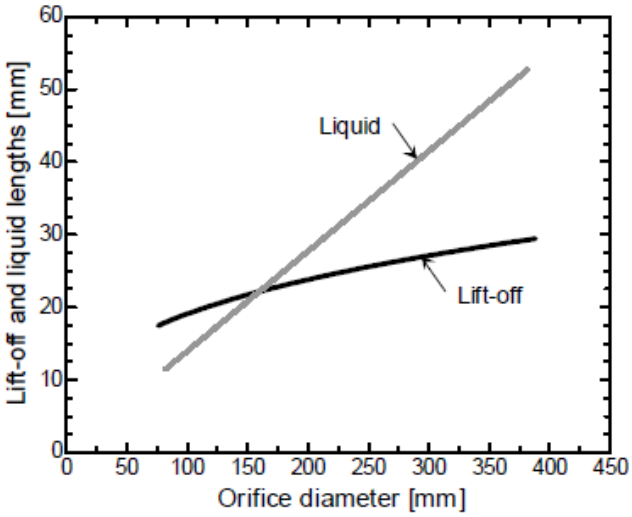

Figure 7-22: influence of the nozzle hole diameter (ambient temperature was 1000K, injection pressure 1380 bars, density 14.8 kg/m3 [7-14]

- Conclusions.

The previous investigations can be summarized according the two following items:

- Concerning the injection system, the positive influence of a reduced nozzle hole diameter on the competition between lift-off length and liquid penetration is quite obvious; Siebers [7-20], Figure 7-23, proposed a schematic drawing to illustrate the situation. Especially with reduced orifice diameters, high values of the injection pressure allow to increase the lift-off length as the liquid penetration is marginally influenced.

- Concerning the thermodynamic conditions, a low ambient temperature, a low air density and a low oxygen content are also important to increase the difference between lift-off length and liquid length.

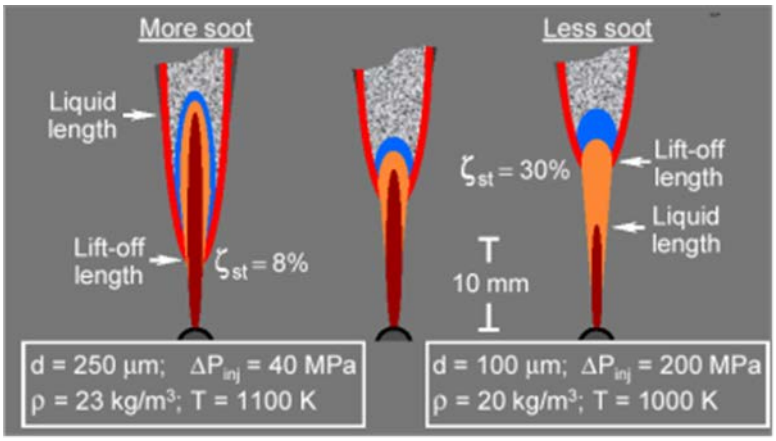

Figure 7-23: mechanism of a low soot diffusive combustion, by Siebers [7-20]

7.2.4.3. Second strategy for a low soot formation.

In 2001, Sasaki and alii [7-5] focused their research activities on the exploitation of the Kamimoto diagram, in the area of low temperature and rich mixture.
In the above paragraphs, the importance of mixture preparation has been clearly identified for reducing the "rich partially premixed reaction zone" present in Figure 7-13; on the contrary, Sasaki used conventional injection systems but tried to avoid the formation of the soot precursors PAH which was described as the second step before soot formation. He demonstrated that PAH formation was dependent on temperature and the idea was therefore to operate the engine with a high amount of EGR.
Basic results presented in Figure 7-24 established that reducing the air/fuel ratio down to values lower than 25 (for the given operation point) inverted the conventional smoke/air fuel ratio tendency and permitted a quite 0 soot level.

Anyway, the experimental conditions investigated were limited to very low load engine points with probably a quite well premixed mixture.

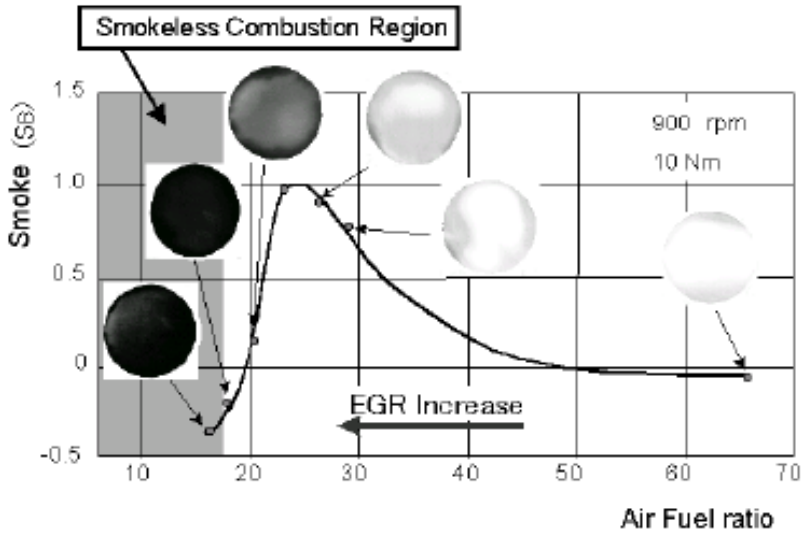

Figure 7-24: reduction of smoke level by use of a huge amount of EGR [7-5]

7.2.5. Basic experiment concerning a non sooting diffusion controlled combustion.

In 2004, Pickett [7-20] showed that a non sooting mixing controlled combustion was possible by using small orifice nozzles and low temperature conditions. The experiments were conducted in a constant volume vessel with a single hole injector –see Figure 7-24. With a 50 µm orifice (right), even if the lift-off length is very much reduced compared to 100µm (left), no soot are observed at very high temperature and quite high equivalence ratio. This result was completely coherent with the influence shown in Figure 7-22.

The situation is another way illustrated by Figure 7-25 and 7-26 where the frontier between non sooting and sooting conditions was moved towards high temperature as the hole diameter was reduced.
The associated publications probably led Stanton [7-13] to propose the combustion strategy illustrated in Figure 7-10 and opened the way to different cooperative programs, like DIAMANP [7-21] or DICO ([7-22] and [7-23]) in France.

Anyway it must be kept in mind that all these experiments have been achieved with single hole injectors; on a real engine, the influence of one spray on the other might probably change the conclusion, at least quantitatively if not qualitatively.

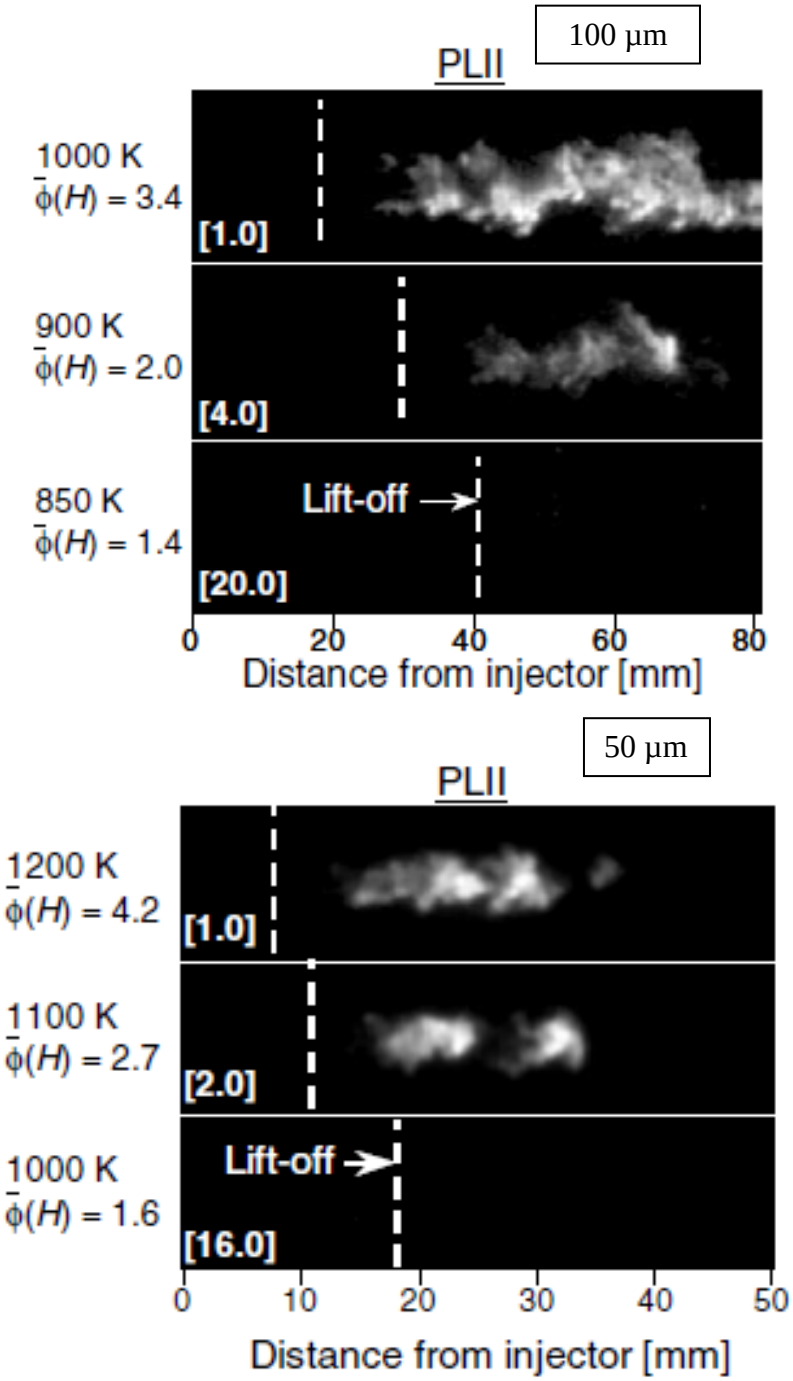

Figure 7-25: PLII images at the central plane of the fuel jet using a 100-µm orifice and a 50µm orifice. The ambient density was 14.8 kg/m3. The PLII images were acquired 3.2 ms after the start-of-injection during mixing-controlled combustion. The vertical dashed line in each image marks the lift-off length location, and the estimated cross-sectional average equivalence ratio at the lift-off length, φ (H), is given at the left. Relative PLII camera gain is given in brackets at the lower left of each image. An increased camera gain corresponds to a lower PLII intensity (i.e. less soot) [7-16]

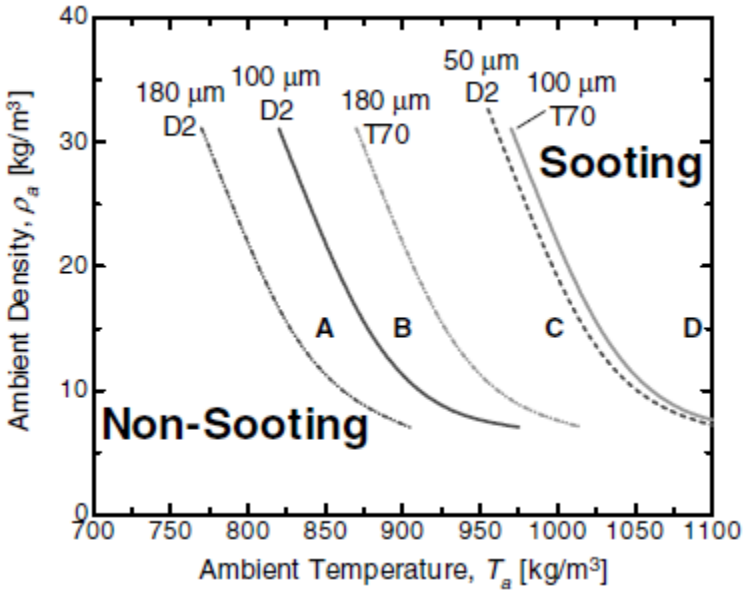

Figure 7-26: Non-sooting mixing-controlled combustion operating regimes as function of ambient gas temperature and density. Injection pressure is 1380 bars [7-20]

7.3. Development of the Lifted Flame Diffusion Controlled LFDC combustion.

7.3.1. Definition of the injection system.

The development of Diesel fuel systems has been driven by two necessities for conventional combustion: on one hand, the power/cylinder increase for top end applications or down-sized engines led to higher and higher injection pressures, over 2000 bars; on the other hand, the need to limit soot emissions governed the reduction of the nozzle holes diameter down to around 100 µm in serial production.
The association of advanced prototyping techniques allowing to machine "full size multi hole nozzles" with orifices around 75 µm and very high rail pressures was a great opportunity to check if the non sooting mixing controlled combustion foreseen by Pickett [7-20] in academic conditions was also suitable for real engines.

The basic tool used for the investigation was a Delphi Multec^{TM} DCR solenoid system [7-24] designed to operate at 2000 bars but which was "pushed" up to 2200 bars for short duration tests (Figure 7-27).

1	Inlet Metering Valve	6	Venturi
2	Inlet Fuel Temperature Sensor	7	High Pressure Discharge Valve
3	High Pressure Pump	8	Rail
4	Rail Pressure Sensor	9	Fuel Filter
5	Injector		

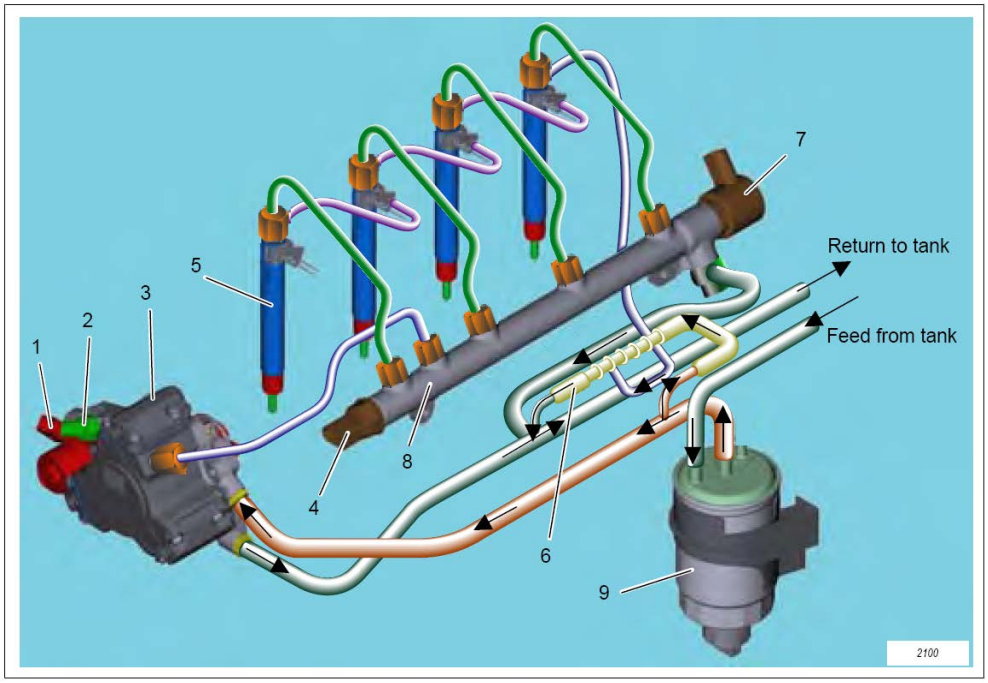

Figure 7-27. Delphi Multec^{TM} DCR common rail system overview [7-24]

The matrix of the different nozzles used is presented in Table 7-2. The configuration with 7 holes of 123µm was quite close to the production definition.

Anyway, as shown in Figure 7-28, an increased rail pressure of 2200 bars associated to a hydraulic flow of 340 ml/min didn't allow to obtain the same injection rate as a hydraulic flow of 480 ml/min associated to 1600 bars. Assuming the same losses between the two nozzles, the 340 ml/min would be equivalent to 400 ml/min due to the maximum pressure increase. That is to say that the peak power, at constant maximum cylinder pressure and temperature before turbine, might be reduced with the lower flows because of longer injection times.

	Hydraulic flow in ml/min			
	680	480	340	240
7 holes	123	104	88	
10 holes		88	74	63
14 holes			63	

Table 7-2: hole diameter in µm for the different nozzles

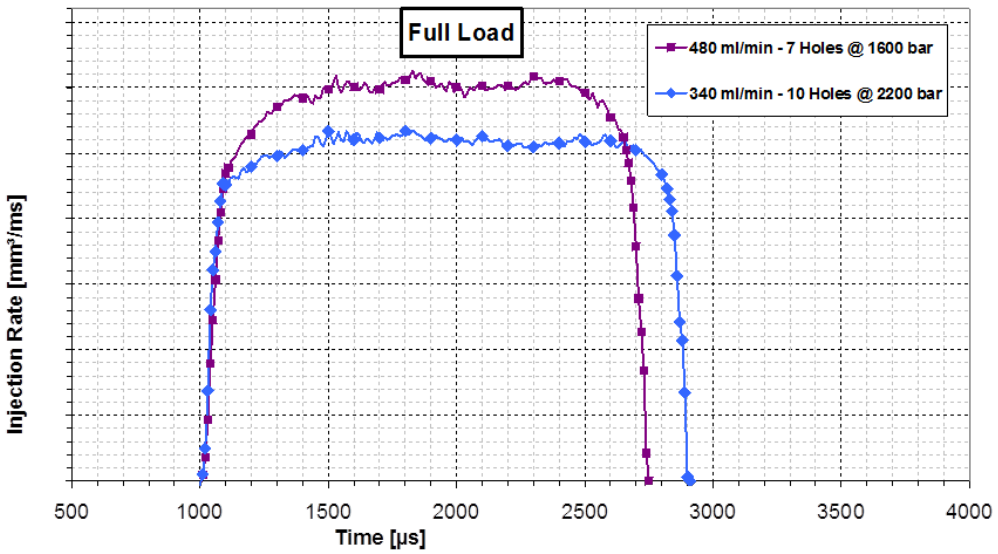

Figure 7-28: measured injection rate for the 7holes/480ml/min1600 bars and 10holes/340l/min/2200 bars [7-23]

Nota Bene: the term "injection pressure" will be used in all the following paragraphs as it is in the majority of the papers published on Diesel engines; nevertheless, this data is generally not known and there is a confusion with the measured "rail pressure", assuming that the pressure losses in the injector are negligible. This fact is obviously wrong and could lead to bad interpretations when injectors with different technologies or suppliers are used, even if is not the case in this program.

7.3.2. Spray investigation: effect of the nozzle definition.

7.3.2.1. Air entrainment.

Two single hole injectors with an external orifice of respectively 113 and 80 µm have been investigated at IMFT using the FPIV –Fluorescent PIV- at ambient temperature ([7-15] and [7-18]).

The experimental set-up didn't allow to use a multi holes injector due to the interaction between the laser sheet and the other sprays. A very long injection duration of 3 ms was chosen to stabilize the measurement which was obtained 2 ms ASOI. The observed area was not disturbed by the vortices present near the spray tip.

Figure 7-29 presents a comparison between the two diameters. The first well known result is that the cumulated mixing ratio –eg the cumulated mass of air entrained by the spray between the orifice and the distance z from the orifice versus the cumulated amount of fuel injected- increases at high air densities; the other interesting point is concerning the positive effect of a reduced hole diameter; for instance, at an air density of 36 kg/m3, the ratio was quite close to 14 at a distance of 22 mm from the orifice with the smaller holes, which roughly corresponds to the stoichiometric conditions; with the 113 µm one,

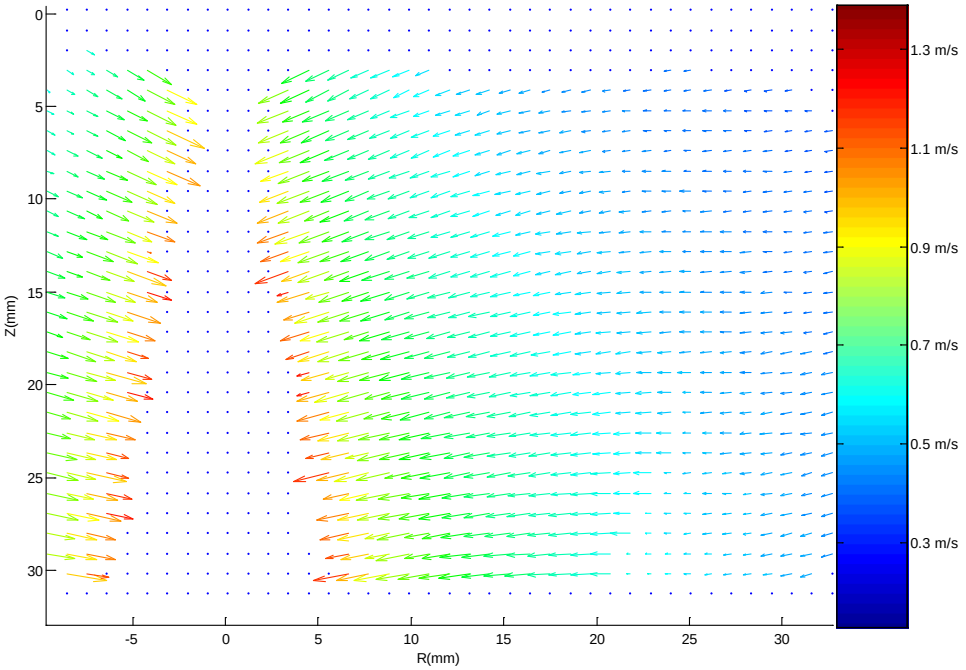

Figure 7-29: velocity field measured by FPIV; hole diameter was 113 µm, injection pressure 700 bars, ambient temperature air density 14.4 kg/m3 [7-25]

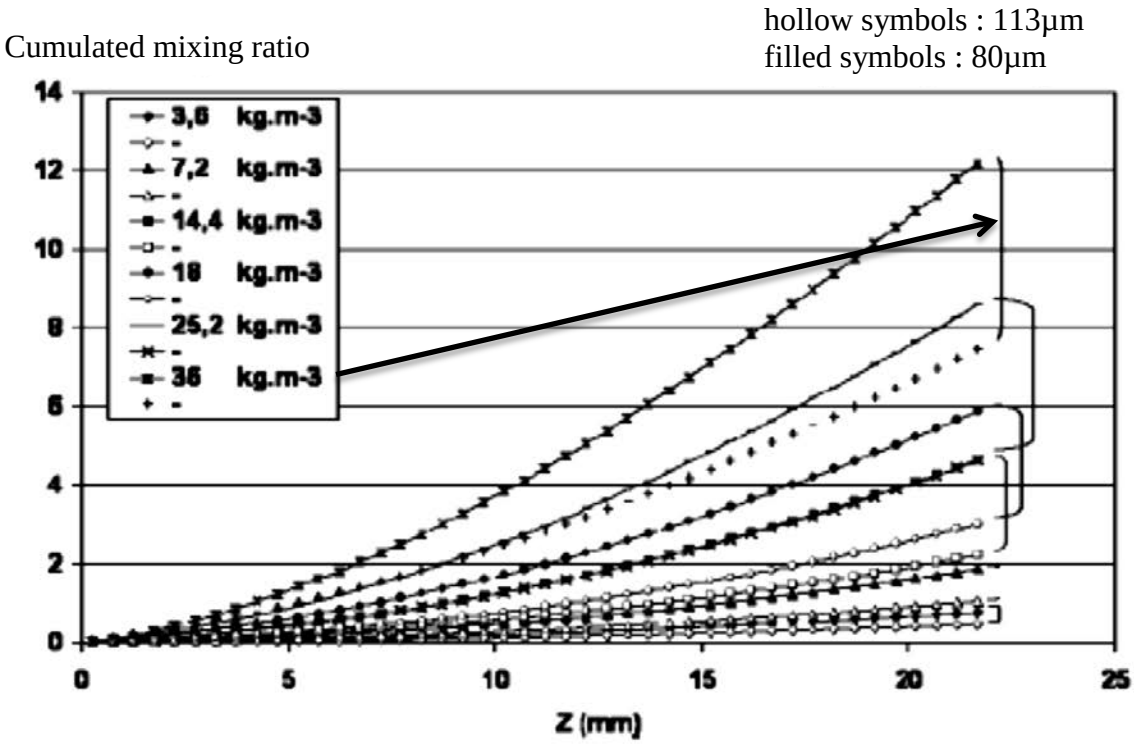

Figure 7-30: cumulated mixing ratio measured on the spray axis at a distance z from the orifice; ambient temperature; injection pressure 700 bars; parameter is the air density in the chamber [7-18]

this ratio was only 8. For a more conventional point at 25 kg/m3 which illustrates thermodynamic conditions at SOI at part load, the difference was smaller - 9 versus 4.5.

7.3.2.2. Spray evaporation.

The second important point was to compare the evaporation rate and the liquid penetration. A Rapid Compression Machine was used at CERTAM to simulate the thermodynamic conditions along the compression stroke and around the injection event. The simulated operating point was set at 2500 rpm with a constant air density of 25 kg/m3 at TDC and an injected fuel mass of 43 mg/stroke corresponding to full load.

- Liquid phase penetration and angle.

Figure 7-31 is an example of the liquid phase visualization at a constant injection pressure of 1240 bars. Mie scattering technique was used.

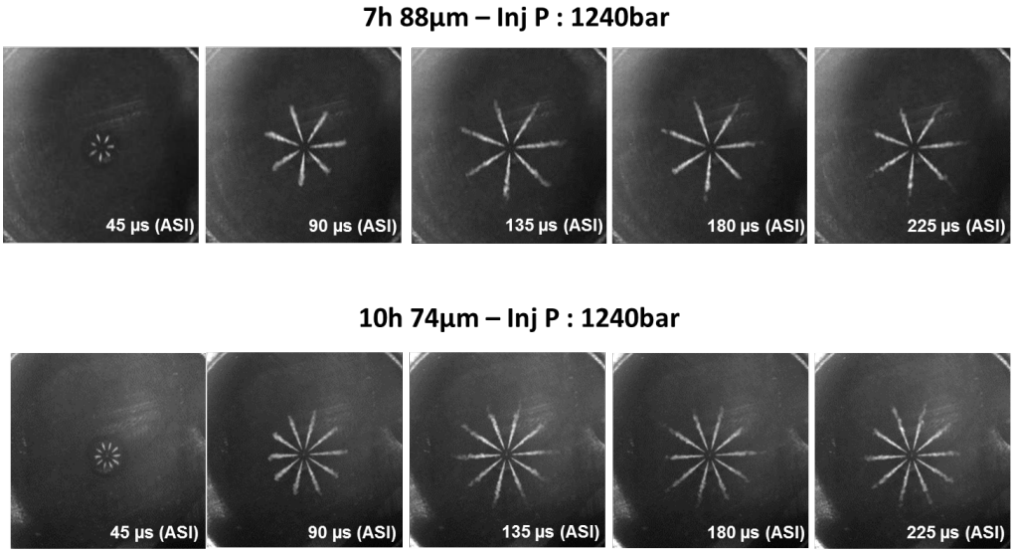

Figure 7-31: liquid phase visualization; injection pressure was 1240 bars; air density 25 kg/m3 [7-23]

Results of the parametric investigation are summarized in the following figure and are coherent with the results of the above Equation (2) –see §1.4.2.

The well-known stability of the liquid penetration above a certain distance from the orifice is observed.

A reduced hole diameter clearly led to a shorter liquid penetration when the spray was established; a 3mm difference between 88 and 63 µm was noticed, larger than the measurement dispersion (vertical segments on the curves). At the same time, the mean cone angle was strongly reduced by around 3° between 88 and 74 µm, indicating a better evaporation as illustrated by Figure 7-32.

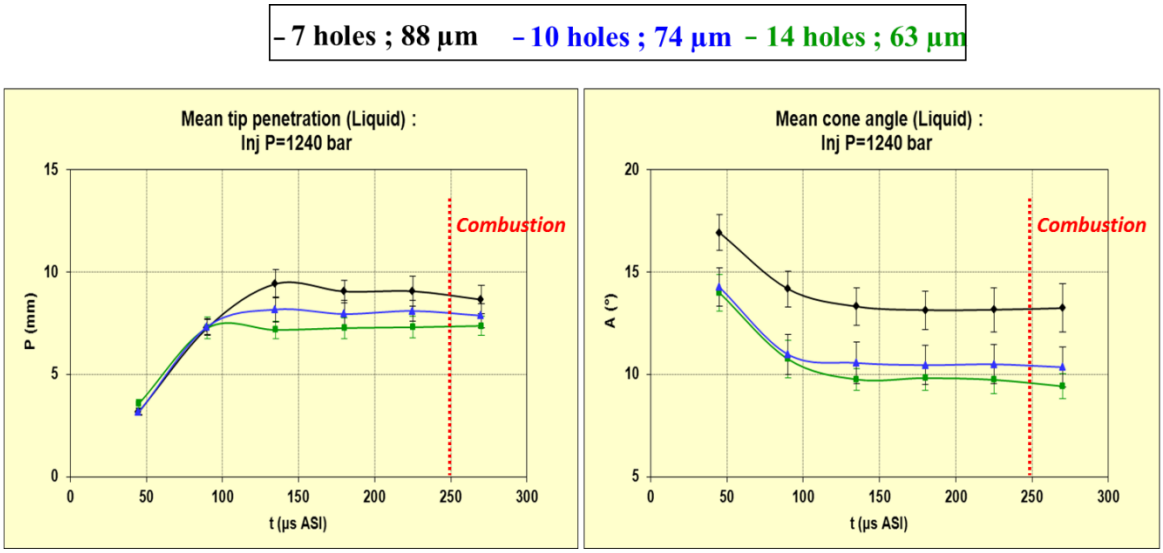

Figure 7-32: liquid penetration and cone angle for different nozzle configurations; injection pressure was 1240 bars; air density was 25 kg/m3

- Vapor phase penetration and angle.

As an example, Figure 7-33 shows photographs obtained with the Schlieren technique; the evolution of the vapor phase at a constant injection pressure of 1240 bars is compared for 10 and 14 holes.

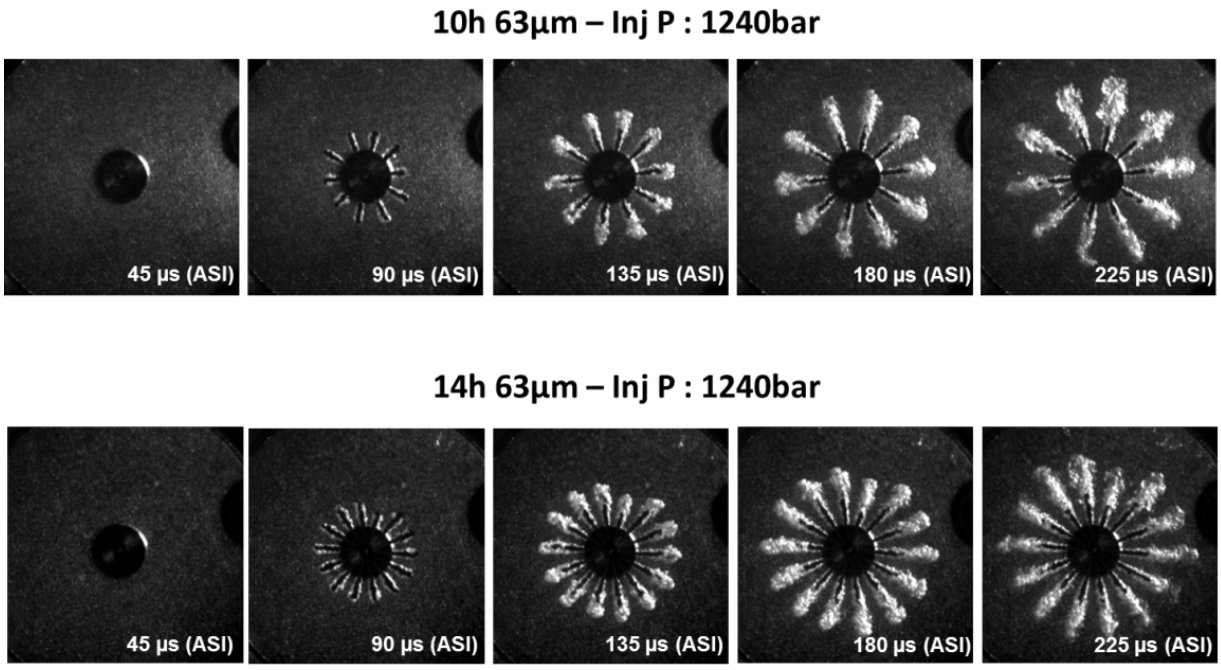

Figure 7-33: comparison between 10 and 14 holes with the same orifice diameter

A continuous increase of the vapor penetration is noticed until combustion occurred; as well as for the cone angle, a small orifice diameter was synonym of small measured values –see Figure 7-34.

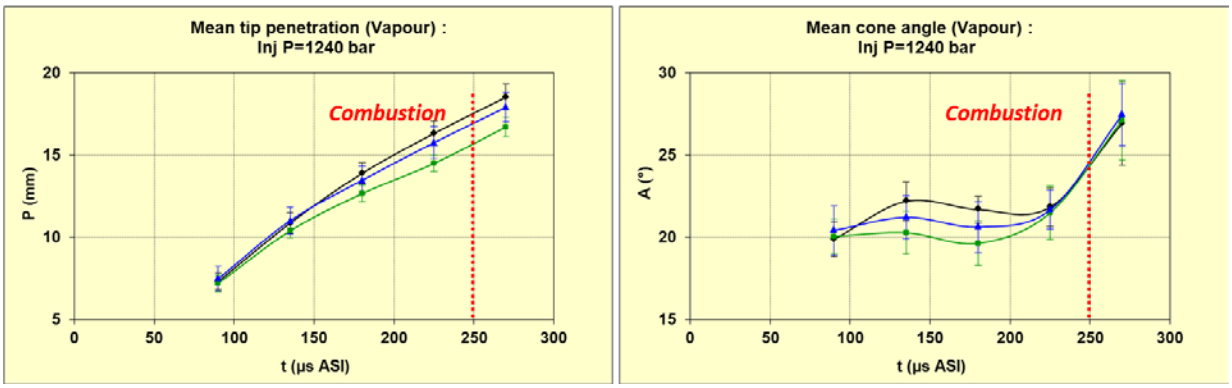

Figure 7-34: vapor penetration and cone angle for different nozzle configurations; injection pressure was 1240 bars; air density was 25 kg/m3

As a clear conclusion concerning the ability of each nozzle configuration to evaporate fuel seemed to be difficult, the use of another parameter was necessary; for this purpose, the Vaporization Index I was defined as the ratio between the projected surface occupied by the vapor versus the total projected surface occupied by the spray (liquid+vapor). Results given in Figure 7-35 attest the interest of the small holes diameter.

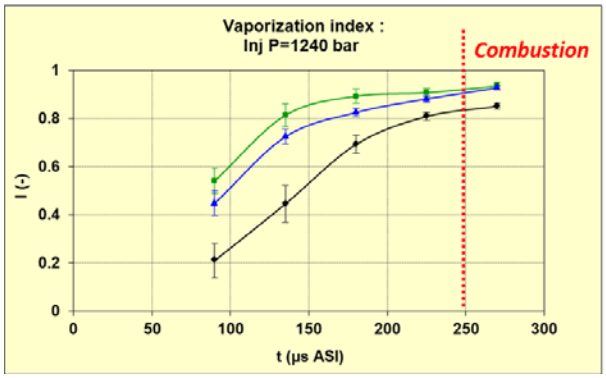

Figure 7-35: vaporization index I for different nozzle configurations; injection pressure was 1240 bars; air density was 25 kg/m3

Figure 7-36 established that, taking the measurement dispersions into account, the number of holes at constant orifice diameter has no significant influence on the liquid and vapor phases, at least until 14 holes and without swirl. This result could –partially, because of the restriction concerning the aerodynamics in the RCM- validate a transposition of the results described § 7.3.2.1 to a full size nozzle.

- Conclusion.

For the mixture preparation aspects, the presented results tend to confirm that reduced orifice diameters provide a significant improvement to achieve a

mixing controlled combustion with a very low soot level as described §7.2.4.3; conditions concerning air entrainment –and therefore equivalence ratio at light-off- and presence of liquid seemed to change positively versus a standard nozzle configuration.

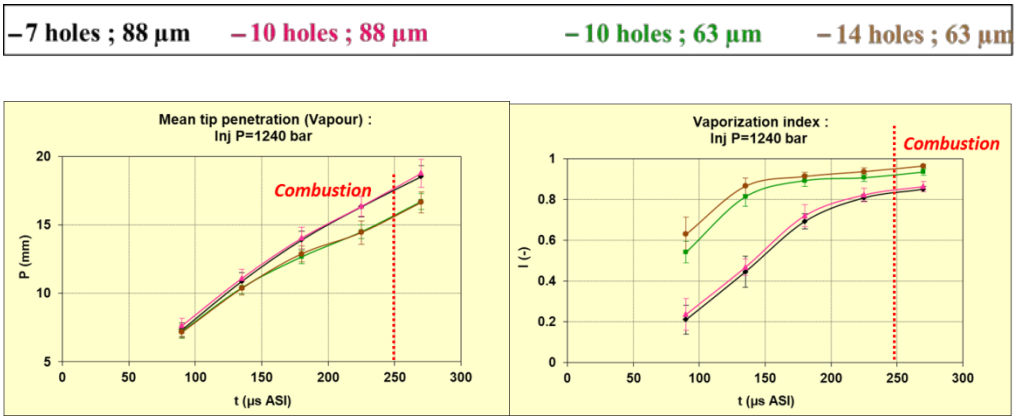

Figure 7-36: influence of the number of holes; injection pressure was 1240 bars; air density was 25 kg/m3

7.3.2.3. Lift-off length.

Laser Induced Fluorescence on the OH radical has been used to determine the first location of the combustion in the spray. Operating conditions in the high pressure high temperature vessel available at IFPEN were constant with an initial air density of 25 kg/m3 and an injection pressure of 1600 bars. Main results are presented in Figure 7-37.

The lift-off length seemed to slightly decrease with the 88µm diameter and to be constant between 104 and 123µm. This result is qualitatively coherent with § 1.4.2 Equation (1) which would have provided a 6% difference between each configuration.

So, this experiment conducted with full size nozzles confirmed the above previous conclusions and established that the difference between liquid penetration and lift-off length increases; for 104µm and 88 µm, the lift-off length was significantly higher than the liquid penetration as they were roughly the same with 123 µm.
The second set of conditions for a soot-less combustion seemed therefore to be fulfilled.

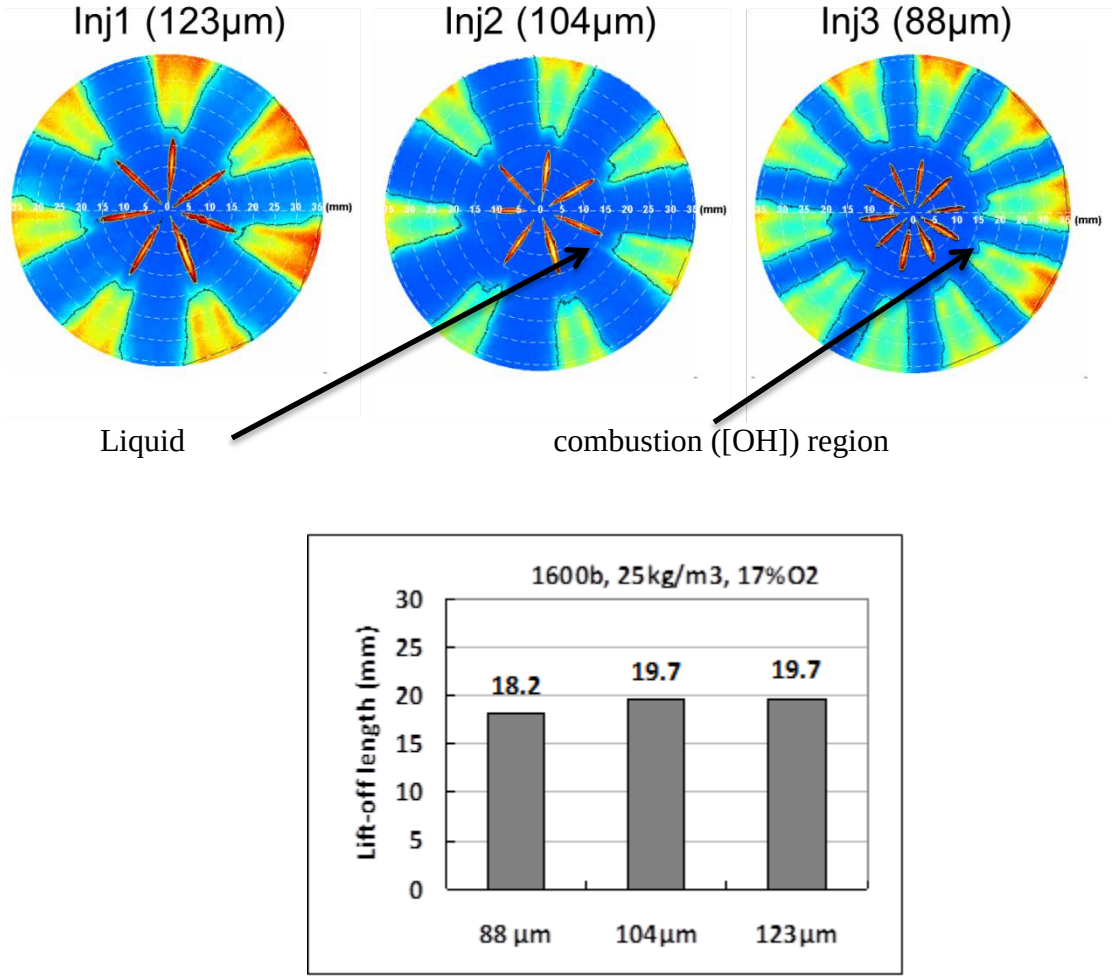

Figure 7-37: effect of the nozzle hole diameter on both the liquid phase and combustion areas; injection pressure was 1600 bars, initial oxygen content 17% and air density 25 kg/m3, temperature 850 K at SOI

7.3.3. Spray investigation: effect of the injection pressure.

7.3.3.1. Spray evaporation.

The same RCM as used in §7.3.2.2 was used to investigate the effect of the injection pressure with the 10 holes 63 µm nozzle. For these experiments, the air density was set at 25 kg/m3.
The effect of increasing the injection pressure from 1240 up to 2000 bars on the evaporation was quite obvious –see Figure 7-38.

Qualitatively, the vapor phase is much more important at high injection pressure, in terms of penetration and cone angle. More quantitative data are presented in Figure 7-39.

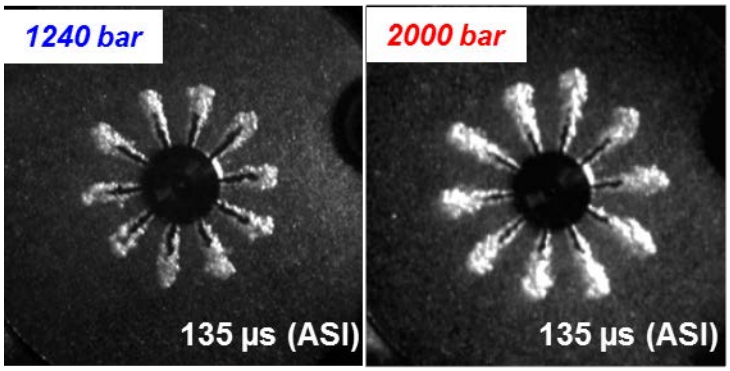

Figure 7-38: effect of the injection on the liquid and vapor phases with a 10 holes nozzle, orifice diameter 63 µm, air density 25 kg/m3

The visualization confirmed the already established property that the liquid phase penetration was very slightly influenced by the injection pressure (see §7.2.4.2. Equation (2)); on the contrary, a small decrease of the mean cone angle has been detected at 2000 bars, which is nevertheless coherent with the increased size of the vapor phase.
Figure 7-40 summarizes the tendency with the already define Vaporization Index, tendency which was confirmed by the same tests with the 7 holes 104µm at 1240, 1600 and 2000 bars

The positive effect of the injection pressure on the evaporation rate has been demonstrated but, in conclusion, two points might be kept in mind within the frame of the Lifted Flame Diffusive Combustion:

- The liquid penetration is not significantly influenced by the injection pressure.
- The vapor penetration slightly increases with high injection pressures; this point is particularly important for designing an optimized piston bowl, wide enough to promote mixing between air and fuel vapor.

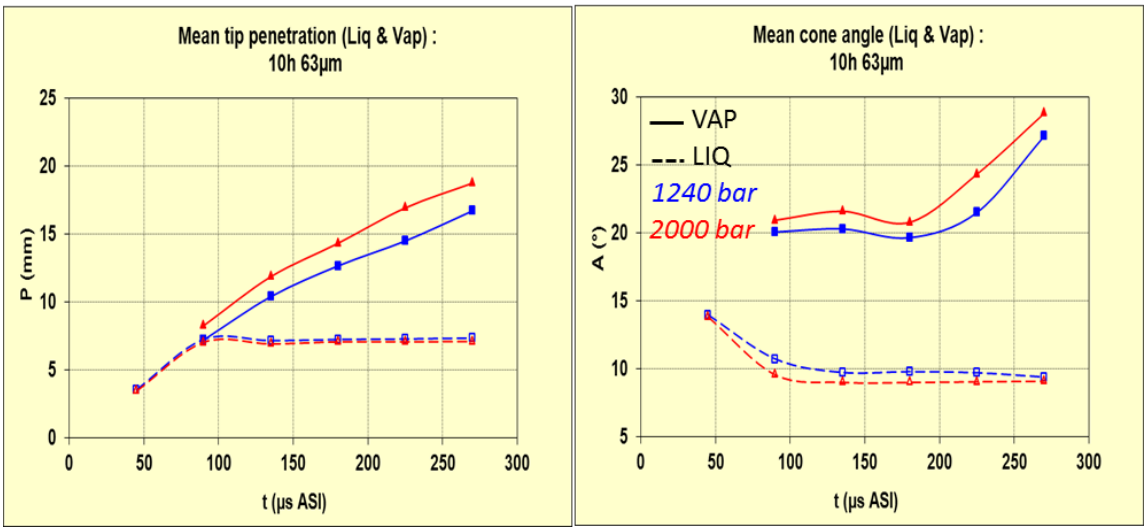

Figure 7-39: liquid and vapor penetration (left) and cone angle (right) according to the injection pressure – same conditions as in Figure 7-36.

.

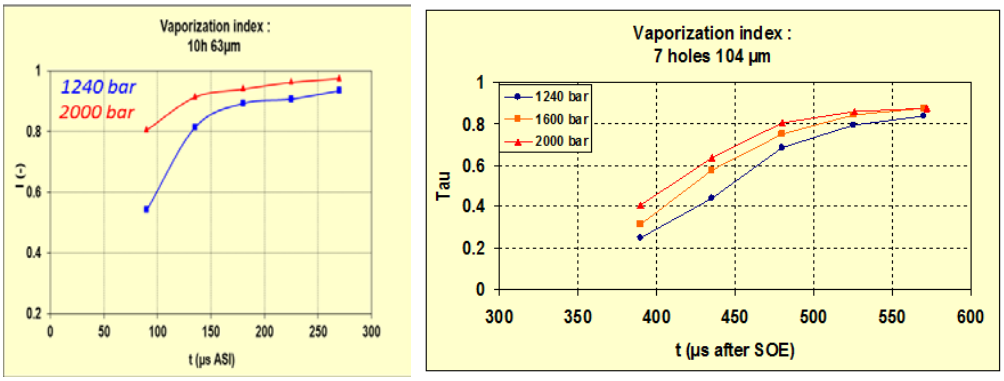

Figure 7-40: influence of the injection pressure on the vaporization index – same conditions as in Figure 7-37

7.3.3.2. Lift-off length.

For both 80 µm (Figure 7-41) and 63 µm (not represented), the lift-off length slightly increases with higher pressures. This result is coherent with the literature –see §7.2.4.2 Equation (1) with a relatively low order of magnitude because of the square root between pressure and velocity; in the presented case, the calculated increase would be around 13% -eg a bit more than 1mm !

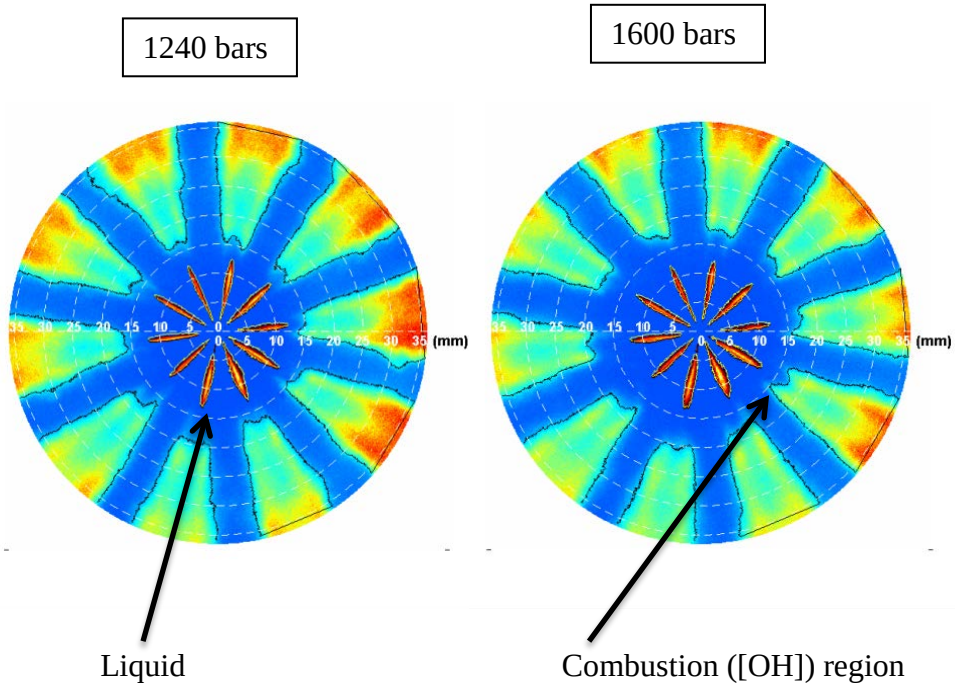

Figure 7-41: effect of the injection pressure on both liquid penetration and lift-off length. Nozzle hole orifice 80µm, air density 25 kg/m3, Oxygen content 17%, temperature 850K at SOI

7.3.4. Lift-off length: effect of the oxygen content.

With the same methodology, the effect of a reduced oxygen content, simulating EGR, from 17 down to 13% has been investigated –see Figure 7-42.

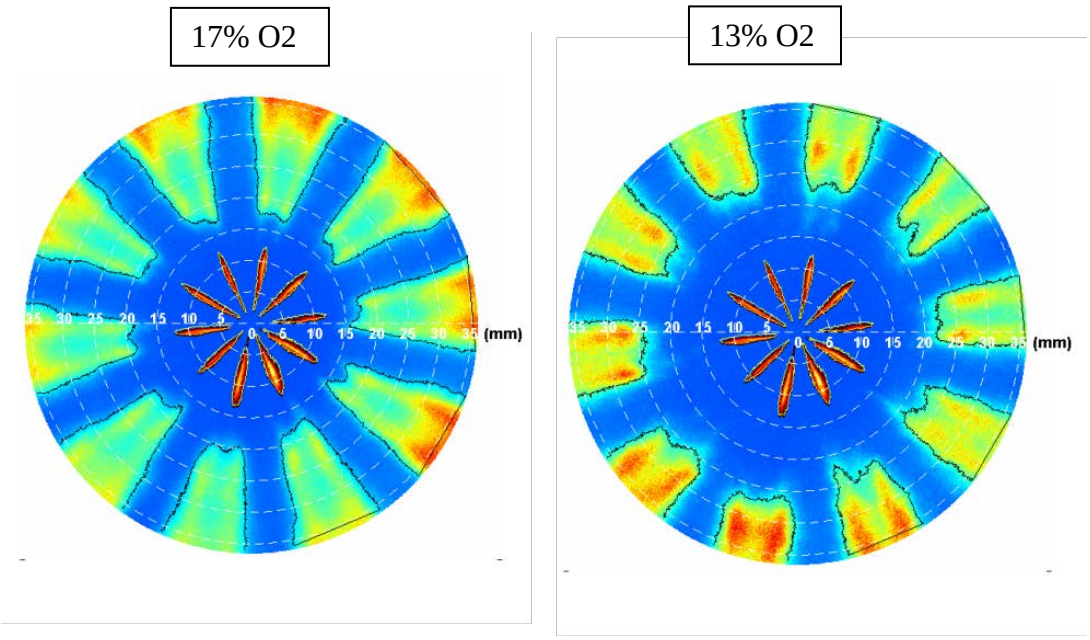

Figure 7-42: effect of the oxygen content on both liquid penetration and lift-off length. Nozzle hole orifice 80 µm, air density 25 kg/m3, Injection pressure 1600 bars, temperature 850 K at SOI

A reduction between 2 and 5 mm of the lift-off length has been measured; that was the highest sensitivity noticed between the tested parameters. In fact, the auto ignition of the mixture was retarded due to the lack of oxygen or, with other words, a higher distance was necessary for the spray to entrain the same amount of oxygen as thermodynamic conditions were unchanged.
This result was coherent with the more academic investigation summarized §7.2.4.2.
This result leads to schedule that the EGR rate might be an efficient way for achieving LFDC.

7.4 Tests on a single cylinder engine.

7.4.1. Operating points and reference configuration.

The aim of the program was to test the strategy described §7.2.3 –eg to use a LTC Mild HCCI tuning at low engine loads, and then, where the noise becomes an important drawback in premixed mode, a LFDC at higher loads – see Figure 7-43.

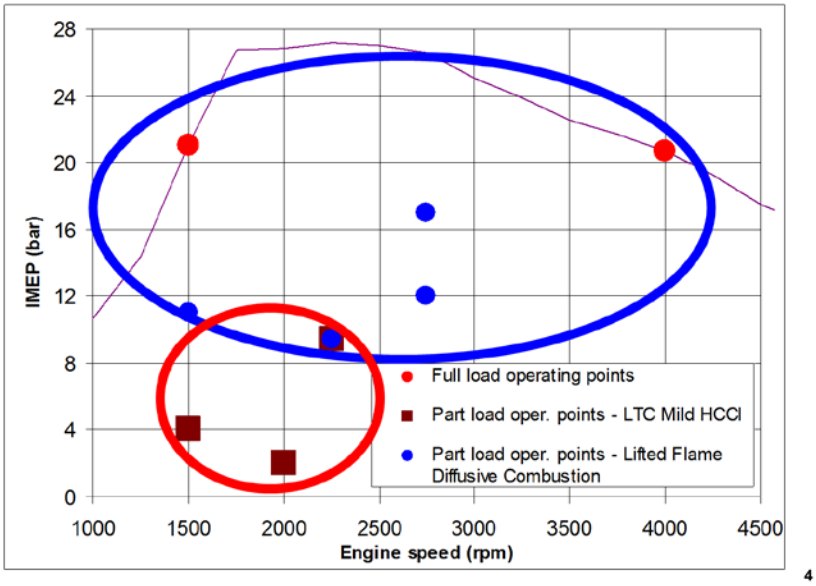

Figure 7-43: operating points chosen on the H9M single cylinder engine

The engine was fitted with the quite conventional piston bowl designed for Euro 6 applications and represented in Figure 7-44.

For the reference, the standard nozzle with 7 holes of 123 µm outlet diameter, 330 cm3/100bars/30s of hydraulic flow and 1600 bars injection pressure, was used.

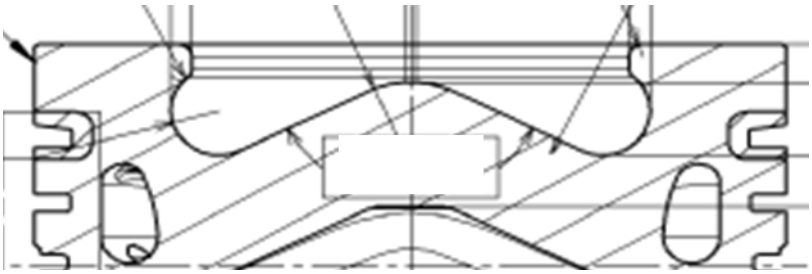

Figure 7-44: piston bowl design – maximum bowl diameter was 51mm for a given bore of 80 mm

7.4.2. Full load points.

7.4.2.1. Peak power at 4000 rpm.

This high speed operating point was particularly interesting because almost all the combustion phase occurred in diffusion mode as shown by the Heat Release Rate HRR chart in Figure 7- 45, with a great importance given to mixture preparation.

On the other hand, the injection duration was mostly important because of the limitation of the turbine inlet temperature; in the investigated case, the four injectors were not equivalent as shown Table 7-3.

Number of holes	Holes diameter in µm	Std hydraulic flow Q in cm3/100bars/min	Injection pressure P in bars	Q'
7	123	680	1600	272
7	104	480	2050	217
10	88	480	2050	217
10	74	340	2150	158

Table 7-3: comparison of the different injectors. $Q' = Q * P^{0.5} * 0.01$

Q' is quite proportional to the injection duration at the rated injection pressure.

Despite a longer injection duration –and thereby a longer combustion phase as observed on the heat release chart- the smallest 7 holes injector provided quite the same power as the standard one with a significant advantage in smoke level for equivalence ratios higher than 0.7.
The explanation came from the increased injection pressure associated to the low orifice diameter which allowed better liquid atomization, higher air entrainment and fuel evaporation rate and lower local equivalence ratio as seen in the previous paragraphs.

Concerning the 10 holes configurations, the 88 µm was probably penalized by the too high standard swirl level, generating spray overlap, richer local mixtures between the sprays and thereby a lower combustion velocity and a high production of soot. The situation was very much improved by reducing the swirl level from 1.6 down to 1 with the 74 µm nozzle. In this case the peak power target was almost achieved even if the injection duration was still too long.

7.4.2.2 Maximum Torque at 1500 rpm.

Following the tests at peak power, the focus was made on the nozzles with the smallest orifice diameters.
On this operating point, the smoke level was the limiting factor for the torque, even if the maximum cylinder pressure was also limited to 170 bars.
Figure 7-46 summarized the results obtained with the three more interesting configurations.

The important fact is that, with an adapted low swirl level of 1.0 and an optimized injection pressure, the nozzles with 74and 63µm diameter orifices allowed to achieve the highest torque at constant smoke level.

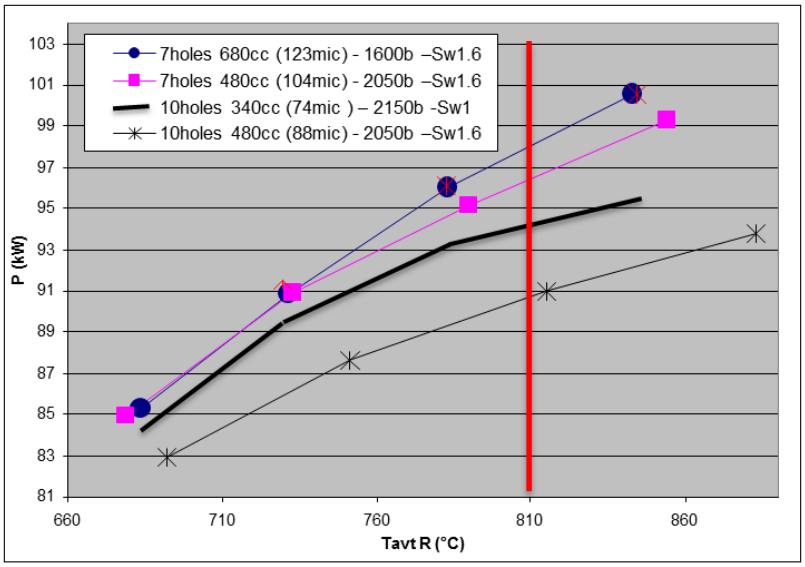

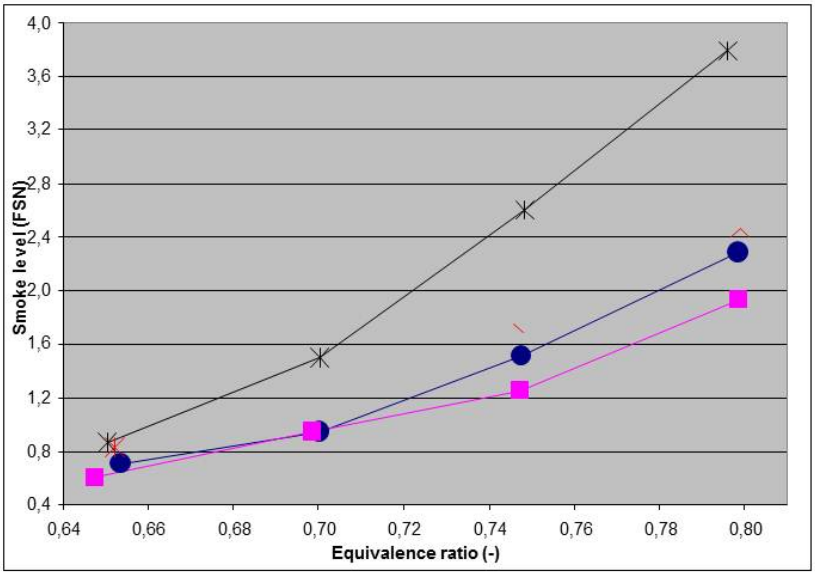

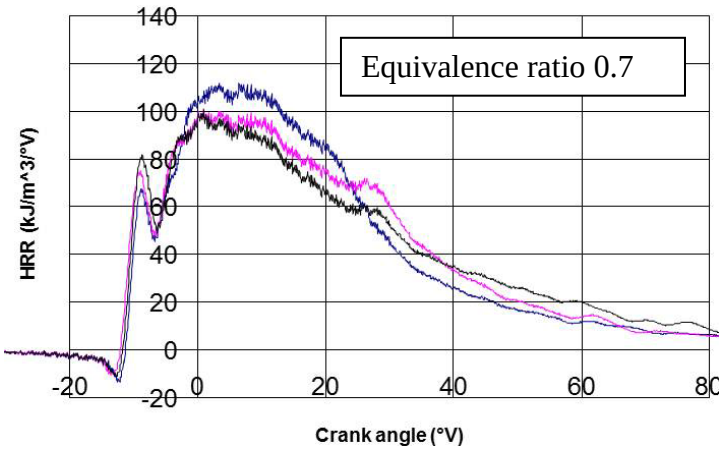

Figure 7-45: full load operation at 4000 rpm – cylinder peak pressure limited to 170 bars. The red bar represents the limit for turbine inlet temperature.

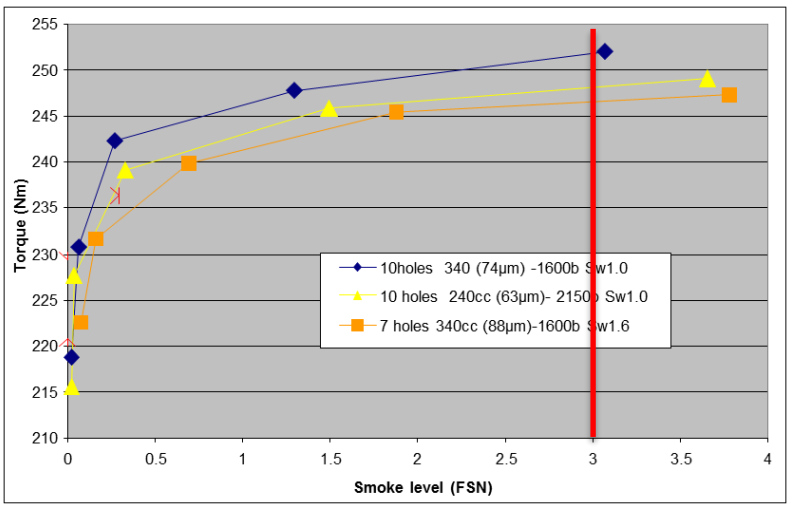

Figure 7-46: full load operation at 1500 rpm – cylinder peak pressure limited to 170 bars – the red bar represents the smoke limit.

7.4.2.3. Conclusion for full load performances.

With an optimized low swirl level, the association of nozzles with small orifice diameters and very high injection pressures allows to fulfill the peak power and torque targets.
For the future, injection pressures up to 2500 bars seem to be feasible in mass production within the following years. In this case a new value of Q' could be lowered from 217 down to 196 and so a new optimum value for Q would be around 390cc/100bars/min. Assuming that the discharge coefficient of the holes is independent of the diameter, the product $n * d^2$ where n is the number of orifices and d their diameter, might be constant; so new potential nozzles could be forecasted as:

10 holes and 70 µm diameter
12 holes and 64 µm diameter
14 holes and 59 µm diameter

Availability of prototypes led us to go on testing the new reference 7 holes 88 µm and two other one as a 10 holes/74 µm and 14 holes/63 µm.

7.4.3 Part load operating points.

7.4.3.1. LTC Mild HCCI conditions.

- 1500rpm and 4 bars IMEP

At this very low engine load the smoke level is near zero and the main questions are concerning ISFC and HC emissions, respectig a dedicated noise limit.
Figure 7-47 presents ISFChp results for the previously selected nozzles. A good behavior was observed for the two 10 holes configurations at the

NOx target of 0.1 mg/s. No difference was noticed for HC emissions, which was coherent because all the nozzles had the same sack hole volume.

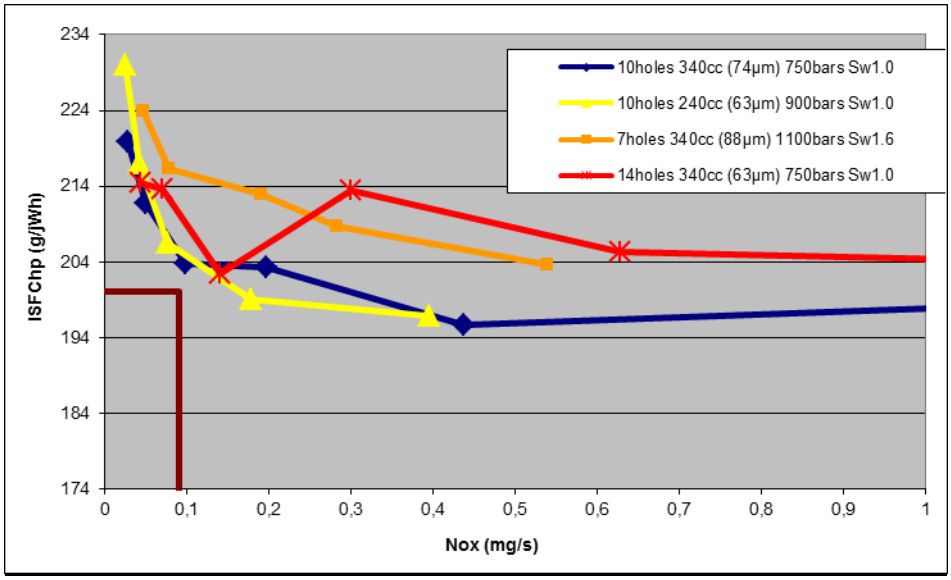

Figure 7-47: ISFC versus NOx at 1500rpm and 4bars IMEP

Results at 2000 rpm 2 bars IMEP were quite similar.

- 2250 rpm 9.4 bars IMEP

For this operating point, which was at the limit between Mild HCCI and LFDC strategies, the target for Euro 6 was to set the IOF/NOx trade-off within the brown rectangle in the chart represented by Figure 7-48.
Only the 14 holes nozzle didn't fulfill to the objectives, one time again probably because the swirl level was still too high.
At the NOx target, the smallest orifices with the 10 holes nozzle provided a quasi negligeble soot level of 0.15 mg/s.
All the configurations showed the same ISFC/NOx compromise.

- Conclusion:

In the low load/low speed area the best results were obtained with the smallest orifice diameters as long as it was possible to reduce the swirl level when the number of holes increased.

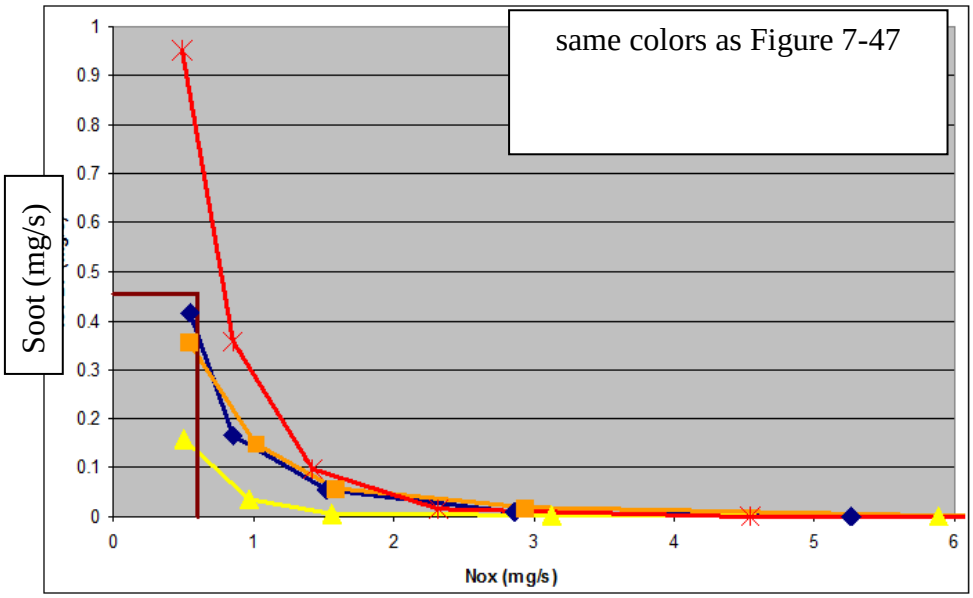

Figure 7-48: Soot versus NOx at 2250 rpm and 9.4 bars IMEP, constant noise level 87 dBA

7.4.3.2. LFDC operating points.

- Reference point at 2250 rpm 9.4 bars IMEP

The 10 holes 88 µm nozzle associated to a swirl level reduced to 1.0 was used.
According to the strategy developped by Akihama and presented in §7.2.4.3, the engine tuning was modified step by step.

The first one consisted in advancing the injection timing versus the conventional mode, in order to get a very stable combustion even with a high amount of EGR as seen in Figure 7-49. Noise level was obviously increased from 87.5 dBA up to 93 dBA. The pilot injection was canceled in order to avoid any warm-up of the gases and to secure the longest possible lift-off length.

On this basis, the second step aimed to reduce the peak of heat release by adding EGR and therefore increasing the equivalence ratio from 0.65 up to 0.85 –Figure 7-50. With this new tuning, the minimum NOx level of 0.3 g/kWh was achieved with an increased equivalence ratio of 0.85 instead of 0.65 and a corresponding smoke level of 4.5 instead of 2.7.

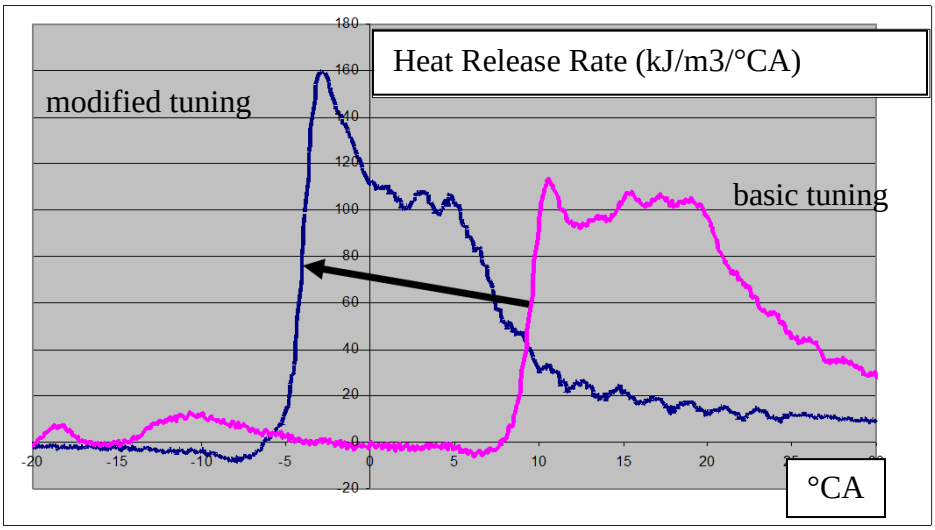

Figure 7-49: heat release rate versus CA for basic tuning (main injection at +1°CA) and modified tuning (main injection at -31°CA). All other parameters kept constant as intake pressure = 1.6 bar, equivalence ratio 0.65, O2 content 16.5%, injection pressure 1300 bars

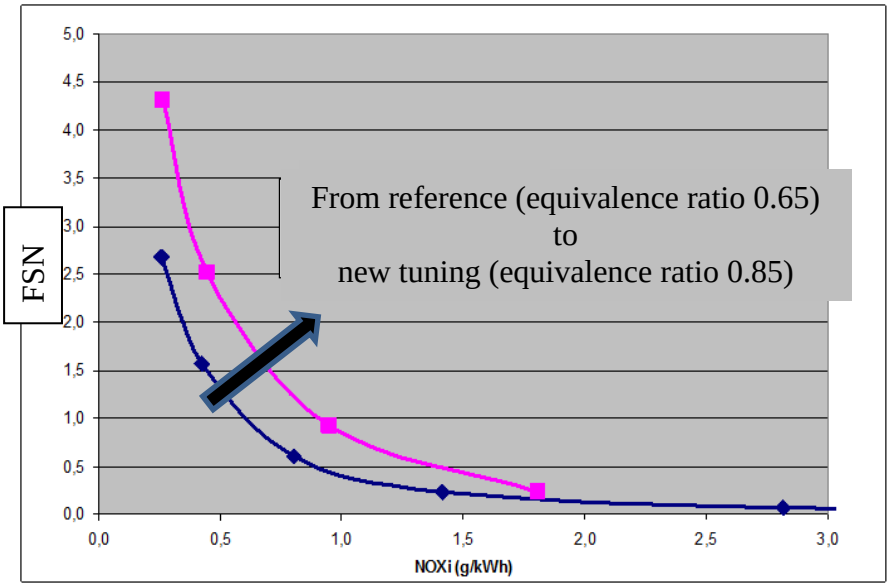

Figure 7-50: effect of the equivalence ratio on the NOx/soot trade-off

To reach the conditions described in §7.2.4.2, it was therefore necessary to one time again significantly increase the EGR level; but, at the same time, the pressure boost had to be set from 1.6 bars up to 3.1 bars in order to have a sufficient percentage of oxygen to keep the same engine load. At the same noise level, the injection pressure was increased from 1300 to 2200 bars. The effect on the heat release rate is shown in Figure 7-51; the premixed mode still noticeable with 11.7% of Oxygen completely disappeared as the temperature at SOI increased due to the EGR.

In these conditions, the evolution of the NOx/soot trade-off completely changed –see Figure 7-52- and, after a peak of soot, both pollutants decreased significantly until both reaching quite a 0 level.

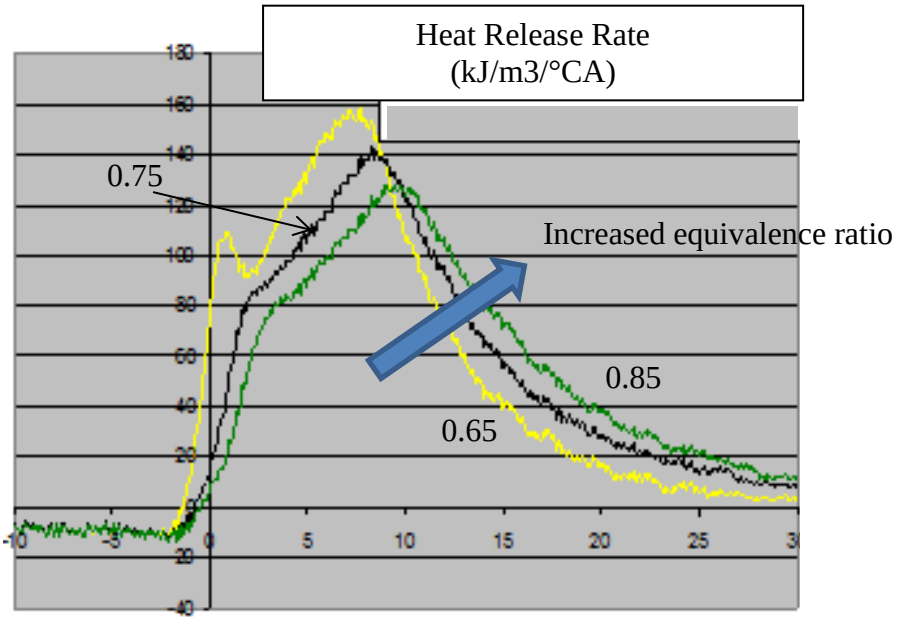

Figure 7-51: effect of the EGR rate on the HRR (Pinj 2200 bars, intake pressure 3.1 bars); O2 levels are 11.7% (equivalence ratio 0.65), 10.2% (0.75), 8.8% (0.85)

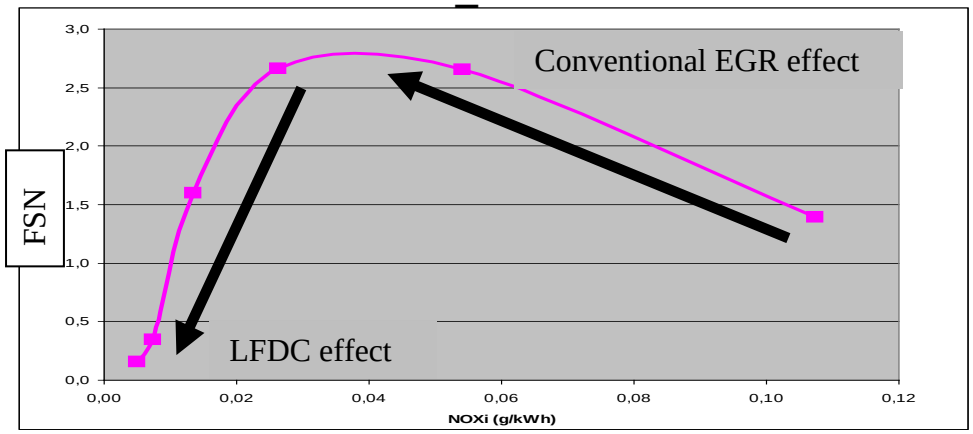

Figure 7-52: soot/NOx trade-off in LFDC mode (Pinj 2200 bars, intake pressure 3.1 bars) – the black arrows represent an increase of the equivalence ratio from around 0.65 up to around 0.85

Nevertheless, the fuel consumption increased significantly (Figure 7-53) due to both a high level of HC and CO and a worse combustion phasing in the cycle. The penalty in unburnt emissions was the consequence of the high EGR rate, generating a too low temperature at the end of the combustion, during the expansion stroke, and reducing the post-oxidation – cf §7.2.2.1.

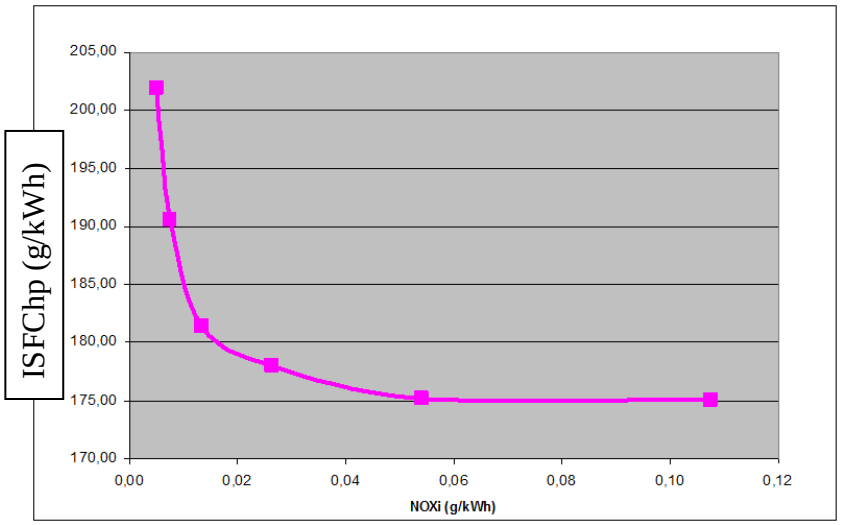

Figure 7-53: ISFChp in LFDC mode (Pinj 2200 bars, intake pressure 3.1 bars)

- Other operating points and influence of the nozzle definition.

Two other points defined in §7.4.1. have also been investigated with the same strategy. The ability to achieve a "0 NOx, 0 smoke" was confirmed as shown in Figures 7-54 and 7-55. On the same graphs, the influence of the nozzle hole diameter and of the number of holes are also presented; all the tests have been achieved with a swirl level of 1.0, except the basic 7 holes injector which was associated to a level of 1.6.

At 2750 rpm, the capability of the air system used on the bench was not sufficient to provide enough fresh air to the engine. This was also the reason why higher loads have not been investigated.

Nevertheless, the LFDC has also been achieved and the smallest nozzle holes always provided the best results concerning the NOx/soot trade-off but also the amplitude of the soot peak before LFDC.

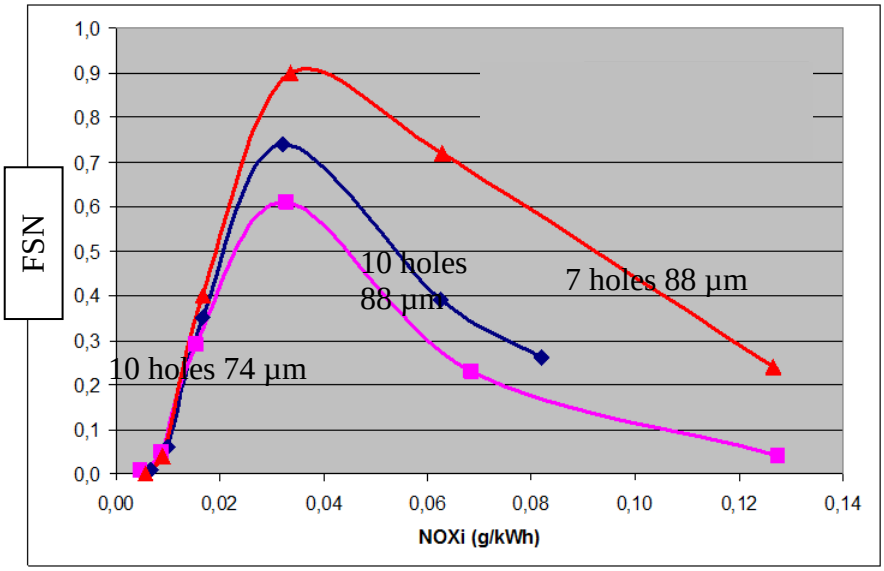

Figure 7-54a: 1500 rpm 9 bars IMEP; injection pressure 1200 bars

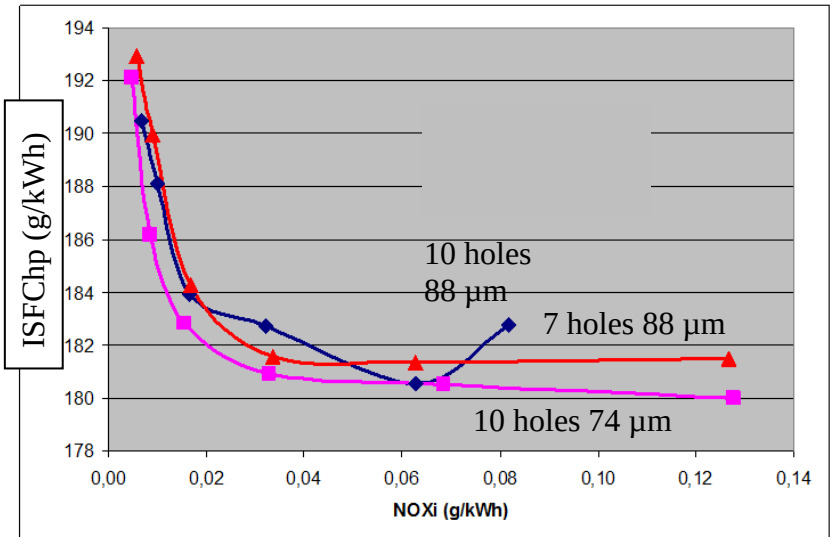

Figure 7-54b: 1500 rpm 9 bars IMEP; injection pressure 1200 bars

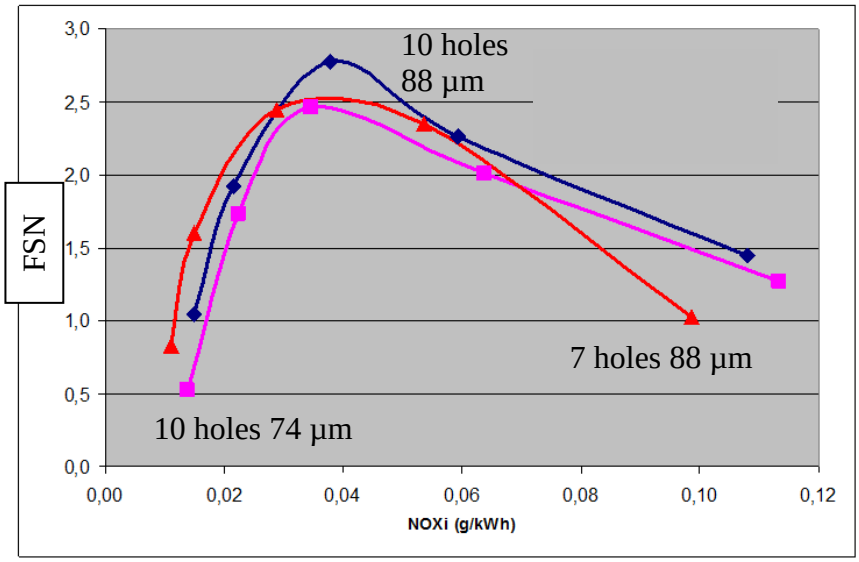

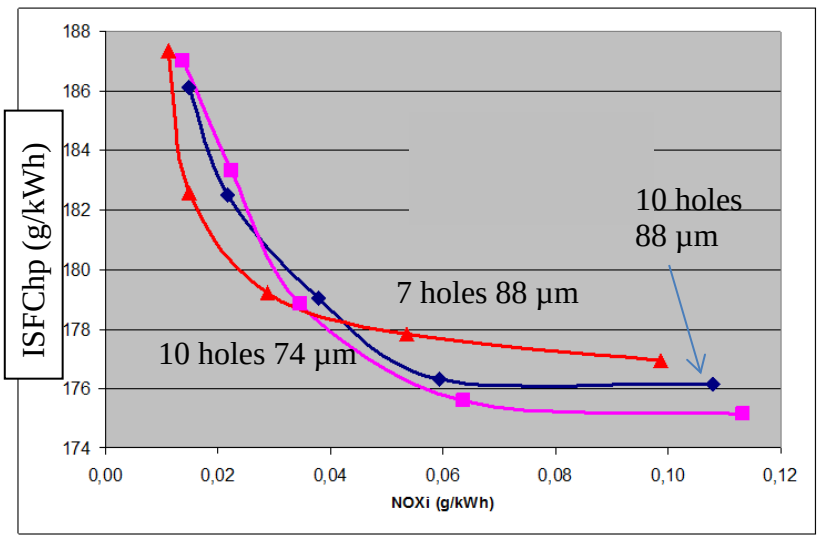

Figure 7-55: 2750rpm 9bars IMEP 1800 bars

7.4.3.3. Thermodynamic analysis at 2250 rpm 9.4 bars IMEP in LFDC mode.

The first interesting way to analyze the results obtained by LFDC was to use a quite simple analysis based on the 1st law of the thermodynamics. On the given operating point, different LFDC tunings obtained with the 10 holes 88 µm 2200 bars configuration were compared to the Mild HCCI mode with the standard 7 holes 123 µm 1600 bars injector.

As observed before, the premixed combustion peak on the heat release rate disappeared with the two highest EGR levels. The maximum HRR level decreased as well due to a "colder combustion" –see Figure 7-56.

Figure 7-57 represents the enthalpy split between the different loss sources and the indicated work; the low pressure loop, highly dependent upon the EGR and boosting systems, was not represented here. The main result was concerning the importance of the unburned components HC and CO in the LFDC mode as noticed §7.4.3.2. This explained the reduction of the indicated work observed with LFDC compared to the soot peak location. This drawback was partially compensated by different gains:

- A reduction of the exhaust losses due to a combustion timing closer to TDC. Nevertheless the reduction of the exhaust enthalpy would have a negative effect as a high turbocharging level was needed.
- A reduction of the thermal losses to the cylinder liner as there was no more premixed combustion; the flame volume was concentrated in the central zone of the cylinder, reducing contacts between the diffusive flame and the wall. On the contrary, heat losses are a bit higher in Mild HCCI mode because of the importance of the premixed mode.

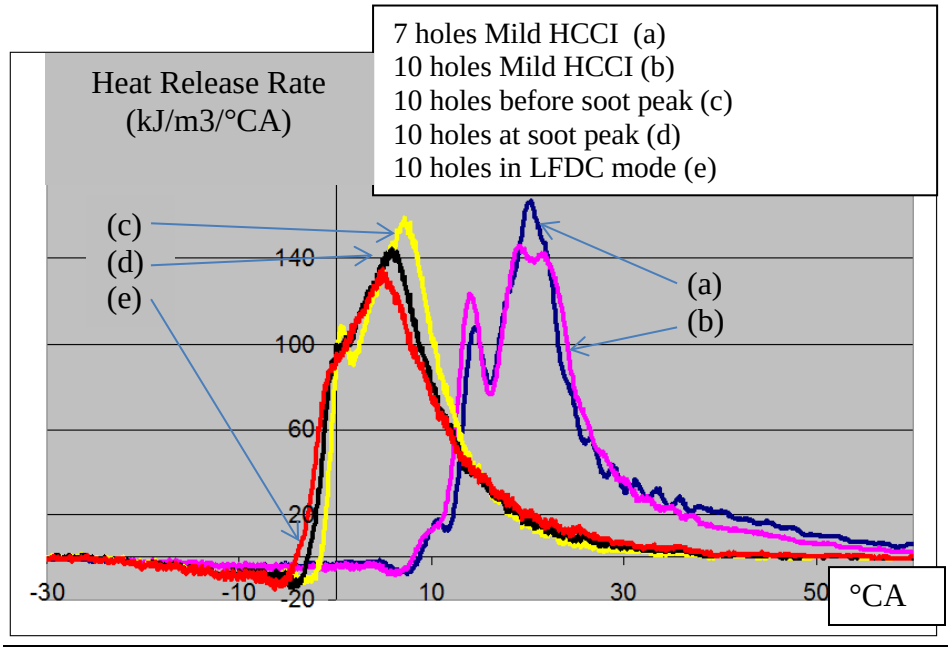

Figure 7-56: comparison of the heat release at 2250 rpm 9.4bars IMEP

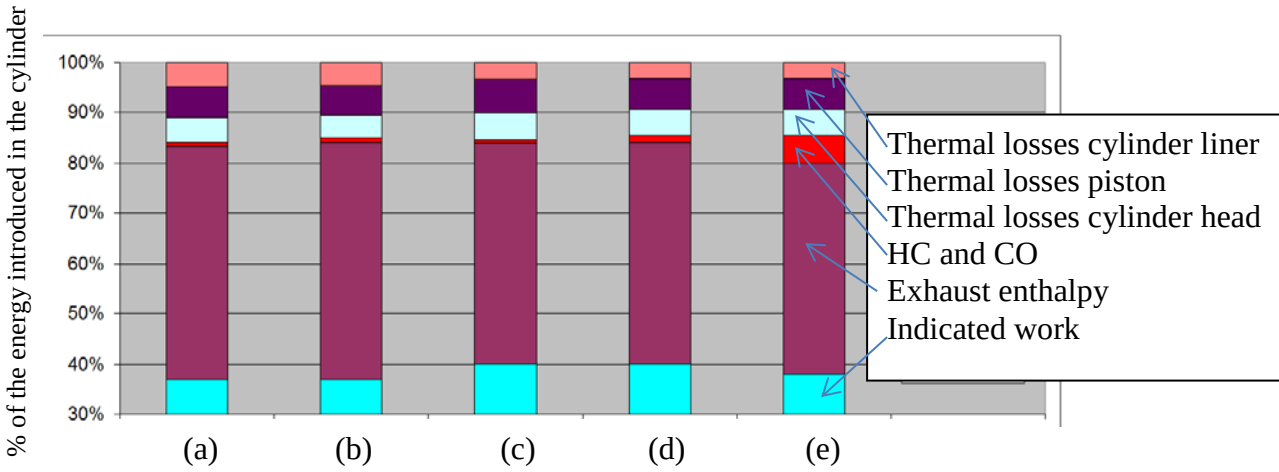

Figure 7-57: split of the introduced energy for the same configurations as in Figure 7-55 (high pressure loop only)

7.4.3.4. 3D analysis at 2250 rpm 9.4bars IMEP in LFDC mode.

Another point of view would be to analyze the physics explaining the deep change between the conventional NOx/soot behavior before the soot peak –eg the soot level increases as the EGR rate is higher- and after –eg the increase of the EGR rate leads to a decrease of both NOx and soot, until they reach a value close to 0. To achieve this task, a 3D simulation was conducted using the Star CD code. Instead of directly comparing soot concentrations –it is well known that the soot models do not provide quantitative results with high EGR levels- two analysis were chosen:

- The observation of both lift-off and liquid length as well as the temperature field (Figure 7-60) to confirm the internal and external previous analysis in constant volume vessel based on mixture preparation and seen in §7.2.4.1 to 7.2.4.3.
- The combustion history traced on the Kamimoto diagram (Figure 7-61) to evaluate the impact of thermodynamic conditions (see §7.2.4.4.)

The chosen tests have been achieved with the 10 holes 88 µm nozzle and the two EGR levels (or equivalence ratios) are illustrated in Figure 7-58.

The comparison of the heat release rate for points A and B is presented in Figure 7-59 for both simulation and test.

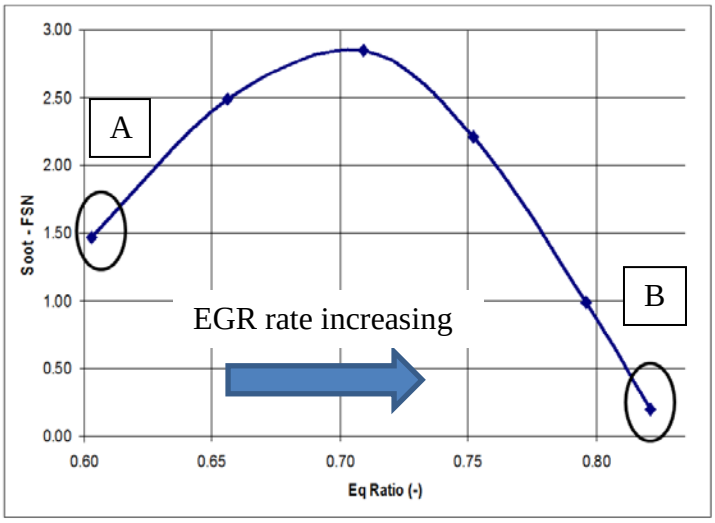

Figure 7-58: soot versus equivalence ratio at 2250 rpm 9.4 bars IMEP – injection pressure 2200 bars 10 holes 88 µm nozzle– boost pressure 3.1 bars – Swirl 1.0

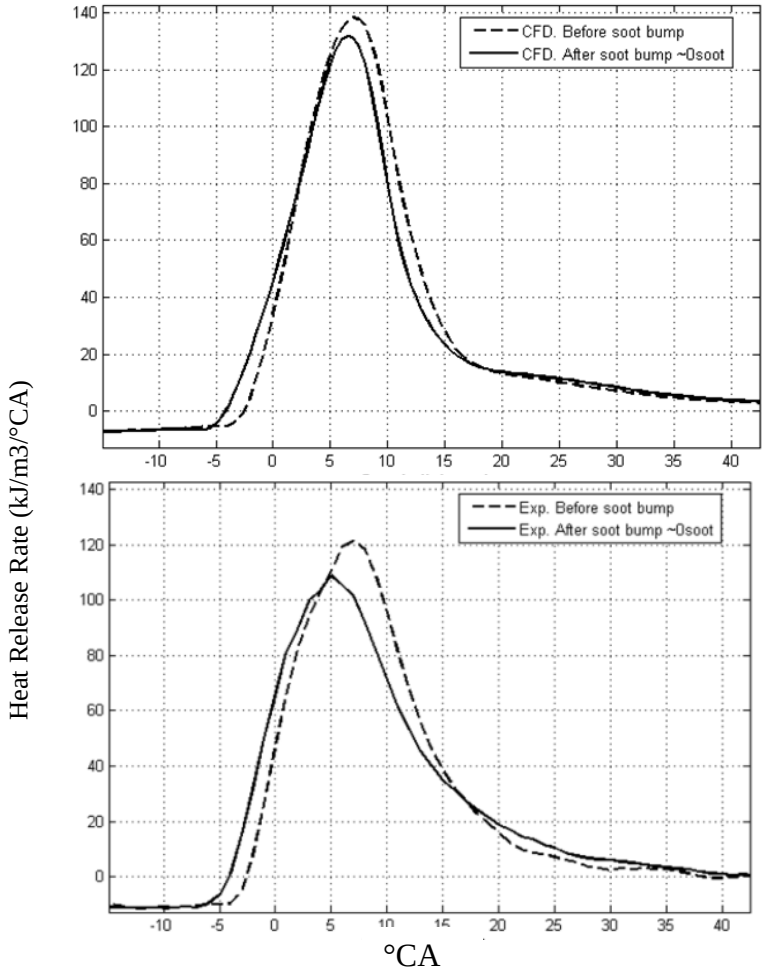

Figure 7-59: comparison of simulated (upper graphic) and experimental (lower graphic) heat release for points A (dotted line) and B (plain line)

Even if the simulation has over-estimated the maximum value of the HRR, the CA timing versus TDC was correctly reproduced as well as the relative position of the traces for points A and B.
Figure 60 establishes significant differences between points A and B, which greatly explain the existence of the LFDC:

- There is no major difference on the equivalence ratio map for both points

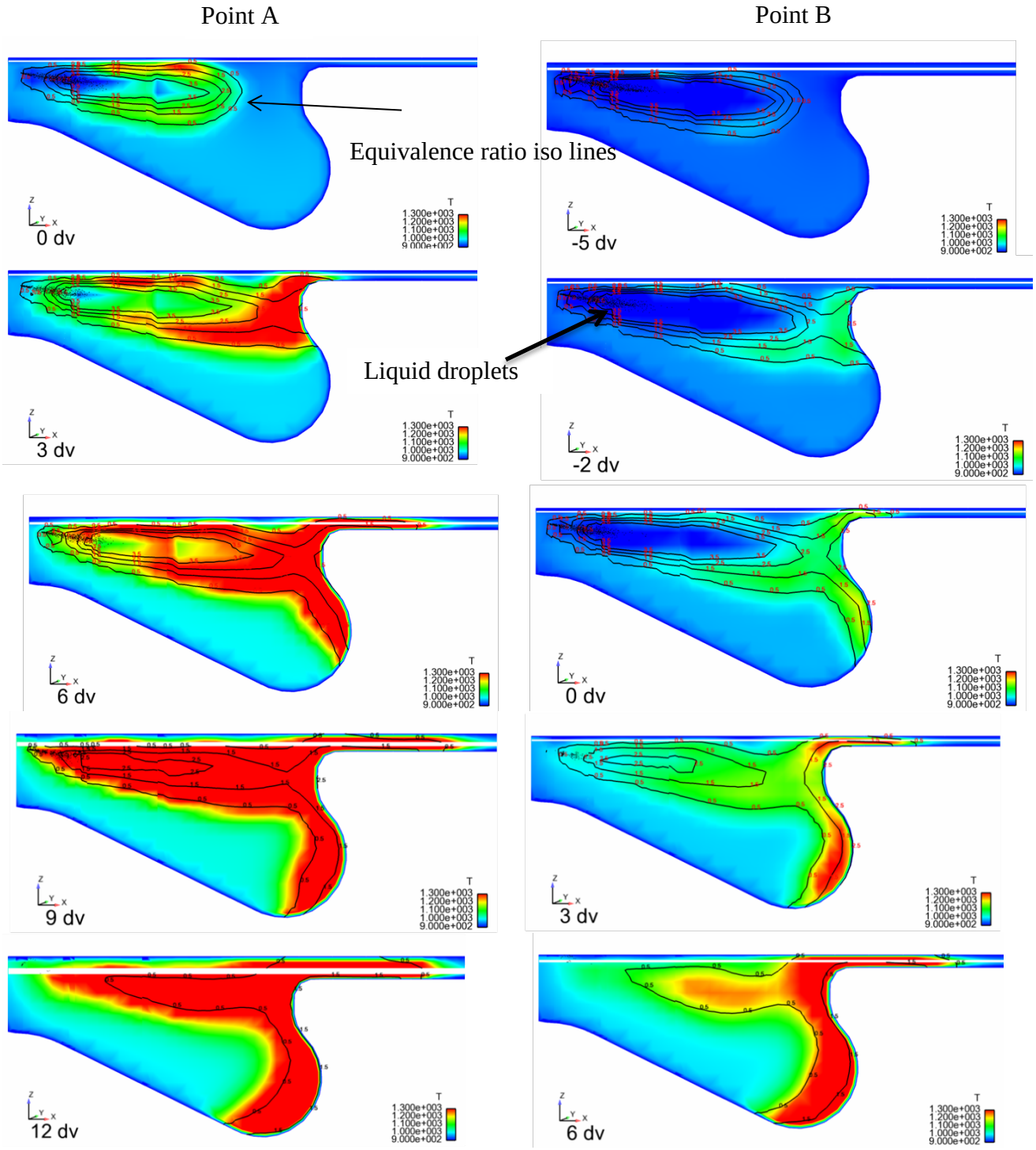

Figure 7-60: temperature field, equivalence ratio iso lines and liquid droplets at the same timing after SOI. CA (dv) indications are referring to the absolute timing versus TDC

- The high temperature area (particularly the red zone) remains smaller for point B than for point A due to the thermodynamic effect of the EGR. This explains the quicker evaporation rate and liquid droplets decrease for point A.
- The combustion and the high temperature zone were propagating upstream the spray direction in both cases but, as they reached the liquid droplets 6°CA after TDC for point A, they remained quite far at least until injection stopped for point B. This is exactly what was awaited from LFDC.

Nevertheless, the evolution of the hot zone towards the liquid droplets during the expansion cycle was not observed during the tests in the constant volume vessel –see § 7.3.4. This fact was probably due to the much larger volume available in the vessel which leads to a higher heat diffusion in the surrounding gases and thereby a relatively slower increase of the local temperature. This could explain the fact that a lower oxygen concentration had to be achieved on the engine than in the vessel to obtain a proper LFDC –eg 8 to 9% versus 12 to 13%. This had obviously an impact on the availability of such a high EGR level around 70% on the engine.
All these observations confirm the previous evaluations and diagnosis involving the impact of the mixture preparation on the possibility to achieve a sootless diffusive combustion.

On the other side, the impact of the thermodynamic conditions has been evaluated. The evolution of the equivalence ratio and the temperature as combustion was developing is presented in Figure 7-61.

First of all, as the mixture preparation was approximately unchanged between points A and B, the equivalence ratio in the chamber was not greatly modified. On the contrary, the huge amount of EGR used with point B led to strongly reduce the temperature and therefore kept the mixture far away from the soot and NOx peninsula as it can be noticed between 366 and 375 °CA. Nevertheless, the intersection of the mixture zone with the area where oxidation of CO and HC was possible was significantly more limited with point B than with point A, which could explain the lack of efficiency observed §7.4.3.3.

7.4.4 Conclusion.

The LFDC has been obtained on high load operating points; confirming the investigation led by Sasaki [7-5] –see §7.2.4.3.- with conventional nozzles, the thermodynamic effect due to a very low combustion temperature seems to be predominant even if very small nozzle orifices have a significant benefit via a large distance between liquid penetration and lift-off length.

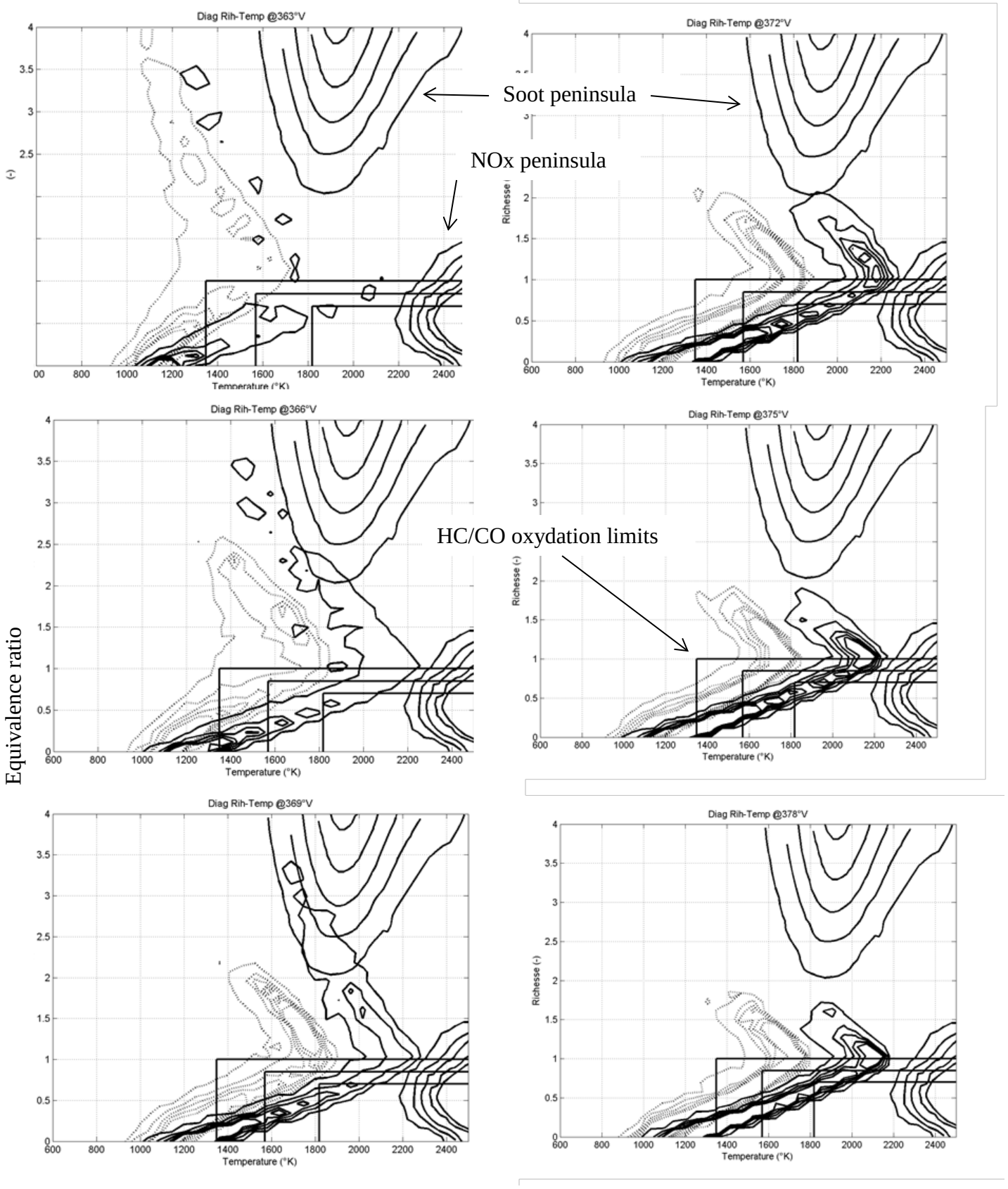
Diag Rih-Temp @363°V
Diag Rih-Temp @372°V
Soot peninsula
NOx peninsula
Diag Rih-Temp @366°V
Diag Rih-Temp @375°V
HC/CO oxydation limits
Equivalence ratio
Diag Rih-Temp @369°V
Diag Rih-Temp @378°V
Temperature (°K)
Richesse (-)

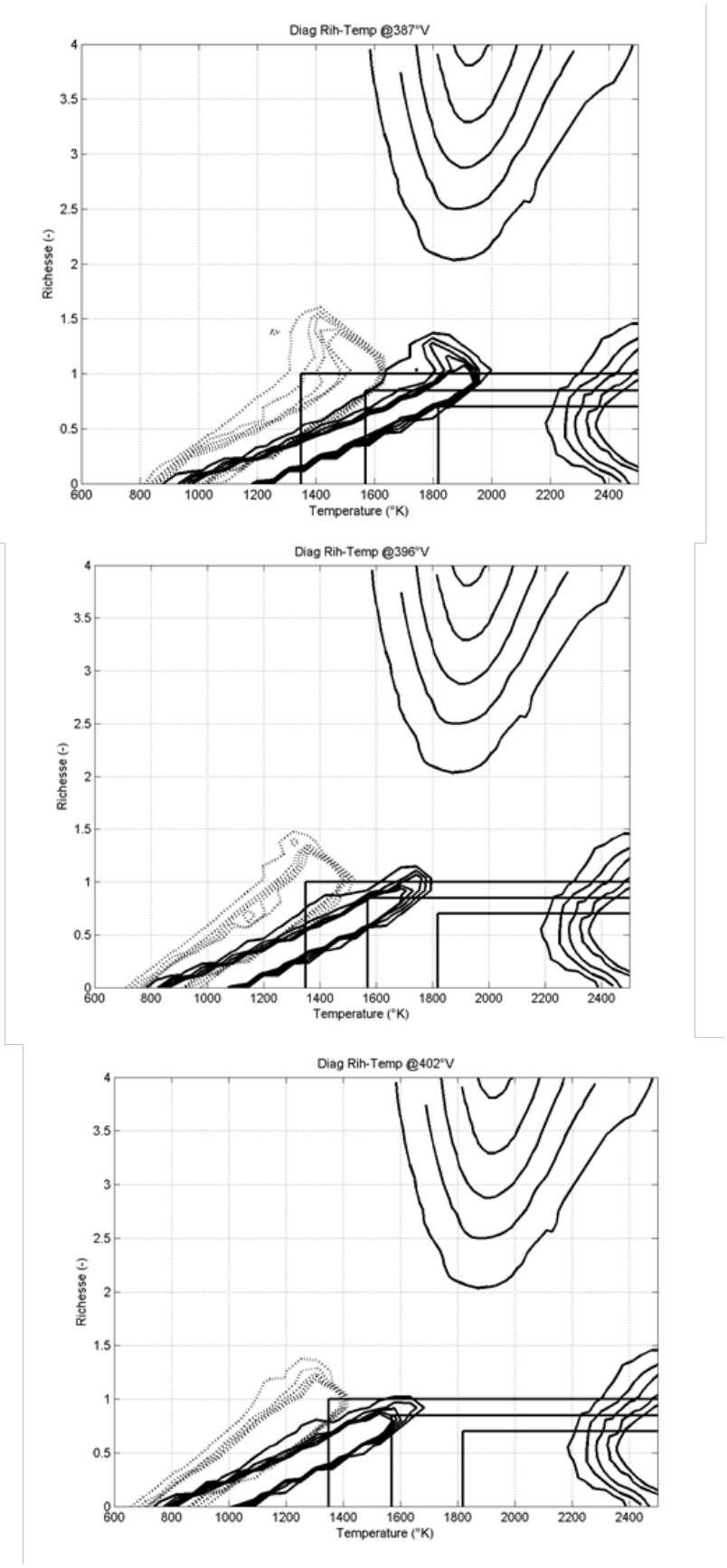

Figure 7-61: combustion trace in the Kamimoto diagram for points A (dark lines) and B (light lines) °V (°CA) are refering to the absolute position versus TDC.

7.5. Conclusion.

One time again in the history of the Diesel engine, the advances achieved with the injection system and particularly with the nozzle geometry have allowed to obtain significant improvements in mixture preparation and combustion.

In this chapter, the investigation and the development of the combustion system have been led by the physics of the phenomena which govern mixture preparation, beginning with results published by an international laboratory, even if they were limited to academic tests with a single hole prototype injector. The research of a lift-off length completely disconnected with the penetration length of the liquid phase pushed to machine nozzles with smaller and smaller outlet orifices until the limit of the technical possibilities and to investigate much higher injection pressures and unconventional engine tunings. Advanced optical techniques have been used to explain the resulting spray behavior in different operating conditions, more and more linked to actual engine conditions, with always a look at the previous investigation. For example, the interest of a low oxygen content for dissociating liquid and combustion was first suggested by the bibliographic analysis and then confirmed by the tests in the constant volume vessel.

The optimization of the air system involving swirl ratio, charging pressure and EGR, was only a consequence of the physical phenomena we tried to reproduce on the engine. They were linked to the necessity to obtain a sufficient hydraulic flow to achieve the targeted power density and an increase of the number of holes was the only solution to cope with the reduced holes diameter.

At the same time, questions concerning the relative importance of the mixture preparation and the thermodynamics arose, even if this last item was not initially within the frame of the work; a parallel investigation, mainly based on the use of simulations, demonstrated the first order of importance of the temperature conditions in the results; the LTC not only helped to avoid the premixed combustion mode and to reach LFDC but also, on a much more conventional way, reduced the potentiality of soot and NOx formation.

Finally, even if the EGR and boost levels won’t be feasible for industrial applications in the near future, tests achieved in Mild HCCI and conventional combustion modes at full load proved the interest of small orifices associated to very high injection pressures; it is also the role of the engineers to follow a dedicated target –for instance here LFDC- but also to remain open-minded and to explore collateral solutions which were not obvious at the beginning of the research work.

Bibliography.

[7-1] JE. Dec: A Conceptual Model of DI Diesel Combustion Based on Laser-Sheet Imaging
SAE 970873

[7-2] S.Kook, C.Bae, P.Miles, D.Choi, L.Pickett: The Influence of Charge Dilution and Injection Timing on Low-Temperature Diesel Combustion and Emissions
SAE 2005-01-3837

[7-3] P.Miles: Sources of UHC and CO in Low Temperature Diesel Combustion Systems
Thiesel 2010

[7-4] S.Kimura, O.Aoki, H.Ogawa, S.Muranaka, Y.Enomoto: New Combustion Concept for Ultra-Clean and High-Efficiency Small DI Diesel Engines
SAE 99-01-3681

[7-5] S.Sasaki, K. Akihama, Y. Takatori, K.Inagaki, AM.Dean: Mechanism of the Smokeless Rich Diesel Combustion by Reducing Temperature
SAE 2001-01-0655

[7-6] B.Walter, B. Gatellier: Development of the High Power NADI Concept using Dual Mode Diesel Combustion to achieve Zero Nox and Particulate Emissions
SAE 2002-01-1744

[7-7] S. Kimura, O. Aoki, Y. Kitahara and E. Aiyoshizawa: Ultra Clean Combustion Technology Combining a Low-Temperature and Premixed Combustion Concept for Meeting Future Emission Standards
SAE 2001-01-0200

[7-8] G.Coma, P.Gastaldi, JP.Hardy: HCCI, risks and potentialities
Haus der Technik Essen 2008

[7-9] M.Besson, N.Hilaire, H.Lahjaily, P.Gastaldi: Diesel Combustion study at full load using CFD and Design of Experiments.
SAE paper 2003-03-36.

[7-10] P.Gastaldi, JP.Hardy: Advantages and limits of HCCI combustion modes for Diesel Engines
Thiesel Valencia 2006

[7-11] G.Coma, P.Gastaldi, JP.Hardy: HCCI Verbrennung, Traum oder Realität?
13.Aachener Kolloquium – 2004

[7-12] P.Gastaldi, S.Dehoux, JP.Hardy: Mild HCCI, a worldwide combustion system for very low emissions?
AVL Symposium – Baden 2008.

[7-13] D.Stanton: Advanced combustion technology to enable high efficiency clean combustion.
Deer Symposium- 2008

[7-14] D.Siebers, B.Higgins: Flame Lift-Off on Direct-Injection Diesel Sprays Under Quiescent Conditions
SAE 2001-01-0530

[7-15] A.Arbeau: Etude de l'entraînement d'air dans un spray haute pression. Diagnostics optiques et application à l'injection Diesel
PhD report – Toulouse 2004

[7-16] L.Pickett, D.Siebers, C.Idicheria: Relationship Between Ignition Processes and the Lift-Off Length of Diesel Fuel Jets
SAE 2005-01-3843

[7-17] D.Siebers: Flame lift-off and mixing controlled combustion
Deer Symposium 2008

[7-18] V.Sepret: Application de la PIV sur traceurs fluorescents à l'étude de l'entraînement d'air par un spray Diesel. Influence de la densité ambiante et du diameter de trou d'injecteur.
PhD report – Toulouse 2009

[7-19] D.Siebers, B.Higgins, L.Pickett: Flame Lift-Off on Direct-Injection Diesel Fuel Jets: Oxygen Concentration Effects
SAE 2002-01-890

[7-20] L.Pickett, D.Siebers: Non-Sooting, Low Flame Temperature Mixing-Controlled DI Diesel Combustion
SAE 2004-01-1399

[7-21] DIAMANP (DIesel A Maitrise de l'Acoustique, des NOx et des Particules): rapport final à l'ADEME
Paris 2009

[7-22] DICO (Diffusive Combustion): rapport final à l'ANR
Paris 2012

[7-23] G.Bruneaux, F.Defransure, C.Garsi, P.Gastaldi, B.Griffaton, J.Kashdan, JP.Le Ru, B.Lombard, LM.Malbec, B.Nicolas, E.Topenot: DICO, a new step towards emission free diffusive combustion
Thiesel – Valencia 2012

[7-24] N.Guerrassi, P.Bercher, P.Geurts, G.Meissonnier, N.Milovanovic: Light Duty Common Rail Injection Technology for High Efficiency Clean Diesel Engines
SIA - Rouen 2010

[7-25] B.Argueyrolles, S.Dehoux, P.Gastaldi, JP.Hardy: From conventional to Mild HCCI and Lifted flame combustions: the new steps to develop low emissions high efficiency Diesel engines.
Thiesel – Valencia 2010

Chapter 8

Conclusion

Following the same frame as in the previous chapters, three topics will constitute the conclusions of the present work: the first one will concern the future of the combustion engine, the second one the necessary developments and improvements of experimental and numerical tools, and the third one some new ideas emphasizing the interest of a closer cooperation between the research laboratories and the industry.

8.1. Threatens and potential for the internal combustion engine.

The combustion engine nowadays is a mass production product, with thereby a stronger and stronger pressure on both design and manufacturing costs. To secure a sufficient level of profitability, automotive and truck manufacturers have to reduce the diversity of the models sold over the world while taking into account the different customer expectations, the different regulations, the different fuel qualities, and eventually the production tools available in each region. This requirement necessitates to develop robust combustion systems whose hardware could be adapted by dedicated tuning strategies, like the Mild HCCI [8-1]. For instance, the Diesel engines delivered in the USA must be capable of accepting fuels with highly different cetane numbers; for actual applications, a closed loop combustion, frequently based on the CA50 optimization, is used with the help of cylinder pressure sensors.

A second challenge is constituted by the necessity to optimize a more and more difficult trade-off between, on one hand the demand for high performances and driving pleasure, especially in quite rich countries, and, on the other hand, the involvement for drastically reducing CO_2 emissions –ie fuel consumption- and for coping with tighter and tighter pollutant emissions regulations for NO_x, soot, HC and CO. In the race for finding the acceptable compromise between all these requirements, the internal combustion engine will be more and more challenged by electric powertrains –hybrids or vehicles powered by batteries only. If the cost to CO_2 performance is nowadays in favor of the ICE, progress in electric motors and energy storage has to be considered in the future, as shown in Figure 8-1.

In this competition, the efficiency and the cost of the after-treatment systems, especially for nitrogen oxides with SCR or NO_x traps, will govern the targets for engine out emissions and thereby the ability to improve fuel consumption for both Diesel and direct injection stratified gasoline engines.

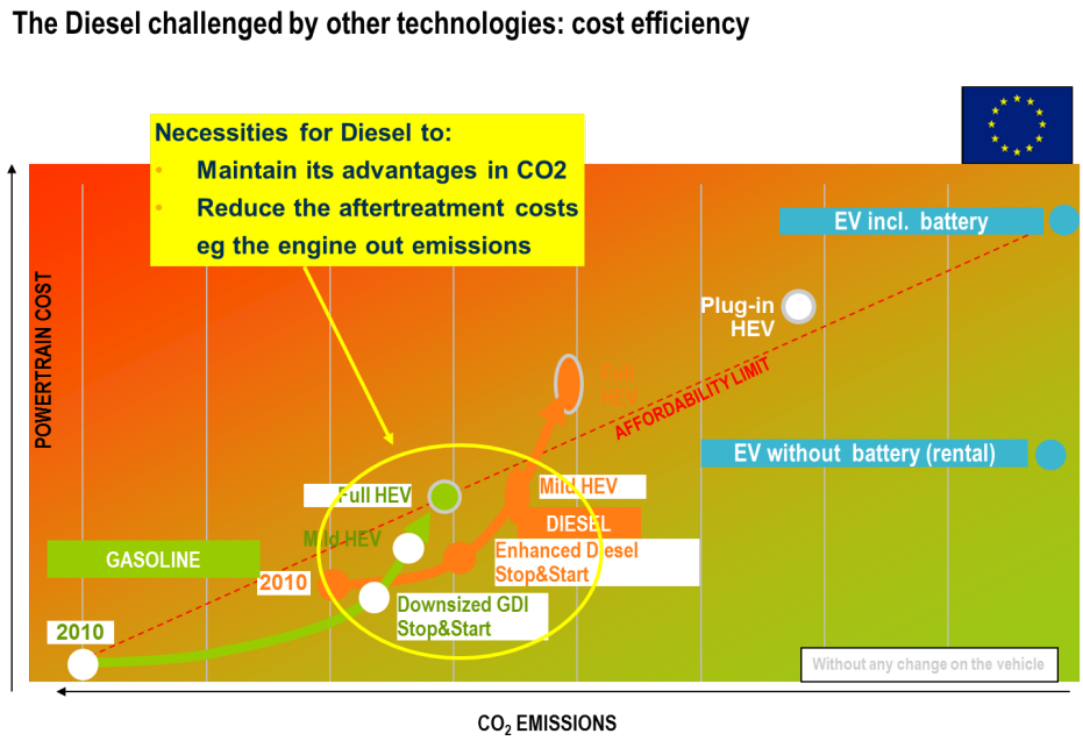

Figure 8-1: trade-off between CO_2 and cost for different powertrain technologies [8-2]

.

8.1.1. Potential solutions for the SI powertrain.

For the SI powertrain, progress in high pressure indicated cycle efficiency will be linked to an increase of the compression ratio, that is to say to the ability to accept values higher than 11; concerning pumping losses, both a strong downsizing, with super or turbo chargers to achieve the necessary levels of power, and unthrottled operation capabilities, especially for large displacement engines, will be considered.

The most important barrier to operate the engine at high cylinder pressures is linked to abnormal combustions, like knock or “super knock”; late investigation have shown that the addition of controlled quantities of EGR could avoid the occurrence of auto-ignition in the chamber by reducing the overall gas temperature [8-3]. The physics of “super knock” phenomena is on the contrary much more difficult to handle, with perhaps an influence of oil droplets coming from the sump through the piston rings and generating hot spots in the chamber [8-4].

Stratification is, apart from reducing the displacement, another way to avoid high pumping losses at low operating load for mid or large size engines. Chapters 5 and 6 have shown that spray guided and air guided SI stratified systems both rely on the ability to govern mixture preparation in the cylinder – ie with other words the fuel repartition or the air/fuel ratio distribution. Fundamentally, both of the systems could achieve a satisfactory stratification at low engine load until idle, with an acceptable presence of fuel in the vicinity of the spark plug to secure ignition and to avoid unacceptable misfiring occurrences. This ability leads to a dramatic reduction of the pumping losses

by operating the engine at WOT, and thereby an increase of the effective efficiency. But, as the first concept is mainly influenced by the spray behavior in different thermodynamic conditions, with a quite robust squish air motion, the second design is highly sensitive to cycle to cycle aerodynamic fluctuations, transporting more or less fuel vapor to the plug according to the tumble intensity and position in the chamber. The difficulties to cope with these last dispersions within the frame of mass production engines is clearly challenging and would require costly on line controls during the cylinder head manufacturing. It is the reason why spray guided systems seem to have the greatest potential in the future.

Nevertheless, the availability of performant injectors, with a high pressure capability –ie over 100 bars or even more as the MID3S was limited to 80 bars- and a low spray angle sensitivity in a wide range of thermodynamic conditions, covering WOT and part load lambda 1.0 operations, remains a key requirement. The association of such a spray with a squish motion has proven to be efficient in Chapter 5.

Concerning pollutant emissions, the necessity to limit soot, whose production mechanism is quite different from what has been understood on CI engines, will be clearly a must for direct injection. As fine particles are mainly resulting from the interaction between the spray and the piston head, an accurate evaluation of the droplets penetration in various ambient conditions is mandatory. If the engine out emissions can't be reduced, the use of a particles filter will be necessary despite their relatively high cost.

8.1.2. Potential solutions for Diesel.

On a CI engine, the efficiency can't be optimized without integrating NVH and pollutant emissions limits; if a significant progress is awaited with advanced NOx after-treatment systems, like the SCR, soot production will have to be carefully managed due to the impact of CSF regeneration on fuel consumption, but also for the presence of carbon particles in the lubricating oil.

An interesting way to evaluate the different improvement sources in terms of efficiency is to compare a large bore industrial powertrain, whose development was only led by fuel economy, and a passenger car one as illustrated by Figure 8-2 [8-5].

Besides the noticeable impact of the air system –but the range of operating points is much reduced on an industrial engine-, the following progress axis are identified:

- A high air mass flow and thereby a reduced equivalence ratio associated with efficient air coolers to improve the cycle efficiency, mainly via the compression polytropic coefficient
- The combustion velocity, with a quick heat release and an optimized mass burnt center of gravity associated to a lower engine speed. This

improvement would have a positive influence on both the thermodynamic efficiency but also on the expansion polytropic coefficient.

- Low wall losses due to engine geometry, low temperature combustion phasing and very low swirl levels

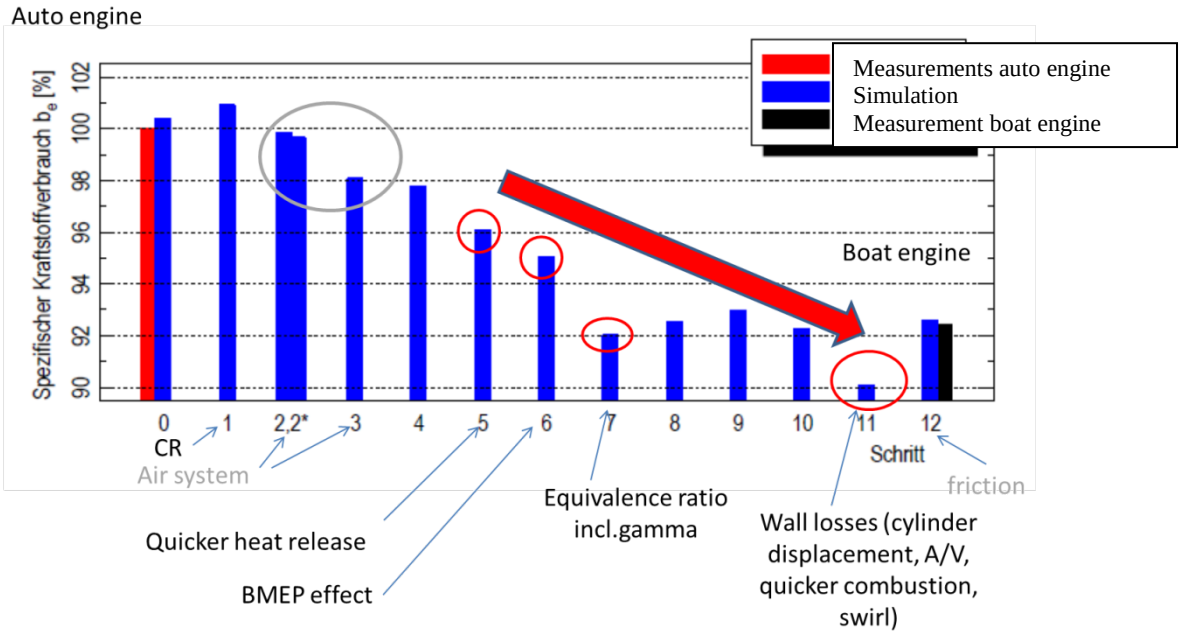

Figure 8-2: model change between an automotive and a marine engine at maximum load [8-5]

Among these three main items, enhancing combustion highly relies on mixture preparation and on the ability to limit noise and soot emissions. As seen in chapter 7, this strategy requires to improve the diffusion controlled combustion by promoting a better spray atomization with shorter injection durations. It could be reasonably assumed that the continuous increase of the rail pressure would lead to 3000 bars in the near future, for both heavy duty and passenger cars applications, allowing a rough 20% decrease of the injection length –and furthermore of the combustion duration- together with a 50% increase of the Weber number compared to current 2000 bars systems ([8-6], [8-7]). Keeping the hydraulic flow at the same level, a new trade-off between the size of the hole and the number of holes will have to be investigated in order to reduce soot or to allow an increase of the EGR rate, in the direction of the LFDC as shown in chapter 7. The optimization of such a combustion system will necessitate a good understanding of atomization, spray behavior and air/fuel interaction.

8.2. Tools development.

The mixture preparation process will undoubtedly remain at the heart of the combustion improvement for both Diesel and GDI engines. Keeping this scope in

mind, the capability to investigate actual operating conditions will be more and more important for both 3D simulation, visualization, or for the common use of both tools:

- the identification of the spray characteristics and the capability to compute them correctly
- the capability to investigate mixture preparation –eg the interaction between the fuel and the surrounding gases- in a real engine, leading to an accurate evaluation of the local equivalence ratio in the chamber.

8.2.1. Spray characteristics.

The aim of this investigation is to properly define the spray formation and to calibrate the different available models. The first point is to secure the knowledge of the boundary conditions for the experiments –eg rail pressure, fuel temperature and physical properties, back temperature and pressure. The ECN consortium for the testing environment, or the physical data base built within the frame of the NADIA project, could therefore be very helpful to improve the spray simulation [8-8].

The knowledge of the actual fuel pressure in the nozzle sack will rely on 1D hydraulic simulation, correlated with flow rate measurements on the bench; thereafter, the characterization of the flow in the nozzle holes will be obtained with more sophisticated 3D calculations involving cavitation models [8-9], [8-10]. If the last generations of nozzles were developed in order to improve the discharge coefficient, new products will probably mitigate efficient conical shapes with a minimum level of cavitation in order to manage coking [8-11]. All these data will be used to define the spray boundary conditions at the outlet orifice of the nozzle.

A parallel use of Mie scattering and Schlieren will allow to provide the necessary results –liquid and vapor penetration and angle- to calibrate the fuel models. An important challenge will consist in optimizing the different model coefficients for the very high injection pressures - ie up to 3000 bars for Diesel or to 3 or 400 bars for gasoline- as most of them were optimized a long time ago at quite lower levels. The identification of the spray structure, perhaps by the mean of X-ray measurements, will be helpful to identify the actual physical phenomena to be taken into account in the models [8-12], [8-13].

8.2.2. Mixture preparation.

The interest of endoscopic visualizations achieved in an actual engine has been illustrated in Chapter 5; improvements in lighting techniques, with continuous lasers for instance, in very high speed numeric cameras and the availability of endoscopes transmitting UV light would allow to dramatically increase space and time resolutions in order to register a whole cycle, from the beginning of the injection to the end of the combustion. This is of primary importance to capture and understand cycle to cycle variations, particularly at low load and speed for GDI. The evolution of the liquid spray versus walls and

plugs would provide important information concerning the ability to ignite and the risks of soot formation; for Diesel, the smoke clouds motion could easily be followed for evaluating the post-oxidation capability of the combustion system and the potential contact between soot and oil on the cylinder liner.

In parallel, a significant progress has been achieved with single cylinder optical engines, now able of reaching peak combustion pressures and IMEP corresponding to mid low operations. This tool would be wise to obtain detailed quantitative results, imaging the equivalence ratio repartition in the chamber with LIF techniques or the evolution of soot with LII or LEM.

8.3. R&D context.

The three combustion systems investigated in the previous chapters clearly have necessitated an intensive use of new tools and methodologies; this situation is quite frequent in the industry, and particularly in the field of the automotive engineering, where the development of a new concept is generally due to the evolution of pollutant regulations, power densities, or to the availability of new components like injectors or ignition systems. For instance, as described in Chapter 6, the introduction of the air guided stratified combustion needed to acquire the knowledge of the equivalence ratio and thereby to develop LIF techniques. At the end of this work, it seemed interesting to have a brief overview of the development cycle for a new project and of the imbrication of tools and product developments.
Figure 8-3 is summarizing a V representation of what could be this cycle [8-14].

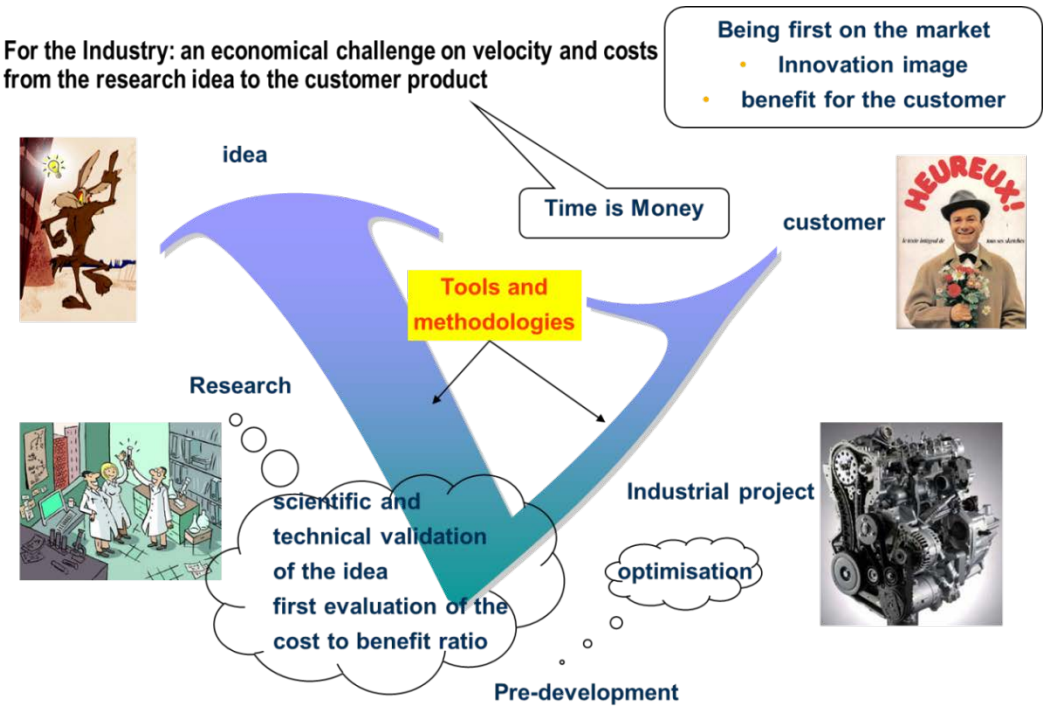

Figure 8-3: schematic overview of a project development scheme

During the research phase, the actual potential of the idea has to be clearly evaluated in terms of cost to benefit for the final customer; this important job sometimes necessitates new tools to capture and understand the inherent physical phenomena and to provide methodological guidelines for the forthcoming pre-development and for the optimization phase.

Ideally, these tools currently exist in the company or in academic laboratories because their necessity has been anticipated earlier, but in some cases, they unfortunately have to be developed, or adapted, during the project; in this case, because of short industrialization timings, they can't be really optimized and their accuracy remains at least perfectible.

To avoid this uncomfortable situation, a close cooperation between Research, this word covers both internal activities but also partnerships with universities and laboratories, and Industry, is mandatory to evaluate the needs as soon as possible, to provide enough time for choosing the best technique in terms of accuracy, difficulties and necessary knowledge, and to adapt it within the planning, as proposed in Figure 8-4. The Research partner would thereafter have to provide the complete "ready to use" tool with the associated methodology and the analysis of the accuracy to the Industry or propose to operate it internally according to its complexity.

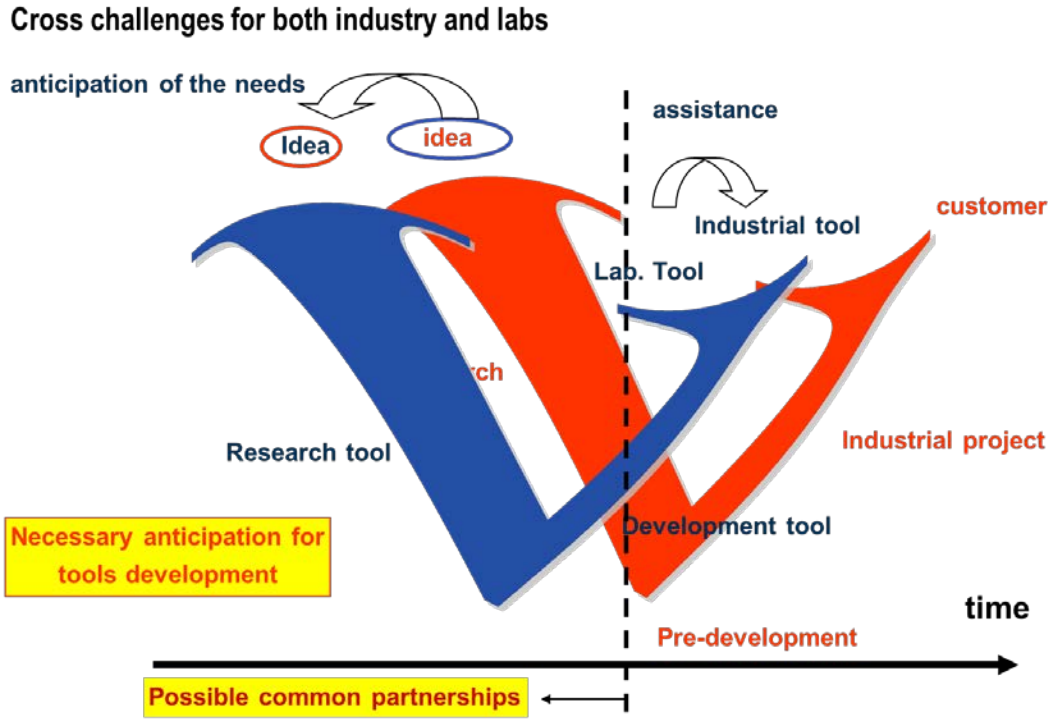

Figure 8-4: ideal timing for tools and project development

Bibliography.

[8-1] P.Gastaldi, S.Dehoux, JP.Hardy: Mild HCCI, a worldwide combustion system for very low emissions?
AVL symposium – Baden 2008

[8-2] J.Prost: keynote speech
SIA Rouen 2012

[8-3] K. Kumano, S.Yama : Analysis of Knocking Suppression Effect of Cooled EGR in Turbo-Charged Gasoline Engine
SAE 2014-01-1217

[8-4] O. Welling, J.Moss, J.Williams, N.Collings : Measuring the Impact of Engine Oils and Fuels on Low-Speed Pre-Ignition in Downsized Engines
SAE 2014_01-1219

[8-5] Technologietransfer zu Ubertragung von CO2- und Schadstoffemissions-potentialen zwischen verschiedenen Motorarten
FVV final report 2013

[8-6] K.Natti, A.Sinha, C.Hoerter, P.Andersson, J.Andersson, C.Lohmann, D.Schultz, N.H.Cho, R.Winsor : Studies on the Impact of 300 MPa Injection Pressure on Engine Performance, Gaseous and Particulate Emissions
SAE 2013-01-0897

[8-7] J.Johnson, J.Naber, S-Y.Lee, G.Hunter, R.Truemner, T.Harcombe : Correlations of Non-Vaporizing Spray Penetration for 3000 Bar Diesel Spray Injection
SAE 2013-024-0033

[8-8] J.M. Desantes, R. Payri, J. Gimeno, P. Marti-Aldaravi : Simulation of the First Millimeters of the Diesel Spray by an Eulerian Spray Atomization Model Applied on ECN Spray A Injector
SAE 2014-01-1418

[8-9] B.Argueyrolles, S.Dehoux, P.Gastaldi, L.Grosjean, F.Lévy, A.Michel, D.Passerel: Influence of injector nozzle design and cavitation on coking phenomenon
SAE 2007-01-1896

[8-10] F.Payri, V.Bermudez, R.Payri, F.J.Salvador: The influence of cavitation on the internal flow and the spray characteristics in Diesel injection nozzles
Fuel, vol 83 – 2004.

[8-11] F.Payri, J.Arrègle, J.J.Lopez, S.Hermens: Effect of cavitation on the nozzle outlzet flow, spray and flame formation in a Diesel engine
SAE 2006-01-1391

[8-12] M-C. Lai, Y.Zheng, X-B.Xie, S.Moon, Z.Liu, J.Gao, X.Zhang, K.Fezzaa, J.Wang, J.Shi : Characterization of the Near-Field Spray and Internal Flow of Single-Hole and Multi-Hole Sac Nozzles using Phase Contrast X-Ray Imaging and CFD
SAE 2011-01-0681

[8-13] C.Powell**:** Fuel Injection and Spray Research Using X-Ray Diagnostics
Deer Symposium 2012

[8-14] P.Gastaldi : keynote speech
Thiesel 2012

Bibliography

1) Ahmed A., Dupont A., Gastaldi P., Stéphan D.: Entwicklung eines neuen Brennraums für einen luftgeführten DI-Otto Motor mittels neuster experimenteller und computergestüzter Entwicklungstools.- 9.Aachener Kolloquium 2000 – Appears as [6-11]

2) Arbeau A., Bazile R., Charnay G., Gastaldi P.: A New Application of the Particle Image Velocimetry (PIV) to the Air Entrainment in Gasoline Direct Injection Sprays - SAE 2004-01-1948 – Appears as [3-23]

3) Arbeau A.: Etude de l'entraînement d'air dans un spray haute pression. Diagnostics optiques et application à l'injection Diesel - PhD report – Toulouse 2004 – Appears as [7-15]

4) Arcoumanis C., Badami M., Flora M., Gavaises M.: Cavitation in Real-Size Multi-Hole Diesel Injector Nozzles - SAE 2000-01-1249 – Appears as [3-10]

5) Argueyrolles B., Dehoux S., Gastaldi P., Grosjean L., Lévy F., Michel A., Passerel D.: Influence of injector nozzle design and cavitation on coking phenomenon - SAE 2007-01-1896 – Appears as [8-9]

6) Argueyrolles B.,Dehoux S.,Gastaldi P., Hardy J.P.: From conventional to Mild HCCI and Lifted flame combustions: the new steps to develop low emissions high efficiency Diesel engines – Thiesel – Valencia 2010 - Appears as [7-25]

7) Audi France – press book on the FSI system presented at the Paris Motor Show - Paris - September 2001. Appears as [6-19]

8) Baron.E: Elements d'automobiles – Pollution - Techniques de l'ingénieur – 2013 - Appears as [1-4]

9) Besson M., Hilaire N., Lahjaily H., Gastaldi P.: Diesel Combustion study at full load using CFD and Design of Experiments - SAE paper 2003-03-36 – Appears as [7-9]

10) Bird A.L.: Characteristics of nozzles and sprays for oil engines, Second World Power Conference- Berlin 1930 – Appears as [2-1]

11) Bruneaux G., Defransure F., Garsi C., Gastaldi P., Griffaton B., Kashdan J., Le Ru J.P., Lombard B., Malbec L.M., Nicolas B., Topenot E.: DICO, a new step towards emission free diffusive combustion - Thiesel – Valencia 2012 – Appears as [7-23]

12) Cavallino F.: Fuel Efficiency Evolution and Air Quality Improvement in Italy - SAE 962484 – Appears as [2-12]

13) Closeup: Gasoline DI could make waves soon - Ward's Engine Update – 03/1992 – Appears as [6-4]

14) Coma G., Gastaldi P., Hardy J.P.: HCCI Verbrennung, Traum oder Realität? - 13.Aachener Kolloquium – 2004 – Appears as [7-11]

15) Coma G., Gastaldi P., Hardy J.P.: HCCI, risks and potentialities - Haus der Technik Essen 2008 – Appears as [7-8]

16) Cordes D., Pischke P., Kneer R.: Influence of Injection and Ambient Conditions on the Nozzle Exit Spray of an Outwardly Opening GDI Injector - SAE 2012-01-0396 – Appears as [3-24]

17) Cossali G., Brunello G.,Coghe A.: LDV characterization of Air Entrainement in Transient Diesel Sprays - SAE 910178 – Appears as [3-15]

18) de Boer C.D., Grigg D.W.: Gasoline Engine Combustion – The Nebula Combustion Chamber - SAE 885148 – Appears as [2-13]

19) Dec J.E.: A Conceptual Model of DI Diesel Combustion Based on Laser-Sheet Imaging - SAE 970873 – Appears as [7-1]

20) Desantes J.M., Payri R., Garcia J.M., Salvador F.J.: A Contribution to the Understanding of Isothermal Diesel Spray Dynamics - Fuel, vol. 86 – 2007 – Appears as [3-8]

21) Desantes J.M., Payri R., Gimeno J., Marti-Aldaravi P. : Simulation of the First Millimeters of the Diesel Spray by an Eulerian Spray Atomization Model Applied on ECN Spray A Injector - SAE 2014-01-1418 – Appears as [8-8]

22) Desantes J.M., Payri R., Salvador F.J., de la Morena J.: Cavitation effects on Spray characteristics in the near nozzle field - SAE 2009-24-0037 – Appears as [3-13]

23) Desantes J.M., Payri R., Salvador F.J., Gimeno J. : Prediction of Spray Penetration by Means of Spray Momentum Flux - SAE 2006-01-1387 – Appears as [4-26]

24) DIAMANP (DIesel A Maitrise de l'Acoustique, des Nox et des Particules): rapport final à l'ADEME -Paris 2009 – Appears as [3-2] and [7-21]

25) DICO (Diffusive Combustion): rapport final à l'ANR - Paris 2012 – Appears as [3-1] and [7-22]

26) Dupont A., Floch A., Baby X.: In-cylinder flow investigation in a GDI 4 valve engine : bowl shape piston effects on swirl and tumble motions - FISITA 1998 – Appears as [4-21] and [6-14]

27) E.F.Obert : Internal Combustion Engines and Air Pollution - Harper and Row – Appears as [5-1]

28) EIA International Energy Outlook 2011 – Appears as [1-2]

29) Eifler W.: Untersuchungen zur Struktur des instationären Dieselöleinspritzstrahles im Düsennahbereich mit der Methode der Hochfrequenz-Kinematografie - PhD report – Kaiserlautern – 1990 – Appears as [3-12]

30) European Patents:
R.Leboeuf, P.Gastaldi, C.Voisin : EP 0997622
A.Floch, P.Gastaldi, JC.Lucas, D.Stéphan : EP 1068433

31) Fath A., Münch K.U., Leipertz A.: Spray Break-Up Process of Diesel Fuel Investigated Close to the Nozzle - ICLASS – Seoul – 1997 – Appears as [3-4]

32) Fischer J., Kettner M., Nauwerck A., Pfeil J., Spicher U.: Influence of an Adjustable Tumble System on In-Cylinder Air Motion and Stratification in a Gasoline Direct Injection Engine - SAE 2002-01-1645 – Appears as [6-13]

33) Flynn P.F., Durrett R.P., Hunter G.L., zur Loye A.O., Akinyemi O.C., Dec J.E., Westbrook J.W.: Diesel Combustion: An Integrated View Combining Laser Diagnostics, Chemical Kinetics, And Empirical Validation - SAE 99-01-0509 – Appears as [3-16]

34) Fraidl G.K., Piock W.F., Wirth M.: Gasoline Direct Injection: Actual Trends and Future Strategies for Injection and Combustion Systems - SAE 960465 – Appears as [5-2]

35) Fröba A.P., Rabenstein F., Munch K.U., Leipertz A.: Mixture of TEA and Benzene as a new seeding material for the quantitative two-dimensional LIEF Imaging of Vapor and Liquid Fuel inside SI Engines - Combustion and Flame – 1998 – Appears as [4-14]

36) Gastaldi P. : keynote speech - Thiesel 2012 – Appears as [8-14]

37) Gastaldi P., Clivillé F.: Moteur multicylindre à injection d'essence, comportant 3 soupapes par cylinder - French Patent n°89/10440, European Patent n° EP0412009 – Appears as [5-12]

38) Gastaldi P., Dehoux S., Hardy J.P.: Mild HCCI, a worldwide combustion system for very low emissions? - AVL Symposium – Baden 2008. – Appears as [7-12] and [8-1]

39) Gastaldi P., Gervais D.: Application of various Laser Induced Fluorescence techniques as tools for developping a new air guided Direct Injection SI combustion chamber - Esslingen – 2000 – Appears as [4-15] and [6-16]

40) Gastaldi P., Hardy J.P.: Advantages and limits of HCCI combustion modes for Diesel Engines - Thiesel Valencia 2006 – Appears as [7-10]

41) Gastaldi P., Préterre C.: Entwicklung neuer Methoden zur Analyse von direkteinspritzenden Ottomotoren - 8.Aachener Kolloquium, 1999 – Appears as [6-12]

42) Gastaldi P., Soler T.: Visualisation des jets d'injection sur et hors moteur - Renault internal report n° 17/91 – Rueil 1991 – Appears as [4-5] and [5-14]

43) Gastaldi P.: Compte rendu des essais sur culasse MID3S - Renault internal report n°26 – 02/90 – Appears as [5-15]

44) Gastaldi P.: Présentation de la culasse MID3S - Renault internal report n°126 – 01/89 – Appears as [5-11]

45) Gelalles A.G: Effect of orifice length diameter ratio on fuel sprays for compression ignition engines - NACA report 402 – 1931- Appears as [2-2]

46) Gervais D., Gastaldi P.: a comparison of two quantitative Laser Induced Fluorescence Techniques applied to a new air guided direct injection SI engine - SAE 2002-01-750 Appears as [6-17]

47) GIEC, Climate Change 2007, The Physical Science Basis, Cambridge University Press 2007 - Appears as [1-3]

48) Graff Seherr-Stoss H-C: die Brennstoffzuführung bei schnelllaufenden Verbrennungsmotoren - Kultur und Technik – 1/1987 – Appears as [5-4]

49) Guerrassi N., Bercher P., Geurts P., Meissonnier G., Milovanovic M.: Light Duty Common Rail Injection Technology for High Efficiency Clean Diesel Engines

50) Hartmann G.: Clerget (1875 – 1943), un motoriste de genie - Editions de l'Officine, 2004 – Appears as [2-3]

51) Haupais A.: Contribution à l'étude de la combustion dans un moteur Diesel -PhD report – Lyon 1981 – Appears as [2-9]

52) Higgins B., Siebers D.: Measurement of the Flame Lift-Off Location on DI Diesel Sprays Using OH Chemiluminescence - SAE 2001-01-0918 – Appears as [3-17]

53) Hiroyasu H. : Diesel Engine Combustion and its Modeling - Comodia – 1985 – Appears as [2-11]

54) Hiroyasu H.: Diesel Engine Combustion and its Modeling - University of Hiroshima – 1982 – Appears as [4-17]

55) Huh K.Y., Gosman A.D.: Phenomenological Model of Diesel spray atomization - International Conference on Multiphase Flows – Tsukuba – 1991 – Appears as [3-5] and [4-23]

56) Idicheria C.A., Pickett L.M.: Soot Formation in Diesel Combustion under High-EGR Conditions - SAE 2005-01-3834 – Appears as [3-18]

57) Iwamoto Y., Noma K., Nakayama O., Yamauchi T., Ando H.: Development of Gasoline Direct Injection Engine - SAE 970541- Appears as [6-5]

58) Jain B.C., Rife J.M., Keck J.C.: A Performance Model for the Texaco Controlled Combustion, Stratified Charge Engine - SAE 760116 – Appears as [2-15]

59) JD Power forecast 2012 release - Appears as [1-1]

60) Johnson J., Naber J., Lee S-Y, Hunter G., Truemner R., Harcombe T. : Correlations of Non-Vaporizing Spray Penetration for 3000 Bar Diesel Spray Injection - SAE 2013-024-0033 – Appears as [8-7]

61) Jourde J.P., Hauet B.: Development of a Pressure-Time type Electromagnetic Injector for Direct Injection in a 2-Stroke Spark Ignition Engine - SAE 885132 – Appears as [5-13]

62) Kakuho A.,Yamaguchi K., Hashizume Y., Urushihara T.,Itoh I., Tomita E.: A Study of Air Fuel Mixture Formation in Direct Injection SI Engines - SAE 2004-01-1946 – Appears as [6-18]

63) Kakuhou K., Urushihara T., Itoh I., Takagi Y.: Characteristics of Mixture Formation in a Direct Injection SI Engine with Optimized In-Cylinder Swirl Air Motion - SAE 99010505 – Appears as [6-7]

64) Khuong Ahn Dung: The Eulerian-Lagrangian Spray Atomization (ELSA) model of the Jet Atomization in CFD - PhD report – Valencia 2012 – Appears as [1-5]

65) Kim J.U., Golding B., Nocera D.G., Schock H.J., Keller P. : Exciplex Fluorescence Visualization Systems for Pre-Combustion Diagnosis for an Automotive Gasoline Engine - SAE 960826 – Appears as [4-11]

66) Kimura S., Aoki O., Kitahara Y. and Aiyoshizawa E.: Ultra Clean Combustion Technology Combining a Low-Temperature and Premixed Combustion Concept for Meeting Future Emission Standards - SAE 2001-01-0200 – Appears as [7-7]

67) Kimura S., Aoki O., Ogawa H., Muranaka S., Enomoto Y.: New Combustion Concept for Ultra-Clean and High-Efficiency Small DI Diesel Engines - SAE 99-01-3681- Appears as [7-4]

68) Knapp M., Andresen P., Luczak A., Beushausen V., Hentschel W. : Vapor/Liquid Visualization with Laser Induced Exciplex Fluorescence in an S.I.Engine for Different Fuel Injection timings - SAE 961122 – Appears as [4-10]

69) Kook S., Bae C., Miles P., Choi D., Pickett L.: The Influence of Charge Dilution and Injection Timing on Low-Temperature Diesel Combustion and Emissions - SAE 2005-01-3837 – Appears as [7-2]

70) Kumano K., Yama S. : Analysis of Knocking Suppression Effect of Cooled EGR in Turbo-Charged Gasoline Engine - SAE 2014-01-1217 – Appears as [8-3]

71) Lai M-C, Zheng Y., Xie X-B., Moon S., Liu Z., Gao J., Zhang X., Fezzaa K., Wang J., Shi J. : Characterization of the Near-Field Spray and Internal Flow of Single-Hole and Multi-Hole Sac Nozzles using Phase Contrast X-Ray Imaging and CFD - SAE 2011-01-0681 – Appears as [8-12]

72) Lebas R., Blokkeel G., Beau P.A., Demoulin F.X. : Coupling Vaporization Model with the Eulerian-Lagrangian Spray Atomization Model (ELSA) in Diesel Engine Conditions - SAE 2005-01-0213 – Appears as [4-22]

73) Liu X., Kyoung-Su Lm,Wang Y., Wang J., Tate M.W., Ercan A., Schuette D.R., Gruner S.M.: Ultrafast and Quantitative X-Tomography and Simulation of Hollow-Cone Gasoline Direct-Injection Sprays - SAE 2007-01-1847 – Appears as [3-22]

74) Luftwaffe Handbuch - Daimler Benz DB601A -– October 1940 – Appears as [2-4]

75) Maly R.: Improved Otto cycle by enhancing the final phase of combustion - Contractors meeting on Combustion Research – Brussels 1988 – Appears as [4-3]

76) Manin J.: Analysis of Mixing Processes in Liquid and Vaporized Diesel Sprays through LIF and Rayleigh Scattering Measurements - PhD report – Valencia – 2011 – Appears as [3-3]

77) Margot X., Payri R., Gil A., Chavez M., Pinzello A. : Combined CFD-Phenomenological Approach to the Analysis of Diesel Sprays under Non-Evaporative Conditions - SAE 2008-0-0962 – Appears as [4-27]

78) Marie J.J.: Diagnostics optiques: application à l'étude de la combustion dans les moteurs thermiques - Renault internal report n°0812/88/1205 – Rueil 1988 – Appears as [4-4]

79) Mauger C.: Cavitation dans un micro-canal, modèle d'injecteur Diesel: methods de visualization et influence de l'état de surface - PhD report – Lyon 2012 – Appears as [3-11]

80) May M.G. : the high compression lean burn spark ignited 4-stroke engine - I Mech E 1979 – Appears as [2-14]

81) May M.G., Spinnler F.: Betriebserfahrungen mit hochverdichteten Ottomotoren nach dem May Fireball-Verfahren - MTZ 06/78 – Appears as [5-8]

82) May M.G.: The High Compression Lean Burn Spark Ignited 4-Stroke Engine Journal of I-Mech 1979 – Appears as [5-9]

83) Melton L.A. : Applied Optics – 1983 – Appears as [4-9]

84) Miles P.: Sources of UHC and CO in Low Temperature Diesel Combustion Systems

85) Mitsubishi Motors Begins Research on In-cylinder Injection Technology of Gasoline Engine – EGIS "The Japan Automobile Letter" – 05/1992- Appears as [6-2]

86) MMC close to a production DI gasoline 4-stroke - RD's Engine and Vehicle Technology Update – 02/1992 – Appears as [6-1]

87) Munch K.U., Kramer H., Leipertz A.: Investigation of Fuel Evaporation Inside the Intake of a SA Engine Using Laser Induced Exciplex Fluorescence with a New Seed - SAE 961930 – Appears as [4-12]

88) Musculus M.P.B.: Heavy-Duty Low-Temperature and Diesel Combustion & Heavy-Duty Combustion Modeling - FY 2010 DOE Vehicle Technologies Program Annual Merit Review – Appears as [3-20]

89) NADIA_bio (New Advanced Direct Injection Analysis for bio fuels): rapport final à l'ANR - Paris 2011- Appears as [3-9]

90) Namazian M., Hanson S., Lyford-Pike E., Sanchez-Barsse J., Heywood J., Rife J.: Schlieren visualization of the flow and density fields in the cylinder of a spark-ignited engine - SAE 800044 – Appears as [4-1]

91) Natti K., Sinha A., Hoerter C., Andersson P.,.Andersson J., Lohmann C., Schultz D., Cho N.H., Winsor R. : Studies on the Impact of 300 MPa Injection Pressure on Engine Performance, Gaseous and Particulate Emissions - SAE 2013-01-0897 – Appears as [8-6]

92) Ortolan G., Deschamps B.: Separate Vapor-Liquid Visualization with Laser Induced Exciplex Fluorescence Applied to Gasoline Direct Injection Engines - 10th Gordon Research Conference on Laser Diagnostics (Poster) – Ciocco – 1999 – Appears as [4-13]

93) Payri F., Arrègle J., Lopez J.J., Hermens S.: Effect of cavitation on the nozzle outlzet flow, spray and flame formation in a Diesel engine - SAE 2006-01-1391 – Appears as [8-11]

94) Payri F., Bermudez V., Payri R., Salvador F.J.: The influence of cavitation on the internal flow and the spray characteristics in Diesel injection nozzles - Fuel, vol 83 – 2004. Appears as [8-10]

95) Pickett L., Siebers D., Idicheria C.: Relationship Between Ignition Processes and the Lift-Off Length of Diesel Fuel Jets - SAE 2005-01-3843 Appears as [7-16]

96) Pickett L., Siebers D.: Non-Sooting, Low Flame Temperature Mixing-Controlled DI Diesel Combustion - SAE 2004-01-1399 – Appears as [7-20]

97) Pinchon P., Levesque R.: Visualisation de la combustion dans les moteurs - Rapport IFP/GSM n° 32732 – Rueil 1985 – Appears as [4-2]

98) Pischinger A&F : Gemischbildung und Verbrennung in Dieselmotor - Springer Verlag Wien – 1957 – Appears as [2-5]

99) Powell C.: Fuel Injection and Spray Research Using X-Ray Diagnostics - Deer Symposium 2012 – Appears as [8-13]

100) Prost J.: keynote speech - SIA Rouen 2012 – Appears as [8-2]

101) Ramirez A.I.,Som S., Aggarwall S.K., Kastengren A.L., El Hannouny E.M., Longman D.E., Powell C.F.: Characterizing Spray Behavior of Diesel Injection Systems Using X-Ray Radiography - SAE 2009-01-0846 – Appears as [3-7]

102) Reboux J., Puechberty D., Dionnet F.: A new approach of Planar Laser Induced Fluorescence applied to Fuel/Air ratio measurement in the compression stroke of an optical SI engine - SAE 941988 – Appears as [4-6]

103) Reboux J., Puechberty D., Dionnet F.: Study of mixture inhomogeneities and combustion development in a SI engine using a new approach of Laser Induced Fluorescence (FARLIF) - SAE 961205 – Appears as [4-7]

104) Reitz R.D., Diwakar R.: Effect of drop breakup on fuel sprays - SAE 860469 – Appears as [3-6]

105) Reitz R.D., Diwakar R.: Structure of High Pressure Fuel Sprays - SAE 870598 – Appears as [4-24]

106) Reitz, Bracco: on the dependence of the spray angle and other spray parameters on nozzle design and operating conditions - SAE 790494 – Appears as [2-7]

107) Reitz, Bracco: ultra high speed filming of atomizing jets - Physic fluids - 1979 – Appears as [2-8]

108) Ren W., Shen J., Nally J.F.: Geometrical Effects Flow Characteristics of a Gasoline High Pressure Swirl Injector - SAE 971641- Appears as [6-10]

109) Ricou F.P., Spalding D.P.: Measurements of entrainment by axisymmetric turbulent jets -Journal of Fluid Mechanics -11 – 1960 – Appears as [3-14]

110) Sacadura J.C., Robin L., Dionnet F., Gervais D., Gastaldi P., Ahmed A.: Experimental Investigation of an Optical Direct Injection S.I. Engine using Fuel Air Ratio Laser Induced Fluorescence - SAE 2000-01-1794 – Appears as [4-8] and [6-15]

111) Sasaki S., Akihama K., Takatori Y., Inagaki K., Dean A.M.: Mechanism of the Smokeless Rich Diesel Combustion by Reducing Temperature - SAE 2001-01-0655 – Appears as [7-5]

112) Schäppertons H., Emmenthal K.D., Grabe H.J., Oppermann W.: VW's Gasoline Direct Injection (GDI) Research Engine - SAE 910054 – Appears as [5-6]

113) Scherenberg H. : Der Erfolg der Benzin Einspritzung bei Daimler-Benz" - MTZ 07/61 pp. 241 -245 – Appears as [5-3]

114) Schweitzer P.H.: Penetration of Oil Spray - Pennsylvania State College Bulletin – 1937 – Appears as [4-16]

115) Scussel, Simko A.O.,Wade W.R. : the Ford PROCO Engine Update - SAE 780699 – Appears as [5-5]

116) Sepret V.: Application de la PIV sur traceurs fluorescents à l'étude de l'entraînement d'air par un spray Diesel. Influence de la densité ambiante et du diameter de trou d'injecteur - PhD report – Toulouse 2009 – Appears as [7-18]

117) Shahed S.M., Chiu W., Lyn W.T. : a mathematical model of Diesel combustion- I.Mech – Cranfield – 1975 – Appears as [2-10]

118) Shelby M.H., VanDerWege B.A., Hochgreb S.: Early Spray Development in Gasoline Direct-Injected Spark Ignition Engines - SAE 980160 – Appears as [3-21]
SIA - Rouen 2010 – Appears as [7-24]

119) Siebers D., Higgins B., Pickett L.: Flame Lift-Off on Direct-Injection Diesel Fuel Jets: Oxygen Concentration Effects - SAE 2002-01-0890 – Appears as [3-19] and [7-19]

120) Siebers D., Higgins B.: Flame Lift-Off on Direct-Injection Diesel Sprays Under Quiescent Conditions - SAE 2001-01-0530 – Appears as [7-14]

121) Siebers D.: Flame lift-off and mixing controlled combustion - Deer Symposium 2008 – Appears as [7-17]

122) Solver M., Klahr D., Torres A.: An Unstructured Parallel Solver for Engine Intake and Combustion Stroke Simulation - SAE 2002-01-1120 – Appears as [4-20]

123) Stanton D.: Advanced combustion technology to enable high efficiency clean combustion - Deer Symposium- 2008 – Appears as [7-13]

124) Tatsuta H., Matsumura M.,Yajima J.,Nishide H.: Mixture Formation and Combustion Performance in a new Direct-Injection SI V6 engine - SAE 981435 – Appears as [6-6]

125) Technologietransfer zu Ubertragung von CO2- und Schadstoffemissions- potentialen zwischen verschiedenen Motorarten - FVV final report 2013 – Appears as [8-5]
Thiesel 2010 – Appears as [7-3]

126) Toyota plans DI gasoline engine in 1993 - Ward's Engine Update – 10/1992 – Appears as [6-3]

127) Tsao K.C., Dong Y., Xu Y.: Investigation of Flow Spray and Flow Field in a Direct Injection Diesel Engine via Kiva II Program - SAE 901616 – Appears as [4-19]

128) Wakuri: Studies of the penetration of fuel spray in a Diesel engine - JSME n°9 – 1960 – Appears as [2-6]

129) Walter B., Gatellier B.: Development of the High Power NADI Concept using Dual Mode Diesel Combustion to achieve Zero Nox and Particulate Emissions - SAE 2002-01-1744 – Appears as [7-6]

130) Welling O., Moss J., Williams J., Collings N. : Measuring the Impact of Engine Oils and Fuels on Low-Speed Pre-Ignition in Downsized Engines - SAE 2014_01-1219 – Appears as [8-4]

131) Wojdas O. : Numerical simulation for the Diesel engine development - PhD report – INSA Lyon – 2010 – Appears as [4-25]

132) Wolters P., Grigo M., Walzer P.: Betriebsverhalten eines direkteinspritzenden Ottomotors mit luftgeführter Gemischbildung - 6.Aachener Kolloquium 1997 – Appears as [6-8]

133) Wurster W.: Grundsatzuntersuchungen am Ottomotor mit direkter Einspritzung (Porsche AG) - Technische Akademie Wuppertal – 09/1989 – Appears as [5-7]

134) Zellat M., Rolland T., Poplow F.: Three Dimensional Modelling of Combustion and Soot Formation in an Indirect Injection Diesel Engine - SAE 900254 – Appears as [4-18]

135) Zwei neue Motoren von Jaguar - MTZ 5/1988 – Appears as [5-10]